MODERN NEUROSURGERY AND NEUROANATOMY

EDITED BY: Albert Sufianov, Ilgiz Fanilevich Gareev, Ozal Beylerli and Daming Zhang
PUBLISHED IN: Frontiers in Surgery

frontiers Research Topics

ISSN 1664-8714
ISBN 978-2-83250-088-0
DOI 10.3389/978-2-83250-088-0

About Frontiers

Frontiers is more than just an open-access publisher of scholarly articles: it is a pioneering approach to the world of academia, radically improving the way scholarly research is managed. The grand vision of Frontiers is a world where all people have an equal opportunity to seek, share and generate knowledge. Frontiers provides immediate and permanent online open access to all its publications, but this alone is not enough to realize our grand goals.

Frontiers Journal Series

The Frontiers Journal Series is a multi-tier and interdisciplinary set of open-access, online journals, promising a paradigm shift from the current review, selection and dissemination processes in academic publishing. All Frontiers journals are driven by researchers for researchers; therefore, they constitute a service to the scholarly community. At the same time, the Frontiers Journal Series operates on a revolutionary invention, the tiered publishing system, initially addressing specific communities of scholars, and gradually climbing up to broader public understanding, thus serving the interests of the lay society, too.

Dedication to Quality

Each Frontiers article is a landmark of the highest quality, thanks to genuinely collaborative interactions between authors and review editors, who include some of the world's best academicians. Research must be certified by peers before entering a stream of knowledge that may eventually reach the public - and shape society; therefore, Frontiers only applies the most rigorous and unbiased reviews.
Frontiers revolutionizes research publishing by freely delivering the most outstanding research, evaluated with no bias from both the academic and social point of view.
By applying the most advanced information technologies, Frontiers is catapulting scholarly publishing into a new generation.

What are Frontiers Research Topics?

Frontiers Research Topics are very popular trademarks of the Frontiers Journals Series: they are collections of at least ten articles, all centered on a particular subject. With their unique mix of varied contributions from Original Research to Review Articles, Frontiers Research Topics unify the most influential researchers, the latest key findings and historical advances in a hot research area! Find out more on how to host your own Frontiers Research Topic or contribute to one as an author by contacting the Frontiers Editorial Office: frontiersin.org/about/contact

MODERN NEUROSURGERY AND NEUROANATOMY

Topic Editors:
Albert Sufianov, I.M. Sechenov First Moscow State Medical University, Russia
Ilgiz Fanilevich Gareev, Peoples' Friendship University of Russia, Russia
Ozal Beylerli, Peoples' Friendship University of Russia, Russia
Daming Zhang, First Affiliated Hospital of Harbin Medical University, China

Citation: Sufianov, A., Gareev, I. F., Beylerli, O., Zhang, D., eds. (2022). Modern Neurosurgery and Neuroanatomy. Lausanne: Frontiers Media SA. doi: 10.3389/978-2-83250-088-0

Table of Contents

frontiers | Frontiers in Surgery

TYPE Editorial
PUBLISHED 17 August 2022
DOI 10.3389/fsurg.2022.993898

Check for updates

OPEN ACCESS

EDITED BY
Philipp Taussky,
Beth Israel Deaconess Medical Center, Harvard Medical School, United States

*CORRESPONDENCE
Ilgiz Gareev
ilgiz_gareev@mail.ru

SPECIALTY SECTION
This article was submitted to Neurosurgery, a section of the journal Frontiers in Surgery

RECEIVED 14 July 2022
ACCEPTED 28 July 2022
PUBLISHED 17 August 2022

CITATION
Gareev I, Beylerli O, Sufianov A and Zhang D (2022) Editorial: Potential clinical applications of circulating microRNAs in neurosurgery. Front. Surg. 9:993898.
doi: 10.3389/fsurg.2022.993898

Editorial: Potential clinical applications of circulating microRNAs in neurosurgery

Ilgiz Gareev[1,2]*, Ozal Beylerli[1,2], Albert Sufianov[1,2,3] and Daming Zhang[4]

[1]Department of Neurosurgery, Federal Center of Neurosurgery, Tyumen, Russia, [2]Educational and Scientific Institute of Neurosurgery, Peoples' Friendship University of Russia (RUDN University), Moscow, Russian Federation, [3]Department of Neurosurgery, Sechenov First Moscow State Medical University (Sechenov University), Moscow, Russia, [4]Department of Neurosurgery, The First Affiliated Hospital of Harbin Medical University, Harbin, China

Editorial on the Research Topic
Potential clinical applications of circulating microRNAs in neurosurgery

By Gareev I, Beylerli O, Sufianov A, Zhang D. (2022) Front. Surg. 9: 993898. doi: 10.3389/fsurg.2022.993898

Neurosurgical pathology occupies a special place in surgical practice. As with other surgical specialties, this is a century-old specialization of the industry. In modern neurosurgery, for a qualitative approach to the treatment of patients with various diseases of the central nervous system (CNS), it is necessary to solve many diagnostic issues related to the peculiarities of this narrowly focused branch of medicine. One of the urgent problems in neurosurgery is the search for diagnostic and prognostic biomarkers for several neurosurgical pathologies, such as brain tumors or intracranial aneurysms with high risk rupture, the diagnostic methods of which currently require significant improvements. In modern neurosurgery, the search for predictive biomarkers, especially in brain tumors and cerebrovascular disease, is of paramount importance, since the introduction of these indicators into clinical practice will quickly determine the optimal treatment for each patient. Diagnosis plays a crucial role in making a prognosis and choosing the best therapy for brain tumors. Despite significant recent advances in the diagnosis of brain tumors using various modifications of imaging techniques followed by histopathological examination, tumor detection is still limited by its size and location, as well as by the heterogeneity of its tissue (1). In this regard, it is necessary to develop new diagnostic approaches that, together with the available methods, will improve the accuracy of diagnosis. A promising approach is fluid biopsy, which involves finding and measuring the levels of various circulating molecules in human body fluids such as blood or cerebrospinal fluid (CSF). In addition, given that computed tomography angiography (CTA), magnetic resonance angiography (MRA), and selective cerebral angiography (SCA) are either unavailable or do not provide clear evidence of possible rupture of intracranial aneurysms (IAs), accurate and reliable analysis of the molecular profile in biological fluids can help in the early diagnosis and prognosis of rupture, as well as likely mortality and morbidity or prognostic outcome of patients with subarachnoid

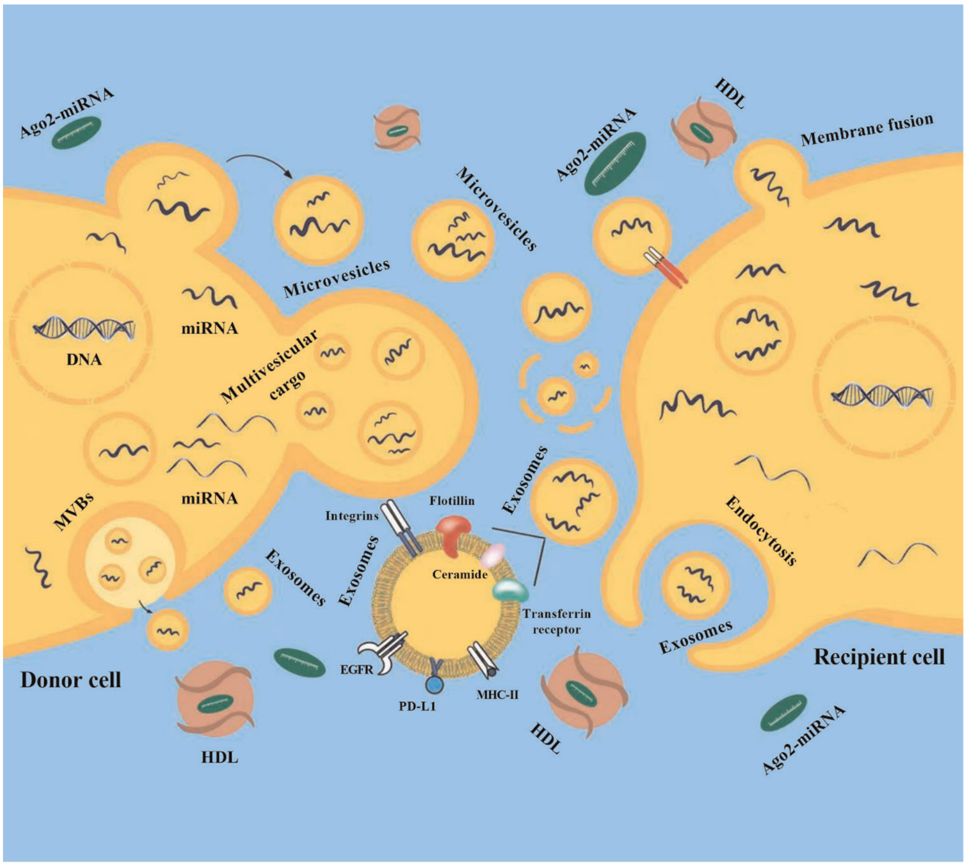

FIGURE 1
Release of microRNAs (miRNAs) into the extracellular environment. Released miRNAs are transported by extracellular vesicles (EVs) and transferred to recipient cells (from donor cells) where they regulate post-transcriptional gene expression. Membrane exosomes are released from cells as endosomes containing multivesicular bodies (MVBs) that fuse with the plasma membrane. Microvesicles (MVs) are released from the plasma membrane *via* outward budding. Multivesicular cargo (MVC) is released by membrane budding during apocrine secretion. EVs and their miRNAs cargo are transferred to recipient cells (from donor cells) after endocytosis or membrane fusion. MiRNAs can also be secreted outside of vesicles. Most circulating miRNAs are in a non-vesicular form, namely, they are associated with Ago2 proteins (Ago2-miRNA complex). In addition to the Ago2 protein, high-density lipoproteins (HDL) are reported to be involved in the mechanism of intercellular communication and are involved in the transport and delivery of miRNAs. EGFR, epidermal growth factor receptor; PD-L1, programmed death-ligand 1; MHC-II, major histocompatibility complex class II.

hemorrhage (SAH) to stratify patients admitted to hospitals (1). MicroRNAs (miRNAs) are promising candidates for the role of such biomarkers. This is due to tissue specificity and a high rate of changes in miRNAs expression, combined with the possibility of these molecules leaving cells into the extracellular space/biological fluids in a form that is stable to degradation (**Figure 1**) (2).

Many studies have been published on the diagnostic significance of circulating miRNAs in primary and metastatic brain tumors, cerebrovascular disease (e.g., hemorrhage stroke and SAH), osteochondrosis, and traumatic brain injuries, etc. For instance, one prospective multi-center observational study identified a panel of 762 plasma miRNAs for each patient to establish these circulating miRNAs signatures specific to glioblastoma, and was capable of distinguishing them from malignant non-glial brain tumors (primary CNS lymphomas (PCNSL) and brain metastases (BM)) (NCT03630861, ClinicalTrials.gov). The EVTRNA study (NCT04230785, ClinicalTrials.gov) analyzed the differentiated expression pattern of circulating miRNAs by next-generation sequencing (NGS) in acute ischemic stroke (IS) patients before and/or after endovascular treatment. The candidate circulating miRNAs were verified as the biomarker and regulator for the progression and prognosis of acute IS with endovascular treatment.

Circulating miRNAs are attractive candidates for monitoring cerebrovascular disease (3). It is assumed that changes in expression of circulating microRNAs in biological fluids occur earlier than currently known biomarkers (e.g., markers of inflammation and repair, which include troponin, D-dimer, C-reactive protein, chemokines, and cytokines). Recently, a number of studies have been carried out, showing that circulating miRNAs may be more preferable as biomarkers since they can be detected early in the development of the disease, whereas protein structures like D-dimer and C-reactive protein are found in the blood only when a significant amount of damage has already occurred (4, 5). In addition, concentrations of D-dimer or C-reactive protein can also be increased in other pathologies, including thrombosis, infections, and myocardial infarction.

The stability and availability of circulating miRNAs in biological fluids make them new non-invasive biomarkers of particular interest in modern neurosurgery. The areas of application of circulating miRNAs will not only cover brain tumors or cerebrovascular disease but may also extend to many other neurosurgical pathologies. However, to minimize the variability of results, it is necessary to standardize sample processing procedures, detection methods, and, above all, normalization strategies. In addition, another breakthrough that we are now seeing is the study of miRNAs in extracellular vesicles such as exosomes, which are now available through various isolation methods, allowing them to be studied as biomarkers according to their cellular origin.

Author contributions

All authors listed have made a substantial, direct, and intellectual contribution to the work and approved it for publication. All authors contributed to the article and approved the submitted version.

Conflict of interest

The authors declare that the research was conducted in the absence of any commercial or financial relationships that could be construed as a potential conflict of interest.

Publisher's note

All claims expressed in this article are solely those of the authors and do not necessarily represent those of their affiliated organizations, or those of the publisher, the editors and the reviewers. Any product that may be evaluated in this article, or claim that may be made by its manufacturer, is not guaranteed or endorsed by the publisher.

References

1. Barnett SR, Nozari A. The preoperative evaluation of the neurosurgical patient. *Int Anesthesiol Clin*. (2015) 53(1):1–22. doi: 10.1097/AIA.0000000000000047

2. Gareev I, Beylerli O, Yang G, Sun J, Pavlov V, Izmailov A, et al. The current state of MiRNAs as biomarkers and therapeutic tools. *Clin Exp Med*. (2020) 20 (3):349–59. doi: 10.1007/s10238-020-00627-2

3. Gareev I, Yang G, Sun J, Beylerli O, Chen X, Zhang D, et al. Circulating MicroRNAs as potential noninvasive biomarkers of spontaneous intracerebral hemorrhage. *World Neurosurg*. (2020) 133:e369–75. doi: 10.1016/j.wneu.2019.09.016

4. Zhao Y, Brasier AR. Qualification and verification of protein biomarker candidates. *Adv Exp Med Biol*. (2016) 919:493–514. doi: 10.1007/978-3-319-41448-5_23

5. Backes C, Meese E, Keller A. Specific miRNA disease biomarkers in blood, Serum and plasma: challenges and prospects. *Mol Diagn Ther*. (2016) 20 (6):509–18. doi: 10.1007/s40291-016-0221-4

frontiers in Surgery

CASE REPORT
published: 11 March 2022
doi: 10.3389/fsurg.2022.866476

A Three-Surgeon–Six-Hand Operation Using a 4K-3D Exoscope for Neurological Surgery: A Case Report

Ryota Tamura[1,2], Yuki Kuranari[2] and Makoto Katayama[2]*

[1] *Department of Neurosurgery, Keio University School of Medicine, Shinjuku, Japan,* [2] *Department of Neurosurgery, Kawasaki Municipal Hospital, Kawasaki, Japan*

Background: Advances in digital imaging including evolving of 3-dimensional (3D) exoscope has allowed its use as an alternative to microscopes in neurosurgery. The exoscope can concede wide space around the operating table and patient. Here, we show a three-surgeon–six-hand operative approach using a 4K-3D exoscope. Practical advantages and disadvantages of this approach are discussed.

Clinical Presentation: A 58-year-old male was refered with a 60 mm diameter meningioma in the right frontal convexity. The tumor removal was done by an operator and two assistants with a scrub nurse while viewing images displayed on a 55-inch monitor with integrated 4K and 3D visualization technology retrieved by KINEVO®. Meaningful communication between the operator and two assistants allowed for simultaneous, and precise surgical procedures. Gross total removal was achieved without damaging the brain.

Conclusion: The ocular-free, openness of 4K-3D exoscope allows for a three-surgeon–six-handed operation, which leads to simultaneous surgical maneuvers by multiple hands, shorter operative time, flexible/intermittent brain retraction made by two assistants, and educational benefits owing to the surgical procedure being visually shared.

Keywords: exoscope, 3-dimensional, 4K, KINEVO, six hand, assistant

OPEN ACCESS

Edited by:
Ozal Beylerli,
Federal Center of Neurosurgery, Russia

Reviewed by:
Valentin Pavlov,
Bashkir State Medical University, Russia
Aferin Beilerli,
Harbin Medical University, China

Correspondence:
Ryota Tamura
moltobello-r-610@keio.jp

Specialty section:
This article was submitted to Neurosurgery, a section of the journal Frontiers in Surgery

Received: *31 January 2022*
Accepted: *18 February 2022*
Published: *11 March 2022*

Citation:
Tamura R, Kuranari Y and Katayama M (2022) A Three-Surgeon–Six-Hand Operation Using a 4K-3D Exoscope for Neurological Surgery: A Case Report. Front. Surg. 9:866476. doi: 10.3389/fsurg.2022.866476

INTRODUCTION

The incorporation of visual enhancement technology has transformed the field of neurosurgery to the next generation. The operating microscope (OM) has become the gold standard in neurosurgery (1, 2). However, the OM has some limitations in operative mobility, accessibility and expense. Additionally, the operational view of the OM is limited by the patients position, which can, in cases, leading to an uncomfortable position for the operator and assistant, resulting in intraoperative fatigue. To ameliorate these problems, the 3-dimensional (3D) extracorporeal telescope (exoscope) was created (3, 4). Owing to advances in digital imaging, the 3D exoscope has been increasingly used as an alternative to microscopes in surgery. The 4K-3D exoscope ideally presents the operative environment illustrated broadly in a 3D landscape. The exoscope

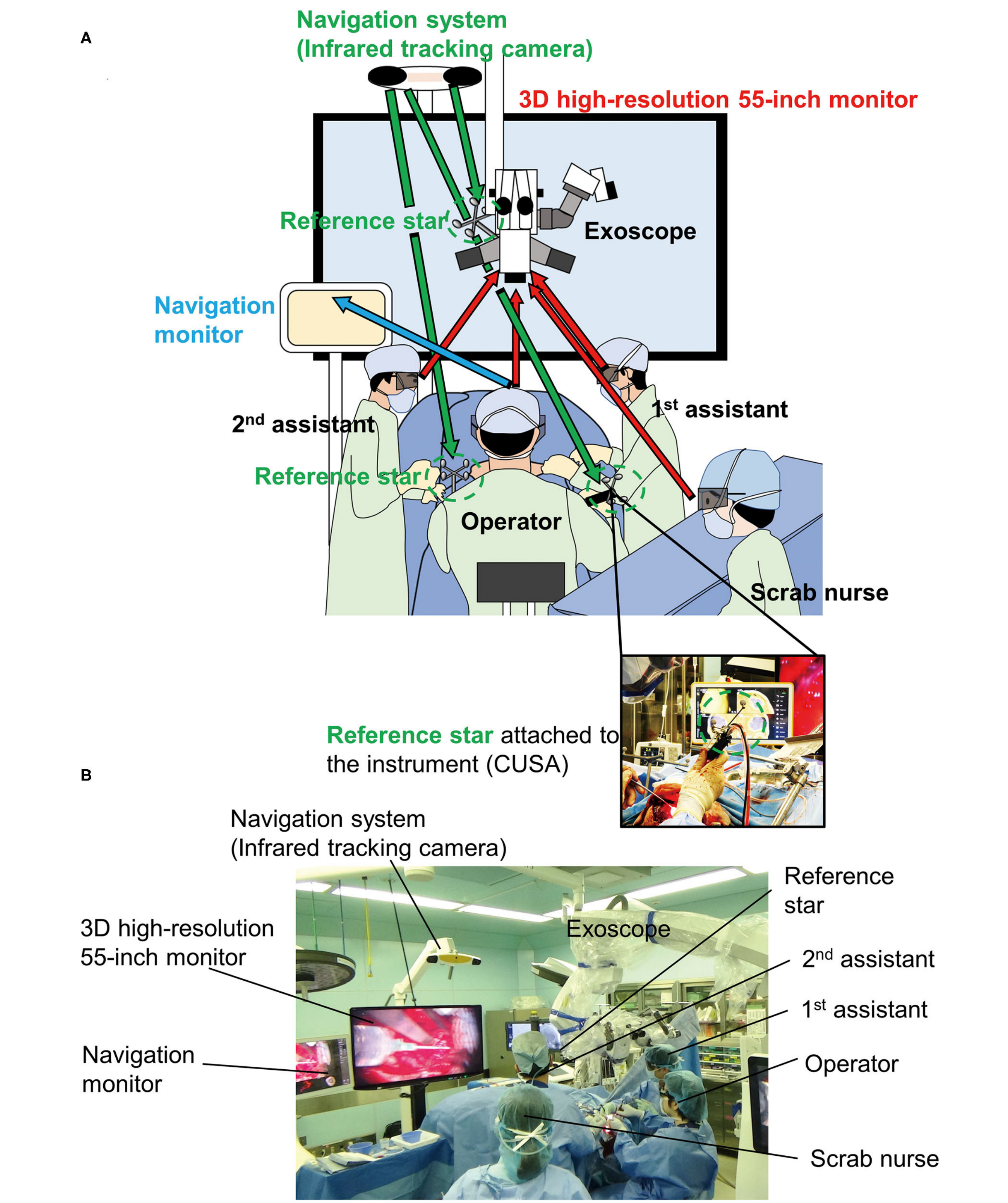

FIGURE 1 | Equipment, operating room setup, and patient positioning. **(A)** Illustration of a three-surgeon–six-hand operation using a 4K-3D exoscope is shown. **(B)** Actual setup in the operation room. Arrows means viewpoint of each staff.

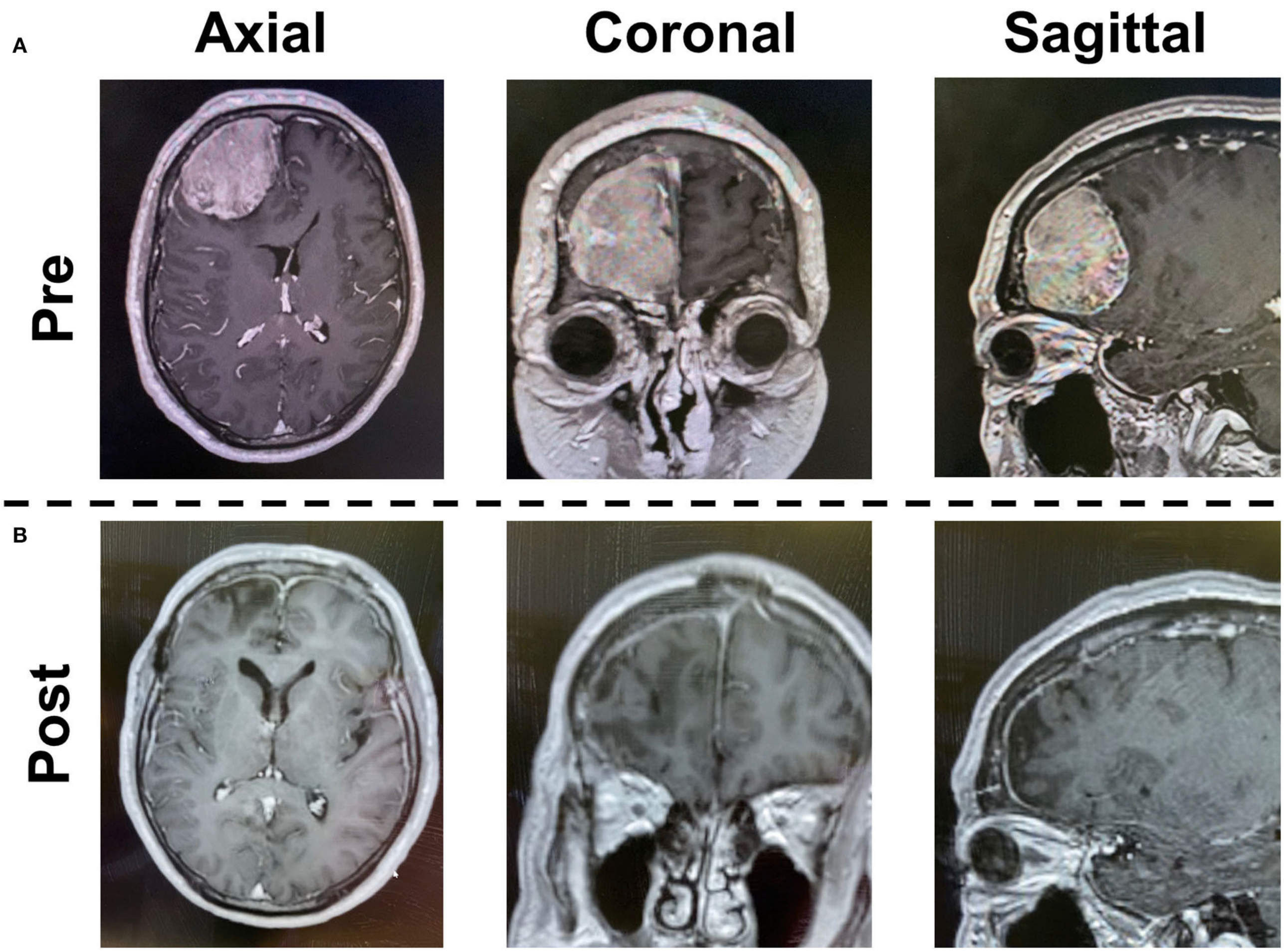

FIGURE 2 | Case presentation. Preoperative **(A)** and postoperative **(B)** gadolinium-enhanced T1-weighted imagings are shown.

is suspended above the surgical field. A 4K monitor is displayed in front of the surgeon, and the operation is performed while watching the monitor and wearing 3D glasses. A surgeon's position is not limited to the microscope' oculars, while freedom in movements during surgery, a higher comfort rate, a lower fatigue after longer procedures have been reported in using a 4K-3D exoscope (5, 6).

The exoscope system can be used for brain tumor, skull base surgery, aneurysm clipping and vascular microanastomosis, both cervical and lumbar complex spine surgery (7). In the last decade, several types of approaches using exoscopes have been developed and adapted to various neurosurgical procedures (8–11).

Similarly, endonasal endoscopic approach has evolved to enable skull base surgery through minimal access ports using pre-existing air spaces. Endoscopy provides excellent magnification, high-definition images and a panoramic view (12). Four-handed technique provides further panoramic views and greater surgical freedom with minimal invasion, and results in fewer complications compared to the two-handed technique (13).

The exoscope has a focal length of 220–650 mm (10, 14, 15). The exoscope will allow for wide space around the operating table and patient. This is especially useful in procedures of surgical assistants with multiple equipment (e.g., navigation devices or ultrasound). The purpose of this study is to show the three-surgeon–six-hand operative approach using a 4K-3D exoscope. The practical advantages and disadvantages of this approach are discussed.

CASE PRESENTATION

Equipment, Operating Room Setup, and Patient Positioning

KINEVO® (Carl Zeiss Meditec AG, Oberkochen, Germany) was used, which contains 4K-3D displays, light filters for 5-aminolevulinic acid and indocyanine video-angiography, pneumatic arms, adjustable operative settings, multiscreen output, longer focus distance and a greater magnification power (10, 14, 15). The operator takes position in front of the patients head with two assistants on both sides. A scrub nurse stands on the operator's dominant hand side between the operator and each assistant.

The KINEVO® camera was placed above the patients head at a high position allowing for open visualization of the monitor.

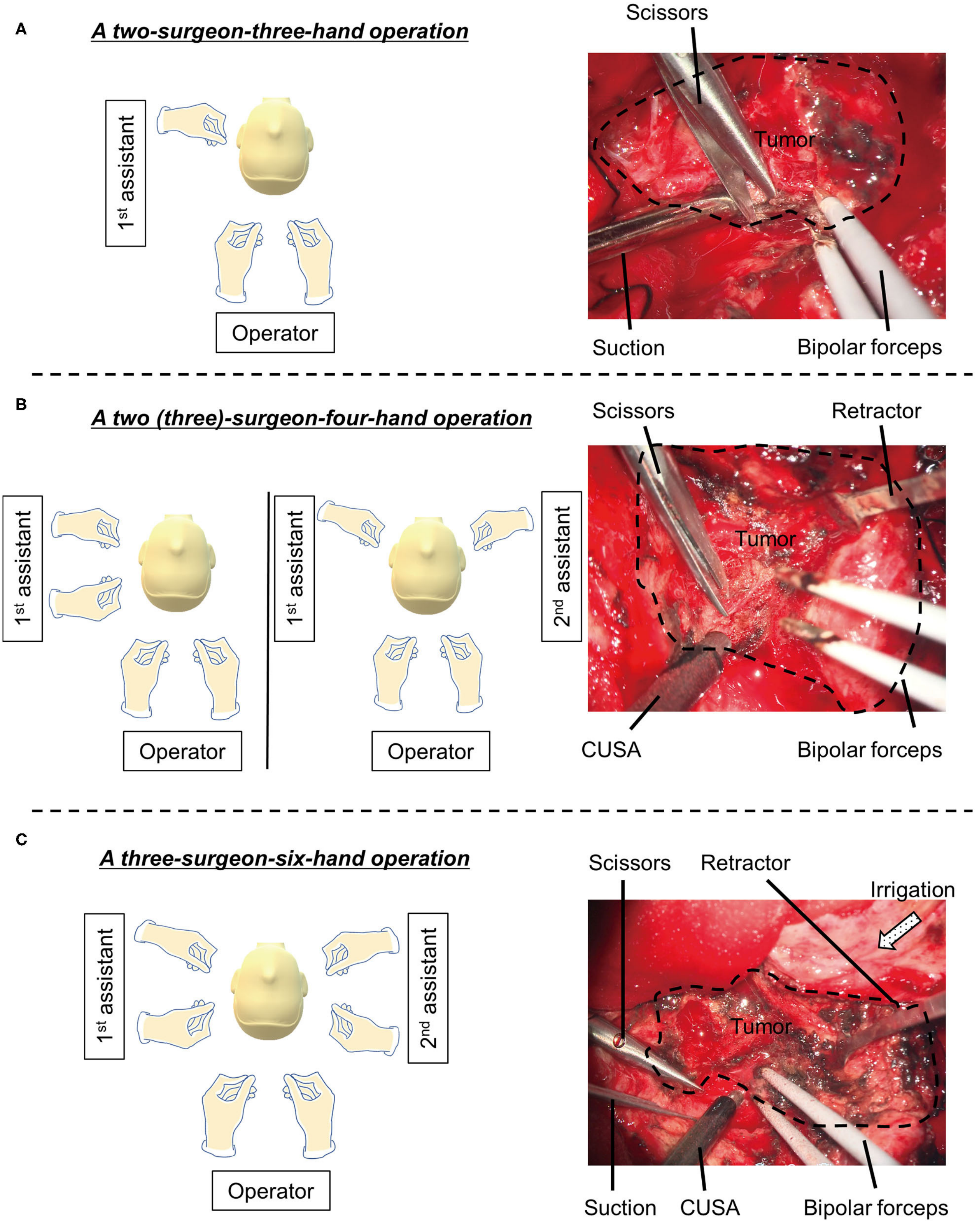

FIGURE 3 | The combination of the experienced operator and assistants. A two-surgeon-three-hand **(A)**, a two (three)-surgeon-four-hand **(B)** and a three-surgeon-six-hand operations **(C)** is illustrated on the left panels. Intraoperative images are shown on the right panels.

TABLE 1 | Advantages and disadvantages of the three-surgeon–six-hand operation using a 4K-3D exoscope.

Advantage	Disadvantage
1. Meaningful communication between the operator and two surgical assistants allows for seamless procedures, leading to shorter operative time. 2. No continuous brain retraction is needed. 3. Two assistants can obtain educational benefits owing to the visually and dynamically shared surgical procedures.	1. Two assistants may feel intraoperative fatigue during looking at the same monitor placed on the caudal side of the patients.

A high-definition view of the surgical field was projected onto a 3D high-resolution 55-inch monitor, which was placed across the room toward the patient's leg side. An operator and two assistants operated with the scrub nurse viewing images (with 3D glasses) of the surgical field on the monitor. We used a neuronavigation system (BrainLab, Munich, Germany) to visualize the tumor and anatomical landmarks. Infrared tracking camera with extended detection and navigation monitor were placed behind, and next to the 55-inch monitor, respectively. The reference star was positioned around the neck caudally from the second assistant (**Figures 1A,B**).

Surgical Procedures

A 58-year-old male presented with a headache. CT demonstrated a 60 mm diameter meningioma in the right frontal convexity. Tumor removal was performed *via* frontal craniotomy (**Figure 2**). A three-surgeon–six-hand operative technique was used with a 4K-3D exoscope, as described above (**Figure 3**). Furthermore, a two-surgeon-three-handed and a two (three)-surgeon-four-handed method was flexibly used (**Figure 3**).

During the operation, the operator mainly used bipolar forceps and CUSA® Clarity (Integra LifeSciences Corporation, NJ, USA). The first and second assistants used micro scissors and suction, or brain retractor and suction. The combination of the experienced operator and two assistants allowed for seamless processing of dissection between the brain and tumor, without exchanging tools from one hand to another. Continuous brain retraction was unnecessary. Gross total removal was achieved without damaging the brain (Simpson's grade I). Postoperative CT scan displayed complete removal of the tumor.

DISCUSSION

In the present study, the three-surgeon–six-hand operation was perfomed using a 4K-3D exoscope, showing some practical advantages. Exoscope has a focal length of 220–650 mm, resulting in wider working space. The camera head of the exoscope does not interfere with the assistants' access to the surgical field during simultaneous surgical procedures. It was not necessary to devise the patient's position, the operators' position, and the arrangement of other surgical equipment. Meaningful communication between the operator and two surgical assistants allowed for seamless procedures, leading to shorter operative time (**Table 1**).

Brain retraction is important to secure surgical space during brain surgery. Surgery without continuous tumor and brain retractors could be performed because two assistants versatilely pulled the tumor or brain to the operator's desired direction. The combination of the experienced operator and assistants lead to seamless, efficient and faster dissection procedures (**Table 1**). With the flexible and intermittent retraction, the brain damage was morphologically minimal with a retraction force (16–18).

Typically, the use of external monitors and glasses can give the audience such as students and residents the same high-resolution view as the surgeon, leading to educational advantages (14). The three-surgeon–six-hand operation also includes special educational benefits of two assistants in addition to all individuals present in the operating room owing to the visually and dynamically shared surgical procedures. Furthermore, the operator may be attuned to surrounding trainees, leading to valuable teaching opportunities (**Table 1**).

An important disadvantage of this approach is the slight difficulty in assisting the operator from both sides for the two assistants, and a relatively distant position of the scrub nurse (**Table 1**). This disadvantage can be reduced by the efficient equipment, operating room setup, and patient positioning. Two assistants may feel intraoperative fatigue looking at the same direction having the 55-inch monitor placed on the caudal side of the patients. However, this is still better than an OM, because the assistant has to look into the other eyepiece of the OM in an uncomfortable position dictated by the primary operator.

The 4K-3D exoscope can allow wide space around the operating table and patient. We can perform the three-surgeon–six-hand operative approach. Further experience is needed to achieve more comfortable maneuverability of surgical instruments during the procedure.

CONCLUSIONS

A three-surgeon–six-hand operation using a 4K-3D exoscope overcomes some limitations in operative mobility, accessibility and educational aspects in the OM. This approach will be further adapted for the use in various neurosurgical diseases.

DATA AVAILABILITY STATEMENT

The original contributions presented in the study are included in the article, further inquiries can be directed to the corresponding author.

AUTHOR CONTRIBUTIONS

RT conceptualized, designed, performed the study, and wrote the manuscript. YK assisted in the acquisition of data. MK assisted with discussion and review of the manuscript. All authors approved the final version.

REFERENCES

1. Herlan S, Marquardt JS, Hirt B, Tatagiba M, Ebner FH. 3D exoscope system in neurosurgery—comparison of a standard operating microscope with a new 3D exoscope in the cadaver lab. *Oper Neurosurg.* (2019) 17:518–24. doi: 10.1093/ons/opz081
2. Siller S, Zoellner C, Fuetsch M, Trabold R, Tonn JC, Zausinger S, et al. A high-definition 3D exoscope as an alternative to the operating microscope in spinal microsurgery. *J Neurosurg Spine.* (2020) 33:705–14. doi: 10.3171/2020.4.SPINE20374
3. Khalessi AA, Rahme R, Rennert RC, Borgas P, Steinberg JA, White TG, et al. First-in-man clinical experience using a high-definition 3-dimensional exoscope system for microneurosurgery. *Oper Neurosurg.* (2019) 16:717–25. doi: 10.1093/ons/opy320
4. Pafitanis G, Hadjiandreou M, Alamri A, Uff C, Walsh D, Myers S. The exoscope versus operating microscope in microvascular surgery: a simulation non-inferiority trial. *Arch Plast Surg.* (2020) 47:242–9. doi: 10.5999/aps.2019.01473
5. Nishiyama K. From exoscope into the next generation. *J Korean Neurosurg Soc.* (2017) 60:289–93. doi: 10.3340/jkns.2017.0202.003
6. Panchal S, Yamada Y, Nagatani T, Watanabe T, Kishida Y, Sayah A, et al. Practice survey to compare and identify the usefulness of neuroendoscope and exoscope in the current neurosurgery practice. *Asian J Neurosurg.* (2020) 15:601–7. doi: 10.4103/ajns.AJNS_339_19
7. Montemurro N, Scerrati A, Ricciardi L, Trevisi G. The exoscope in neurosurgery: an overview of the current literature of intraoperative use in brain and spine surgery. *J Clin Med.* (2021) 11:223. doi: 10.3390/jcm11010223
8. Kwan K, Schneider JR, Du V, Falting L, Boockvar JA, Oren J, et al. Lessons learned using a high-definition 3-dimensional exoscope for spinal surgery. *Oper Neurosurg.* (2019) 16:619–25. doi: 10.1093/ons/opy196
9. Langer DJ, White TG, Schulder M, Boockvar JA, Labib M, Lawton MT. Advances in intraoperative optics: a brief review of current exoscope platforms. *Oper Neurosurg.* (2020) 19:84–93. doi: 10.1093/ons/opz276
10. Sack J, Steinberg JA, Rennert RC, Hatefi D, Pannell JS, Levy M, et al. Initial experience using a high-definition 3-dimensional exoscope system for microneurosurgery. *Oper Neurosurg.* (2018) 14:395–401. doi: 10.1093/ons/opx145
11. Wanibuchi M, Komatsu K, Akiyama Y, Mikami T, Mikuni N. Effectiveness of the 3D monitor system for medical education during neurosurgical operation. *World Neurosurg.* (2018) 109:e105–9. doi: 10.1016/j.wneu.2017.09.113
12. Almeida JP, de Albuquerque LA, Dal Fabbro M, Sampaio M, Medina R, Chacon M, et al. Endoscopic skull base surgery: evaluation of current clinical outcomes. *J Neurosurg Sci.* (2019) 63:88–95. doi: 10.23736/S0390-5616.16.03386-5
13. Castelnuovo P, Pistochini A, Locatelli D. Different surgical approaches to the sellar region: focusing on the "two nostrils four hands technique". *Rhinology.* (2006) 44:2–7.
14. Ricciardi L, Chaichana KL, Cardia A, Stifano V, Rossini Z, Olivi A, et al. The exoscope in neurosurgery: an innovative "point of view". A systematic review of the technical, surgical and educational aspects. *World Neurosurg.* (2019) 124:136–44. doi: 10.1016/j.wneu.2018.12.202
15. Vetrano IG, Acerbi F, Falco J, D'Ammando A, Devigili G, Nazzi V. High-definition 4K 3D exoscope (ORBEYETM) in peripheral nerve sheath tumor surgery: a preliminary, explorative, pilot study. *Oper Neurosurg.* (2020) 19:480–8. doi: 10.1093/ons/opaa090
16. Ahmad FI, Mericli AF, DeFazio MV, Chang EI, Hanasono MM, Pederson WC, et al. Application of the ORBEYE three-dimensional exoscope for microsurgical procedures. *Microsurgery.* (2019) 40:468–72. doi: 10.1002/micr.30547
17. Kanzaki S, Takahashi S, Toda M, Yoshida K, Ogawa K. Pros and cons of the exoscope for otologic surgery. *Surg Innov.* (2021) 28:360–5. doi: 10.1177/1553350620964151
18. Yokoh A, Sugita K, Kobayashi S. Intermittent versus continuous brain retraction. An experimental study. *J Neurosurg.* (1983) 58:918–23. doi: 10.3171/jns.1983.58.6.0918

Conflict of Interest: The authors declare that the research was conducted in the absence of any commercial or financial relationships that could be construed as a potential conflict of interest.

Publisher's Note: All claims expressed in this article are solely those of the authors and do not necessarily represent those of their affiliated organizations, or those of the publisher, the editors and the reviewers. Any product that may be evaluated in this article, or claim that may be made by its manufacturer, is not guaranteed or endorsed by the publisher.

frontiers in Surgery

ORIGINAL RESEARCH
published: 21 March 2022
doi: 10.3389/fsurg.2022.861406

Intraoperative Injection of Normal Saline Through Lumbar Drainage for Transnasal Endoscopic Repair of Complex CSF Leaks

Xiaoming Wei[1,2†], *Fan Zhang*[3†], *Yankai Qiu*[1], *Hong Shen*[1], *Tatiana Ilyasova*[4] and *Li Liu*[1*]

[1] Department of Neurosurgery, The First Affiliated Hospital of Harbin Medical University, Harbin, China, [2] Department of Neurosurgery, First Affiliated Hospital of Yangtze University, Jingzhou, China, [3] Department of Anesthesiology, The First Affiliated Hospital of Harbin Medical University, Harbin, China, [4] Department of Internal Diseases, Bashkir State Medical University, Ufa, Russia

OPEN ACCESS

Edited by:
Ozal Beylerli,
Federal Center of Neurosurgery,
Tyumen, Russia

Reviewed by:
Jiwei Bai,
Capital Medical University, China
Xiaohui Yao,
Shanxi Provincial People's
Hospital, China

***Correspondence:**
Li Liu
h.e2000@hotmail.com

†These authors have contributed equally to this work

Specialty section:
This article was submitted to
Neurosurgery,
a section of the journal
Frontiers in Surgery

Received: 24 January 2022
Accepted: 10 February 2022
Published: 21 March 2022

Citation:
Wei X, Zhang F, Qiu Y, Shen H, Ilyasova T and Liu L (2022) Intraoperative Injection of Normal Saline Through Lumbar Drainage for Transnasal Endoscopic Repair of Complex CSF Leaks. Front. Surg. 9:861406. doi: 10.3389/fsurg.2022.861406

Objective: It is well known that accurate location of the leak in the operation is crucial for repairing cerebrospinal fluid leakage. The study aims to investigate the application of intraoperative injection of normal saline through lumbar drainage in repairing complex leaks.

Methods: The fistulas of all patients with CSF leak were located by computed tomography cisternography (CTC) or heavy T2 magnetic resonance imaging (MRI) before surgery. Before anesthesia, the patient underwent lumbar drainage implantation, and then 20 ml of normal saline was slowly injected through the lumbar drainage to observe the patient's response. The surgical approach was designed based on the preoperative imaging data. When the operation was near to the suspected fistula, normal saline was injected through lumbar drainage (20 ml each time) to confirm the leak location. After CSF leak repair, saline was injected again to confirm whether the repair was successfully.

Result: Of the 5 patients with complex leaks, 4 cases were repaired by transnasal endoscopy method, and 1 case was repaired by transnasal endoscopy method and epidural method. A total of 7 leaks were found during the operation. During the operation, 40–120 ml of normal saline was injected through lumbar drainage. Cauda equina neuralgia was developed in patients who received 120 ml normal saline, which was relieved by intrathecal injection of dexamethasone. During the follow-up of 3 months, 1 case suffered from brain abscess, which was controlled by vancomycin. There was no recurrence of rhinorrhea.

Conclusion: Intraoperative injection of normal saline through lumbar drainage can not only better expose the complex leak but also check the repair effect of the leak during transnasal endoscopic repair, which is effective and avoids side effects.

Keywords: cerebrospinal fluid leak, normal saline, complex leaks, lumbar drainage, neuroendoscopy

INTRODUCTION

Precise exposure of cerebrospinal fluid (CSF) leaks and intraoperative verification of satisfactory repair are essential for transnasal repair of CSF leaks (1, 2). Although there are methods to find leaks before surgery (3), it is difficult to identify complex leaks (such as multiple leaks, leaks with multiple repair failures, and high-flow leaks) during surgery. Even with the methods of increasing intracranial pressure such as breath holding and compression of the jugular vein during surgery (4, 5), leaks are not well exposed, which often enhances the difficulty of surgery or even causes repair failure. Although preoperative lumbar injection of fluorescein is the exact method for the intraoperative tracing of leaks (6), it is an off-label surgical medication with the potential side effects (7, 8). In our practice, we performed intraoperative tracing of the leak by intraoperative injection of normal saline through lumbar drainage, which can further verify whether the repair is successful. From October 2019 to June 2021, five patients with complex leaks were treated at the Department of Neurosurgery, the First Affiliated Hospital of Harbin Medical University. Intraoperative injection of normal saline through lumbar drainage achieved satisfactory outcomes. The summarized experience is as follows.

METHODS

1. The fistulas of all patients with CSF leak were located by computed tomography cisternography (CTC) or heavy T2 magnetic resonance imaging (MRI) before surgery (9).

2. Before anesthesia, the patient underwent lumbar drainage implantation, and then 20 ml of normal saline was slowly injected through the lumbar drainage to observe the patient's response. If the patient had no obvious discomfort, normal saline was injected into the lumbar cistern during the operation; Otherwise, normal saline injection will not be performed.

3. The surgical approach was designed based on the preoperative imaging data. When the operation was near to the suspected fistula, the fistula was searched with endoscope,0 degree or 30 degree, 4 mm in diameter, and 18 cm in length (Karl Storz GmbH & Co KG, Tuttlingen, Germany), and then normal saline was injected through lumbar drainage (20 ml each time) to confirm the leak location. Using different repair methods, the leakage was repaired mainly by "bath-plug method" and nasal septal mucosal flap (10, 11). After successful repair, saline was injected again to confirm whether the repair was successfully.

RESULT

From October 2019 to June 2021, 5 patients of complex leaks were suffered from injection of normal saline through lumbar drainage. Demographic and clinical data of the patients are listed in **Table 1**. Of the 5 patients, 3 had traumatic CSF rhinorrhea and 2 had spontaneous CSF rhinorrhea. Of the 5 patients with complex leaks, 4 cases were repaired by transnasal endoscopy repair, and 1 case was repaired by transnasal endoscopy repair and epidural repair (**Table 1**). A total of 7 leaks were found during the operation, including 1 in tuberculum sellae of sphenoid sinus, 1 in frontal sinus, 1 in ethmoid plate, 1 in lateral recess of sphenoid sinus and 3 in ethmoid sinus roof. During the operation, 40–120 ml of normal saline was injected through lumbar drainage. Cauda equina neuralgia was developed in patients who received 120 mL normal saline, which was relieved by intrathecal injection of dexamethasone. During the follow-up of 3 months, 1 case presented brain abscess, which was controlled by vancomycin. There was no recurrence of rhinorrhea.

TABLE 1 | Patient information.

Case	Age	Sex	Etiology of leak	Location of leak	Number of operation	Complication
1	35	M	Traumatic	Right tuberculum sellae	3	Cauda equina neuralgia
2	50	F	Spontaneous	Right ethmoid sinus roof	1	-
3	56	M	Traumatic	Right frontal sinus and both ethmoid sinus roofs	1	Brain abscess
4	60	M	Traumatic	Ethmoid plate	1	-
5	30	F	Spontaneous	Lateral recess of sphenoid sinus	1	-

CASE PRESENTATION: CASE 1

Case 1 (shown in **Figure 1**) was a 35-year-old male. The patient had a traffic accident 10 years ago, resulting in skull base fracture and CSF leaks. Five years ago, he had purulent meningitis because of the rhinorrhea, and an anti-inflammatory treatment was carried out followed by craniotomy to repair the leaks. During the surgery, extensive fractures of the anterior fossa floor were observed and repaired with an artificial dura mater. However, intracranial infection occurred due to rhinorrhea both 4 and 2 years ago, and the situations were improved after antibiotic and lumbar drainage treatment. One month ago, he came to our hospital because of rhinorrhea and fever again, and the preoperative CTC examination showed a leak in the right tuberculum sellae of sphenoid sinus. The first transnasal repair showed extensive chronic inflammation of the nasal mucosa and the leak was indeed in the right tuberculum sellae. Due to the large size of the leak, muscle, fascia lata and pedicled nasal septum mucosal flaps were applied to repair the leak after the removal of the sphenoid sinus mucosa. The patient had no recurrence of rhinorrhea. On the 16th day after the surgery, the patient developed fever and rhinorrhea. The second surgery showed infection in the sphenoid sinus and the infected muscle and fascia lata was subsequently removed. The nasal septum mucosal flap was used alone to repair the leak. After the surgery, the patient had no fever or intracranial infection but there was intermittent rhinorrhea. Thus, reoperation was performed 18 days after the second surgery, during which, 100 mL of normal saline was injected through lumbar drainage to further clarify that the CSF leak was located in the right tuberculum sellae. The fascia lata was inserted into the leak using the "bath-plug method" (10). After the successful repair, 20 mL of normal saline was injected into the lumbar cistern to verify whether the repair is satisfactory, and a larger fascia was further applied to the outside of the inserted fascia (**Supplementary Video 1**). After awakening from anesthesia, the patient developed a cauda equina irritation sign, which was relieved after intrathecal injection of dexamethasone. During the 3-month follow-up, there was no recurrence of rhinorrhea.

CASE PRESENTATION: CASE 2

Case 2 (shown in **Figure 2**) was a 50-year-old female with spontaneous rhinorrhea and a previous history of breast cancer. After admission, lumbar drainage was performed, and the patient still had massive rhinorrhea. Thus, it was considered to be a "high-flow" leak. Endoscopic exploration of the leak showed significant mucosal edema, which seemed to "disappear" after the removal of the mucosa. 20 mL of normal saline was injected through lumbar drainage, which showed that the leak was "needle-like" in size. The leak was filled using muscle and fascia followed by injecting 20 mL of normal saline to verify whether the repair is satisfactory before packing and fixation. During the 2-month follow-up, there was no recurrence of rhinorrhea.

CASE PRESENTATION: CASE 3

Case 3 (shown in **Figure 3**) was a 56-year-old male. He was admitted because of traumatic rhinorrhea. Preoperative CTC showed three suspected leaks: leaks in the right frontal sinus and both ethmoid sinus roofs. Both ethmoid sinus roofs leaks were confirmed during the surgery. The encephaloceles were observed in both ethmoid sinus roofs. The right frontal sinus was demonstrated to be a leak by further injection of saline. When injection saline, the CSF leak was founded, otherwise there was no CSF leak (**Supplementary Video 2**). The encephaloceles were removed and the leaks were subsequently repaired. The skull defect of the right ethmoid sinus was found to be large, and the two ethmoid sinus roof defect was successfully repaired using thigh adipose tissue and fascia lata followed by injecting 20 mL of normal saline to check the repair. The frontal sinus leak was then repaired by epidural method to close the right frontal sinus by muscle. More than 1 month after discharge, the patient had a brain abscess but no rhinorrhea, which was controlled by vancomycin.

DISCUSSION

Shortcomings of Preoperative Leak Location

There are many methods to locate the leak preoperatively, but whether the imaging method is the most efficient remains undetermined. Eljazzar et al. (12) recommended CT combined with MRI to locate the leak after reviewing numerous literature. The preferred method in our center is the CTC combined with three-dimensional fast-imaging employing steady-state acquisition (3D-FIESTA), which has achieved good results in practical applications. However, during the surgery, we found it difficult to discover some leaks due to abnormal anatomy (traumatic lead) and multiple leaks, which we called complex leaks. To further identify the leaks intraoperatively, the previously commonly used methods are intrathecal fluorescein injection, breath holding, and compression of the jugular vein to increase intracranial pressure. There is no doubt about the role of intrathecal fluorescein injection in further locating the leaks during surgery, but it is off-label use (13), and the consequences are unacceptble once complications occur; intraoperative compression of the jugular vein and breath holding can be used to assist in locating the leaks, but the effect is not significant. So, the above methods limit the further identification of complex leaks. Therefore, how to identify these complex leaks faster and more accurately is particularly important.

Intraoperative Injection of Normal Saline Through Lumbar Drainage

Our experience with the CTC is as follows (9). When the rhinorrhea is not obvious, intrathecal injection of contrast agent followed by injection of 10–20 mL of normal saline can make the patient develop rhinorrhea, achieving the purpose of increasing CTC sensitivity. We assume that the leaks can be exposed intraoperatively by directly increasing the volume of CSF and increasing intracranial pressure with a similar method. It has been reported in the literature that intraoperative injection of normal saline helps fluorescein identify leaks that are more difficult to expose (1, 10). Therefore, we used this method for intraoperative exposure of complex leaks, achieving full exposure and satisfactory repair. However, there is no uniform standard for how much normal saline to inject. It has been reported to be 10–60 mL by Xie et al. (1) and 40–140 mL by Wormald et al. (10). During our surgery of Case 1, 100 mL of saline was injected to fully expose the leak with an abnormal anatomical structure and then 20 mL of saline was injected again to check the repair, with a total of volume of 120 mL. But after awakening from anesthesia, the patient developed cauda equina neuralgia, which was relieved after intrathecal injection of dexamethasone. It is believed that the patient developed this symptom possibly because of excessive saline injection. The treatment experience is as follows: inject 20 mL of normal saline before anesthesia to determine whether there is rhinorrhea and determine the dose of normal saline that needs to be injected at one time during surgery; meanwhile, observe whether there are symptoms of cauda equina stimulation. If yes, the injection of normal saline through lumbar drainage should be slow and the total amount should be small. The symptoms of cauda equina stimulation can be relieved by injecting a small amount of dexamethasone after surgery. In the Case 2, the

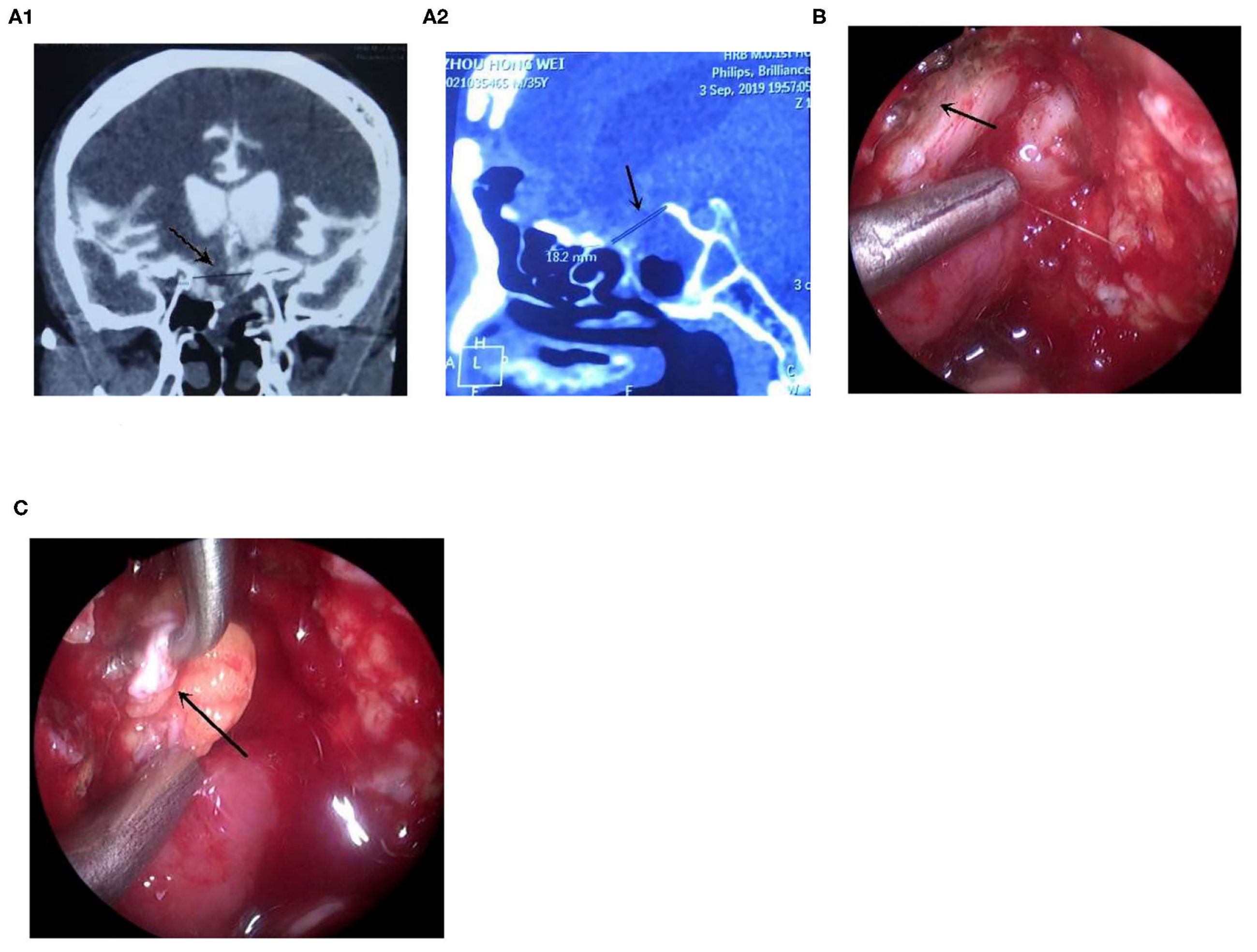

FIGURE 1 | The leak with multiple repair failures was repaired endoscopically. **(A)** The CTC examination showed that the leak was located in the right tuberculum sellae, **(A1)** the coronal CT, **(A2)** the sagittal CT, arrow showed the leak; **(B)** Adequate exposure of the leak after injection of saline; arrow showed the leak. **(C)** The fascia was plugged into the leak using the "bath-plug method," arrow showed the fascia (**Supplementary Video 1**).

intraoperative exploration of the skull base, the skull base did not appear to be abnormal, and CSF flowed from the "needle-like" sized leak only after the injection of saline for repair. A total of 40 mL of saline was injected, and there were no postoperative complications. In the other cases, a total of 40–60 mL of saline was injected to expose the leaks adequately without associated complications.

Compared With Injection of the Fluorescent Agent

We applied the injection of saline through lumbar drainage in the repair of complex CSF leaks. For example, in the case of high-flow leaks or leaks with large defect (more than 1 cm) (14), multiple leaks, and leaks failed to be repaired initially, it is not only possible to find the leaks, but also verify whether the intraoperative repair is satisfactory.

The injection of the fluorescent agent through lumbar drainage is conducted before the start of transnasal endoscopic surgery, so the fluorescent agent can be found when entering the nasal cavity and CSF leaks can be found with the prompt of the fluorescent agent (15, 16). At present, due to preoperative CT cisternography, the accuracy of non-interval magnetic resonance scanning with heavy T2 in judging CSF leaks can reach 95%. Most of the surgeons can determine the initial location of the leak, so it is of little significance to inject the fluorescent contrast agent preoperatively to achieve the detection of the fluorescent contrast agent when entering the nasal cavity.

In our initial detection of the location of the leak and management of structures such as the mucosa around the leak, extensive removal of skull base soft tissue had the risk of further aggravating rhinorrhea due to the patient's

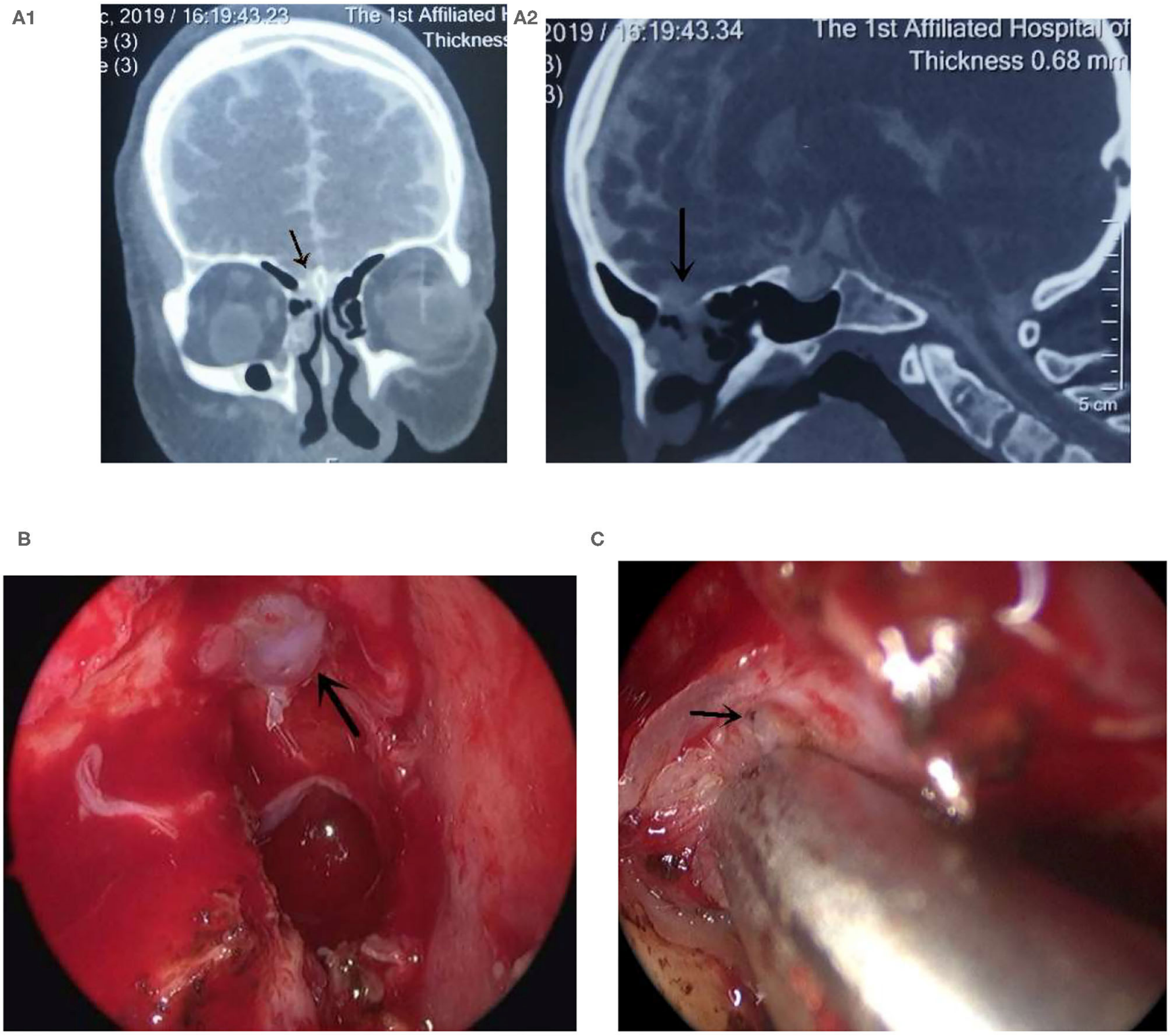

FIGURE 2 | The high-flow leak was repaired endoscopically. **(A)** The CTC examination showed that the leak was located in the right ethmoid pate, **(A1)** the coronal CT, **(A2)** the sagittal CT, arrow showed the leak; **(B)** Arrow showed the edematous mucosa; **(C)** Exposed "pinpoint" leak after the injection of saline through lumbar drainage indicated by the arrow.

extensive skull base defects in Case 1. We only injected normal saline in this case to identify the exact location of the CSF leak, then further injected normal saline after the repair procedure to verify the accuracy of the repair procedure. When multiple leaks were suspected preoperatively, the mucosa around the leak was surgically treated, and the already found leak could not be easily identified due to the patient's reduced cranial pressure. It is very easy for us to identify the leak with certainty by injecting normal saline intraoperatively as in case 3.

We believe that intraoperative injection of normal saline through lumbar drainage is effective and avoids side effects such as spinal cord injury caused by the injection of fluorescent agents through lumbar drainage.

In summary, we believe that the injection of normal saline through lumbar drainage during transnasal endoscopic repair of rhinorrhea, which not only better exposes complex leaks but also verifies the repair effect. However, the sample size in this study is small, which needs to be enlarged to further investigate the advantages and disadvantages.

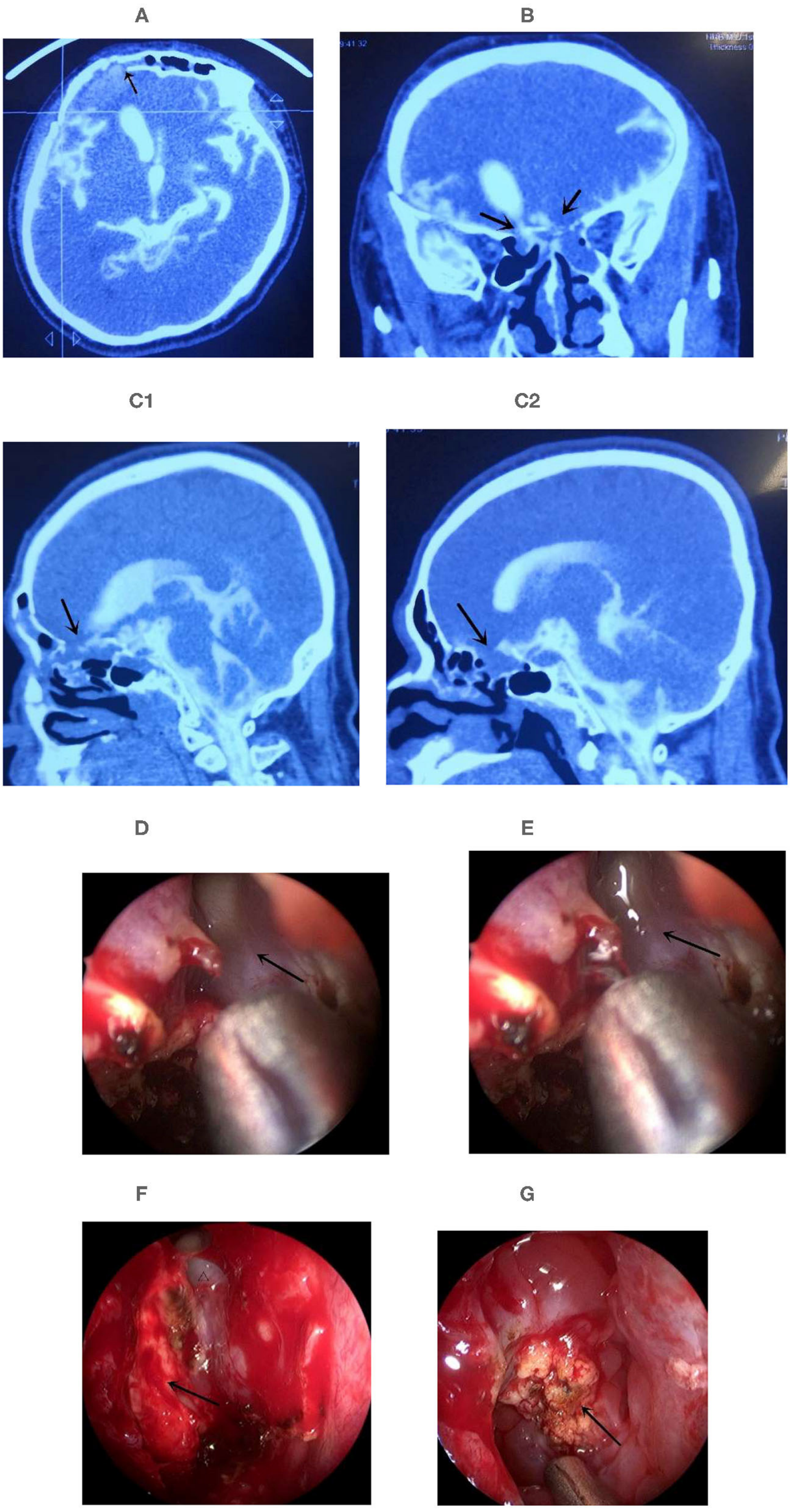

FIGURE 3 | Multiple leaks were repaired by transnasal endoscopy combined with the epidural approach. **(A–C)** The CTC examination located the leaks before surgery. **(A)** The leak was in the right frontal sinus; **(B)** The leak was located in the both ethmoid sinus roofs of the coronal CT. **(C1)** Sagital CT of right ethmoid, **(C2)** Sagital CT of left ethmoid. Arrow show the suspected leak. **(D)** No CSF leak in the right frontal sinus, arrow show the orifice of frontal sinus. **(E)** CSF leak was found in the right frontal sinus when intraoperative injection of 40 mL normal saline through lumbar drainage to expose the leak. Arrow show the CSF in the orifice of frontal sinus. **(F)** Encephaloceles in the right ethmoid sinus roof leakage, arrow show the encephaloceles, triangle indicated the orifice of right frontal sinus; **(G)** Encephaloceles in the left ethmoid sinus roof leakage, arrow show the encephaloceles (**Supplementary Video 2**).

DATA AVAILABILITY STATEMENT

The raw data supporting the conclusions of this article will be made available by the authors, without undue reservation.

ETHICS STATEMENT

Ethical review and approval was not required for the study on human participants in accordance with the local legislation and institutional requirements. The patients/participants provided their written informed consent to participate in this study. Written informed consent was obtained from the individual(s) for the publication of any potentially identifiable images or data included in this article.

AUTHOR CONTRIBUTIONS

XW, FZ, and LL contributed to conception and design of the study. YQ and HS organized the database. TI wrote section of the manuscript. All authors contributed to manuscript revision, read, and approved the submitted version.

FUNDING

This work was supported by Applied Technology Research and Development Program Project of Heilongjiang Provincial Science and Technology Department (GA20C019) and Research Innovation Foundation of First Affiliated Hospital of Harbin Medical University (2020M19).

ACKNOWLEDGMENTS

The authors thank Professor Tianhong Zhang and Professor DaChuan Fan for their instruction of repair of CSF leak.

SUPPLEMENTARY MATERIAL

The Supplementary Material for this article can be found online at: https://www.frontiersin.org/articles/10.3389/fsurg.2022.861406/full#supplementary-material

REFERENCES

1. Xie T, Sun W, Zhang X, Liu T, Ding H, Hu F, et al. The value of 3D-FIESTA MRI in detecting non-iatrogenic cerebrospinal fluid rhinorrhoea: correlations with endoscopic endonasal surgery. *Acta Neurochir.* (2016) 158:2333–9. doi: 10.1007/s00701-016-2988-9
2. Vimala LR, Jasper A, Irodi A. Non-invasive and minimally invasive imaging evaluation of CSF rhinorrhoea - a retrospective study with review of literature. *Pol J Radiol.* (2016) 81:80–5. doi: 10.12659/PJR.895698
3. Le C, Strong EB, Luu Q. Management of Anterior skull base cerebrospinal fluid leaks. *J Neurol Surg B Skull Base.* (2016) 77:404–11. doi: 10.1055/s-0036-1584229
4. Zhou D, Meng R, Zhang X, Guo L, Li S, Wu W, et al. Intracranial hypertension induced by internal jugular vein stenosis can be resolved by stenting. *Eur J Neurol.* (2018) 25:365. doi: 10.1111/ene.13512
5. Godoy DA, Seifi A, Garza D, Lubillo-Montenegro S, Murillo-Cabezas F. Hyperventilation therapy for control of posttraumatic intracranial hypertension. *Front Neurol.* (2017) 8:250. doi: 10.3389/fneur.2017.00250
6. Raza SM, Banu MA, Donaldson A, Patel KS, Anand VK, Schwartz TH, et al. Sensitivity and specificity of intrathecal fluorescein and white light excitation for detecting intraoperative cerebrospinal fluid leak in endoscopic skull base surgery: a prospective study. *J Neurosurg.* (2016) 124:621–6. doi: 10.3171/2014.12.JNS14995
7. Mahaley MS, Odom GL. Complication following intrathecal injection of fluorescein. *J Neurosurg.* (1966) 25:298–9. doi: 10.3171/jns.1966.25.3.0298
8. Wallace JD, Weintraub MI, Mattson RH, Rosnagle R. Status epilepticus as a complication of intrathecal fluorescein case report. *J Neurosurg.* (1972) 36:659–60. doi: 10.3171/jns.1972.36.5.0659
9. Wei XM, Zhang F, Xue YT, Zhang F, Liu L. Application of CT cisternography in locating the fistula of cerebrospinal fluid rhinorrhea. *Chin J Minim Invasive Neurosurg.* (2019) 24:547–51.
10. Wormald PJ, McDonogh M. The bath-plug closure of anterior skull base cerebrospinal fluid leaks. *Am J Rhinol.* (2003) 17:299–305. doi: 10.1177/194589240301700508
11. Hadad G, Bassagasteguy L, Carrau RL, Mataza JC, Kassam A, Snyderman CH, et al. A novel reconstructive technique after endoscopic expanded endonasal approaches: vascular pedicle nasoseptal flap. *Laryngoscope.* (2006) 116:1882–6. doi: 10.1097/01.mlg.0000234933.37779.e4
12. Eljazzar R, Loewenstern J, Dai JB, Shrivastava RK, Iloreta AM. Detection of cerebrospinal fluid leaks: is there a radiologic standard of care? a systematic review. *World Neurosurg.* (2019) 127:307–15. doi: 10.1016/j.wneu.2019.01.299
13. Flynn JP, Pavelonis A, Ledbetter L, Bhalla V, Alvi SA, Chiu AG, et al. The utility of computed tomography and intrathecal fluorescein in the management of cerebrospinal fluid leak. *Am J Rhinol Allergy.* (2020) 34:342–7. doi: 10.1177/1945892419896243
14. Zwagerman NT, Wang EW, Shin SS, Chang Y-F, Fernandez-Miranda JC, Snyderman CH, et al. Does lumbar drainage reduce postoperative cerebrospinal fluid leak after endoscopic endonasal skull base surgery? A prospective, randomized controlled trial. *J Neurosurg.* (2018) 131:1172–78. doi: 10.3171/2018.4.JNS172447
15. Oh J-W, Kim S-H, Whang K. Traumatic cerebrospinal fluid leak: diagnosis and management. *Korean J Neurotrauma.* (2017) 13:63–7. doi: 10.13004/kjnt.2017.13.2.63
16. Jakimovski D, Bonci G, Attia M, Shao H, Hofstetter C, Tsiouris AJ, et al. Incidence and significance of intraoperative cerebrospinal fluid leak in endoscopic pituitary surgery using intrathecal fluorescein. *World Neurosurg.* (2014) 82:e513–23. doi: 10.1016/j.wneu.2013.06.005

Conflict of Interest: The authors declare that the research was conducted in the absence of any commercial or financial relationships that could be construed as a potential conflict of interest.

Publisher's Note: All claims expressed in this article are solely those of the authors and do not necessarily represent those of their affiliated organizations, or those of the publisher, the editors and the reviewers. Any product that may be evaluated in this article, or claim that may be made by its manufacturer, is not guaranteed or endorsed by the publisher.

METHODS
published: 26 May 2022
doi: 10.3389/fsurg.2022.891119

The Guidewire-assisted Drainage Catheter Placement in Chronic Subdural Hematoma

Bingjie Zheng[1‡], Chunlei Wang[1‡], Jinbiao Yao[1], Shiyi Zhu[1], Svetlana Meshcheryakova[2] and Huaizhang Shi[1†]*

[1]Department of Neurosurgery, The First Affiliated Hospital of Harbin Medical University, Harbin, China, [2]Bashkir State Medical University, Republic of Bashkortostan, Ufa, Russia

OPEN ACCESS

Edited by:
Albert Sufianov,
Federal Center of Neurosurgery, Russia

Reviewed by:
Zhifeng Wen,
Shanghai Jiao Tong University, China
Yongxu Wei,
Shanghai Jiao Tong University, China

***Correspondence:**
Huaizhang Shi
shihuaizhang@hrbmu.edu.cn

†Present address:
Huaizhang Shi,
The Department of Neurosurgery, 1st Affiliated Hospital, Harbin Medical University, Harbin, China

‡These authors have contributed equally to this work

Speciality section:
This article was submitted to Neurosurgery, a section of the journal Frontiers in Surgery

Received: 7 March 2022
Accepted: 22 March 2022
Published: 26 May 2022

Citation:
Zheng B, Wang C, Yao J, Zhu S, Meshcheryakova S and Shi H (2022) The Guidewire-assisted Drainage Catheter Placement in Chronic Subdural Hematoma. Front. Surg. 9:891119. doi: 10.3389/fsurg.2022.891119

Background: Chronic subdural hematoma (cSDH) is a common neurosurgical pathology associated with older age. The burr hole drainage is a predominant technique with a lower incidence of recurrence and morbidity. The blind placement of the subdural drain could result in intracerebral hemorrhage. This paper describes a simple and reliable technique for drainage catheter placement in cSDH to reduce intracerebral hemorrhage.

Methods: Forty-nine consecutive patients with cSDH were treated with The Guidewire-assisted Drainage Catheter Placement Technique between July 2019 and June 2021. Epidemiological, clinical and radiographical data were collected and reviewed. The operative technique consists of an angular guidewire tip and catheter. Under the navigation of the guidewire, the catheter is inserted into the subdural space and the length of catheter remaining in the subdural space was 4–5 cm. The catheter was tunneled subcutaneously and fixed at the point where it emerged from the scalp.

Results: Forty-nine consecutive patients underwent 55 The Guidewire-assisted Drainage Catheter Placement. The gender distribution was 37 men and 12 women. The mean age was 69.3 years. The patients presented with headache (31 patients), weakness of limbs (28 patients), speech disturbances (7 patients), and Altered behavior (6 patients). Neither intracerebral hemorrhages nor post-operative seizure occurred. Forty-seven patients were improved after the operation. The recurrence occurred in one patient.

Conclusions: The Guidewire-assisted Drainage Catheter Placement Technique is a reliable method for the insertion of a subdural catheter to evacuate of the Chronic Subdural Hematoma, and is associated with an extremely low risk to cortical structures and cerebral veins.

Keywords: guidewire-assisted technique, chronic subdural hematoma, subdural drain, iatrogenic complications, intracranial hemorrhages

INTRODUCTION

Chronic subdural hematoma (cSDH) is common in neurosurgical practice. The annual incidence of cSDH, at 5 per 100,000 in the general population, can increase to 58 per 100,000 in older age groups (>70 years) (1). There has been a steady, increasing incidence of cSDH as a result of prolonged life expectancy in developing countries in recent years (2).

The conventional therapeutic options for the treatment of cSDH include medical and surgical methods. For symptomatic patients with focal neurological deficit, surgical drainage is regarded as the treatment of choice. Three techniques have been described: twist-drill craniostomy, burr-hole craniostomy, and craniotomy. Recent articles state that burr hole drainage is a superior technique when compared to twist-drill craniostomy and craniotomy, due to a lower incidence of recurrence and morbidity (3–5). Therefore, burr-hole craniostomy with drainage has been popularized around the world. However, a seizure and intracerebral hemorrhage may occur peri-operation, which is mainly induced by a traumatic placement of the subdural drain. Pavlov et al. described a serious intracerebral hemorrhage which was induced by an intracranial cathter (6). Schoedel et al. found that the incidence of procedure-related complications, such as acute rebleed, intracranial bleeding and drainage mispositioning, was 3.9% (7). Hassler et al. reported that 77 complications, believed to be related to the surgical intervention, were observed in 376 patients (8). Therefore, avoiding these procedure-related complications is important for the reduction of mortality and morbidity in cSDH.

The present paper describes a guidewire-assisted technique which may minimize the complication risk of injury to cortical structures and cerebral veins, by using a guiding wire.

METHODS

In this retrospective study, we reviewed the data of 49 patients who underwent the guidewire-assisted drainage catheter placement for cSDH from July 2019 to June 2021 at Department of Neurosurgery, The First Affiliated Hospital of Harbin Medical University. This study was approved by the Harbin Medical University ethic committee. Epidemiological, clinical and radiographical data were collected and reviewed. All patient agreed to publication of clinical details and images.

Surgical Technique

The operation was performed under monitored anesthesia care. The patient was placed typically in the lateral position with the affected side up, and the head elevated at 15 degrees. This position could avoid or reduce the incidence of pneumocephalus. A skin linear incision of approximately 3 cm and single burr-hole was made above the superior temporal line, generally near the parietal bulge. Dura mater and the outer membrane of the subdural hematoma was opened and coagulated by bipolar coagulation. The catheter (14F) with the guidewire at an angle (about 135 degrees) was inserted into the bone hole. The length was about 1 cm in the subdural space. This technique ensures the catheter was placed in the hematoma cavity and closed to the inner surface of the bone due to the angle of the tip. Then, with the wire navigation, the catheter was slowly pushed into the subdural space toward a frontal direction. The catheter length remained in the subdural space was 4–5 cm. Then the wire was slowly withdrawn. The catheter was tunneled subcutaneously and fixed at the point where it emerged from the scalp (**Figure 1**). Continuous irrigation was performed with a sterile saline solution at 37°C until the effluent was clear. The subdural space was filled with saline before closing the skin incision to minimize intracranial air collection. The subdural catheter was connected to a drainage system using a sterile technique.

Statistical Analysis

Means, standard deviations, and medians were reported for continuous variables, and percentages were reported for categorical variables. Continuous variables were analyzed with a t-test, categorical variables were analyzed with a Chi-square test, statistical significance was defined as $p < 0.05$. Statistical analysis was performed using the statistical software SPSS (version 25, IBM Corp.).

RESULTS

Demographics, Comorbidities, and Presentation

Forty-nine consecutive patients underwent 55 The Guidewire-assisted Drainage Catheter Placement. There were 6 bilateral and 43 unilateral hematomas. The mean age was 69.3 years.The

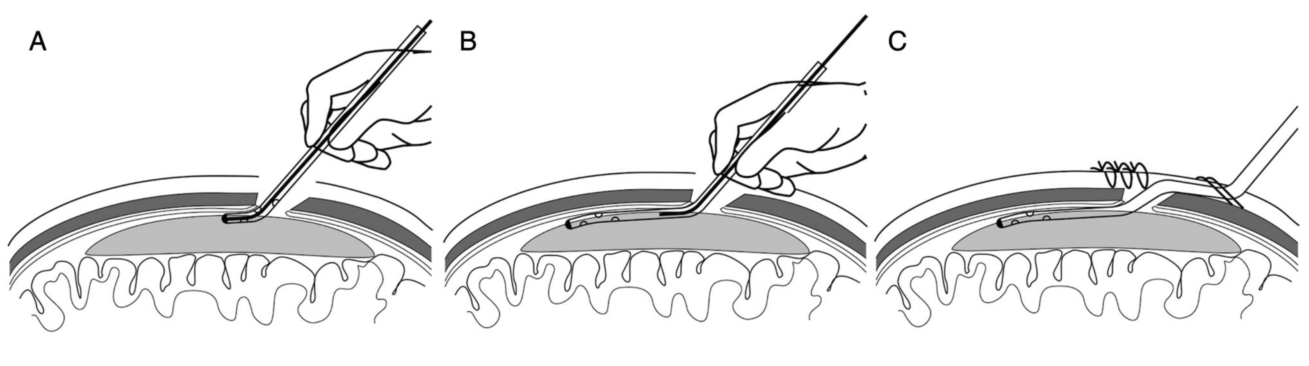

FIGURE 1 | Step-by-step procedure for the guidewire-assisted technique. (**A**) The catheter (14F) with the guidewire at an angle (about 135 degrees) was inserted into the bone hole. (**B**) With the wire navigation, the 4–5 cm catheter was slowly pushed into the subdural space toward the frontal direction. (**C**) The guidewire was slowly withdrawn. The catheter was tunneled subcutaneously and fixed properly.

gender distribution was 37 men and 12 women. The comorbidities included hypertension (34.7%), diabetes mellitus (14.3%) and coronary artery disease (12.2%). The most common presenting symptom was headache which was present in 65.3% of the patients. Other presenting symptoms included weakness of limbs in 28(57.1%), speech disturbances in 7 (14.3%), and Altered behavior in 6(12.2%) the patients (**Table 1**).

Radiological, Clinical Outcomes and Copmplication

Preoperative and Postoperative measurements of hematoma thickness were displayed in **Table 2**. The maximal thickness of hematoma before operation ranged from 1.61–3.61 cm (2.31 ± 0.43 cm). After the evacuation, SDH maximal thickness was decreased to 0.21–2.31 cm (1.08 ± 0.46 cm)($P = 0.000$,). The neurological status at admission was compared with that at the day of hospital discharge. The mean mRS at admission was 2.2. It was 1.0 at discharge ($P = 0.000$,). The neurological status of 45 patients (91.8%) improved after the operation. Neither intracerebral hemorrhages nor post-operative seizure occurred. The recurrence occurred in three patients (6.1%) at 3 months after surgery (**Table 2**).

Case Illustration

A 54-year-old male was referred to our department with a history of progressive right limbs weakness. He had been involved in a motor vehicle accident approximately one month prior. Physical examination revealed hemiparesis of the right arm and leg. The CT scan showed a large, chronic subdural hematomas on the left (**Figure. 2A**). We used the guidewire-assisted drainage catheter placement in this patient. Post-operatively, the patient's hemiparesis improved rapidly. CT scan one day later revealed the subdural hematomas was disappeared nearly (**Figure 2B**). **Figure 2C** showed the guidewire and catheter used in the operation, the guidewire was bent at an angle of 135 degrees.

TABLE 1 | Summary of demographics, comorbidities, and presentation (*N* = 49 patients).

Parameter	Value
Age (Mean, range)	69.3 years, (39–87)
Male (*N*, %)	37 (75.5%)
Hypertension	17 (34.7%)
Diabetes mellitus	7 (14.3%)
Coronary artery disease	6 (12.2%)
Presentation (*N*, %)	
Headache	31 (65.3%)
Weakness of limbs	28 (57.1%)
Speech disturbances	7 (14.3%)
Altered behavior	6 (12.2%)

TABLE 2 | Result of radiological and clinical outcomes (*N* = 49 patients).

	Preop	Postop	*P*
The maximal thickness of hematoma (cm)	2.31 ± 0.43	1.08 ± 0.46	0.000
The mean mRS	2.2	1.0	0.000

Preop, preoperative; Postop, postoperative.

DISCUSSION

We present a retrospective study of 49 patients with a chronic subdural hematoma consecutively treated with a technique that we have not found reported previously. The guidewire-assisted technique may minimize the complication risk of injury to cortical structures and cerebral veins, by using a guiding wire. It probably could prevent postoperative seizures and severe intracranial hemorrhages.

cSDH is a common neurological condition that usually affects the elderly. At present, burr-hole surgery with a subdural closed-drainage system is the most commonly chosen strategy (9). Level 1 evidence also suggests the placement of a closed subdural drainage system at the time of burr hole evacuation can reduce symptomatic recurrence (4). However, A seizure and intracerebral hemorrhage are the frequent complications which could be a result of blind placement of the subdural drainage system (6, 8). Levin häNi et al found that among patients with subdural catheter drainage, the probability of epilepsy was 3.2%, and the probability of brain tissue injury was 2.8% (10). Another study from Minna rauhala et al found that the probability of epilepsy was 4.8%, and the probability of intracranial hematoma was 1.7% (11). Either with twist-hole or burr-hole methods, the drainage catheter is usually inserted into the subdural space blindly. Thus, the catheter tip may be placed into the brain parenchyma or injure the vessels on the cerebral surface. In addition, the catheter direction is not under control during insertion, and therefore, it can lead to drainage malpositioning (4). In this study, we demonstrated our 49 patients experiences of guidewire-assisted technique which could not only guide drainage, but also prevent damage the brain and vessel. Our results showed no complications such as postoperative seizures and intracranial hemorrhages occurred.

Various techniques have been described to facilitate placement of the drainage system to avoid the complications mentioned above. Some authors used subperiosteal drainage to treat cSDH. When this was compared to subdural drainage, it was found that subperiosteal drainage produced lower intracerebral hematoma and overall mortality, the surgical infection rate was significantly lower. However, repeat operations were higher than when subdural drainage was used (10, 12–15). Fichtner et al. used a nelaton catheter guard for placement of the subdural drain, to reduce the risk of damaging relevant structures such as cortical tissue or bridging veins. However, manipulation of the nelaton catheter may be difficult and complex. The catheter needs to be introduced into a bone hole, and withdrawn from the other hole (16). Therefore, The best way to place a catheter could be to place it into the subdural space which should avoid injuring the brain parenchyma and vessels, and this method should be easy to perform. The guidewire-assisted technique was safe and effective in our series.

The benefits of our proposed technique include increased catheter control and reduced complications when compared to traditional methods. Our technique is similar to the Seldinger

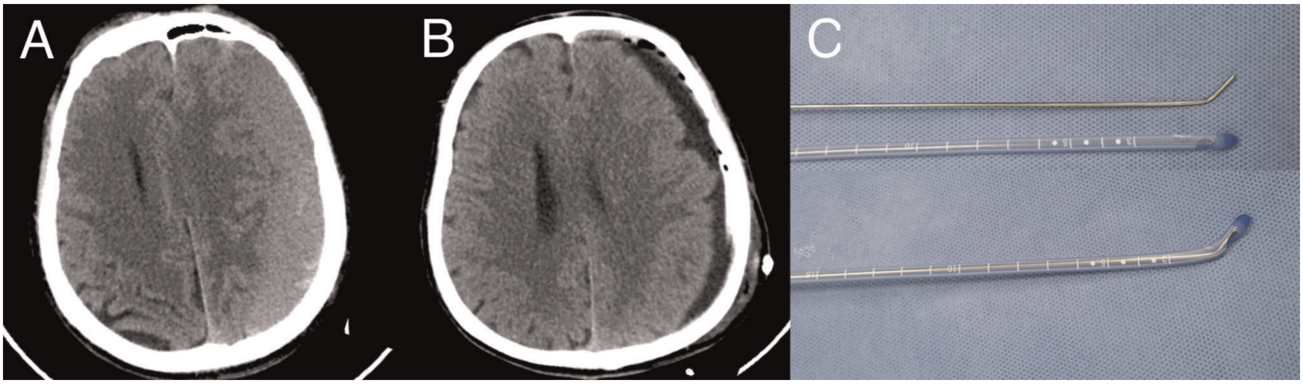

FIGURE 2 | Case illustration. (**A**) The initial CT scan on presentation reveals the left chronic subdural hematoma. (**B**) CT of the head following the placement of drainage demonstrates the almost complete resolution of the left chronic subdural hematoma. (**C**) The guidewire and catheter used in the technique; the guidewire was bent at an angle of 135 degrees.

Technique used in endovascular practice (17). Under guidewire support and navigation, the movement of the tip of the catheter in the subdural space is controlled with greater accuracy. Our guidewire tip is bent and this additional curvature of the wire allows the catheter to be inserted into the subdural space parallel to the surface of the brain, keeping the draining holes in the hematoma. Due to the contact with the hematoma in the subdural space, it is more helpful to drain the hematoma (13). Furthermore, because of the navigation of the wires, the catheters can be successfully implanted into the correct place. In general, the tip of the catheter is toward the frontal direction, as a recent systemic review found, it can reduce the recurrence of subdural hematoma (9). We used the guidewire-assisted technique in forty-nine consecutive patients with chronic SDH. Neither intracerebral hemorrhages nor post-operative seizure occurred and the recurrence only occurred in three patients. The technique described here is a reliable method for the insertion of a subdural catheter and is associated with an extremely low risk to damage cortical structures and cerebral veins.

The length of the catheter in the subdural space is 4–5 cm. A longer length of catheter will possibly damage the cerebrum or vessels at the edge of the hematoma and can induce seizures and intracerebral hemorrhaging. If the length is smaller than 4 cm, because of the stiffness of the catheter, its tip may jump into the brain parenchyma when the hematoma is evacuated rapidly. In addition, the indwelling drainage tube needs to be pushed slowly to prevent damage brain tissue. Meanwhile, attention should be paid to prevent pneumocranium, so as to further prevent recurrence.

Endoscope-assisted evacuation of cSDH is an established, although not widely used, technique. Main advantages of the endoscope-assisted technique are identification of membranes and septations and insertion of a catheter under direct visual control. It results in better placement of catheter in cavity for irrigation and removal of clot and fluid. It was found to be effective for removal of CSDH especially in septate hematomas and multiloculated hematomas (18). However, there needs for special training and the extra equipment (19). Meanwhile, it could increase risk of damage to the cortical surface or membrane due to rigid endoscope or by the rigid suction cannula. The technique described in this paper does not need extra equipment. Furthermore, its simplicity of use, allows for a relatively short learning curve, as seen with junior neurosurgeons. Our technique is associated with an extremely low risk to damage cortical structures and cerebral veins.

The main limitation of this study is that this is a retrospective series. In addition, the mount of patients is low. this may be difficult to get a high level of evidence supporting the use of The Guidewire-assisted Drainage Catheter Placement Technique. Nevertheless, the results suggest that patients with cSDH can benefit from the technique

CONCLUSIONS

The technique described here is a reliable method for the insertion of a subdural catheter and is associated with an extremely low risk of cortical structures and cerebral veins. Additionally, its simplicity of use, allows for a relatively short learning curve, as seen with junior neurosurgeons.

DATA AVAILABILITY STATEMENT

The original contributions presented in the study are included in the article/supplementary material, further inquiries can be directed to the corresponding author/s.

ETHICS STATEMENT

The studies involving human participants were reviewed and approved by This study was approved by the Harbin Medical University Institutional Review Board. Epidemiological, clinical and radiographical data were collected and reviewed. All patient agreed to publication of clinical details and images. The patients/participants provided their written informed consent to participate in this study.

Written informed consent was obtained from the individual (s), and minor(s)' legal guardian/next of kin, for the publication of any potentially identifiable images or data included in this article.

AUTHOR CONTRIBUTIONS

BZ conceptualization, methodology and writing. CW writing (review and editing). JY software, formal analysis. SZ resources, investigation and data curation. HS visualization and supervision. All authors contributed to the article and approved the submitted version.

ACKNOWLEDGEMENTS

We thank International Science Editing (http://www.internationalscienceediting.com) for editing this manuscript.

REFERENCES

1. Kudo H, Kuwamura K, Izawa I, Sawa H, Tamaki N. Chronic subdural hematoma in elderly people: present status on Awaji Island and epidemiological prospect. *Neurol Med Chir (Tokyo)*. (1992) 32:207–9. doi: 10.2176/nmc.32.207
2. Baechli H, Nordmann A, Bucher HC, Gratzl O. Demographics and prevalent risk factors of chronic subdural haematoma: results of a large single-center cohort study. *Neurosurg Rev*. (2004) 27:263–6. doi: 10.1007/s10143-004-0337-6
3. Weigel R, Schmiedek P, Krauss JK. Outcome of contemporary surgery for chronic subdural haematoma: evidence based review. *J Neurol Neurosurg Psychiatry*. (2003) 74:937–43. doi: 10.1136/jnnp.74.7.937
4. Santarius T, Kirkpatrick PJ, Ganesan D, Chia HL, Jalloh I, Smielewski P, et al. Use of drains versus no drains after burr-hole evacuation of chronic subdural haematoma: a randomised controlled trial. *Lancet*. (2009) 374:1067–73. doi: 10.1016/S0140-6736(09)61115-6
5. Lega BC, Danish SF, Malhotra NR, Sonnad SS, Stein SC. Choosing the best operation for chronic subdural hematoma: a decision analysis. *J Neurosurg*. (2010) 113:615–21. doi: 10.3171/2009.9.JNS08825
6. Pavlov V, Bernard G, Chibbaro S. Chronic subdural haematoma management: an iatrogenic complication. Case report and literature review. *BMJ Case Rep*. (2012) 2012:bcr1220115397. doi: 10.1136/bcr.12.2011.5397
7. Schoedel P, Bruendl E, Hochreiter A, Scheitzach J, Bele S, Brawanski A, et al. Restoration of functional integrity after evacuation of chronic subdural hematoma-an age-adjusted analysis of 697 patients. *World Neurosurg*. (2016) 94:465–70. doi: 10.1016/j.wneu.2016.07.027
8. Rohde V, Graf G, Hassler W. Complications of burr-hole craniostomy and closed-system drainage for chronic subdural hematomas: a retrospective analysis of 376 patients. *Neurosurg Rev*. (2002) 25:89–94. doi: 10.1007/s101430100182
9. Brodbelt A, Warnke P. Outcome of contemporary surgery for chronic subdural haematoma: evidence based review. *J Neurol Neurosurg Psychiatry*. (2004) 75:1209–10. doi: 10.1136/jnnp.74.7.937
10. Hani L, Vulcu S, Branca M, Fung C, Z'Graggen WJ, Murek M, et al. Subdural versus subgaleal drainage for chronic subdural hematomas: a post hoc analysis of the TOSCAN trial. *J Neurosurg*. (2019) 30:1–9. doi: 10.3171/2019.5.JNS19858
11. Rauhala M, Helen P, Huhtala H, Heikkila P, Iverson GL, Niskakangas T, et al. Chronic subdural hematoma-incidence, complications, and financial impact. *Acta Neurochir (Wien)*. (2020) 162:2033–43. doi: 10.1007/s00701-020-04398-3
12. Zumofen D, Regli L, Levivier M, Krayenbuhl N. Chronic subdural hematomas treated by burr hole trepanation and a subperiostal drainage system. *Neurosurgery*. (2009) 64:1116–21. doi: 10.1227/01.NEU.0000345633.45961.BB.
13. Bellut D, Woernle CM, Burkhardt JK, Kockro RA, Bertalanffy H, Krayenbuhl N. Subdural drainage versus subperiosteal drainage in burr-hole trepanation for symptomatic chronic subdural hematomas. *World Neurosurg*. (2012) 77:111–8. doi: 10.1016/j.wneu.2011.05.036
14. Soleman J, Lutz K, Schaedelin S, Kamenova M, Guzman R, Mariani L, et al. Subperiosteal vs subdural drain after burr-hole drainage of chronic subdural hematoma: a randomized clinical trial (cSDH-Drain-Trial). *Neurosurgery*. (2019) 85:E825–34. doi: 10.1093/neuros/nyz095
15. Zhang JJY, Wang S, Foo ASC, Yang M, Quah BL, Sun IS, et al. Outcomes of subdural versus subperiosteal drain after burr-hole evacuation of chronic subdural hematoma: a multicenter cohort study. *World Neurosurg*. (2019) 131:e392–e401. doi: 10.1016/j.wneu.2019.07.168
16. Fichtner J, Beck J, Raabe A, Stieglitz LH. The nelaton catheter guard for safe and effective placement of subdural drain for two-burr-hole trephination in chronic subdural hematoma: a technical note. *J Neurol Surg A Cent Eur Neurosurg*. (2015) 76:415–7. doi: 10.1055/s-0034-1396435
17. Seldinger SI. Catheter replacement of the needle in percutaneous arteriography. A new technique. *Acta Radiol Suppl (Stockholm)*. (2008) 434:47–52. doi: 10.1080/02841850802133386
18. Yadav YR, Ratre S, Parihar V, Bajaj J, Sinha M, Kumar A. Endoscopic management of chronic subdural hematoma. *J Neurol Surg A Cent Eur Neurosurg*. (2020) 81:330–41. doi: 10.1055/s-0039-1698388
19. Majovsky M, Masopust V, Netuka D, Benes V. Flexible endoscope-assisted evacuation of chronic subdural hematomas. *Acta Neurochir (Wien)*. (2016) 158:1987–92. doi: 10.1007/s00701-016-2902-5

Conflict of Interest: The authors declare that the research was conducted in the absence of any commercial or financial relationships that could be construed as a potential conflict of interest.

frontiers | Frontiers in Surgery

ORIGINAL RESEARCH
published: 18 April 2022
doi: 10.3389/fsurg.2022.887249

Multiparametric MR Imaging Features of Primary CNS Lymphomas

Rustam Talybov[1], Ozal Beylerli[1], Vadim Mochalov[1], Alexey Prokopenko[1], Tatiana Ilyasova[2], Tatiana Trofimova[3], Albert Sufianov[1,4] and Yang Guang[5,6]**

[1] Federal Center of Neurosurgery, Tyumen, Russia, [2] Bashkir State Medical University, Ufa, Russia, [3] V.M. Bekhterev Psychoneurological Research Institute, St. Petersburg, Russia, [4] Department of Neurosurgery, Sechenov First Moscow State Medical University (Sechenov University), Moscow, Russia, [5] Department of Neurosurgery, The First Affiliated Hospital of Harbin Medical University, Harbin, China, [6] Institute of Brain Science, Harbin Medical University, Harbin, China

OPEN ACCESS

Edited by:
Francesco Certo, Neurological Surgery Unit University of Catania, Italy

Reviewed by:
Галина (Galina) Доровских (Dorovskikh), Омский государственный медицинский университет Омск, Russia
Andrey Tulupov, International Tomography Center (RAS), Russia

***Correspondence:**
Yang Guang
yangguang1227@163.com
Albert Sufianov
sufianov@gmail.com

Specialty section:
This article was submitted to Neurosurgery, a section of the journal Frontiers in Surgery

Received: *01 March 2022*
Accepted: *18 March 2022*
Published: *18 April 2022*

Citation:
Talybov R, Beylerli O, Mochalov V, Prokopenko A, Ilyasova T, Trofimova T, Sufianov A and Guang Y (2022) Multiparametric MR Imaging Features of Primary CNS Lymphomas. Front. Surg. 9:887249. doi: 10.3389/fsurg.2022.887249

Objective: Primary central nervous system lymphomas (PCNS) are relatively rare tumors, accounting for about 4% of all brain tumors. On neuroimaging, they are characterized by a low MR signal in T1, isointense in T2, bright uniform contrast enhancement, and diffusion restriction. The aim of this study is to note the lack of effectiveness of the MR/CT perfusion technique in complex multiparametric imaging in the differential diagnosis of primary lymphomas of the central nervous system in comparison with highly malignant gliomas and brain metastases.

Materials and Methods: This prospective study included 80 patients with CNS tumors examined/operated at the Federal Center for Neurosurgery (Tyumen, Russia) from 2018 to 2021. The patients were divided into 4 groups: group 1 consisted of 33 cases with primary CNS lymphomas (10 cases with atypical manifestations according to perfusion parameters and 23 cases of classic CNS lymphomas), group 2 with anaplastic astrocytomas—14 cases, group 3—23 cases with glioblastomas and group 4—10 cases with solitary metastatic lesions. The study was carried out on a General Electric Discovery W750 3T magnetic resonance tomograph, a Canon Aquilion One multispiral X-ray computed tomograph (Gadovist 7.5 ml, Yomeron 400 mg–50 ml). Additionally, immunohistochemical analysis was carried out with the following markers: CD3, CD20, CD34, Ki-67, VEGF.

Results: It has been established that MR/CT perfusion is not a highly sensitive method for visualizing primary CNS lymphomas, as previously thought, but at the same time, the method has a number of undeniable advantages that make it indispensable in the algorithm of a complex multiparametric diagnostic approach for this type of tumor. Nevertheless, PLCNS is characterized by an atypical manifestation, which is an exception to the rule.

Conclusions: The possibilities of neuroimaging of primary lymphomas, even with the use of improved techniques for collecting MR/CT data, are limited and do not always allow reliable differentiation from other neoplasms.

Keywords: CT, MRI, neuroradiology, perfusion, PCNSL

INTRODUCTION

Lymphomas of the central nervous system are divided into two subgroups: primary and secondary. Primary central nervous system lymphomas (PCNSL) are relatively rare, usually highly malignant tumors with an average lifespan of up to 30 months. Even less common are low-grade primary lymphomas, which have an indeterminate incidence. Secondary lymphomas are caused by the spread of a systemic lesion that originated outside the central nervous system, as part of its progression or as an isolated recurrence. The frequency of occurrence strictly depends on the histological subtype (1–4). There are difficulties in making a diagnosis of central nervous system lymphoma with a "standard" Magnetic resonance imaging (MRI) study (1, 2). Classical features with high specificity are found in immunocompetent patients who have not received therapy; in other cases, characteristic semiotics are absent (5) and are often similar to manifestations of highly malignant gliomas. At the same time, the differential diagnosis of these neoplasms is extremely important, since therapy and prognosis have significant differences (2, 6).

PCNSL is characterized by a classic group of signs due to histological features (hypercellularity, high nuclear/cytoplasmic ratio, disintegration of the blood-brain barrier) (7, 8). In immunocompetent patients, the lesion is usually solitary [multifocality occurs in 20–40% (5)] with intraaxial localization [dural lymphoma is a rare subtype (9)]. The changes are located in the periventricular white matter or in the superficial parts of the brain parenchyma (5, 8, 10), the lesion is mainly supratentorial, less often the stem and cerebellum are involved in the process, and rarely the spinal cord (11, 12). Quite typical spread to the contralateral side along the fibers of the corpus callosum, restriction of diffusion [low values on the Apparent diffusion coefficient (ADC) map, lower than malignant gliomas and metastases (8, 13–16)], mild perifocal edema (5, 17), intense and homogeneous accumulation of contrast agent (5, 8). Sometimes there is a pattern of annular contrast (8, 11) or linear contrast enhancement along the perivascular spaces (10, 18). Hemorrhages are rarely visualized (5, 19). Multifocal lesions are more typical for human immunodeficiency virus (HIV)-associated lymphoma (30–80%), often with uneven, peripheral or annular contrast enhancement due to necrotic changes (20–

TABLE 1 | Average absolute (BF, BV) and normalized (BFn, BVn) numerical values of blood flow parameters in tumors depending on histological affiliation.

Type of tumor	BF ± StDev ml/100g/min	BFn ± StDev	BV ± StDev ml/100g/min	BVn ± StDev
Anaplastic astrocytoma	156.25 ± 26.51	3.85 ± 0.62	20.64 ± 4.02	4.5 ± 1.01
Glioblastoma	290.78 ± 16.13	8.69 ± 1.02	35.61 ± 2.98	8.39 ± 0.73
Metastasis	300.12 ± 25.51	6.75 ± 0.67	37.62 ± 3.97	7.12 ± 1.04
Typical PCNSL	43.11 ± 3.84	1.05 ± 0.05	2.67 ± 0.19	0.92 ± 0.12
Atypical PCNSL	155.7 ± 18.03	4.7 ± 0.45	17.8 ± 1.51	5.9 ± 0.41

StDev, statistical deviation, PCNSL, primary central nervous system lymphoma.

TABLE 2 | Key characteristics of observations of patients with primary cerebral lymphomas.

Age	Male	Number of affected nodes	Localization (subcortical/ periventricular)	ADC values x10-6 mm2/s	Severity of edema	Character contrasting	The presence of hemorrhages	Histological diagnosis	rCBV score vs. normal contralateral white matter (number of times)
32	F	Multiple	Subcortical	450	Pronounced	Homogeneous	No	B-cell lymphoma	×6.0
47	M	Multiple	Subcortical	420	Pronounced	Homogeneous	Yes	B-cell lymphoma	×6.5
53	F	Multiple	Subcortical	457	Moderate	Homogeneous	No	Verification was not carried out	×7.5
55	M	Multiple	Subcortical Periventricular	500	Weak	Homogeneous	No	B-cell lymphoma	×5.0
59	M	Solitary	Periventricular	520	Weak	Homogeneous	No	Verification was not carried out	×5.1
61	F	solitary	periventricular	580	pronounced	homogeneous	No	B-cell lymphoma	×6.2
66	M	Solitary	Subcortical	570	Weak	Homogeneous	No	B-cell lymphoma	×7.0
67	F	Solitary	Subcortical	490	Pronounced	Homogeneous	Yes	B-cell lymphoma	×7.0
67	F	Solitary	Periventricular	500	Moderate	Homogeneous	Yes	B-cell lymphoma	×7.0
71	M	Solitary	Subcortical	539	Pronounced	Homogeneous	No	B-cell lymphoma	×3.0

M, male; F, female; ADC, apparent diffusion coefficient; rCBV, relative cerebral blood volume.

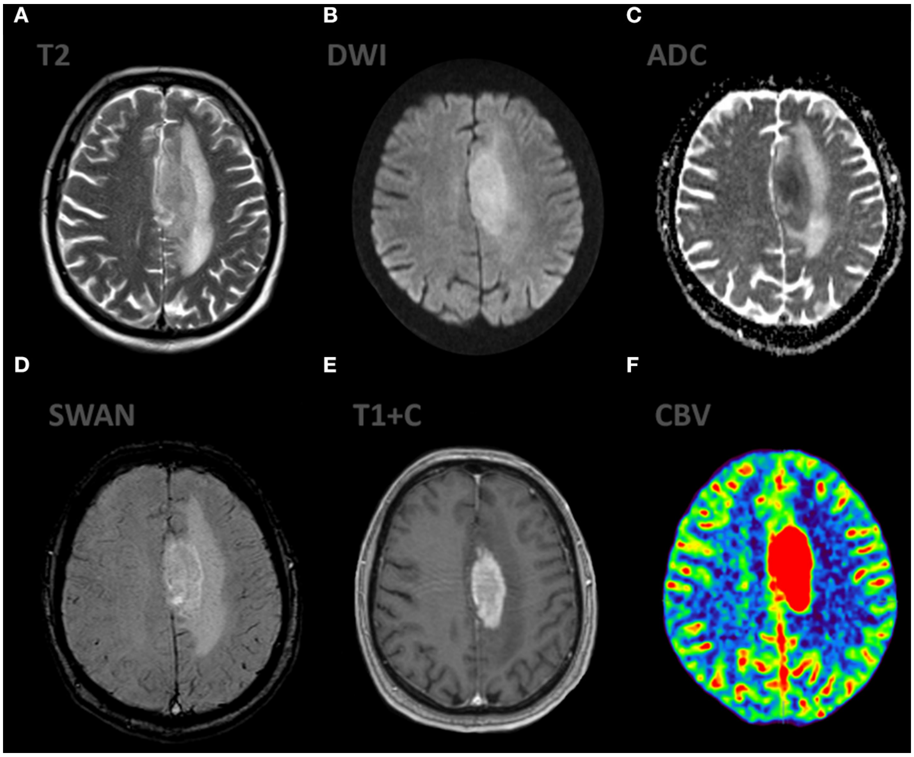

FIGURE 1 | Patient V., male 61 y.o. presented with acute right sided weakness. Axial Brain MRI and CT-perfusion. MRI ax: **(A)** T2WI; 6, **(B)** DWI, **(C)** ADC, **(D)** SWAN, **(E)** T1 + CE. CT ax: **(F)** CT-perfusion (CBV map). There is a well circumscribed mass in the left frontal region with surrounding vasogenic edema on T2WI. The mass has low SI on ADC map indicating high cellular density. The contrast enhancement is bright and uniform. CT-perfusion map shows increased rCBV level.

22). Spontaneous hemorrhages are also more frequently observed in immunocompromised patients (20). Secondary lymphoma is predominantly characterized by leptomeningeal spread in about two-thirds of cases, while intraaxial involvement occurs in only 30% of cases (23). Leptomeningeal metastasis often involves the cisternal portions of the cranial nerves, spinal cord sheaths, and spinal roots (24), which is no different from leptomeningeal processes of any other etiology.

In the context of the correlation between the degree of biological aggression of the tumor and its angiogenic activity, perfusion studies provide valuable information on the delivery of arterial blood to the capillary bed of the tumor tissue, including such parameters as cerebral blood volume (CBV) and cerebral blood flow (CBF) (8, 25–27). Primary lymphomas show low maximum relative CBV values (1, 8, 28–30), which is consistent with histopathological findings indicating the absence of neovascularization (1, 6, 8, 28–30), and is fundamentally different from malignant gliomas or solitary metastases. This finding explains the hypothesis of a lower microvascular density of lymphoma, since neovascularization is not a histological characteristic of PCNSL. In addition, low values of the percentage of signal intensity recovery are noted, also presumably due to massive leakage of the contrast agent into the interstitial space during the passage of the bolus through highly permeable vessels. The latter is explained by the angiocentric nature of growth, in which tumor cells are grouped around already existing brain vessels, inducing their immunoreactive changes (1, 2, 14). There is a known correlation of parameters measured during computed tomography (CT)/MR perfusion with the mitotic index and the degree of malignancy of gliomas. Thus, it has been established that tumor CBV normalized to CBV of the unaltered white matter of the contralateral hemisphere is a biomarker of glioma neoangiogenesis (31). It is believed that improved imaging techniques implemented in multiparametric mapping (mpMRI) can reliably distinguish central nervous system lymphoma from high-grade glioma and metastases (8, 30, 32), but the relationship between perfusion parameters and lymphoma aggression has not been adequately studied.

MATERIALS AND METHODS

The study was approved by the local ethics committee of the Federal Center for Neurosurgery, Tyumen, Russia. Written informed consent for diagnostic manipulations was obtained from all participating patients. The total number of patients with PCNSL, gliomas (Grade 3–4) and MTS who received neurosurgical care in the Department of Neurooncology of the Federal Center for Neurosurgery, Tyumen, Russia. and a pathomorphological conclusion was 80 people (of which 51 were men, 29 were women), their age ranged from 32 to 82 years, mean age was 54 years, median was 58 years. Of these, the diagnosis of PLCNS was made in 33 patients, among whom 10

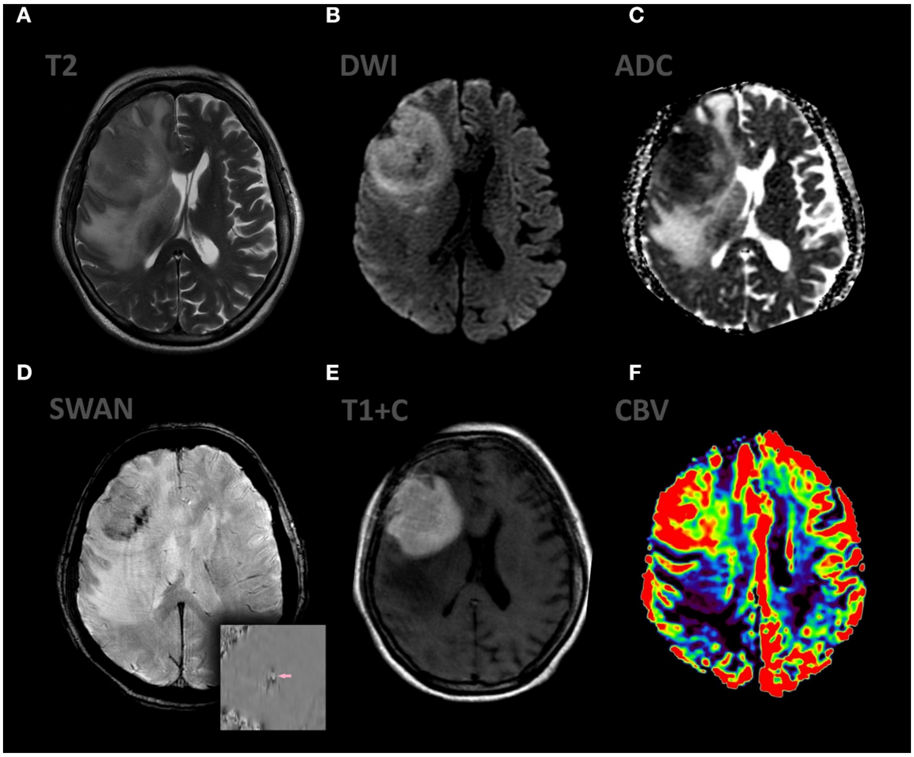

FIGURE 2 | Patient A., female 67 y.o. presented with left sided weakness and altered mental status. MRI ax: **(A)** T2WI; 6, **(B)** DWI, **(C)** ADC, **(D)** SWAN, **(E)** T1 + C, **(F)** DSC-PWI. Axial Brain MRI: there is a large intraaxial mass in right frontal lobe with extensive peritumoral edema on T2WI and mild mass effect. The mass has restricted diffusion and bright, homogeneous contrast enhancement. Most of the tumor exhibits hyperperfusion. SWAN indicates small amounts of hemorrhage.

cases of lymphoma showed atypical signs according to perfusion. Anaplastic astrocytoma (AA) was diagnosed in 14 patients (not otherwise specified (NOS), isocitrate dehydrogenase (IDH) status was not determined), glioblastoma (GB)—in 23 patients (NOS, IDH status was not determined), solitary metastatic lesions (sMTS)—in 10 patients.

Patients with atypical manifestations of PCNSL perfusion made up a group of observations: a total of 10 people, aged from 32 to 71 years. Neurological manifestations differed depending on the localization of the tumor, a combination of motor and sensory disorders, indicating a multifocal lesion. Information on hormone therapy and HIV status was not available.

The results of MRI with contrast and dynamic dynamic susceptibility contrast (DSC-T2*) perfusion, multislice computed tomography (MSCT) with perfusion study were of decisive importance for the diagnosis. MRI was performed on a GE 3T Discovery W750 tomograph using an 8-channel head coil, MSCT was performed on a Canon Aqullion One machine, 640 slices. As a contrast agent in the MR study, the Gadovist paramagnetic was used with a dose calculation of 0.1 ml/kg IV; in the perfusion CT study, Iomeron 400 was used at a dose of 50 ml IV, injected into the cubital vein using an automatic injector with injection rate of 5 ml/s. The perfusion protocol included a dynamic series of CT sections performed every second for 60 s, performed by an interval type of scanning at an X-ray tube voltage of 80 kV and a current-time product of 150 mAc. The total radiation exposure (effective dose) for the entire CT examination was no more than 3–4 mSv. The MR study protocol included the following pulse sequences: gradient echo (T1-weighted images "BRAVO"), spin echo (T2-weighted images), susceptibility-weighted angiography (SWAN), Diffusion-weighted magnetic resonance imaging (DWI) with the construction of maps of the apparent diffusion coefficient (ADC), DSC-T2*. Image post-processing was carried out on GE "Advantage Window 4.5" and "Vitrea Advanced Visualization" graphics stations. Blood flow parameters were assessed using two perfusion maps: CBF—ml/100 g/min; CBV—ml/100 g. To normalize blood flow parameters, region of interest (ROI) was used in the intact white matter of the semioval centers (the value of blood flow in the tumor/value in the intact white matter). The normalized blood flow parameters were calculated as the ratio of the values of the parameters in the area of interest to the intact brain substance. Statistical processing of the obtained results was carried out using the methods of descriptive statistics and correlation analysis.

Eight patients underwent biopsy, of which in six cases the lesion was solitary and in two cases it was multifocal. Stereotactic biopsy was performed using 3D navigation (Brainlab). Verification of the obtained data was carried out using histological and immunohistochemical research methods.

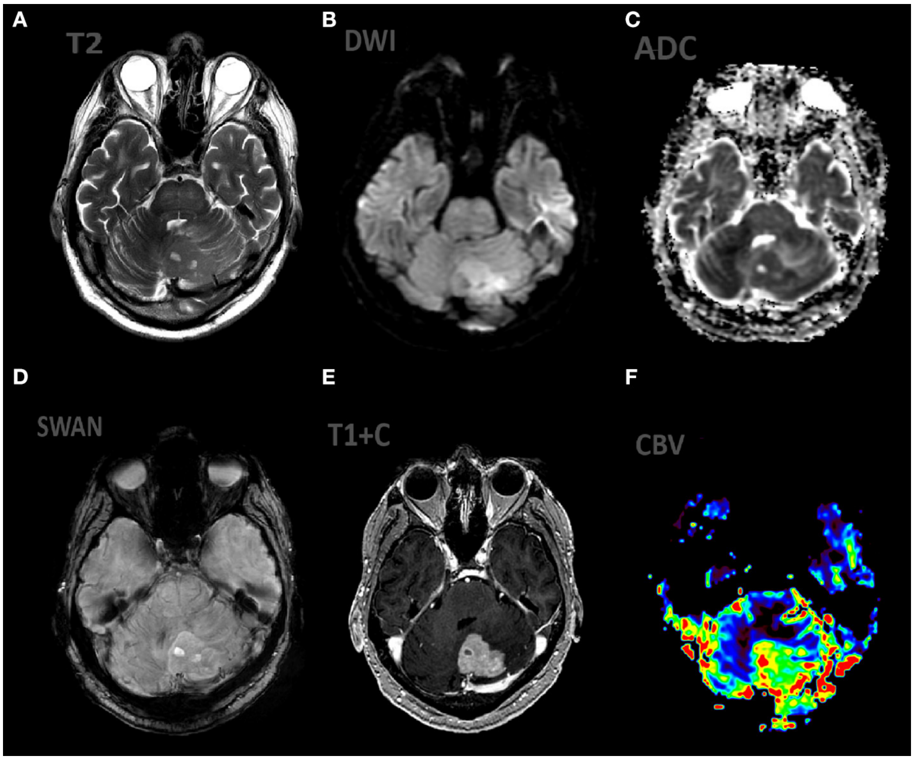

FIGURE 3 | Patient V., male, 66 y.o. presented with gate disturbances. MRI ax: **(A)** T2WI; 6, **(B)** DWI, **(C)** ADC, **(D)** SWAN, **(E)** T1 + C, **(F)** DSC-PWI. Axial Brain MRI: there is lesion in periventricular white matter, the lesion involve left cerebellar peduncle, hemisphere. The lesion demonstrates high SI on T2WI, restricted diffusion (with low ADC values), homogeneous contrast enhancement, elevated rCBV values.

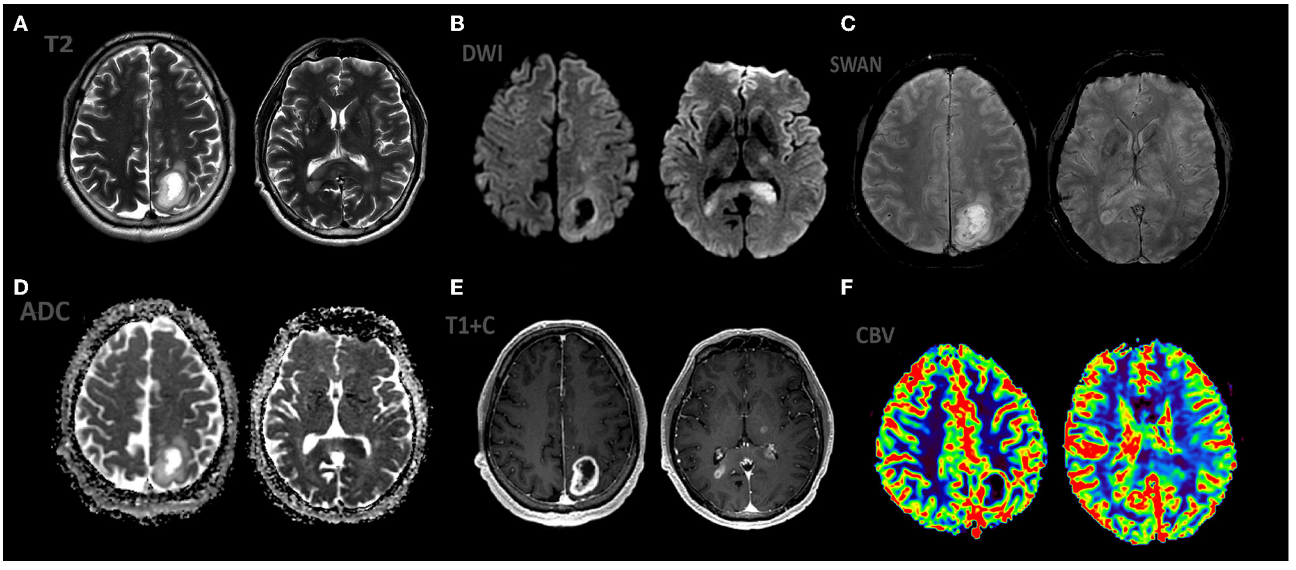

FIGURE 4 | Patient S., male 55 y.o. presented with right sided weakness and memory loss. MRI ax: **(A)** T2WI; 6, **(B)** DWI, **(C)** ADC, **(D)** SWAN, **(E)** T1 + C, **(F)** DSC-PWI. Axial Brain MRI: there is a intraaxial mass in left parietal lobe with low peritumoral edema on T2WI, another mass in the splenium of the corpus callosum and left thalamus. All mass parts have restricted diffusion and bright, homogeneous contrast enhancement and hight rCBV values.

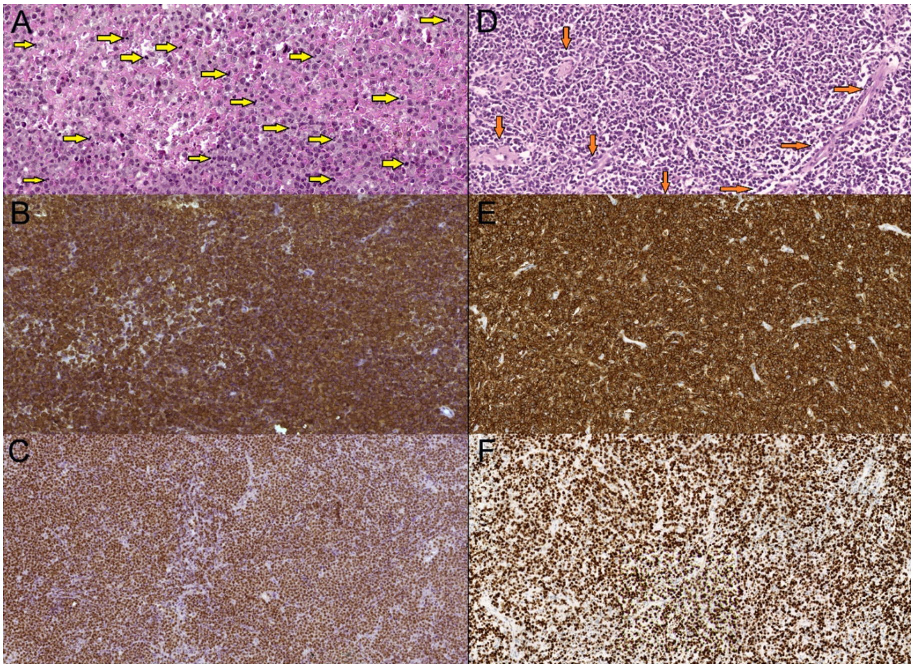

FIGURE 5 | Primary diffuse large cell B-cell CNS lymphomas, mag. x20. **(A,D)**—hematoxilin-eosin stain—hypercellular tumorous tissue with infiltrative growth, cells have centroblasts morphology. Multiple mitoses present (A—yellow arrows), tumorous vessels (D—orange arrows). **(B,E)**—CD20 marker (B-lymphocytic antigen)—prominent membranes CD20+ expression. **(C,F)**—Ki-67 (MIB-1) marker—high proliferation index Ki-67—more than 90%.

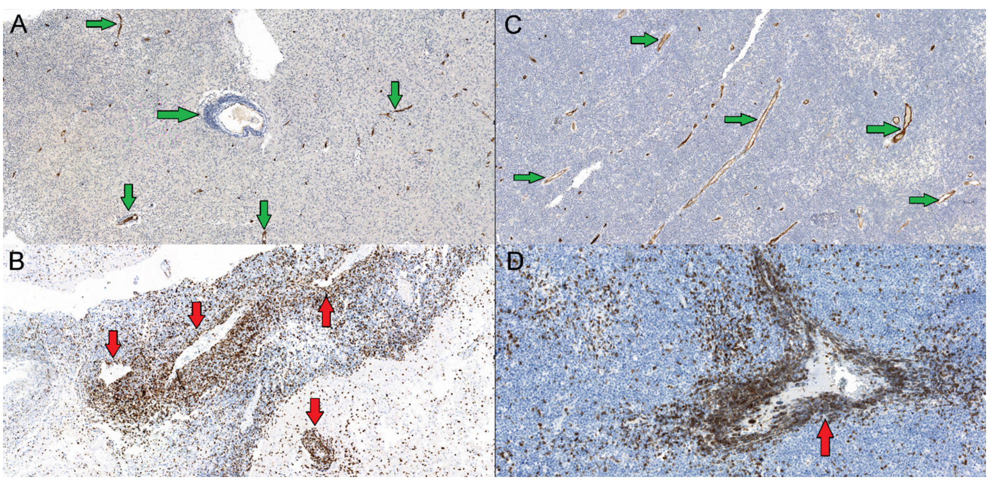

FIGURE 6 | (A,C)—CD34 marker (hematopoetic and endothelial cells progenitor marker)—tumor is vascularised by low caliber capillaries and arterioles, endothelium expresses CD34+ (green arrows), proliferation is scarce. **(B,D)**—CD3 marker (T-cells co-receptor)—more wide vessels locally seen with an impression of an "empty lumen", and abundant perivascularCD3+ T-lymphocytes infiltration caused by vessels walls increased permeability (red allows).

Immunohistochemical analysis included the following range of markers: CD3, CD20, CD34, Ki-67, vascular endothelial growth factor (VEGF).

Taking into account the similar imaging characteristics of PCNS lymphomas with high-grade gliomas (Grade 3–4) and solitary metastatic lesions, a detailed comparative analysis of all tumors was performed using both routine and specialized MR sequences: DWI, SWI or SWAN, dynamic contrasting with the construction of perfusion maps, which form the basis of complex mpMRI.

RESULTS

In the course of the study, an analysis of the MRI and CT perfusion data of 80 patients was performed, followed by the allocation of 4 groups based on the histological diagnosis: group

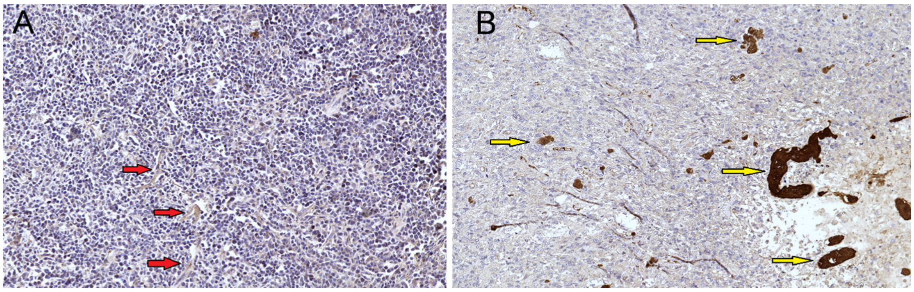

FIGURE 7 | (A) Primary diffuse large cell B-cell CNS lymphomas, mag. ×20. VEGF marker, lymphomas showed no increased expression of VEGF (vascular endothelial growth factor) (red arrows). **(B)** GBM demonstrated expression of VEGF factor (control group) and showed massive antibody expression in proliferating vessels (yellow arrow).

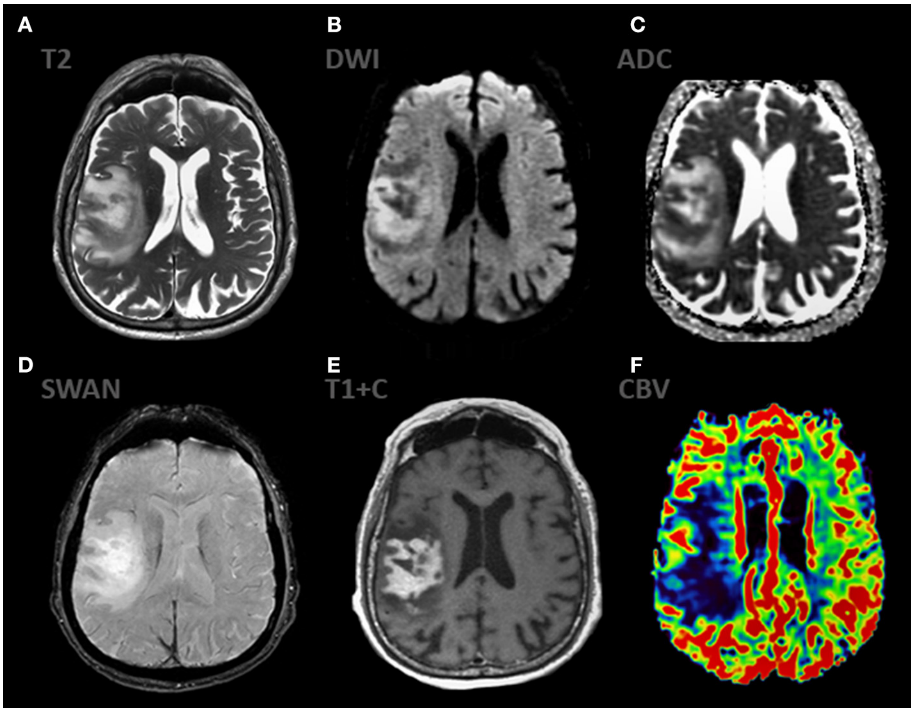

FIGURE 8 | mpMRI ax: **(A)** T2WI; 6, **(B)** DWI, **(C)** ADC, **(D)** SWAN, **(E)** T1 + C, **(F)** DSC-PWI show classic appereance of PCNSL. The mass shows predominantly solid, intense contrast enhancement and has extensive peripheral T2-hyperintensiry. The enhancing component of the lesion demonstrates striking restricted diffusion (ADC 450-490 × 10^{-6} mm^2/s) indicating high cellularity. The mass demonstrates low rCBV values.

1—14 cases with AA, group 2—23 cases with GB, group 3—10 cases with (sMTS) and group 4—33 cases of PLCNS, divided into 2 subgroups: (a) classic—23 cases; (b) atypical—10 cases.

Parameters in group 1: blood flow velocity (BF) in anaplastic astrocytomas ranged from 32.2 to 190.8 ml/100 g/min, blood flow volume (BV)—from 0.53 to 4.79 ml/100 g. The averaged maximum and normalized blood flow values are shown in **Table 1**.

The 2nd group of patients (with GB) was characterized by high absolute and normalized blood flow parameters.

In the 3rd group of patients (with solitary MTS), high rates of CBF and CBV were revealed.

The 4th group of patients (with PLCNS) showed both low (most of them—23 cases) and high (10 atypical cases) values on perfusion maps (**Table 1**).

The results are presented in **Table 2** and **Figures 1–4**.

In the entire group of patients with suspected primary lymphoma, information about HIV status and hormonal therapy was missing. In six cases, the lesion was represented by a solitary tumor node with severe perifocal edema. In four cases, two or more tumor nodes were visualized against the background of edema. In all cases, the changes were characterized by intraaxial localization (periventricular and subcortical), intense and homogeneous contrast enhancement, and low ADC

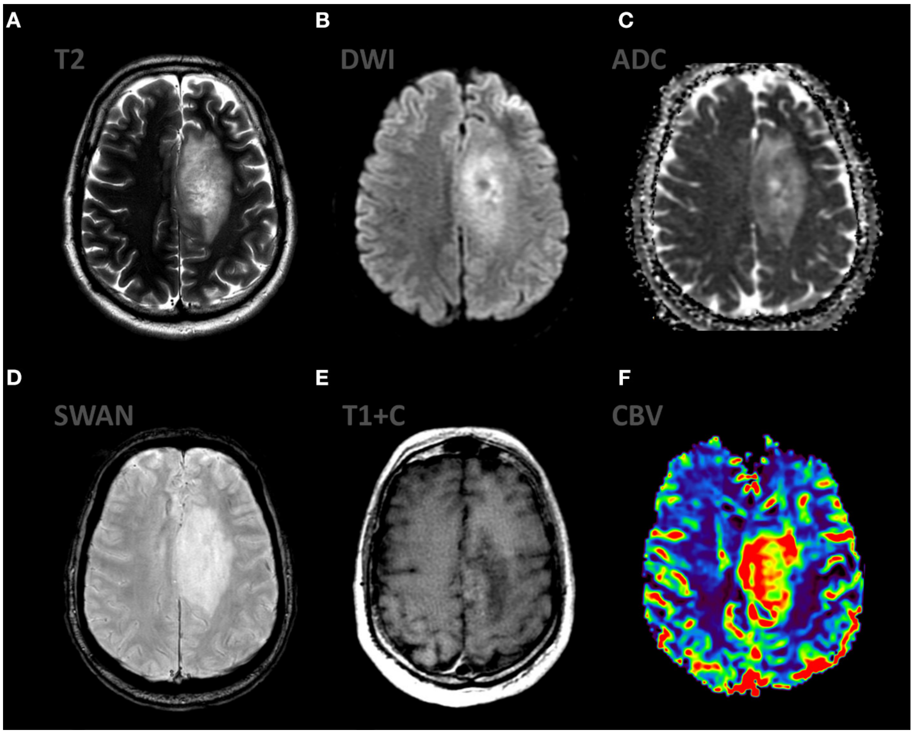

FIGURE 9 | mpMRI ax: **(A)** T2WI; 6, **(B)** DWI, **(C)** ADC, **(D)** SWAN, **(E)** T1 + C, **(F)** DSC-PWI demonstrate the typical appereance of anaplastic astrocytoma (Grade III WHO 2016). There is infiltrative mass in the left frontal region with mild vasogenic edema on T2WI. This mass has low signal on ADC, partial enhancement and high rCBV values.

values. In three cases, hemorrhages were noted. MR DSC and CT perfusion showed hypervascularization with rCBV values ranging from 3.0 to 7.5 times compared to normal white matter.

Histological studies in all these cases revealed hypercellular tumor tissue with infiltrative growth, high mitotic activity and severe perivascular lymphocytic infiltration, increased endothelial permeability. In immunohistological studies, the tumor tissue totally expressed CD20+, the vascular endothelium was brightly stained in reaction to CD34+ and expressed extremely weakly VEGF. T-lymphocytes were positive in reaction with anti-CD3+. The proliferative activity index for Ki-67 was extremely high, over 90%. According to the results of immunohistological studies, lymphoproliferative diseases (primary B-cell lymphoma) were diagnosed (**Figures 5–7**).

DISCUSSION

Undoubtedly, modern qualitative and quantitative imaging tools implemented on CT and MRI cannot compete with invasive techniques in the reliability of determining the histopathological nature of the tumor. Despite this, the main non-invasive method for diagnosing brain tumors is MRI with complex mpMRI mapping (**Figure 8**). The classic imaging manifestations of primary lymphoma of the central nervous system include a group of rather specific criteria according to mpMRI mapping and are as follows: a mass showing a homogeneous and pronounced contrast enhancement, accompanied by moderate perifocal edema, usually without a mass effect, limiting the diffusion of molecules water with low ADC values within 400–600 × 10–6 mm^2/s (0.4–0.6/100mm^3), which has low values of rCBV (1, 26, 29–32). It is generally accepted that, when quantified based on CT and MR perfusion techniques, primary lymphomas show low maximum relative values of rCBV compared with poorly differentiated glial lesions and metastases (1, 8, 28–30, 32).

The differential diagnostic range includes high grade gliomas (anaplastic astrocytoma and glioblastoma) and solitary metastatic lesions (**Figures 9**,**10**).

Malignant gliomas are characterized by an annular contrast pattern with uneven wall thickness, reflecting necrosis ("crown effect"), a combination of vasogenic edema and a non-contrasting infiltrative tumor component, a distinct mass effect, and average values of the ADC in the range of $745 \pm 135 \times 10^{-6}$ mm^2/s (for GBM), within $1{,}067 \pm 276 \times 10^{-6}$ mm^2/s (for AA), elevation of rCBV values by 6.9 ± 3.12 times compared to unchanged white matter, the presence of intratumoral vascular shunts and a low-intensity rim due to the breakdown of products blood test for SWAN (1, 28–33) (**Figure 11**).

sMTS have radiological manifestations similar to those of GBM: a ring-shaped contrasting pattern with a central zone of necrosis, hemorrhage. The differences are the average values of the ADC within $919.4 \pm 200 \times 10^{-6}$ mm^2/s, the absence of a diffuse tumor component in the vasogenic edema and the absence of a tendency to form pathological shunts, which explains the lower perfusion values (1, 28, 30, 32, 34).

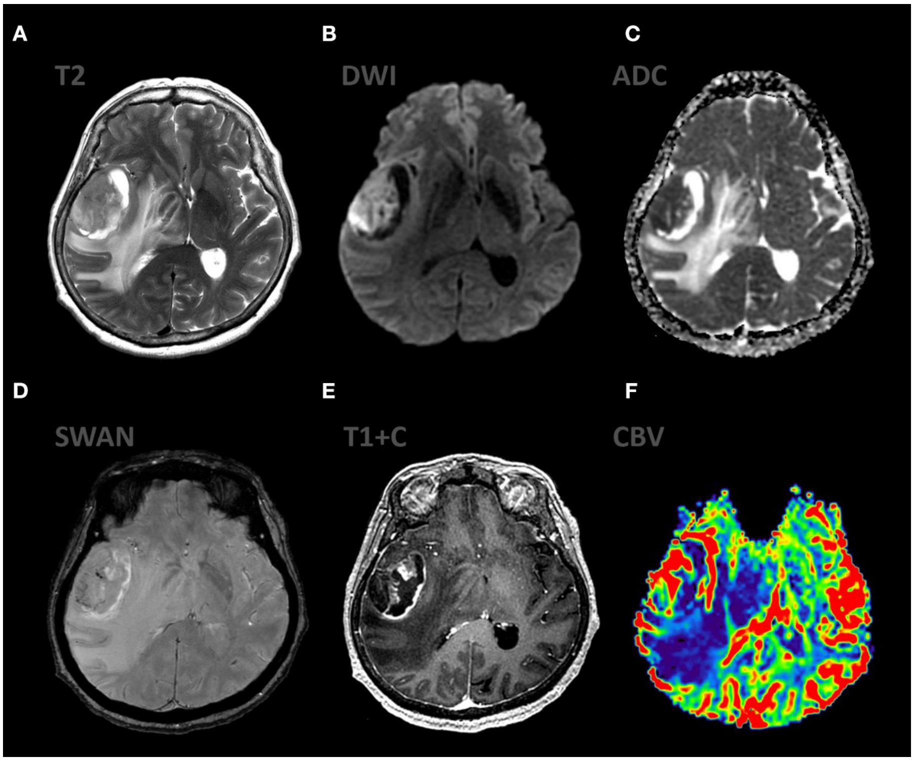

FIGURE 10 | mpMRI ax: **(A)** T2WI; 6, **(B)** DWI, **(C)** ADC, **(D)** SWAN, **(E)** T1 + C, **(F)** DSC-PWI show the classic appereance of GBM (grade IV WHO 2016). The mass shows ring enhancing pattern associated with extensive peripheral T2-hyperintensity and moderate mass effect. The enhancing component of the lesion demonstrates restricted diffusion (ADC 800–900 × 10^{-6} mm^2/s), also the mass shows high values rCBV.

In our studies, all cases of lymphomas corresponded to the classical radiological features (intense and homogeneous contrast enhancement, peritumoral vasogenic edema, and low intratumoral ADC values) except for 10 cases showing hypervascularization with rCBV values that exceeded the values of unchanged white matter by 3.0–7.5 times and hemorrhages that occurred in three cases (see Results), which, according to some authors, is extremely uncharacteristic for the lymphoproliferative process.

PCNS lymphomas may mimic high-grade glioma or metastatic disease, showing a similar morphology and infiltrative growth pattern. High grade gliomas and metastases are distinguished by the presence of neoangiogenesis, the biomarker of which is an increase in rCBV obtained using contrast MR (DSC-T2*) or perfusion CT. Our experience shows that the use of perfusion techniques, which are considered highly sensitive and highly specific for assessing neovascularization, does not always make it possible to distinguish lymphoma from other aggressive brain tumors, since, despite the absence of neoangiogenesis, an increase in rCBV values is often found in PCNS lymphomas, which must be due to some interaction of the tumor with the vasculature of the brain. Instead of forming new ones, PLCNS infiltrates existing vessels. Neoplastic cells proliferate angiocentrically, surround the vessels in a "perivascular cuff" type, and diffusely or in the form of a well-defined front invade the healthy brain parenchyma. In the predominant number of our cases, among PLCNS with hyperperfusion, an increase in rCBV values is observed in a ring-like manner at the periphery of the tumor, where tumor cells interact with the vessels of the unchanged parenchyma.

Analysis of the data obtained from the assessment of immunoreactivity using antibodies to VEGF, CD3, CD20, CD31, CD34 established the absence of signs of neoangiogenesis and the presence of very high values of the proliferative activity index (Ki-67 > 90%), indicating a pronounced biological aggression.

It is noteworthy that against the background of diffuse hemorrhages into the tumor, detected in several patients, there were additional changes in the diameter of capillaries and arterioles according to the type of "vasodilation" with increased wall permeability, which may be due to inflammatory activity, the phase of inflammation or the duration of the process. The data obtained suggest that hyperperfusion of lymphomas is not associated with the activation of neoangiogenesis, as in the cases of glioblastomas and metastases, but is most likely associated with hemodynamic changes in the characteristics of blood vessels. Moreover, increased expression of VEGF (vascular endothelial growth factor) in lymphoma is associated with greater survival (8). Despite a similar increase in rCBV values in our observations, it is not possible to assume the presence of an identical mechanism of vascularization. It is noteworthy that similar mechanisms of an increase in the diameter of blood vessels and an increase in rCBV values, leading to vasodilation,

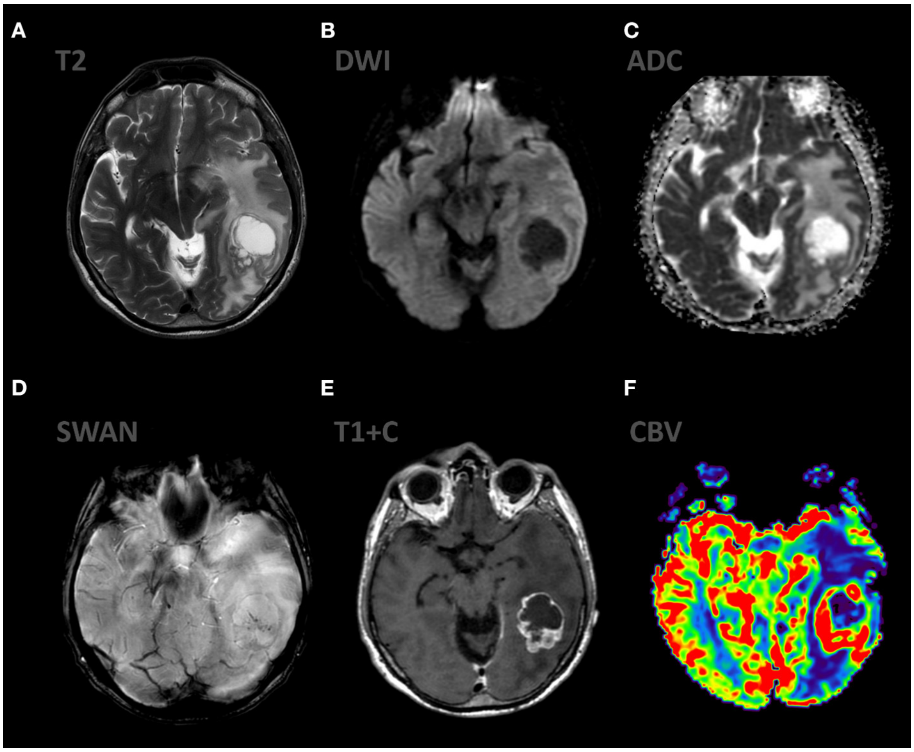

FIGURE 11 | mpMRI ax: **(A)** T2WI; 6, **(B)** DWI, **(C)** ADC, **(D)** SWAN, **(E)** T1 + C, **(F)** DSC-PWI show classic appereance of solitary brain metastasis. There is a lesion with ring-like enhancing pattern and strong peripheral T2-hyperintensiry. Vasogenic edema is out of proportion with tumor size. The enhancing component of the lesion demonstrates high rCBV values.

have been described in multiple sclerosis during the formation of a new acute lesion before the disintegration of the blood-brain barrier or during reactivation of chronic foci (35). Perfusion MR or CT data, which make it difficult to distinguish lymphoma from other aggressive intracerebral tumors, are probably due to the immune response of healthy vessels of the border zone to PLCNS cell invasion and perivascular infiltration (36–38).

CONCLUSIONS

Today, if a neuroradiologist is faced with the task of making a differential diagnosis of intracerebral formations, performing multiparametric MRI mapping is a key condition for obtaining the necessary information about the nature of the tumor. It is generally accepted that knowledge of perfusion parameters (CBV) is critical. However, our study demonstrates the lack of reliability of MR and CT perfusion in cases of PCNS lymphomas. Even mpMRI does not always reliably distinguish lymphoma from other malignant brain tumors (high-grade gliomas and metastases). The use of stereotactic biopsy with histopathological matching remains the "gold" standard in the diagnosis of PCNS lymphomas.

DATA AVAILABILITY STATEMENT

The raw data supporting the conclusions of this article will be made available by the authors, without undue reservation.

ETHICS STATEMENT

Written informed consent was obtained from the individual(s), and minor(s)' legal guardian/next of kin, for the publication of any potentially identifiable images or data included in this article.

AUTHOR CONTRIBUTIONS

RT, TT, and AS: conceptualization. VM, AP, and OB: data curation. OB, AS, TI, and YG: formal analysis. RT: investigation. OB: project administration. RT and TT: resources. OB, RT, and TI: software. AS and TT: supervision. OB, TI, and TT: validation. RT and OB: roles/writing—original draft. RT and YG: writing—review and editing. All authors contributed to the article and approved the submitted version.

REFERENCES

1. Hartmann M, Heiland S, Harting I, Tronnier V, Sommer C, Ludwig R. Distinguishing of primary cerebral lymphoma from high-grade glioma with perfusion-weighted magnetic resonance imaging. *Neurosci Lett.* (2003) 338:119–22. doi: 10.1016/S0304-3940(02)01367-8
2. Hakyemez B, Erdogan C, Bolca N, Yildirim N, Gokalp G, Parlak M. Evaluation of different cerebral mass lesions by perfusion-weighed MR imaging. *J Magn Reson Imaging.* (2006) 24:817–24. doi: 10.1002/jmri.20707
3. Wong ET. Management of central nervous system lymphomas using monoclonal antibodies: challenges and opportunities. *Clin Cancer Res.* (2005) 11:7151s—57s. doi: 10.1158/1078-0432.CCR-1004-0002
4. Mohile NA, Abrey LE. Primary central nervous system lymphoma. *Semin Radiat Oncol.* (2007) 17:223–29. doi: 10.1016/j.semradonc.2007.02.008
5. Haldorsen IS, Krakenes J, Krossnes BK, Mella O, Espeland A, CT. and MR imaging features of primary central nervous system lymphoma in Norway, 1989–2003. *AJNR Am J Neuroradiol.* (2009) 30:744–51. doi: 10.3174/ajnr.A1447
6. Sugahara T, Korogi Y, Shigematsu Y, Hirai T, Ikushima I, Liang L, et al. Perfusion-sensitive MRI of cerebral lymphomas: a preliminary report. *J Comput Assist Tomogr.* (1999) 23:232–7. doi: 10.1097/00004728-199903000-00011
7. Koeller KK, Smirniotopoulos JG, Jones RV. Primary central nervous system lymphoma: radiologic-pathologic correlation. *Radiographics.* (1997) 17:1497–526. doi: 10.1148/radiographics.17.6.9397461
8. Trofimova TN, Savintseva ZHI, Skvortsova TY. Monography: Cerebral Glial Tumors Radiology.(2020).
9. Iwamoto FM, Abrey LE. Primary dural lymphomas: a review. *Neurosurg Focus.* (2006) 21:E5. doi: 10.3171/foc.2006.21.5.6
10. Go JL, Lee SC, Kim PE. Imaging of primary central nervous system lymphoma. *Neurosurg Focus.* (2006) 21:E4. doi: 10.3171/foc.2006.21.5.5
11. Kuker W, Nagele T, Korfel A, Heckl S, Thiel E, Bamberg M, et al. Primary central nervous system lymphomas (PCNSL): MRI features at presentation in 100 patients. *J Neurooncol.* (2005) 72:169–77. doi: 10.1007/s11060-004-3390-7
12. Buhring U, Herrlinger U, Krings T, Thiex R, Weller M, Kuker W, et al. features of primary central nervous system lymphomas at presentation. *Neurology.* (2001) 57:393–96. doi: 10.1212/WNL.57.3.393
13. Senocak E, Oguz KK, Ozgen B, Mut M, Ayhan S, Berker M, et al. Parenchymal lymphoma of the brain on initial MR imaging: a comparative study between primary and secondary brain lymphoma. *Eur J Radiol.* (2010) 57:393–96. doi: 10.1016/j.ejrad.2010.01.017
14. Calli C, Kitis O, Yunten N, Yurtseven T. Perfusion and diffusion MR imaging in enhancing malignant cerebral tumors. *Eur J Radiol.* (2006) 58:394–403. doi: 10.1016/j.ejrad.2005.12.032
15. Zacharia TT, Law M, Naidich TP, Leeds NE. Central nervous system lymphoma characterization by diffusion-weighted imaging and MRspectroscopy. *J Neuroimaging.* (2008) 18:411.17. doi: 10.1111/j.1552-6569.2007.00231.x
16. Schroeder PC, Post MJ, Oschatz E, Stadler A, Bruce-Gregorios J, Thurnher MM. Analysis of the utility of diffusionweighted MRI and apparent diffusion coefficient values in distinguishing central nervous system toxoplasmosis from lymphoma. *Neuroradiology.* (2006) 48:715–20. doi: 10.1007/s00234-006-0123-y
17. Schlegel U, Schmidt-Wolf IG, Deckert M. Primary CNS lymphoma: clinical presentation, pathological classification, molecular pathogenesis and treatment. *J Neurol Sci.* (2000) 181:1–12. doi: 10.1016/S0022-510X(00)00385-3
18. Eichler AF, Batchelor TT. Primary central nervous system lymphoma: presentation, diagnosis and staging. *Neurosurg Focus.* (2006) 21:E15. doi: 10.3171/foc.2006.21.5.16
19. Coulon A, Lafitte F, Hoang-Xuan K, Martin-Duverneuil N, Mokhtari K, Blustajn J, et al. Radiographic findings in 37 cases of primary CNS lymphoma in immunocompetent patients. *Eur Radiol.* (2002) 12:329–40. doi: 10.1007/s003300101037
20. Thurnher MM, Rieger A, Kleibl-Popov C, Settinek U, Henk C, Haberler C, et al. Primary central nervous system lymphoma in AIDS: a wider spectrum of CT and MRI findings. *Neuroradiology.* (2001) 43:29–35. doi: 10.1007/s002340000480
21. Fine HA, Mayer RJ. Primary central nervous system lymphoma. *Ann Intern Med.* (1993) 119:1093–104. doi: 10.7326/0003-4819-119-11-199312010-00007
22. Haldorsen IS, Krakenes J, Goplen AK, Dunlop O, Mella O, Espeland A. AIDS-related primary central nervous system lymphoma: a Norwegian national survey 1989–2003. *BMC Cancer.* (2008) 8:225. doi: 10.1186/1471-2407-8-225
23. Hill QA, Owen RG, CNS. prophylaxis in lymphoma: who to target and what therapy to use. *Blood Rev.* (2006) 20:319–32. doi: 10.1016/j.blre.2006.02.001
24. Bierman P, Giglio P. Diagnosis and treatment of central nervous system involvement in non-Hodgkin's lymphoma. *Hematol Oncol Clin North Am.* (2005) 19:597–609. doi: 10.1016/j.hoc.2005.05.003
25. Wu O, Ostergaard L, Sorensen AG. Technical aspects of perfusion-weighted imaging. *Neuroimaging Clin N Am.* (2005) 15:623–37, xi. doi: 10.1016/j.nic.2005.08.009
26. Cianfoni A, Colosimo C, Basile M, Wintermark M, Bonomo L. Brain perfusion CT: principles, technique and clinical applications. *Radiol Med.* (2007) 112:1225–43. doi: 10.1007/s11547-007-0219-4
27. Fainardi E, Di BF, Borrelli M, Saletti A, Cavallo M, Sarubbo S, et al. Potential role of CT perfusion parameters in the identification of solitary intra-axial brain tumor grading. *Acta Neurochir Suppl.* (2010) 106:283–87. doi: 10.1007/978-3-211-98811-4_53
28. Lee IH, Kim ST, Kim HJ, Kim KH, Jeon P, Byun HS. Analysis of perfusion weighted image of CNS lymphoma. *Eur J Radiol.* (2009). doi: 10.1016/j.ejrad.2009.05.013
29. Kremer S, Grand S, Remy C, Esteve F, Lefournier V, Pasquire B, et al. Cerebral blood volume mapping by MR imaging in the initial evaluation of brain tumors. *J Neuroradiol.* (2002) 29:105–13.
30. Savintseva ZHI, Skvortsova TY, Trofimova TN, Gurchin AF, Smirnov AV. Differentiation between brain tumor recurrence and radiation injury using diffusion-weighted imaging and perfusion magnetic resonance imaging. *Folia. Neuropathol.* (2015) 48:81–92. doi: 10.22328/2079-5343-2015-4-27-34
31. Law M, Yang S, Babb JS, Knopp EA, Golfinos JG, Zagzag D, et al. Comparison of cerebral blood volume and vascular permeability from dynamic susceptibility contrast-enhanced perfusion MR imaging with glioma grade. *Am J Neuroradiol.* (2004) 25:746–55.
32. Rollin N, Guyotat J, Streichenberger N, Honnorat J, Tran Minh VA, Cotton F. Clinical relevance of diffusion and perfusion magnetic resonance imaging in assessing intra-axial brain tumors. *Neuroradiology.* (2006) 48:150–9. doi: 10.1007/s00234-005-0030-7
33. Lemercier P, Paz Maya S, Patrie JT, Flors L, Leiva-Salinas C. Gradient of apparent diffusion coefficient values in peritumoral edema helps in differentiation of glioblastoma from solitary metastatic lesions. *AJR Am J Roentgenol.* (2014J) 203:163–9. doi: 10.2214/AJR.13.11186
34. Zakaria R, Das K, Radon M, Bhojak M, Rudland PR, Sluming V, Jenkinson MD. Diffusion-weighted MRI characteristics of the cerebral metastasis to brain boundary predicts patient outcomes. *BMC Med Imaging.* (2014) 3:14–26. doi: 10.1186/1471-2342-14-26
35. Wuerfel J, Bellmann-Strobl J, Brunecker P, Aktas O, McFarland H, Villringer A, et al. Changes in cerebral perfusion precede plaque formation in multiple sclerosis: a longitudinal perfusion MRI study. *Brain.* (2004), 127:111 ± 119. doi: 10.1093/brain/awh007
36. Blasel S, Vorwerk R, Kiyose M, Mittelbronn M, Brunnberg U, Ackermann H, et al. New MR perfusion features in primary central nervous system lymphomas: pattern and prognostic impact. *J Neurol.* (2018) 265:647–58. doi: 10.1007/s00415-018-8737-7
37. Sugita Y, Takase Y, Mori D, Tokunaga O, Nakashima A, Shigemori M. Endoglin (CD 105) is expressed on endothelial cells in the primary central nervous system lymphomas and correlates with survival. *J Neurooncol.* (2007) 82:249–56. doi: 10.1007/s11060-006-9281-3
38. Takeuchi H1, Matsuda K, Kitai R, Sato K, Kubota T. Angiogenesis in primary central nervous system lymphoma (PCNSL). *J Neurooncol.* (2007) 84:141–5. doi: 10.1007/s11060-007-9363-x

Conflict of Interest: The authors declare that the research was conducted in the absence of any commercial or financial relationships that could be construed as a potential conflict of interest.

Publisher's Note: All claims expressed in this article are solely those of the authors and do not necessarily represent those of their affiliated organizations, or those of the publisher, the editors and the reviewers. Any product that may be evaluated in this article, or claim that may be made by its manufacturer, is not guaranteed or endorsed by the publisher.

CASE REPORT
published: 19 April 2022
doi: 10.3389/fsurg.2022.875881

Case Report: Esthesioneuroblastoma Involving the Optic Pathways

Vithor Ely B. da Silva[1], *Samuel R. Buniatti*[2], *Felipe D'Almeida Costa*[2], *Mauricio R. Torrecillas*[3], *Jean G. de Oliveira*[1] *and Marcio S. Rassi*[1]*

[1] Department of Neurosurgery, AC Camargo Cancer Center, São Paulo, Brazil, [2] Department of Pathology, AC Camargo Cancer Center, São Paulo, Brazil, [3] Centro de Ensino Superior de Maringá, Maringá, Brazil

Olfactory neuroblastoma, or esthesioneuroblastoma, is an uncommon malignant tumor originating from the neural crest that commonly occurs in the upper nasal cavity. Its ectopic origin is extremely rare, especially when located in the optical pathways. This paper reports the case of a giant ectopic esthesioneuroblastoma of the optic pathways that were surgically treated through a cranio-orbital-zygomatic (COZ) craniotomy with extensive resection, in addition to a literature review. The patient is a 46-year-old female presenting with a 4-month history of visual loss in the left eye. Since she was previously blind in the right eye from a traumatic injury, it was evolving to loss of bilateral vision. Imaging depicted an expansive infiltrating lesion involving the entire path of the right optic nerve, extending to the optic chiasm, cisternal portion of the left optic nerve, bilateral optic tract, and hypothalamus. Investigation of pituitary function was unremarkable. Esthesioneuroblastoma is a rare tumor with poorly defined standard clinical management. Its ectopic presentation makes the diagnosis even more challenging, making it difficult to manage these cases properly. Surgeons should be aware of this rare possibility, as early aggressive treatment is likely to be associated with better results.

Keywords: esthesioneuroblastoma, ectopic tumor, cranio-orbito-zygomatic approach, skull base, olfactory neuroblastoma/esthesioneuroblastoma

OPEN ACCESS

Edited by:
Albert Sufianov,
Federal Center of Neurosurgery, Russia

Reviewed by:
Hidehito Kimura,
Kobe University, Japan
Fabio Ferreli,
Humanitas University, Italy

***Correspondence:**
Marcio S. Rassi
marcio.rassi@accamargo.org.br

Specialty section:
This article was submitted to Neurosurgery, a section of the journal Frontiers in Surgery

Received: *14 February 2022*
Accepted: *21 March 2022*
Published: *19 April 2022*

Citation:
da Silva VEB, Buniatti SR, Costa FD'A, Torrecillas MR, de Oliveira JG and Rassi MS (2022) Case Report: Esthesioneuroblastoma Involving the Optic Pathways. Front. Surg. 9:875881. doi: 10.3389/fsurg.2022.875881

BACKGROUND

Olfactory neuroblastoma, or esthesioneuroblastoma, is a malignant rare tumor that usually occurs in the upper aspect of the nasal cavity due to its origin from the olfactory neuroepithelium with neuroblastic differentiation (1). It frequently extends from the upper part of the nasal cavity to the upper part of the septum, the upper nasal conchae, the roof of the nose, and the cribriform plate of the ethmoidal sinus. Those located outside this region, where the olfactory neuroepithelium does not normally exist, have been reported as ectopic (2). Its ectopic origin is extremely rare, especially when located in the optical pathways.

We report the case of giant ectopic esthesioneuroblastoma that extended along the optic nerve, leading to visual loss, and requiring neurosurgical treatment.

CLINICAL PRESENTATION

The patient is a 46-year-old female presenting with a 4-month history of visual loss in the left eye. Since she was previously blind in the right eye from a traumatic injury, it was evolving to loss of bilateral vision. Imaging depicted an expansive infiltrating lesion involving the entire path of the right optic nerve, extending to the optic chiasm, cisternal portion of the left optic nerve, bilateral optic tract, and hypothalamus (**Figure 1**). Investigation of pituitary function was unremarkable.

Patient consent was obtained, and surgical removal was performed by the senior author through a cranio-orbital-zygomatic (COZ) approach *via* Transylvanian and pre-temporal routes (**Supplementary Video**).

After the procedure, the patient showed visual improvement in the left eye, with transient diabetes insipidus on the first

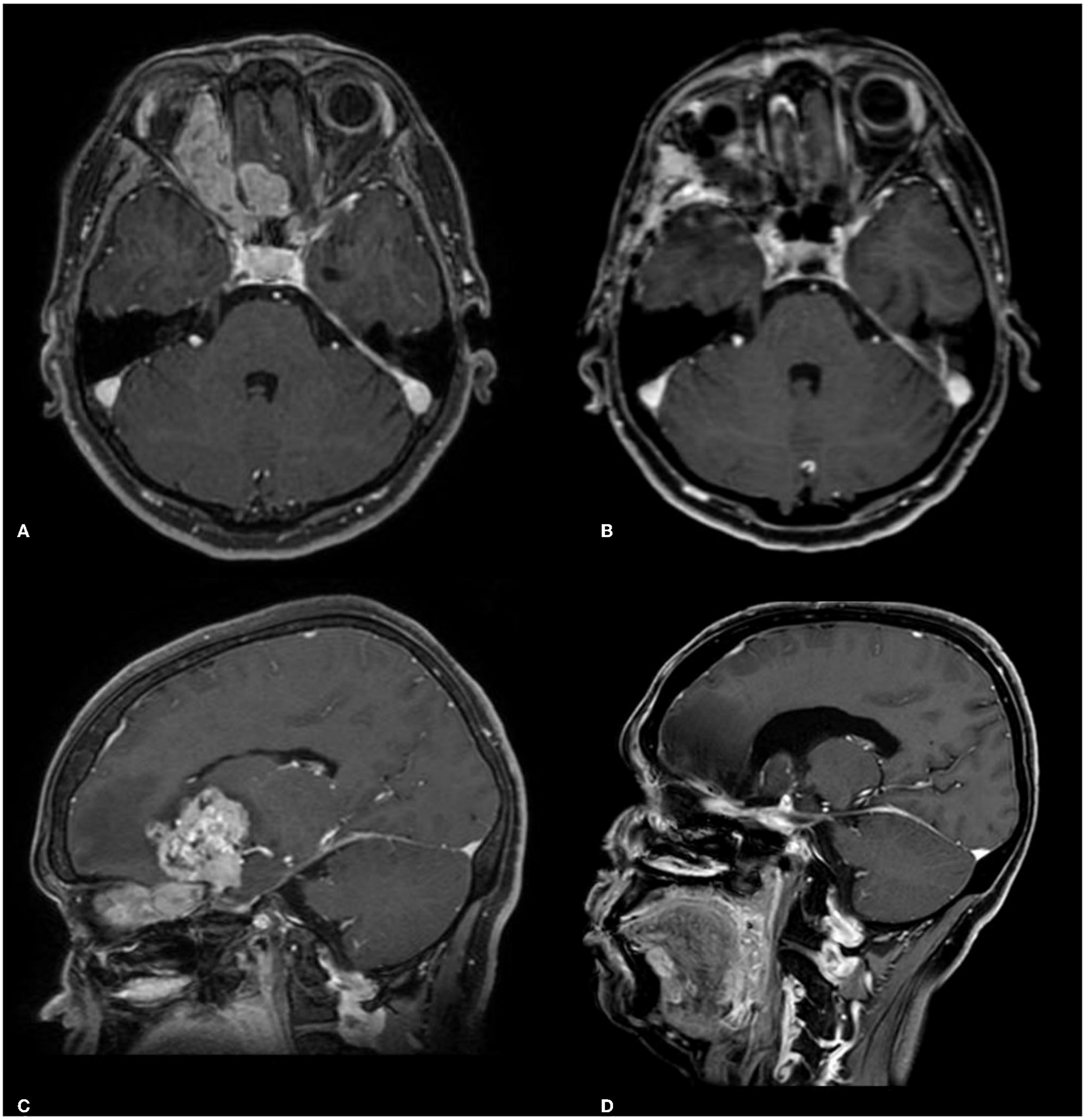

FIGURE 1 | Preoperative post-contrast T1-weighted MRI **(A,C)** and postoperative images **(B,D)**.

postoperative day. Pathology showed an olfactory neuroblastoma grade III of Hyams (**Figure 2**). Treatment was continued with adjuvant radiotherapy.

Postoperative imaging showed gross total resection, in addition to the absence of metastatic foci along the neuroaxis or lymph node involvement, characterizing a T4N0M0 tumor according to Dulguerov et al. (3), or stage C using the modified Kadish classification (4).

DISCUSSION

Esthesioneuroblastoma is a rare tumor with sparse data in the literature. It predominantly occurs in young adults, and the age of presentation varies from 40 to 70 years, with men and women equally affected (1). Although the exact cell type and location have not yet been defined, the common assumption is that it is derived from cells in the neural crest of the upper nasal cavity (5).

Clinical symptoms depend on the location and extension of the tumor, and, therefore, nasal symptoms, such as epistaxis, nasal obstruction, and anosmia, are the most common (5). However, other symptoms, such as headache, diplopia, visual loss, and seizures can also occur. Due to its rarity and unusual presentation, ectopic olfactory neuroblastoma becomes a disease that is difficult to suspect, merging with other types of tumors.

Neither of the two clinical staging systems, TNM by Dulguerov et al. or the modified Kadish classification is ideally geared to the staging of ectopic olfactory neuroblastoma. The most critical information seems to be whether the tumor extends to the anterior cranial fossa and orbit and whether it is related to lymphadenopathy, as this has the greatest impact on treatment planning and prognosis (6).

The theory to explain the ectopic origin of these tumors is speculative and is based on the idea that there may be ectopic cell debris during embryologic development (7). The theory supporting the origin of ectopic esthesioneuroblastoma was first suggested by Jakumeit in 1971 and is the theory of the terminal nervous system (8). Embryologically, the olfactory placode is divided into two systems; the first system contains the olfactory nerve and the vomeronasal nerve, and the second system contains the terminal nerve that develops immediately caudal to the first. Both will degenerate into fetal life. The terminal nerve ganglion and neurons spread diffusely across the cribriform plate, nasal septum, nasal mucosa, Bowman's gland, mucosa naris, crista Galli, and hypothalamus. The persistence of these cells beyond fetal life can provide the source of ectopic esthesioneuroblastoma.

Another possible theory, provided by Zappia et al., describes a model of blocked migration of neuronal cells from the olfactory placode that may provide the origin of these tumors in a case of Kallman syndrome, which is a congenital condition defined by the absence of olfactory bulbs and pituitary hypoplasia. Even patients, who do not have Kallman's syndrome, may exhibit less

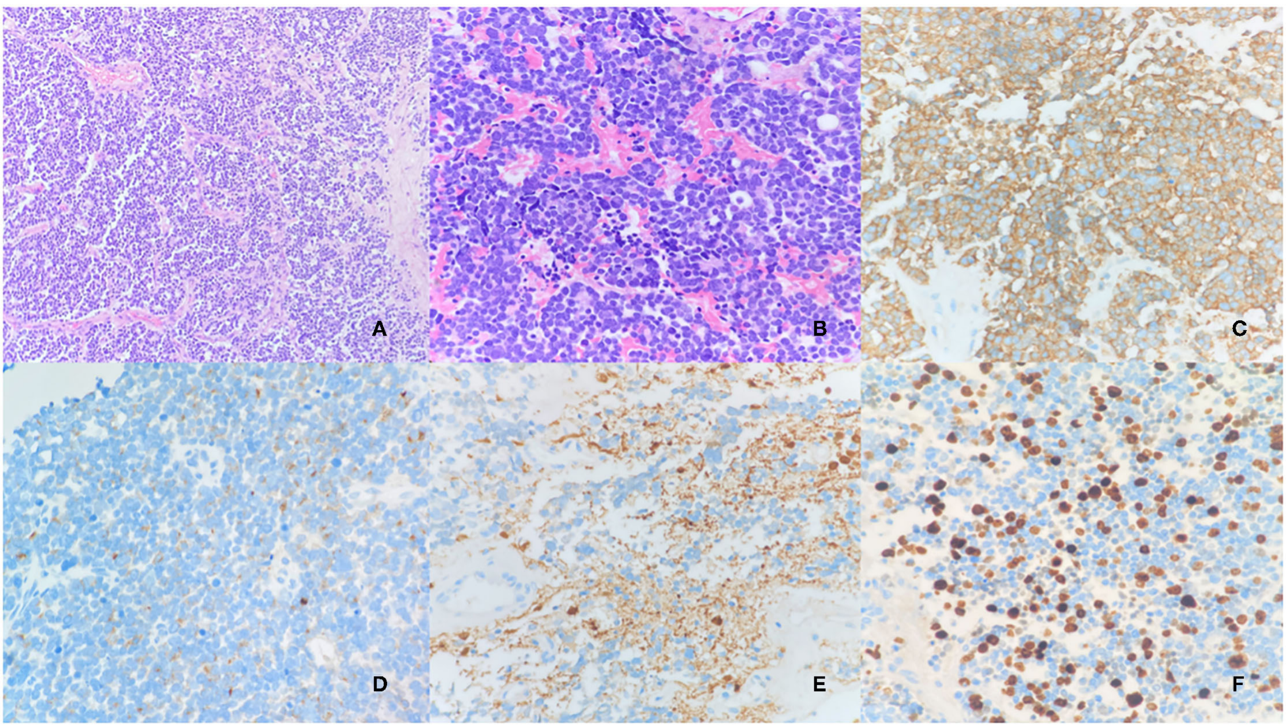

FIGURE 2 | Olfactory neuroblastoma (Hyams III). Proliferation of cells forming lobe sketchs, separated by vascular and hylinized fibrous stroma. HE 10x **(A)**. The cells are hyperchromatic, pleomorphic, and sometimes arranged in gland-like rings or tight annular formations with a true lumen (Flexner–Wintersteiner rosettes). Some mitotic figures can be seen. HE 20x **(B)**. Immunohistochemical stains: Synaptophysin **(C)**; Chromogranin **(D)**; S100: positive in sustentacular periphery cells **(E)**; Ki-67 **(F)**.

disorderly migration along the pathway, which may progress to an esthesioneuroblastoma in the future (9).

The treatment of esthesioneuroblastoma is controversial, mainly due to its rarity and lack of data in the literature to support therapeutic regimens, with surgical resection followed by postoperative radiotherapy, being the option that showed better treatment results in retrospective reports, compared to isolated radiotherapy, although orbital invasion is associated with adverse survival outcomes (5, 10). The classifications of Kadish, Dulguerov, and Hyams help predict prognosis and guide treatment, with no superiority of any (5). In the case presented, we chose a cranio-orbital-zygomatic craniotomy to allow good brain exposure and provide several routes to the tumor location, including Transylvanian and pretemporal. Adjuvant radiotherapy in the surgical bed complemented the operative treatment in this patient.

The role of chemotherapy in the treatment of these patients is still questionable. Neoadjuvant chemotherapy has been reported to show positive responses in locally advanced cases and appears to play an important role, especially in tumors with difficult resection (5). In the initial stage, some groups advocate platinum-based therapy whenever possible, while other groups postpone chemotherapy treatment. More studies with longer follow-ups are needed to interpret the results.

CONCLUSION

Esthesioneuroblastoma is a rare tumor with poorly defined standard clinical management. Its ectopic presentation makes the diagnosis even more challenging, making it difficult to manage these cases properly. Surgeons should be aware of this rare possibility, as early aggressive treatment is likely to be associated with better results.

DATA AVAILABILITY STATEMENT

The original contributions presented in the study are included in the article/**Supplementary Material**, further inquiries can be directed to the corresponding author/s.

ETHICS STATEMENT

Written informed consent was obtained from the individual(s) for the publication of any potentially identifiable images or data included in this article.

AUTHOR CONTRIBUTIONS

All authors listed have made a substantial, direct, and intellectual contribution to the work and approved it for publication.

SUPPLEMENTARY MATERIAL

The Supplementary Material for this article can be found online at: https://youtu.be/mtwYw89NnFk

Supplementary Video 1 | Cranio-orbito-zygomatic approach for ectopic esthesioneuroblastoma.

REFERENCES

1. Limaiem F, Das JM. Esthesioneuroblastoma. In: *Treasure Island* (FL). (2021).
2. Matsunaga M, Nakagawa T, Sakamoto T, Ito J. Sphenoid esthesioneuroblastoma arising from the hindmost olfactory filament. *Auris Nasus Larynx*. (2015) 42:170–2. doi: 10.1016/j.anl.2014.10.003
3. Dulguerov P, Calcaterra T. Esthesioneuroblastoma: The UCLA Experience 1970-1990. *Laryngoscope*. (1992) 102:843–849. doi: 10.1288/00005537-199208000-00001
4. Kadish S, Goodman M, Wang CC. Olfactory neuroblastoma—A clinical analysis of 17 cases. *Cancer*. (1976) 37:1571–1576. doi: 10.1002/1097-0142(197603)37:3<1571::AID-CNCR2820370347>3.0.CO;2-L
5. Wu K, Avila SA, Bhuyan R, Matloob A, Del Signore AG, Hadjipanayis C, Chelnis J. Orbital invasion by Esthesioneuroblastoma: a comparative case series and review of literature. *Orbit*. (2020) 41:1–14. doi: 10.1080/01676830.2020.1852262
6. Wormald R, Lennon P, O'Dwyer TP. Ectopic olfactory neuroblastoma: report of four cases and a review of the literature. *Eur. Arch Oto-Rhino-Laryngology*. (2011) 268:555–60. doi: 10.1007/s00405-010-1423-8
7. Zahedi FD, Gendeh BS, Husain S, Kumar R, Kew TY. Ectopic esthesioneuroblastoma of the sphenoclivus: a rare entity. *Indian J Otolaryngol Head Neck Surg*. (2017) 69:125–9. doi: 10.1007/s12070-016-0978-0
8. Jakumeit HD. Neuroblastoma of the olfactory nerve. *Acta Neurochir*. (1971) 25:99–108. doi: 10.1007/BF01808865
9. Lin JH, Tsai DH, Chiang YH. A primary sellar esthesioneuroblastomas with unusual presentations: a case report and reviews of literatures. *Pituitary*. (2009) 12:70–75. doi: 10.1007/s11102-007-0081-3
10. Li R, Tian S, Zhu Y, Yan L, Zhu W, Quan H, et al. Management of orbital invasion in esthesioneuroblastoma: 14 years' experience, Radiat. *Oncol*. (2019) 14:1–12. doi: 10.1186/s13014-019-1313-1

Conflict of Interest: The authors declare that the research was conducted in the absence of any commercial or financial relationships that could be construed as a potential conflict of interest.

Publisher's Note: All claims expressed in this article are solely those of the authors and do not necessarily represent those of their affiliated organizations, or those of the publisher, the editors and the reviewers. Any product that may be evaluated in this article, or claim that may be made by its manufacturer, is not guaranteed or endorsed by the publisher.

frontiers | Frontiers in Surgery

PERSPECTIVE
published: 25 April 2022
doi: 10.3389/fsurg.2022.892470

Comparing Two Improved Techniques With the Traditional Surgical Techniques for Intra and Extramedullary Spinal Tumor Resection: A Report of 280 Cases

Kamaliddin Djumanov[1], Gayrat Kariev[1,2], Gennady Chmutin[3,4], Gennady Antonov[5], Egor Chmutin[3], Gerald Musa[3], Adam Maier[3] and Alina Shumadalova[6]*

[1] Republican Specialized Scientific and Practical Medical Center of Neurosurgery, Tashkent, Uzbekistan, [2] Department of Neurosurgery, Tashkent Pediatric Medical Institute, Tashkent, Uzbekistan, [3] Department of Nervous Diseases and Neurosurgery, Peoples' Friendship University of Russia (RUDN University), Moscow, Russia, [4] Federal State Budgetary Institution of Medical Department of Moscow "Morozov Children's City Clinical Hospital of Medical Department of Moscow", Moscow, Russia, [5] 3rd Central Military Clinical Hospital Named After A.A. Vishnevsky Under the Ministry of Defense of the Russian Federation, Krasnogorsk, Russia, [6] Department of General Chemistry, Bashkir State Medical University, Ufa, Russia

OPEN ACCESS

Edited by:
Ilgiz Fanilevich Gareev,
Federal Center of Neurosurgery,
Tyumen, Russia

Reviewed by:
Bipin Chaurasia,
Neurosurgery Clinic, Nepal
Keneshbek Yrysov,
Kyrgyz State Medical
Academy, Kyrgyzstan

***Correspondence:**
Gerald Musa
gerryMD@outlook.com

Specialty section:
This article was submitted to Neurosurgery, a section of the journal Frontiers in Surgery

Received: *09 March 2022*
Accepted: *28 March 2022*
Published: *25 April 2022*

Citation:
Djumanov K, Kariev G, Chmutin G, Antonov G, Chmutin E, Musa G, Maier A and Shumadalova A (2022) Comparing Two Improved Techniques With the Traditional Surgical Techniques for Intra and Extramedullary Spinal Tumor Resection: A Report of 280 Cases. Front. Surg. 9:892470. doi: 10.3389/fsurg.2022.892470

Objectives: Spinal tumors remain a challenging problem in modern neurosurgery. The high rate of postoperative morbidity associated with intramedullary tumors makes the need for safer surgical techniques invaluable. This study analyses our experience with the treatment of spinal cord tumors and compares traditional management and a new different surgical approach to intramedullary tumors with an associated hydrosyringomyelia.

Materials and Methods: This retrospective study compared standard surgical techniques and 2 newer modified techniques for intra and extramedullary spinal tumors at the Neurosurgery center for spinal cord tumors of the Republic of Uzbekistan. Preoperative neurological status was recorded with the ASIA/ISNCSCI scale. Postoperative outcome was graded using the Nurrick score.

Results: Of the 280 cases, there were 220 (78.5%) extramedullary and 60 (21.5%) with intramedullary spinal tumors. The control and main group had 159 (56.8%) and 121 (43.2%) patients, respectively. Severe compression myelopathy (ASIA- A, B, C) was 217 (77.5%) patients i.e., ASIA A-39 (13.9%); B-74 (26.4%), and C-104 (37.1%). In 74 extramedullary tumors (33.6%) treated with the new method, good postoperative outcomes in 44 cases (59.5%) with OR = 1.9; 95% CI 1.1–3.3 ($p < 0.05$). Thirty-seven (61.7%) intramedullary tumors were treated with the newer modified technique. There was no difference with the standard method ($p = 0.15$). However, when comparing postoperative Nurick grade 1–2 with grade 3–4, the newer strategy was superior with improvement in 24 (65%) patients, OR = 3.46; 95% CI 1.2–10.3 ($p < 0.05$).

Conclusion: When compared with standard methods, the proposed newer modified strategy of surgical treatment of spinal cord tumors with the insertion of a syringosubarachnoid shunt in the presence of an associated hydrosyringomyelia is associated with better postoperative outcome (Nurick 1 and 2) in 64.8%.

Keywords: spinal cord tumors, syringohydromyelia, differentiated surgical tactics, intramedullary tumors, extramedullary tumors, Nurick score

INTRODUCTION

The term "spinal cord tumors" includes all oncological processes in the region of the spinal column. They are generally classified as: intramedullary, extramedullary (emanating from the inner layer of the dura, dental ligament, pial membrane, intradural part of the spinal root), extradural tumors that are also further divided into primary tumors originating from the vertebra, periosteum, ligaments, cartilage, the outer layer of the dura mater and secondary (metastatic) tumors (1, 2). Spinal cord tumors account for 2% of all neoplasms, 3% of nervous system tumors, and 20% of tumors of the central nervous system in adults. The ratio of spinal to brain tumors is around 1: 9. Most often, spinal cord tumors are observed in the socially active group of people aged 30–50 years, which makes this problem one of great relevance in medicine today. However, surgery of spinal tumors is one of the most difficult problems of neurosurgery. Among the tumors of the spinal cord, according to modern authors, extramedullary tumors predominate and constitute up to 70% of all spinal tumors. The results of surgical treatment of spinal cord tumors depend on many factors: the duration of the disease, the extent of neurological deficit, the radicality of tumor removal, and the extent of intraoperative trauma to the spinal cord (3, 4). All these factors should be considered in combination (3, 5).

To date, the main method of treating spinal cord tumors is surgical excision. However, indications for specific surgical approaches to these tumors are still insufficiently developed and depend on the anatomical location of the tumor, histological diagnosis, and the aggressiveness of the neoplasm (3, 6, 7). Currently, the results of spinal cord tumor surgery are still unsatisfactory, and far from perfect (8). The high rate of postoperative morbidity calls for the need for further research aimed at improving the results of spinal tumors treatment. This study analyses our experience with the treatment of spinal cord tumors and compares traditional management and a new different surgical approach to intramedullary tumors with an associated hydrosyringomyelia.

MATERIALS AND METHODS

Study Design, Setting, and Participants

This was a retrospective study. Case files of all patients with surgically managed spinal tumors between 2014 and 2021 were extensively analyzed. All patients were managed at the Republican Specialized Scientific and Practical Medical Center of Neurosurgery in Tashkent, Uzbekistan during this period. The patients were divided into two groups i.e., the control and the main group depending on the when the patients were managed and the procedure used. The control group included patients treated according to standard traditional tumor resection strategies between 2014 and 2017. The main study group included patients managed using a newer modified strategy between 2018 and 2021 at the Neurosurgery center for spinal cord tumors of the Republic of Uzbekistan.

The newer modified surgical strategy were basically improvements on traditional methods of removing tumors of extra- and intramedullary localization. For extramedullary tumors, the essence of the method is to conduct internal decompression of the tumor, to minimize traumatization of the spinal cord and main vessels. In this method, the intracapsular part is removed in small fractions. The tumor debulking begins with the areas farthest from the great vessels, the roots of the spinal cord, and the spinal cord itself.

In the surgical treatment of intramedullary tumors associated with an intramedullary cyst, the newer modified strategy involved inserting a syringosubarachnoid bypass shunt after excision of intramedullary tumors. This is done to prevent the re-accumulation of cerebrospinal fluid and the expansion of the intramedullary dead space remaining after tumor excision.

A 6–8 cm piece is fashioned from the standard 3mm silicone tubing used for ventriculoperitoneal shunts. Following the standard microsurgical approach and microsurgical tumor resection, the proximal end of the already prepared tube is inserted into the resection cavity and advanced either cranially or caudally depending on the location, into the syrinx cavity. Patency was confirmed by CSF egress through the tube. The distal end of the tube was placed in the subdural space and anchored to the overlying dura using a 6-0 silk suture to avoid shunt migration (**Figure 1**). The dura was closed in a water tight fashion using 6-0 polypropylene monofilament. The remainder of the closure was performed in a standard multilayer fashion for a spinal procedure.

The indications for surgical intervention in the reviewed cases included; the mere presence of a tumor, compression of the spinal cord or its roots, and neurological deficit of varying severity. **Figures 2**, **3** illustrate examples of two extramedullary tumors managed in this study, a C1-C2 anterolateral neuroma and caudal equina ependymoma, respectively.

Preoperative severity of neurological deficit was graded according ASIA/ISNCSCI scale (2015). For a comparative assessment of the postoperative neurological status, the Nurick scale (NS) was used i.e., Grade 1- complete regression of neurological symptoms, grade 2- improvement, grade 3- No change, and grade 4- deterioration of neurological status.

Statistical Analysis

The statistical analysis was carried out using the IBM SPSS 23 program. The Chi-squared criterion (χ^2) was used to determine the presence of association, the strength of the association was determined using the odds ratio (OR) with a 95% confidence

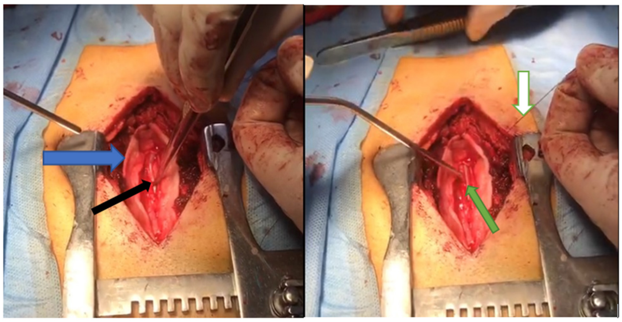

FIGURE 1 | Intraoperative images showing the insertion of the syringosubarachnoid shunt. The dura is opened (blue arrow), the tube is inserted into the resection dead space and into the syrinx (black arrow). The shunt is seen laying in the resection dead space is anchored to the overlying dura using a 6-0 silk suture (white arrow).

FIGURE 2 | MRI of the cervical spine, preoperative and 2 days post-surgery. A 36-year-old with a Neuroma on the ventral surface of the spinal cord, at the level of C1-C2 (blue arrow). Control MRI shows total tumor removal using an improved method (orange arrow).

interval (95% CI). The significance level was set at $p < 0.05$, for all analyses.

RESULTS

The reviewed cases included 280 patients, 220 (78.5%) patients had extramedullary tumors and 60 patients (21.5%) with intramedullary spinal tumors. These different histological diagnoses were analyzed as shown in **Table 1**. In both groups, meningiomas and neuromas were the most common extramedullary tumors while ependymoma was the most frequent intramedullary tumor. The control group managed with standard techniques included 159 (56.8%) managed between 2014 and 2017 while the main study group included 121 (43.2%) managed with the modified methods between 2017 and 2021.

Based on the ASIA/ISNCSCI scale (2015), the total number of patients with compression myelopathy syndrome (groups A, B, C) was 217 (77.5%) patients i.e., ASIA A-39 (13.9%); B-74 (26.4%), and C-104 (37.1%). The ambulant patients were 63 (21.5%) i.e., ASIA D 47 (16.8%); and E-16 (5.7%).

In 74 (33.6%) cases with extramedullary tumors, underwent an improved newer method of surgical removal of extramedullary tumors.

Multiple comparisons with the patients that had the standard traditional method showed a statistically significant difference in treatment outcomes ($p = 0.03$). Using the newer modified surgical method for extramedullary tumors showed better postoperative outcomes in 44 cases (59.5%) with OR = 1.9; 95% CI 1.1–3.3 ($p < 0.05$) (**Table 2**).

In 37 (61.7%) cases of intramedullary tumors with an associated intramedullary cyst underwent the newer modified technique. When comparing the two treatment methods for intramedullary tumors, there was no statistically significant difference observed ($p = 0.15$). However, when comparing postoperative Nurick grade 1–2 with grade 3–4, the use of the newer modified method described above demonstrated improvement in the postoperative neurological status in 24 (65%) patients with OR = 3.46; 95% CI 1.2 to 10.3 ($p < 0.05$) (**Table 3**).

DISCUSSION

Surgical removal of spinal cord tumors remains the main, highly effective method of treatment. The technique and tactics of treatment of this pathology were developed in the 1980s of the twentieth century (7, 9–11). Most neurosurgeons recommend total tumor resection in all possible cases (10, 12). However, although postoperative residual tumor is an important predictor of progression, the aggressiveness of resection should be cautiously weighed against the risk of new postoperative neurological deficit (13). Modern approaches to the surgical treatment of spinal cord tumors are aimed at increasing the number of minimally invasive techniques, the use of accurate diagnostic methods, and modern equipment and tools. The use of minimally invasive accesses for the removal of spinal cord tumors has recently been highlighted in a large number of publications (3, 10, 14). Minimal bone resection when accessing the extradural space (hemilaminectomy), according to Yu et al. (14), has several advantages: maximum preservation of the stability of the spine, reduction in the volume of intraoperative blood loss, reduction of muscle dissection, reduction in the duration of the operation and, as a result, a decrease in postoperative pain syndrome and faster physical rehabilitation. The need to use minimally invasive surgical access to maintain the stability of the spine was demonstrated by Byvaltsev et al. (10) in a multicenter study.

In any case, the goal of treating spinal cord tumors is total surgical removal with the possible preservation of orthopedic stability. At the same time, the question of choosing different options for removing tumors, depending on the anatomical location of tumors, remains relevant. When removing

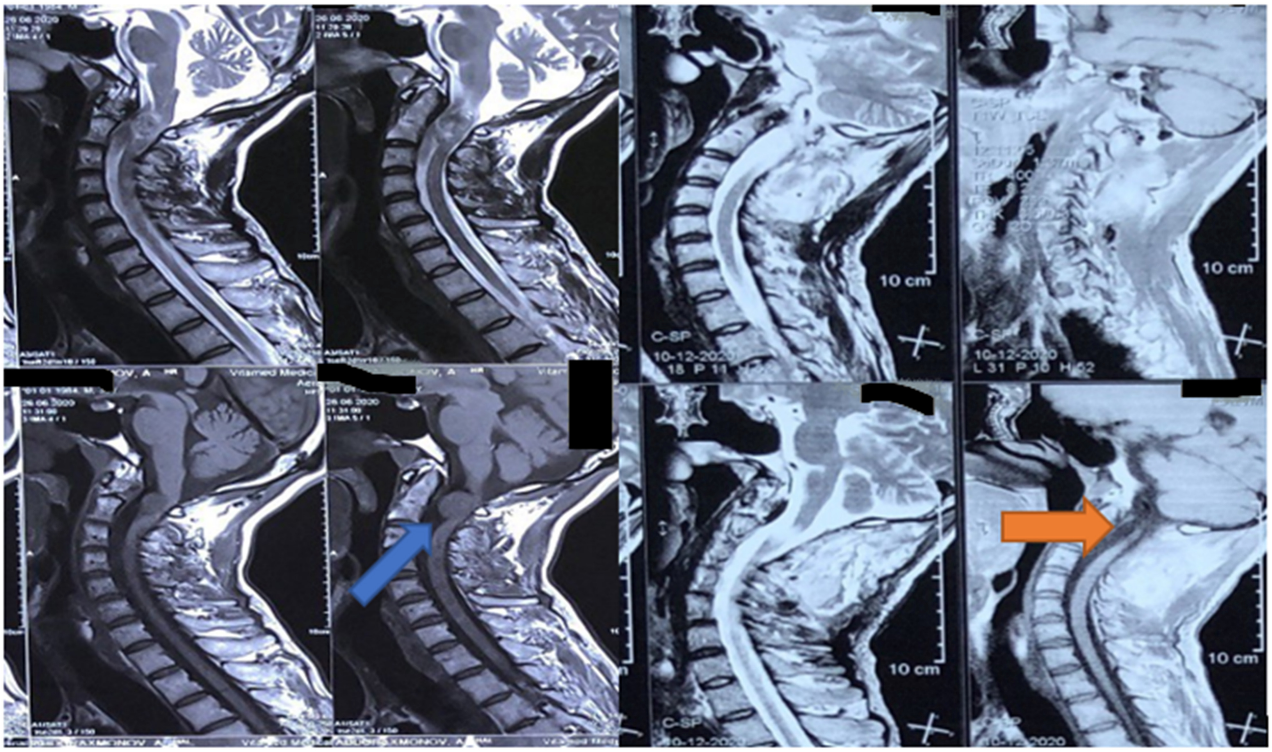

FIGURE 3 | A pre-and post-surgery MRI of 32 years old with ependymoma of the roots of the cauda equina and syringomyelia between L3-L5 (blue arrow).

intramedullary tumors, the use of microsurgical techniques and minimally invasive accesses can significantly improve the results of surgical treatment and reduce the chances of relapses (6). Anteriorly located extramedullary spinal cord tumors are challenging tasks for the neurosurgeon (10, 15). In some cases, the use of an anterior approach is required for their radical removal. With the ventrally and ventrolaterally located thoracic spine tumors, some authors (16) suggest the use of endoscopic techniques. The use of endoscopy or endoscopic assistance in the resection of spinal cord tumors is a relatively new direction in spinal neuro-oncology.

Intraoperative electrophysiological monitoring is necessary for spinal neurosurgical clinics, especially with intramedullary located tumors. In our study, intraoperative electrophysiological monitoring was used in 12 cases. According to a study of the outcomes of surgical treatment of intradural tumors of the spinal cord conducted by Nambiar and Kavar (12), the frequency of radical resections, according to their data, was 72.3%. A good premorbid clinical stage was the most significant predictor of a positive outcome at discharge and follow-up. The authors concluded that the surgical outcome depends on the premorbid, preoperative, postoperative clinical stage, the degree of radicality of tumor resection, localization, and histological stage of the tumor. This is similar to our findings.

The use of minimally invasive methods for removing spinal cord tumors has advantages in terms of the earlier restoration of lost neurological functions (11, 14). In our opinion, there is a need for a balance between the size of the approach and the possibility of complete removal of the tumor. We, like many authors (2, 6, 10, 17, 18), believe that minimally invasive neurosurgery should primarily be minimally invasive only to neural structures and that tumor resection has to be safe with minimal to no damage to the normal surrounding tissues. The microsurgical technique described for extramedullary tumors emphasizes piece meal tumor removal and starting the initial dissection far from the neural tissue where possible. This in

TABLE 1 | Distribution of the spinal tumors by histological diagnosis.

Histology	Control group	Main group	Total
Meningioma	43	27	70 (25.0%)
Neuroma	28	21	49 (22.3%)
Ependymoma	9	12	21 (9.5%)
Astrocytoma	9	10	19 (6.8%)
Hemangioblastoma	5	7	12 (4.3%)
Chondroma	5	6	11 (3.9%)
Reticulosarcoma	7	4	11 (3.9%)
Osteosarcoma	3	6	9 (3.2%)
Myeloma	4	2	6 (2.2%)
Osteoma	3	2	5 (1.8%)
Other	43	24	67 (23.9%)
Total	159 (56.8%)	121 (43.2%)	280 (100%)

TABLE 2 | Results of surgical treatment of extramedullary tumors.

Nurick score	Advanced (new) method	%	Traditional method	%	*p*-value
Grade 1	21	28.4	17	11.6	$\chi^2 = 8.7, p = 0.03$
Grade 2	23	31.1	47	32.3	
Grade 3	22	29.7	64	43.8	
Grade 4	8	10.8	18	12.3	
Total	74	100	146	100	

TABLE 3 | Results of surgical treatment of intramedullary tumors.

Nurick scale	Advanced (New) method	%	Traditional method	%	*p*-value
Grade 1	9	24.3	3	13.0	$\chi^2 = 5.9, p = 0.15$
Grade 2	15	40.5	5	21.7	
Grade 3	9	24.3	8	34.8	
Grade 4	4	10.8	7	30.4	
Total	37	100	23	100	

theory reduces the trauma on the neural tissue and allows for clear identification of the tumor, texture and location by the time the neural elements are encountered. This method was superior to traditional tumor removal techniques $p < 0.05$.

Thus, numerous studies (3, 10, 19) have shown that the use of modern operating technologies can avoid instability of the spine, reduce the surgical wound size and infectious complications, the intensity of post-operative pain, the volume of intraoperative blood loss, and the frequency of recurrence of tumor growth.

Syringomyelia associated with intramedullary tumors results from intramedullary tissue damage secondary to hemorrhage or infarction, and resulting from direct secretory ability of intramedullary tumor (20). Some authors consider the presence of a syrinx a favorable prognostic sign because they are commonly associated with non-infiltrative tumors with distinct cleavage planes than more diffuse, infiltrative tumors (21). Whether or not it should be drained remains the question. Some authors have concluded that the syringes resolve spontaneously, we believe the continued pressure on the spinal cord from the syrinx and the fluid collection in the resection cavity can impair the microcirculation and delay recovery in some cases. Other intramedullary cysts like arachnoid cysts have been managed with fenestration with good results (22). Insertion of a syringosubarachnoid shunt as described in the improved method was associated with improved neurological outcome (Nurrick 1 and 2). However, there was no statistically significant difference in overall outcomes.

Tumor resection has to be safe with minimal to no damage to the normal surrounding tissues (13). The microsurgical technique described for extramedullary tumors emphasizes piece meal tumor removal and starting the initial dissection far from the neural tissue where possible. This in theory reduces the trauma on the neural tissue and allows for clear identification of the tumor, texture and location by the time the neural elements are encountered. This method was superior to traditional tumor removal techniques $p < 0.05$.

The limitations of the study includes: low number of patients as this would have affected the significance of our results. We also believe a more comprehensive randomized study would be more informative on the validity of the new improved techniques. The patients' comparisons were not corrected for tumor type and or age but just the procedure performed. This would be very helpful for future to improve the validity of the results.

CONCLUSION

Spinal tumors are associated with a high postoperative morbidity. Choosing the optimal surgical approach requires adequate preoperative assessment taking into account multiple patient and tumor factors. We recommend the use of the newer modified techniques described for extramedullary and intramedullary tumors. These procedures were associated with improved postoperative outcome (Nurick 1 and 2) i.e., 59.5 and 64.8% for extramedullary and intramedullary tumors, respectively.

DATA AVAILABILITY STATEMENT

The original contributions presented in the study are included in the article/supplementary material, further inquiries can be directed to the corresponding author/s.

ETHICS STATEMENT

The studies involving human participants were reviewed and approved by Institutional Review Board at the Republican Specialized Scientific and Practical Medical Center of Neurosurgery. The Ethics Committee waived the requirement of written informed consent for participation. Written informed consent was obtained from the individual(s) for the publication of any potentially identifiable images or data included in this article.

AUTHOR CONTRIBUTIONS

KD, GK, and GC: substantial contributions to the conception or design of the work. AS, AM, and GM: acquisition, analysis, and interpretation of data for the work. GK, KD, and GM: drafting and critical revision of the manuscript for important intellectual content. GC, GK, GA, GM, and AM: final approval of the version to be published. All authors contributed to the article and approved the submitted version.

FUNDING

The publication was carried out with the support of the Peoples Friendship University of Russia (RUDN) Strategic Academic Leadership Program.

REFERENCES

1. Gaidar BV, Dulaev AK, Orlov VP, Nadulich KA, Teremshonok AV. Surgical treatment of patients with thoracic and lumbar spine injuries. *Hirurgiâ Pozvonočnika.* (2004) 3:40–5.
2. Sama A, Giradi F, Cammisa FP Jr. Spinal tumors. *Spine*. (2002) 6:1456–78.
3. Konovalov NA, Shishkina LV, Asyutin DS, Onoprienko RA. Extradural spinal cord hemangioblastoma (case from practice and review of literature). *J Neurosurg*. (2016) 6:88–92. doi: 10.17116/neiro201680688-92
4. Zozulia Iu A, Polishchuk NE, Slyn'ko EI. The surgical treatment of medullocervical tumors. *J Issues Neurosurg.* (1998) 1:6–10.
5. Voronov V. *Congenital Malformations of Spinal Cord and Spine in Children*. St Petersburg, FL (1998). p. 53.
6. Akshulakov SK, Kerimbayev TT, Aleinikov VG, Maev EZ, Pazylbekov TT. Surgical treatment of intramedullary tumors of the spinal cord. *Neurosurg Neurol Kazakhstan*. (2011) 2:14–6.
7. Vetrile S, Kolesov S. *Craniovertebral Pathology*. Moscow: M: Medicine (2007).
8. Baber WW, Numaguchi Y, Kenning JA, Harkin JC. Periosteal chondroma of the cervical spine: one more cause of neural foramen enlargement. *Surg Neurol*. (1988) 29:149–52. doi: 10.1016/0090-3019(88)90074-2
9. Angevine PD, Kellner C, Haque RM, McCormick PC. Surgical management of ventral intradural spinal lesions. *J Neurosurg Spine*. (2011) 15:28–37. doi: 10.3171/2011.3.SPINE1095
10. Byval'tsev VA, Sorokovikov VA, Damdinov BB, Belykh EG, Sereda ÉV, Panasenkov SI, Grigor'ev EG. Factors affecting the outcome of surgical management for extramedullary spinal cord tumors: a multicenter study. *J Issues Neurosurg.* (2014) 78:15–23. doi: 10.17116/neiro201478615-23
11. Dzukaev DN, Semchenko VI, Dreval ON. A new technology in the treatment of pathological spinal fractures. *J Issues Neurosurg.* (2009) 3:19–22
12. Nambiar M, Kavar B. Clinical presentation and outcome of patients with intradural spinal cord tumours. *J Clin Neurosci*. (2012) 19:262–6. doi: 10.1016/j.jocn.2011.05.021
13. Samuel N, Tetreault L, Santaguida C, Nater A, Moayeri N, Massicotte EM, et al. Clinical and pathological outcomes after resection of intramedullary spinal cord tumors: a single-institution case series. *Neurosurg Focus*. (2016) 41:E8. doi: 10.3171/2016.5.FOCUS16147
14. Yu Y, Zhang X, Hu F, Xie T, Gu Y. Minimally invasive microsurgical treatment of cervical intraspinal extramedullary tumors. *J Clin Neurosci*. (2011) 18:1168–73. doi: 10.1016/j.jocn.2010.12.043
15. Aabo K, Walbon-Jørgensen S. Central nervous system complications by malignant lymphomas: radiation schedule and treatment results. *Int J Radiat Oncol Biol Phys*. (1986) 12:197–202. doi: 10.1016/0360-3016(86)90094-5
16. Jenny B, Rilliet B, May D, Pizzolato G. Transthoracic transvertebral approach for resection of an anteriorly located, calcified meningioma. *Case Rep Neurochirurgie*. (2002) 48:49–52.
17. Campanacci M, Boriani S, Savini R. Staging, biopsy, surgical planning of primary spinal tumors. *La Chirurgia degli organi di movimento*. (1990) 75(1 Suppl.):99–103.
18. Guidetti B, Mercuri S, Vagnozzi R. Long-term results of the surgical treatment of 129 intramedullary spinal gliomas. *J Neurosurg*. (1981) 54:323–30. doi: 10.3171/jns.1981.54.3.0323
19. Alper M, Bilkay U, Keçeci Y, Çelik N, Sabah D, Zileli M, et al. Transsacral usage of a pure island TRAM flap for a large sacral defect: a case report. *Ann Plastic Surg*. (2000) 44:417–21. doi: 10.1097/00000637-200044040-00011
20. Blegvad C, Grotenhuis J, Juhler M. Syringomyelia: a practical, clinical concept for classification. *Acta Neurochirurgica*. (2014) 156:2127–38. doi: 10.1007/s00701-014-2229-z
21. Samartzis D, Gillis CC, Shih P, O'Toole JE, Fessler RG. Intramedullary spinal cord tumors: part I-epidemiology, pathophysiology, and diagnosis. *Global Spine J*. (2015) 5:425–35. doi: 10.1055/s-0035-1549029
22. Novegno F, Umana G, Di Muro L, Fraioli B, Fraioli MF. Spinal intramedullary arachnoid cyst: case report and literature review. *Spine J*. (2014) 14:e9–15. doi: 10.1016/j.spinee.2013.10.051

Conflict of Interest: The authors declare that the research was conducted in the absence of any commercial or financial relationships that could be construed as a potential conflict of interest.

frontiers | Frontiers in Surgery

ORIGINAL RESEARCH
published: 06 May 2022
doi: 10.3389/fsurg.2022.915818

Basal Cisternostomy for Severe TBI: Surgical Technique and Cadaveric Dissection

L. Giammattei[1]*, *D. Starnoni*[1], *M. Messerer*[1,2] *and R. T. Daniel*[1,2]

[1]*Department of Neurosurgery, Lausanne University Hospital, Lausanne, Switzerland,* [2]*Faculty of Biology and Medicine, University of Lausanne, Lausanne, Switzerland*

Introduction: Cisternostomy is emerging as a novel surgical technique in the setting of severe brain trauma. Different surgical techniques have been proposed with a variable degree of epidural bone work. We present here the surgical technique as it is currently performed in our Institution.

Methods: Anatomical dissection of one adult cadaveric head, injected and non-formalin fixed was perfomed. A large right fronto-temporo-parietal craniotomy was accomplished. Extradural sphenoidal drilling till opening of the superior orbital fissure was performed. The microsurgical anatomy of basal cisternostomy was then explored.

Results: A step by step description of the surgical technique, enriched with cadaveric and intraoperative images, was made.

Conclusion: Basal cisternostomy is a promising surgical technique that does not necessarily include complex surgical maneuvers. Trained neurosurgeon can safely implement it in their clinical practice.

Keywords: severe brain trauma, decompressive craniectomy (DC), skull base, cisternostomy, cadaveric dissection

OPEN ACCESS

Edited by:
Ilgiz Fanilevich Gareev, Federal Center of Neurosurgery, Russia

Reviewed by:
Jutty Parthiban, Kovai Medical Center and Hospitals (KMCH), India
Hidehito Kimura, Graduate School of Medicine, Kobe University, Japan

Correspondence:
Lorenzo Giammattei
lore1985nch@gmail.com

Speciality section:
This article was submitted to Neurosurgery, a section of the journal Frontiers in Surgery

Received: *08 April 2022*
Accepted: *19 April 2022*
Published: *06 May 2022*

Citation:
Giammattei L., Starnoni D., Messerer M. and Daniel R. T. (2022) Basal Cisternostomy for Severe TBI: Surgical Technique and Cadaveric Dissection. Front. Surg. 9:915818. doi: 10.3389/fsurg.2022.915818

INTRODUCTION

Severe traumatic brain injury (TBI) is a life-threatening condition which is associated with substantial morbidity and mortality (1). The pathogenesis of TBI includes a primary injury related to a physical injury to the brain and a delayed secondary injury caused by the subsequent molecular, chemical and inflammatory cascades that can result in brain oedema, ischemia and intracranial hypertension. Cisternostomy is a novel surgical technique that has been proposed to prevent the development of secondary brain injury and treat associated increase in intracranial pressure (2, 3). A previous clinical study of our group (4) has showed that adjuvant cisternostomy is associated with an improved outcome (both at early and long term), improved brain oxygenation, better control of ICP and shorter ICU stay when compared to standard decompressive craniectomy (DC). A recent randomized trial by Chandra et al. (5) has also confirmed the benefit of cisternostomy in terms of outcome and ICP control when compared to standard DC. However, discordances exist between the different authors concerning the surgical technique (6). The aim of this study is to illustrate in details the surgical technique employed in our Institution with the support of cadaveric dissection and intraoperative surgical images in order to guide neurosurgeons interested in implementing this promising technique in their clinical practice.

METHODS

Surgical Case Series

The following described surgical technique has been employed in a standardized manner in a previously published retrospective surgical series of 18 patients treated with adjuvant cisternostomy (AC group) that were compared to 22 patients that underwent decompressive craniectomy (DC group) in case of severe brain trauma (4). The AC group included 13 patients that were surgically treated as primary procedure (patients presenting a unilateral mass effect lesion) and 5 patients that were treated as secondary procedure (refractory intracranial hypertension despite medical therapy). The DC group included 11 patients that treated as primary procedure and 11 patients treated as secondary procedure. The surgical procedure of the AC group included cisternostomy as an adjunct procedure to standard DC. AC was associated with significant shorter duration of mechanical ventilation and ICU stay, as well as better Glasgow coma scale at discharge. The outcome difference was particularly relevant when AC was performed as primary procedure. Patients in the AC group also had significant lower average post-surgical ICP values, higher PbO2 values and required less osmotic treatments as compared with those treated with DC alone.

Cadaveric Dissections

The anatomical dissections were performed at the neuroanatomy laboratory of the Lausanne University Hospital, Switzerland. The surgical anatomy of cisternostomy was described using 1 adult cadaveric head injected with colored latex, non formalin-fixed. The procedure was performed with standard microsurgical instruments, high-speed drill (Midas Rex; Medtronic, Minneapolis, MN, USA) and a surgical microscope (Leica Camera AG, Wetzler, Germany). The operative video was recorded using a 2D/4K camera (Karl Storz GmbH, KG, Tuttlingen, Germany) connected to the microscope. The head was fixed with a three-pins Mayfield clamp, contra laterally turned to 60 for the soft tissues dissection and craniotomy. The contralateral turn was then changed to 30 in order to perform the sphenoidal drilling and the cisternostomy. The microscope was used to perform the sphenoidal drilling, to open the basal cisterns and to place the cisternal drain. Each step of the surgical technique is described in details. Tips and tricks of each step according to the experience of our group are also presented, with accompanying cadaveric dissections and intraoperative illustrative pictures. A video illustrating in details the cadaveric dissection is also added (video 1).

SURGICAL TECHNIQUE

Positioning

The patient is placed in the supine position with 30 degrees of head elevation to decrease the intracranial pressure. The head, fixed in a skull-clap system, is contralaterally turned of 60 degree and extended in order to have the malar eminence as highest point of the specimen. During surgery the absence of jugular stenosis on both sides should be verified. This contralateral turn will facilitate the first part of surgery that approximates that of a standard trauma-flap procedure. It is important to verify that the patient is adequately secured onto the table to enable table tilt to obtain 30 degree of head turn in order to facilitate the sphenoidal drilling and the cisternal opening.

Skin Incision and Soft Tissue dissection

A frontotemporal skin incision is performed in order to give access to frontal, parietal bone and temporal bones including the anterolateral skull base. The incision often goes beyond the midline to obtain a basal craniotomy. The inferior limit of this skin incision should be at the level of the zygoma and vey next to the tragus in order to avoid injury to the branches of the facial nerve. A monolayer myocutaneous flap is elevated through subperiosteal dissection. The muscle bulk is reflected anterolaterally and kept retracted with multiple small hooks. The dissection should proceed till identification of the orbital rim, supraorbital nerve and possibly the root of the zygoma inferiorly that will give a precise idea of the position of the middle fossa floor (**Figure 1A**).

Craniotomy

Multiple burr holes are performed: one at the level of the key-hole, one anterior and one posterior to the coronal suture, paying attention to be at least 2 cm far away from the midline, one at the level of the parietal bone, one at the level of the squamous part of the temporal bone just superior to the root of the zygoma. A large craniotomy (15×12 cm in diameters) is obtained with the aid of a craniotome (**Figure 1B**). The craniotomy should be basal and the surgeon must pay attention to avoid entering the orbit. The supraorbital nerve can be considered as a good anatomical landmark to help surgeon to design a craniotomy that would allow a lateral subfrontal access. The bone flap is elevated and epidural bleeding is controlled using multiple dural tenting sutures.

Epidural Drilling

The surgical table is then modified in order to have the head turned of 30 degree to facilitate anatomical orientation for the sphenoidal drilling and the intradural phase. Considering the clinical contest of raised intracranial hypertension it is important to focus first on the last part of remaining squamous part of the temporal bone and the greater sphenoid wing. It is very important to obtain a craniotomy that is flush with the middle fossa. This will enable to relieve the pressure on the temporal lobe. The temporal dura and frontal dura are then gently dissected from the skull base avoiding unintentional pressure onto the brain. The second step of this epidural drilling is now to shave the orbital roof in order to enable the surgeon to obtain a trajectory that is parallel to the skull base thus reducing frontal lobe manipulation. The third steps consists of drilling the sphenoidal bone till exposure of the meningo-orbital band and opening of the SOF (**Figure 1C,D**).

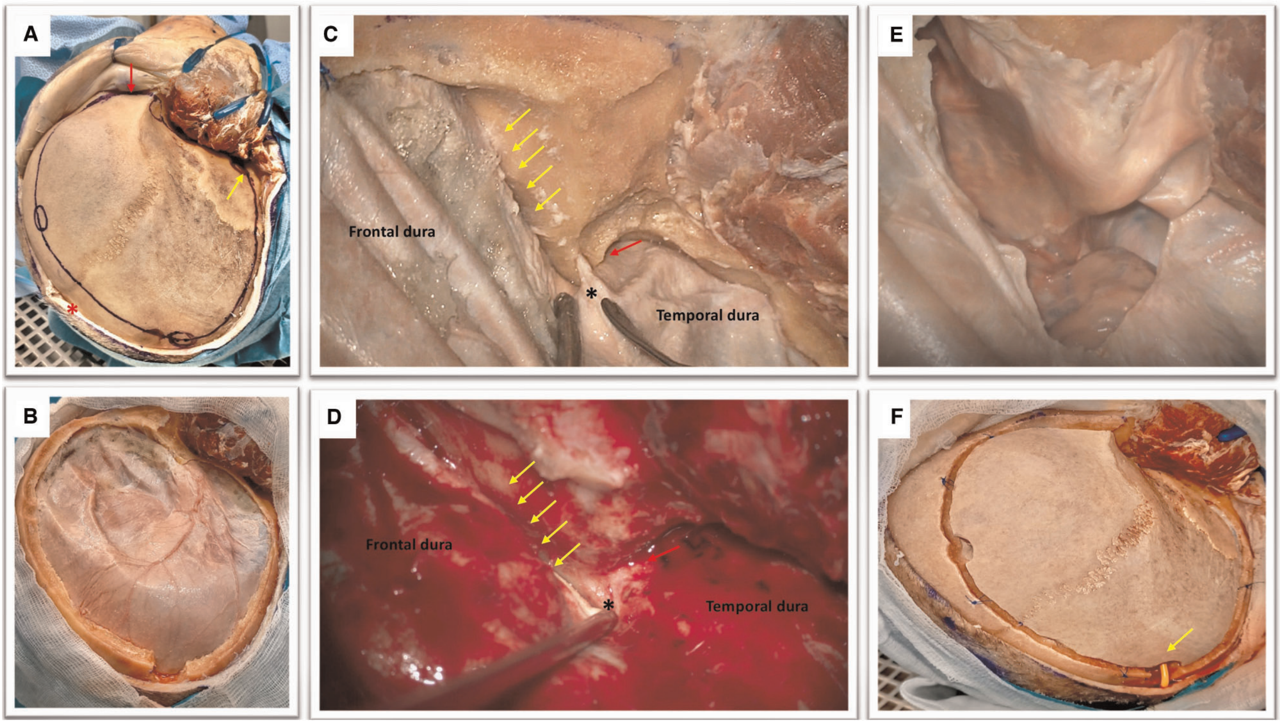

FIGURE 1 | (**A**) Cadaveric dissection obtained after the elevation of soft tissues. The temporal muscle is retracted anteriorly with multiple hooks. The coronal suture is seen as well as the fontal, parietal, the squamous part of the temporal bones, the key hole and the orbital rim (red arrow). Please note the position of the midline (red asterisk) and the root of the zygoma (yellow arrow) that can be easily palpated in order to perform a craniotomy that is flush with the middle fossa. Note that the soft tissues are dissected till obtaining a visualization of the supra-orbital nerve and the orbital rim (red arrow).This is an essential step to perform a basal craniotomy that will enable the subsequent intradural elevation of the frontal lobe. Please note the position of the frontal and parietal burr holes that should be at a proper distance from the midline (approximately 2 cm) to avoid the risk of injury to the superior sagittal sinus. The key hole has an antero-superior location with respect to the pterion and should avoid transgression of the orbit with an appropriate direction of the perforator that should point in a posterior direction. (**B**) The obtained craniotomy allows an adequate fronto-basal access that would be increased by the epidural sphenoid drilling. The remaining part of the greater wing of the temporal bone is also drilled in order to expose the middle fossa floor and rapidly provide temporal lobe decompression. (**C**,**D**) Epidural sphenoidal drilling is accomplished by flattening the skull base to obtain a lateral subfrontal access (according to the direction of the yellow arrows) and continued till the opening of the superior orbital fissure (red arrow). The meningo-orbital band is identified (black asterisk); this is a dural band that tethers the frontotemporal dura to the orbit and is attached to the lateral part of the superior orbital fissure. The epidural drilling is usually stopped at this point. (**E**) A basal durotomy is performed and this small dural flap is antero-laterally retracted to increase the skull base view. (**F**) If the bone flap is replaced, care should be taken to ensure that the subcutaneously tunneled cisternal drain is not kinked (yellow arrow).

Dural Opening

A small semicircular opening of the dura is perfomed staying close to the basal part of the craniotomy (**Figure 1E**). Dural tack-up sutures are applied in order to avoid an epidural bleeding that can perturb the intradural phase. The dura over the convexity can be opened in a later stage if needed (i.e., evacuation of an hematoma, removal of cerebral contusions) after the accomplishment of cisternostomy.

Opening of the Basal Cisterns and Lamina Terminalis

The first step is represented by obtaining a correct orientation of the operative microscope that allows a surgical view parallel to the skull base. To achieve a lateral subfrontal approach, a certain amount of frontal lobe manipulation is required. As a general rule the light of the operative microscope should be directed half on the brain and half on the skull base. The frontal lobe elevation should be performed very gently, cottonoids can be employed to protect the brain and to dry the surgical field in case of profuse intraoperative venous bleeding. It is also important to be careful with the distal part of the surgical intruments that can produce also iatrogenic contusions of the frontal lobe. Eventual component of hematoma that is on the way to the cisterns can be aspirated to reduce the intracranial pressure and facilitate the procedure. The olfactory nerve will inevitably cross the optic nerve; this is a very useful landmark to precisely localize the optic nerve and the internal carotid artery. The first cistern to be addressed is the optico-carotid cistern. Once the optico-carotid cistern has been opened the microscope should be oriented in a more antero-posterior direction in order to expose and open the Liliequist's membrane (2A). The Liliequist's membrane is usually composed by two leaves: the diencephalic and the

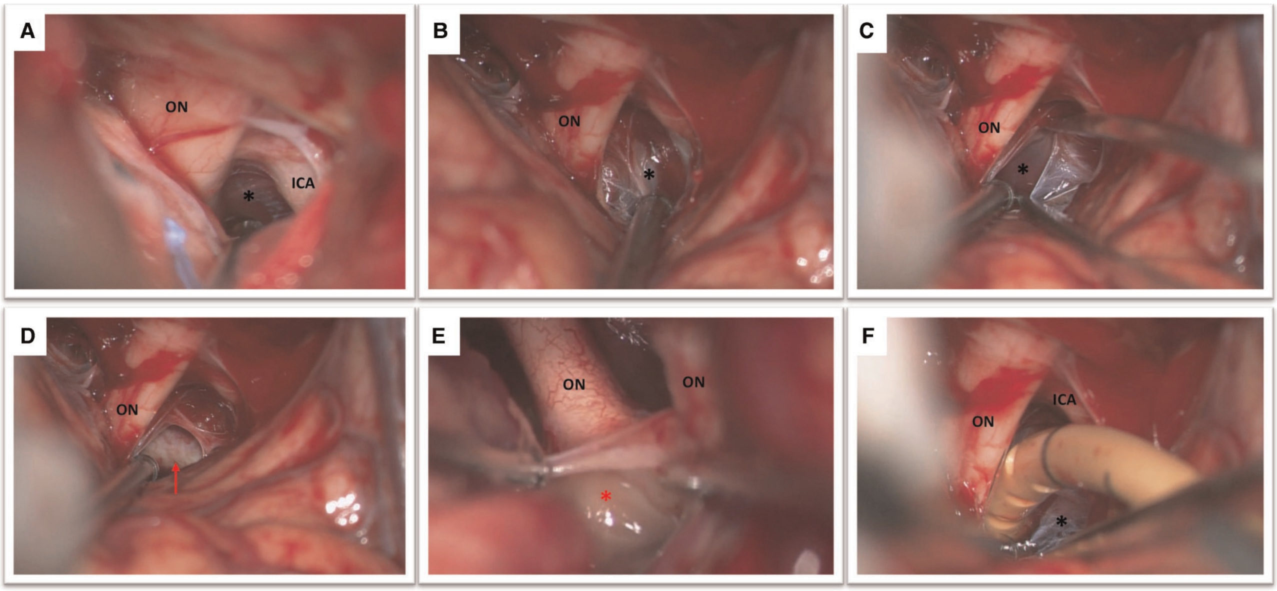

FIGURE 2 | (**A**) This figure shows the view obtained after the opening of the optico-carotid cistern with optic nerve (ON), internal carotid artery (ICA) and Liliequist's membrane (black asterisk). (**B**) The optic nerve (ON) and the diencephalic leaf of the Liliequist's membrane (black asterisk) are seen. (**C**) The diencephalic leaf is opened enabling the exposure of the mesencephalic leaf (black asterisk). (**D**) The dorsum sellae (red arrow) becomes clearly visible (**E**) Both optic nerves and the lamina terminalis (red asterisk) are visible in this picture. (**F**) Note the position of the catheter which is placed in between the optic nerve (ON) and the internal carotid artery (ICA) passing through Liliequist's membrane (black asterisk) into the prepontine cistern.

mesencephalic one (**Figure 2B–E**). The homolateral optic nerve should be followed posteriorly onto the chiasm and optic tract to identify and open the lamina terminalis (**Figure 2E**). A gentle mobilization of the homolateral A1 segment is in general required to perform this last task.

Cisternal Drain Positioning

A standard EVD drain is first subcutaneously tunneled and then the drain is inserted under the microscope at the level of the optico-carotid cistern possibly reaching the prepontine cistern. The position of the drain (the distal end) is verified under the microscope (**Figure 2F**). It is important to verify that it is effectively placed inferior to the level of the dorsum sellae, which would reduce drain displacement. As soon as the drain is correctly positioned the proximal part of the catheter need to be stitched to the skin to avoid inadvertent drain displacement. The bone flap can be replaced in case of a lax brain obtained at the end of the procedure also in accordance with Institutional Protocol (**Figure 1F**).

Post-Operative Course

A postoperative CT scan is usually performed the day after surgery. We usually set the drainage in order to obtain around 5–10 cc of CSF per hour for 5–7 days after the surgical procedure. The amount of drainage can be adapted also according to the post-operative values of ICP. The amount of CSF drainage is gradually decreased and the cisternal drain is removed usually 7 days after surgery.

DISCUSSION

Cisternostomy represents a novel surgical strategy to treat severe TBI. There are now several publications that show encouraging results for cisternostomy over traditional methods of treatment for sTBI (4, 5, 7). Different surgical techniques have been described in the literature some including an extradural anterior clinoidectomy (and posterior clinoidectomy in some cases) (8) and other less aggressive ones (4, 5). However, there has an undue emphasis given to the complexity of the surgical approach which has generated resistance to this technique within the neurosurgical community, that is essentially undeserved (9). Therefore it is essential that this surgical technique is demystified. Based on the experience of our previously published surgical series we aimed to illustrate in details the surgical technique that is commonly used in our Institution. As presented in the cadaveric dissection and the illustrative intraoperative images, the first part of the surgery consists of a "trauma flap" in order to perform a fronto-temporo-parietal craniotomy/craniectomy that is extended till the middle fossa floor to ensure temporal lobe bony decompression (10). As illustrated in the figures and videos we routinely stop the extradural drilling at the level of the superior orbital fissure. In our experience performing an extradural anterior clinoidectomy is usually not necessary as also reported by other authors (7). The surgical technique of performing an extradural anterior clinoidectomy (EAC) demands specific technical skills, takes a certain amount of time that makes it poorly suitable in a context of urgent surgery and moreover can lead to well described complications in terms of vascular injury, thermic injury to the optic nerve, third nerve palsy and CSF leak (11). A proper basal craniotomy and a rapid extradural sphenoidal drilling till the superior orbital fissure can be rapidly accomplished with an acceptable extra-time of approximately 15–20 min when compared to a standard trauma flap. This slight increase in terms of amount of time has been found also by Chandra et al. (5). It is to be specified that this increased time includes the extradural sphenoidal drilling and the intradural phase of cisternal opening and positioning of the cisternal drain. An enough basal craniotomy, in general allows (12) access to the optico-carotid cistern, following the opening of which, the brain becomes much less tense and allows to complete the rest of the procedure. However, access to the cisterns is more challenging in case of a secondary surgical procedure (patients with refractory intracranial hypertension despite maximal medical therapy), and these cases may require increased surgical expertise and extradural work. The durotomy is also a critical step while dealing with surgeries for intracranial hypertension. Large durotomies will result in brain herniation with potential venous kinking and lacerations of the cortex on the bone edge and secondary brain injury leading to further brain swelling (13–15). To avoid these issues and to render possible an early access to the cisterns, it is mandatory to start with a very basal durotomy in proximity to the optico-carotid cistern. This small durotomy will avoid brain herniation and would leave the vast majority of the frontal lobe covered by the dura thus reducing iatrogenic contusions. If indicated, this small basal durotomy can be enlarged to access other lesions placed more posteriorly like hematomas or contusions. The opening of the Liliequist's membrane allows a communication between the supratentorial and infratentorial basal cisterns. The anatomy of this membrane could be variable as nicely illustrated by Froelich et al. (16). Essentially three main configurations can be identified: one with a single membrane that starts from the arachnoid covering the dorsum sellae and ends between the infundibulum and mammillary bodies, one with a diencephalic leaf and a mesencephalic leaf that run in a separate course and the last one with a single membrane in the anterior part separating in two leaves in the posterior part. The dissection is then continued with the opening of the lamina terminalis that is part of our surgical technique and represents a modification of the initial technique as described by Cherian et al. (8). We believe that this surgical maneuver is important because it allows to drain both the ventricular and cisternal CSF thus resulting in a more efficient drainage, approximately a mean of 200 mL/day, as presented in our previous study. Moreover clinical experience from subarachnoid hemorrhage has showed that the fenestration of both lamina terminalis and Liliequist's membrane is associated with a statistically significant reduction of shunt dependent hydrocephalus, probably because this maneuver relieve obstruction to CSF flow creating an alternative flow pathway (17). The final step of the procedure is represented by the positioning of a standard EVD catheter into the cisternal compartment under microscopic view. We introduce the drain into the optico-carotid cistern and then gently advance it towards the prepontine cistern. The decision to leave out or replace the craniotomy bone flap is open to interesting reflections. Although promising results have been published with cisternostomy as a stand-alone treatment (3, 5, 7), uncertainties are still present given the limited published clinical experience. A reasonable way to proceed would be not to replace the bone flap if the brain does not achieve a complete relaxation after cisternostomy or in case of borderline situations. This should also be done in accordance with Insitutional Protocols. In case of primary procedure, after the evacuation of a mass effect lesion (acute subdural hematoma) the decision whether to replace the bone flap or not is actually based on clinical and intraoperative parameters (18) and still subject to uncertainties that will be possibly clarified by the awaited results of the RESCUE-ASDH trial. The potential advantages of replacing the bone flap at the primary surgery avoids a future cranioplasty that have been reported to be associated with complications like infections, reoperations, extra-axial fluid collection, bone flap resorption and, scalp necrosis (19). In cases of surgery where cisternostomy is performed as a secondary procedure, the bone flap replacement is not always possible due to a more severe brain oedema in these patients. Results of all surgical therapies in this group are suboptimal. This is possibly a reflection of the severity of the trauma and a possible delay in treatment. Further clinical studies need to be done to critically evaluate the true benefits of maximal medical therapy and essentially determine the ideal timing of surgery.

CONCLUSION

Cisternostomy represents a promising surgical technique in the setting of severe brain trauma. We present here a step-by-step description of the surgical anatomy along with cadaveric dissection to illustrate this technique. EAC and other complex surgical maneuvers are not usually required. The surgical procedure can be safely achieved in the majority of cases by surgeons who have had a basic neurosurgical training.

DATA AVAILABILITY STATEMENT

The original contributions presented in the study are included in the article/Supplementary Material, further inquiries can be directed to the corresponding author/s.

AUTHOR CONTRIBUTIONS

LG: Conception and design, drafting of the paper, critically revising the paper, editing of video. DS: Drafing of the paper, critically revising the paper, editing of figures. MM: critically revising the paper, study supervision. RD: conception and design, critically revising, supervision of the study. All authors contributed to the article and approved the submitted version.

REFERENCES

1. Peeters W, van den Brande R, Polinder S, Brazinova A, Steyerberg EW, Lingsma HF, et al. Epidemiology of traumatic brain injury in Europe. *Acta Neurochir (Wien)*. (2015) 157(10):1683–96. doi: 10.1007/s00701-015-2512-7
2. Cherian I, Yi G, Munakomi S. Cisternostomy: replacing the age old decompressive hemicraniectomy? *Asian J Neurosurg*. (2013) 8(3):132–8. doi: 10.4103/1793-5482.121684
3. Giammattei L, Messerer M, Oddo M, Borsotti F, Levivier M, Daniel RT. Cisternostomy for refractory posttraumatic intracranial hypertension. *World Neurosurg*. (2018) 109:460–3. doi: 10.1016/j.wneu.2017.10.085
4. Giammattei L, Starnoni D, Maduri R, Bernini A, Abed-Maillard S, Rocca A, et al. Implementation of cisternostomy as adjuvant to decompressive craniectomy for the management of severe brain trauma. *Acta Neurochir (Wien)*. (2020) 162(3):469–79. doi: 10.1007/s00701-020-04222-y
5. Ramesh Chandra VV, Bodapati Chandra Mowliswara P, Banavath HN, Kalakoti CSR. Cisternostomy vs decompressive craniectomy for the management of traumatic brain injury: a randomized controlled trial. *World Neurosurg*. (2022) 19:S1878-8750(22)00214-5. doi: 10.1016/j.wneu.2022.02.067
6. Volovici V, Haitsma IK. Cisternostomy in traumatic brain injury: time for the world to listen–cerebrospinal fluid release: possibly the missing link in TBI. *World Neurosurg*. (2022) 162:3–5. doi: 10.1016/j.wneu.2022.02.121
7. Parthiban JKBC, Sundaramahalingam S, Rao JB, Nannaware VP, Rathwa VN, Nasre VY, et al. Basal cisternostomy - a microsurgical cerebro spinal fluid let out procedure and treatment option in the management of traumatic brain injury. Analysis of 40 consecutive head injury patients operated with and without bone flap replacement following cisternostomy in a tertiary care centre in India. *Neurol India*. (2021) 69(2):328–33. doi: 10.4103/0028-3886.314535
8. Cherian I, Bernardo A, Grasso G. Cisternostomy for traumatic brain injury: pathophysiologic mechanisms and surgical technical notes. *World Neurosurg*. (2016) 89:51–7. doi: 10.1016/j.wneu.2016.01.072
9. Di Cristofori A, Gerosa A, Panzarasa G. Is neurosurgery ready for cisternostomy in traumatic brain injuries? *World Neurosurg*. (2018) 111:427. doi: 10.1016/j.wneu.2017.11.139
10. Hutchinson PJ, Kolias AG, Tajsic T, Adeleye A, Aklilu AT, Apriawan T, et al. Consensus statement from the international consensus meeting on the role of decompressive craniectomy in the management of traumatic brain injury : consensus statement. *Acta Neurochir (Wien)*. (2019) 161(7):1261–74. doi: 10.1007/s00701-019-03936-y
11. Kulwin C, Tubbs RS, Cohen-Gadol AA. Anterior clinoidectomy: description of an alternative hybrid method and a review of the current techniques with an emphasis on complication avoidance. *Surg Neurol Int*. (2011) 2:140. doi: 10.4103/2152-7806.85981
12. Giammattei L, Messerer M, Belouaer A, Daniel RT. Surgical outcome of tuberculum sellae and planum sphenoidale meningiomas based on Sekhar-Mortazavi Tumor Classification. *J Neurosurg Sci*. (2021) 65(2): 190–9. doi: 10.23736/S0390-5616.18.04167-X
13. Alves OL, Bullock R. « Basal durotomy » to prevent massive intra-operative traumatic brain swelling. *Acta Neurochir (Wien)*. (2003) 145(7):583–6; discussion 586. doi: 10.1007/s00701-003-0055-9
14. Jiang Y-Z, Lan Q, Wang Q-H, Song D-L, Lu H, Wu W-J. Gradual and controlled decompression for brain swelling due to severe head injury. *Cell Biochem Biophys*. (2014) 69(3):461–6. doi: 10.1007/s12013-014-9818-6
15. Shi L, Sun G, Qian C, Pan T, Li X, Zhang S, et al. Technique of stepwise intracranial decompression combined with external ventricular drainage catheters improves the prognosis of acute post-traumatic cerebral hemispheric brain swelling patients. *Front Hum Neurosci*. (2015) 9:535. doi: 10.3389/fnhum.2015.00535
16. Froelich SC, Abdel Aziz KM, Cohen PD, van Loveren HR, Keller JT. Microsurgical and endoscopic anatomy of Liliequist's membrane: a complex and variable structure of the basal cisterns. *Neurosurgery*. (2008) 63(1 Suppl 1): ONS1-8; discussion ONS8-9. doi: 10.1227/01.neu.0000335004.22628.ee
17. Winkler EA, Burkhardt J-K, Rutledge WC, Rick JW, Partow CP, Yue JK, et al. Reduction of shunt dependency rates following aneurysmal subarachnoid hemorrhage by tandem fenestration of the lamina terminalis and membrane of Liliequist during microsurgical aneurysm repair. *J Neurosurg*. (2018) 129(5):1166–72. doi: 10.3171/2017.5.JNS163271
18. Ruggeri AG, Cappelletti M, Tempestilli M, Fazzolari B, Delfini R. Surgical management of acute subdural hematoma: a comparison between decompressive craniectomy and craniotomy on patients treated from 2010 to the present in a single center. *J Neurosurg Sci*. (2022) 66(1):22–7. doi: 10.23736/S0390-5616.18.04502-2
19. Cho YJ, Kang SH. Review of cranioplasty after decompressive craniectomy. *Korean J Neurotrauma*. (2017) 13(1):9–14. doi: 10.13004/kjnt.2017.13.1.9

Conflict of Interest: The authors declare that the research was conducted in the absence of any commercial or financial relationships that could be construed as a potential conflict of interest.

frontiers | Frontiers in Surgery

PERSPECTIVE
published: 10 May 2022
doi: 10.3389/fsurg.2022.900986

Application of Intraoperative Ultrasound Navigation in Neurosurgery

Keith Simfukwe[1,2]*, *Iurii Iakimov*[1,2], *Rinat Sufianov*[2], *Luís Borba*[2,3], *Luciano Mastronardi*[2,4] and *Alina Shumadalova*[5]

[1] Federal Center of Neurosurgery, Tyumen, Russia, [2] Department of Neurosurgery, Sechenov First Moscow State Medical University (Sechenov University), Moscow, Russia, [3] Department of Neurosurgery, Federal University of Paraná, Curitiba, Brazil, [4] Division of Neurosurgery, San Filippo Neri Hospital, Roma, Italy, [5] Depatment of General Chemistry, Bashkir State Medical University, Ufa, Russia

Effective intraoperative image navigation techniques are necessary in modern neurosurgery. In the last decade, intraoperative ultrasonography (iUS), a relatively inexpensive procedure, has gained widespread acceptance.

Aim: To document and describe the neurosurgery cases, in which iUS has been employed as the primary navigational tool. This includes a discussion of the advantages that iUS may possess relative to other forms of neuronavigation.

Conclusion: The application of iUS as an intraoperative navigation tool during neurosurgery holds great potential as it has been shown, relative to other neuronavigation techniques, to be quick, repeatable, and able to provide real-time results.

Keywords: ultrasonography, navigation, neurosurgery, epilepsy, glioma

OPEN ACCESS

Edited by:
Ozal Beylerli,
Federal Center of Neurosurgery, Russia

Reviewed by:
Bipin Chaurasia,
Neurosurgery Clinic, Nepal
Andrey Tulupov,
International Tomography Center (RAS), Russia

Correspondence:
Keith Simfukwe
keithsimfukwe@gmail.com

Specialty section:
This article was submitted to Neurosurgery, a section of the journal Frontiers in Surgery

Received: *21 March 2022*
Accepted: *04 April 2022*
Published: *10 May 2022*

Citation:
Simfukwe K, Iakimov I, Sufianov R, Borba L, Mastronardi L and Shumadalova A (2022) Application of Intraoperative Ultrasound Navigation in Neurosurgery. Front. Surg. 9:900986. doi: 10.3389/fsurg.2022.900986

INTRODUCTION

The ideal intraoperative navigational modality for neurosurgeons is the one that is accurate, user-friendly, and most of all cost-efficient (1–4). Over the last two decades, the most reliable and frequently used intraoperative navigational tools include intraoperative computed tomography (iCT) and intraoperative magnetic resonance imaging (iMRI), with the latter being deemed the "golden standard" (5–7). Despite the effectiveness of the aforesaid intraoperative tools, neurosurgeons still face challenges in the acquisition and use of iCT and iMRI. These challenges include the following: (1) Enormous costs in the acquisition of these tools, especially in low-budget neurosurgical centers and developing countries; (2) Heavy dependence on acquired pre-operative images; (3) At every stage of the procedure; post craniotomy, dural opening, tumor debulking, and resection, the element of brain shift results in varying degrees of loss of accuracy; (4) Inherent lack of soft-tissue resolution and the associated radiation exposure like in the case of iCT. To circumvent these hurdles, more innovative, convenient, and novel generation modes of Intraoperative sonography or ultrasound (iUS) systems have been developed. The iUS is comparatively inexpensive, easy to use, and requires less intraoperative preparation. The two-dimensional (2D) greyscale and three-dimensional (3D) iUS provide real-time, clear, and well-correlated images, which are easily interpreted by the neurosurgeon. Additionally, the ease and flexibility it provides the user make it possible to counter-check the location of the lesion at any stage of the surgery without prolonged workflow stoppages (8). This, therefore, solves the element of brain shift. The iUS does not require pre-existing images before surgery. However, there is a necessity to save the initial image scanned to serve as a baseline check during the surgery.

TABLE 1 | Survey on the applicability of IUS in neurosurgery as a neuronavigation tool.

Participants (41) Country (15) — **Russia (20), Spain (5), Zambia (3), India (2), Algeria (1), Costarica (1), France (1), Greece (1), Iraq (1), Kyrgystan (1), Nepal (1), Uzbekistan (1), Ethiopia (1), Mongolia (1), Palestine (1)**

Questions	Yes	No	ST	N	IDK	G	B	VT	NTL	F	X	Ius	CT	Mri	N	Fmri	Non
Q1. Familiar with neuro-Imaging tools										41.5	68.3	73.	53.7	43.9	78	43.9	2.4
Q2. Neuron Imaging tools are available in facilities										56.1	80.5	78	53.7	41.7	78	53	2.4
Q3. Do you use Intraoperative neuroimaging during brain tumor surgery	51.2	17.1	31.7														
Q4. Have you experienced brain shift during tumor brain surgery*	41.5	19.5	26.8	2.4	9.8												
Q5. Are you familiar with ultrasound intraoperative neuroimaging during brain tumor surgery?	81.8	19.2															
Q6. Dose the use of intraoperative ultra sound neuro imaging improve tumor resection outcome?	73.2	4.9	22														
Q7. How would you grade the use of intraoperative ultrasound neuoimaging during brain tumor surgery?						90.3	9.7										
Q8. How long dose did it take you to learn and apply usage of intraoperative ultrasound?								58.5	41.5								
Q9. How long dose it take to apply usage of intraoperative ultrasound during a procedure?								29.2	70.8								
Epilepsy surgery		GTR	STR	B	NA												
Q10. Do you manage patients with intractable epilepsy?		34.1	17.1														
Q11. Do you use intraoperative neuroimaging during epilepsy surgery?	48.8	39	17.1														
Q12. Have you used intraoperative ultrasound neuroimaging during epilepsy surgery?	43.9	53.7	14.6														
Q13. How would you grade the EOR with aid of intraoperative ultrasound neuroimaging during epilepsy surgery?	31.7									53.6	4.9	4.9	36.6				

St, Sometimes; N, never; IDK, I don't Know; G-Good; B, Bad; NVT, long time; VT, very long time; F, fluoroscopy ; X, X-ray; IUS, intra operative ultrasound; CT, computer temography; EOR , extent of resection; GTR, Gross total resection; STR, subtotal resection; B, biopsy; NA, not attempted.

**Brain shift is the change of a brain lesion position from it's original anatomically located point on MRI. All results are in percentages.*

In this narrative, we reclaiming these findings by outlining our center (Federal Center of Neurosurgery, Tyumen, Russia) experience in the use of iUS during brain, spine, vascular, and epilepsy surgery. We do this by highlighting technical nuances and discussing, with illustrative cases, the spectrum of applications and benefits. Finally, we descriptively evaluate neurosurgeons' experience in using iUS as a neuronavigation tool.

METHODOLOGY

We took a retrospective approach for this investigation, and it involved the extraction of data from a facility database on neurosurgical procedures that were performed between 2015 and December of 2021 at the Federal Center of Neurosurgery, Tyumen Russia. The key criterion for inclusion in the investigation was the documented intraoperative application of iUS during elective surgery. The investigators reviewed a total of 1,330 patient records, with documented brain and spinal lesions. In addition, we also assessed neurosurgeon's experience with the use of intraoperative ultrasound as a neuroimaging through the application of an online survey tool the following link: https://docs.google.com/forms/d/e/1FAIpQLSfqHcExcft3FwcTKiKb2A0b5i828UhnoXe1smoXPDIdH6_g/viewform?usp=sf_link (**Table 1**).

Abbreviations: iUS, intraoperative ultrasonography; iMRI, intraoperative magnetic resonance imaging; iCT, intraoperative computed tomography; LMIC, low-&-middle-income countries; MIC, middle-income countries; HIC, high-income countries; CSF, cerebral spinal fluid; FCD, focal cortical dysplasia; AVM, arteriovenous malformation; LGG, low grade glioma; HGG, high-grade gliomas.

Equipment and Technical Modality

We employed a FlexFocus 800 iUS [BK Medical, Denmark for three-dimensional (3D)] iUS neuro-navigation. We applied a Linear-type and convex transducer (**Figure 1B**; high-frequency Linear 8870), as well as a craniotomy sensor (Craniotomy 8862). We use a frequency of 3.8–10 MHz, a contact surface of 29 × 10 mm. The iUS was done in coronal, sagittal, and axial planes.

Anatomically consistent reference points, as mentioned above, were used for the localization of the lesions. The interpretation of anatomical features on iUS was described by their respective echogenicity reflections' tissue consistency. We described spaces that had no echogenicity, such as ventricles/ CSF spaces as anechogenic. Hypoechoic features were defined in spaces with less echogenicity, such as the brainstem. Isoechogenic structures included the normal brain tissue (white matter) and conversely hyperechoic in tissues with high enchogenicity, such as in gliomas, calcifications, meningiomas, and vascular anatomical structures, such as the choroid plexus (**Figure 2**). Imaging characteristics on iUS were compared with pre- and post-operative CT or MRI images available to assess for concordance.

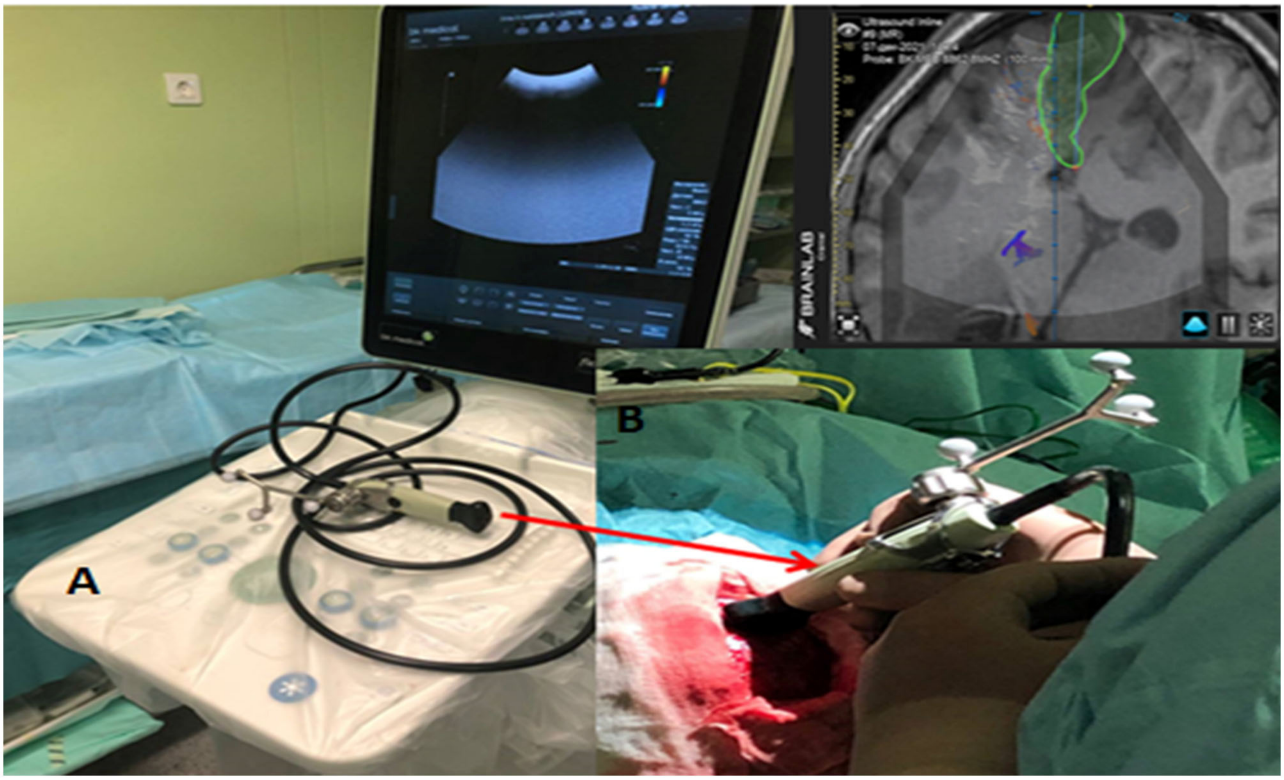

FIGURE 1 | (A) iUS Apparatus - BK Medical flex focus 800 (Denmark) with Sterile convex transducer. **(B)** Integrated Brain lab neuronavigation system (Germany).

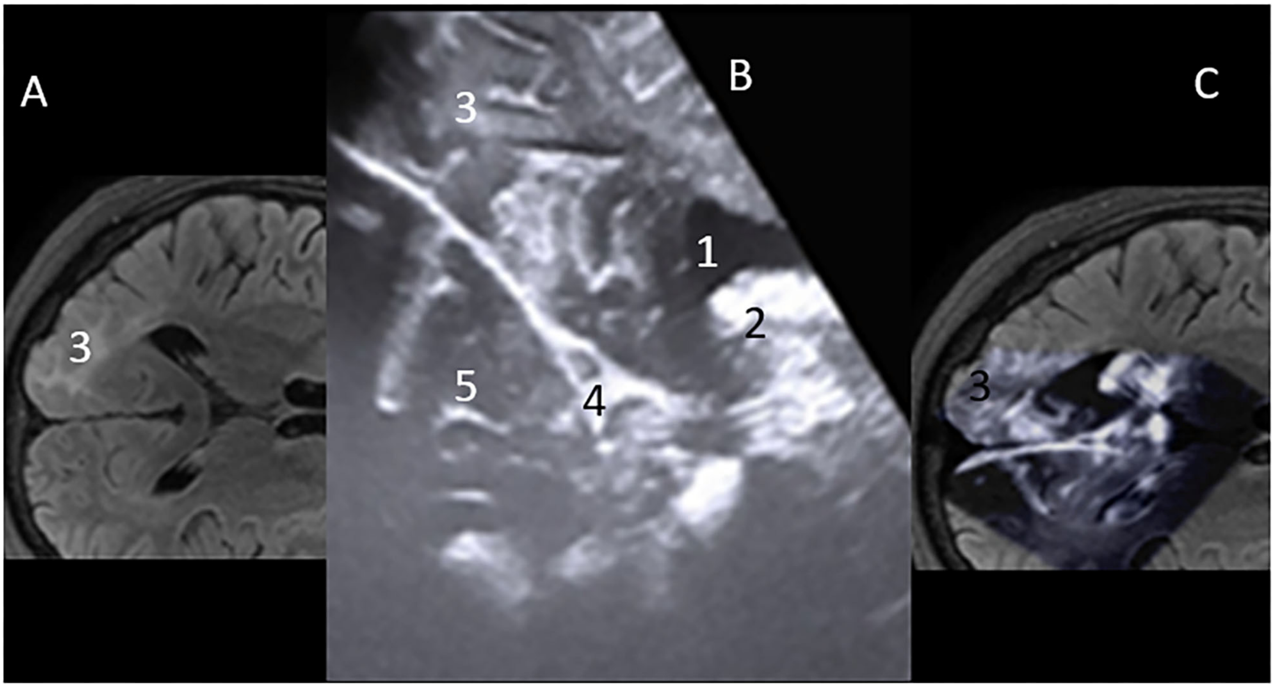

FIGURE 2 | (A) MRI – flair axial view of Rt occipital lobe Focal cortical dysplasia (FCD) lesion-3. **(B)** Mirror iUS Axial view of Rt occipital lobe FCD lesion-3. Cerebral spinal fluid (CSF) in ventricle occipital horn is "Hypoechoic" on iUS-1; "Hyperechoic" futures vascular stuctures, high grade tumors. Here, the choroid plexis is hyperechoic-2. Falx- 4. Normal brain tissue on iUS is "isoechoic"-5. **(C)** Projection on the intraoperative Ultrasound Concordance of lesion location on MRI and iUS.

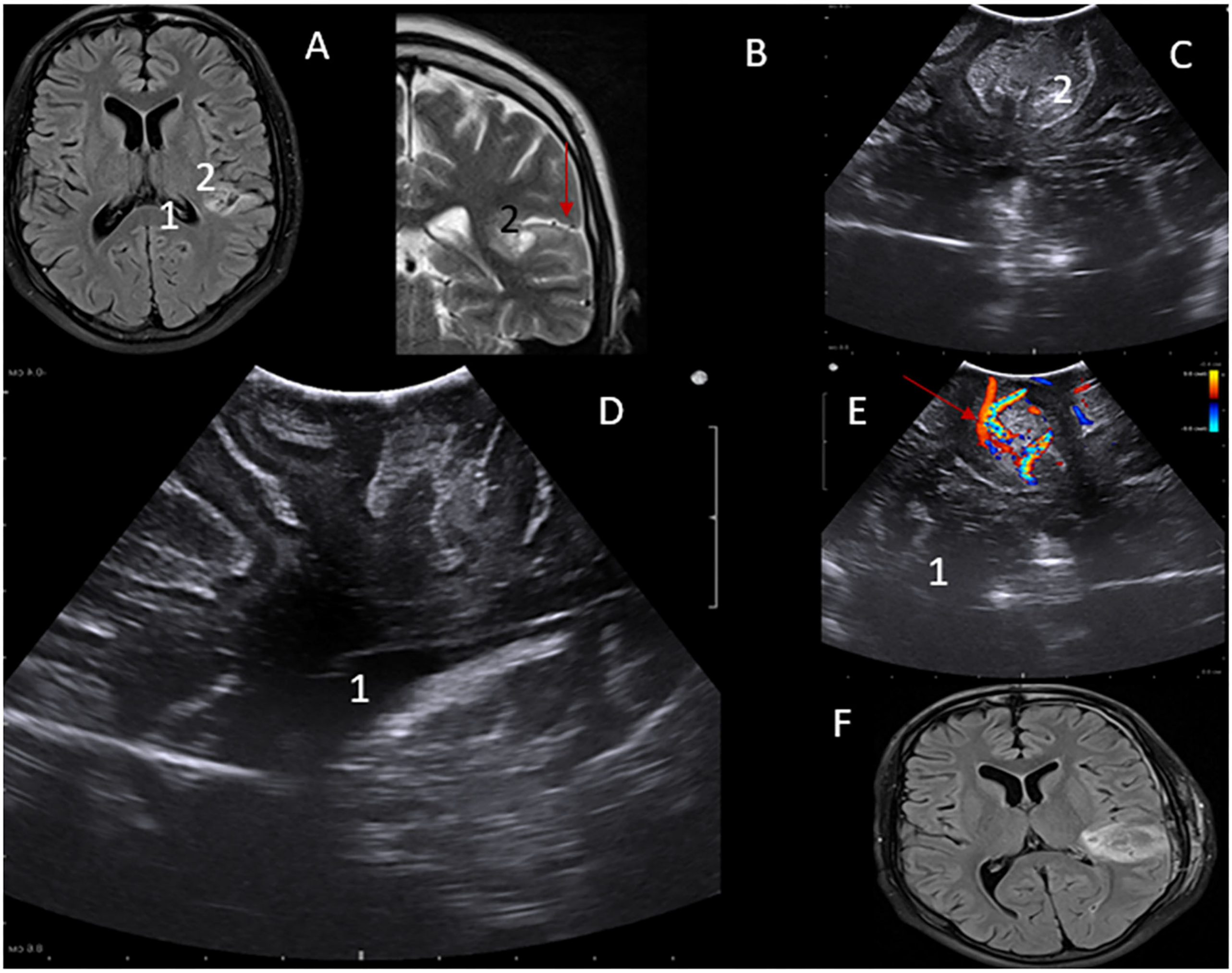

FIGURE 3 | (A) MRI – flair axial view of Lt parital lobe lesion- 1. **(B)** MRI – T2WI MRI coronal view of Lt parietal lobe lesion- 2. iUS depiction of low-grade lesion in axial. **(C,D)** Saggital views Perilesional vascular structures can be visualized using Color Doppler function-Red arrow **(A,E)**. Post-operative MRI showing gross total resection of the lesion **(F)**.

RESULTS

Survey on the Applicability of iUS in Neurosurgery as a Neuronavigation Tool

There are 41 neurosurgeons, 33 males, and eight females, from 15 countries, 12 of whom were from low-and-middle-income countries (LMIC), while three were from middle-income (MIC) and high-income countries (HIC). Regarding years of experience, 73.8% had, at most, 5 years of working experience as neurosurgeons, being relatively junior residents, while 26.2% had at least 6 years of working experience, being individuals at the registrar to consultant professor level.

iUS-Navigated Neurosurgical Cases

All the surgeries were performed by Professor Albert Sufianov at the Federal Center of Neurosurgery, Tyumen, Russia, with the assistance of the same surgical team. Intraoperative ultrasonography was performed after the craniotomy, both before and after opening the dura mater.

Supratentorial Low-Grade Glioma

Low-grade subcortical gliomas can be difficult to locate after the dura mater has been opened. However, as shown in **Figure 3**, LGG are readily identified, and their margins are well-defined by intraoperative ultrasound regardless of pre-operative imaging patterns. This enhances intraoperative lesion delineation and the extent of resection. Features of lesion-vascular interactions and landscape can be also demonstrated while localizing lesions, a vital component for undesirable hemorrhage avoidance.

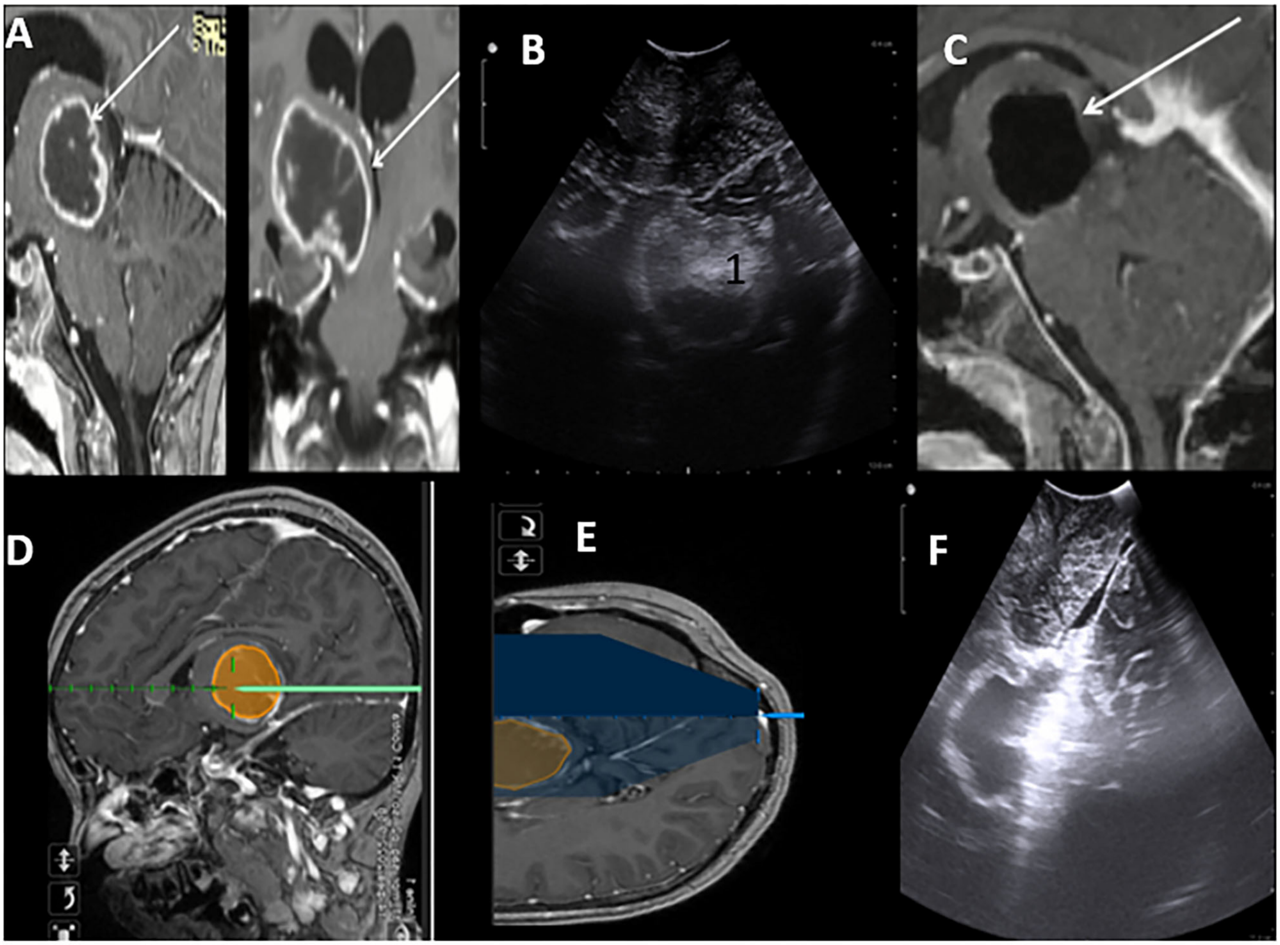

FIGURE 4 | Post Contrast MRI T1WI Sagittal and Coronal sections suggestive of high-grade thalamic glioma (HGG) with cystic central cystic component **(A)**. Brain lab navigation system depicting trajectory to the lesion **(D,E)**. iUS Axil section depicting thalamic hyperechoic lesion **(B)**. Post-resection iUS Sagital section depicting wall of the cavity after complete resection **(F)**. MRI in concordance with ius showing gross total resection of the HGG **(C)**.

Deep High-Grade Gliomas

One of the key challenges during the surgical treatment of high-grade gliomas is the achievement of the optimum balance between maximizing the resection of the lesion and minimizing the effect on healthy tissue (and any potential neurological impairment). It is in this regard that iUS demonstrates one of its key strengths in being able to provide real-time information on the lesion's location and boundaries. On iUS, they demonstrate varying levels of echoicity and are normally heterogenic. Despite being able to detect deep HGGs, intraoperative evaluation of the extent of resection of deep high-grade gliomas may be challenging when in B-mode iUS. This is because both malignant tumor tissue and peritumoral edema are hyperechoic (**Figure 4F**). This poses a notable disadvantage compared to iMRI. It is for this reason that we still advocate for early post-operative MRI images and clinical (at 3 and 6 months, then once a year) follow-up to rule out a residual tumor.

Intraventricular Lesions

In **Figures 5**, **6**, we illustrate two cases of lateral and fourth ventricular lesions resected with iUS guidance along with Bain lab neuronavigation. As illustrated, iUS can be used to highlight even deep-seated brain lesions, to show their relationships with surrounding neural and vascular structures, and to provide real-time and dynamic imaging. As in the previously described cases, the probe is placed over the dura to acquire standard B-mode imaging scans. The lesion is identified on the two axes and is measured. The iUS with brain lab integration, gives greater details of the dimensions of the lesion, about the normal cortical structure during each stage of the procedure, and, therefore, abetting the element of brain shift (**Figures 5C–E**). Even within narrow and deep corridors to the fourth ventricle, lesion dimensions can be captured on the coronal and sagittal axis. Intricate lesion-anatomical structure interrelations of the fourth ventricle can be clearly defined (**Figures 6, 7**).

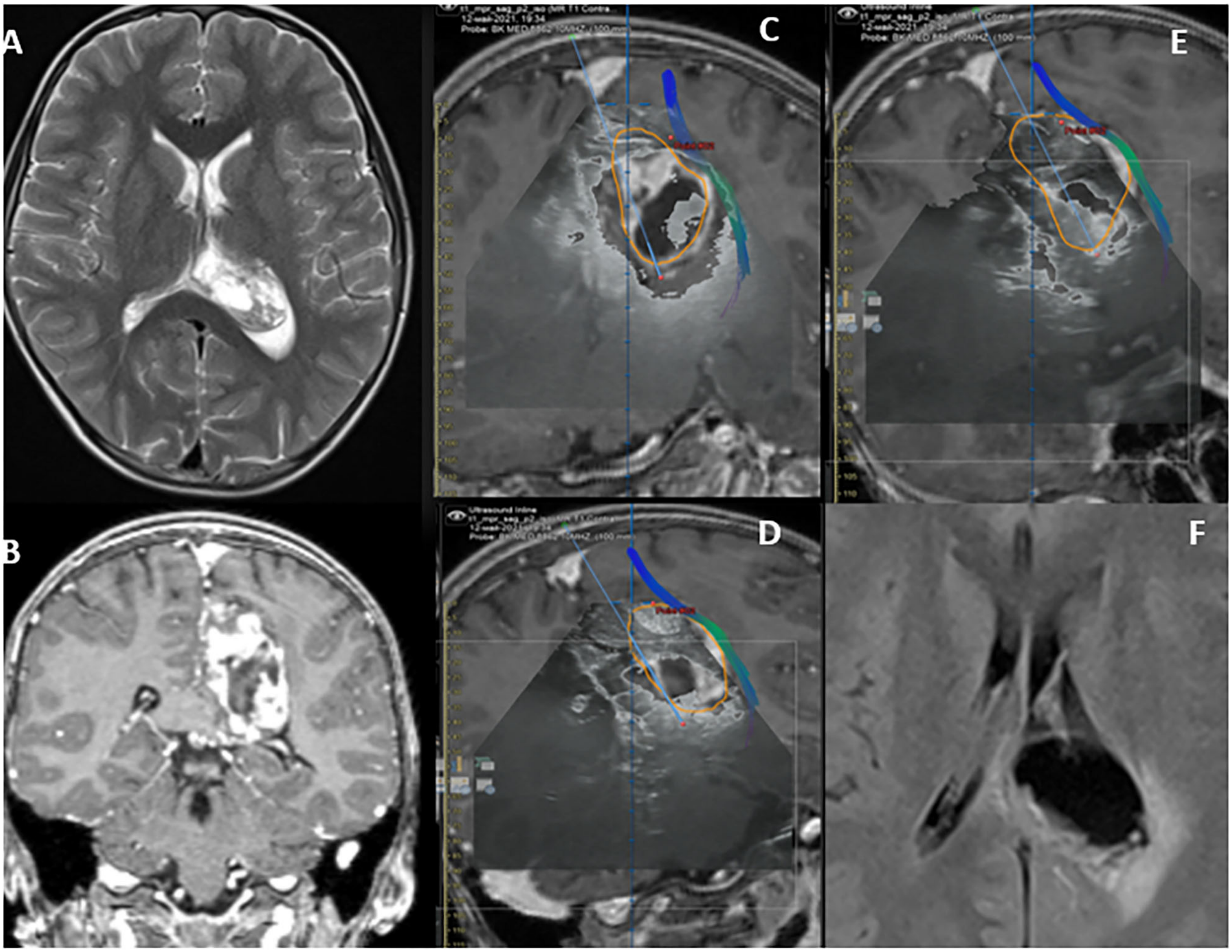

FIGURE 5 | MRI T2 WI Axial parietal- intraventricular cystic lesion **(A)**. Heterogeneous enhancing on T1WI-C as depicted on its coronal section **(B)**. The lesion boundaries are depicted in orange on **(C–E)**, illustrating "Brain shift." Lesion in close proximity with the cortical spinal tracts. Plain axial post-operative TIWI depicting complete resection of the lesion.

Vascular Lesions

Arteriovenous Malformation

The iUS can be used to visualize a range of vascular abnormalities, including arteriovenous malformations (AVM). We illustrate our experience in a case of a 17-year-old female who presented with seizures and worsening headaches. Preliminary CT and MRI were suggestive of a 4-cm left occipital AVM (Spetzer Martin Grade 3). The iUS's Doppler mode allows for the precise imaging of arterial feeders and venous drainage. This mode is extremely valuable in AVM surgery because it depicts vascular flow in real-time. Locating the main arteries and veins of a tumor, as well as the patency of the venous sinuses and proof of the tumor's vascularity, aids in safe removal (**Figure 8**).

Spinal Lesions

The iUS is fairly useful for determining the level and localizing the lesion during spine surgery. We have had remarkable success using iUS for both extramedullary and intramedullary lesions, such as neurofibromas, ependymomas, and astrocytomas, in both extramedullary and intramedullary settings. The iUS can be used to safely aid and remove tumor successfully through the surgery, without disturbing the flow of surgery. The iUS made it easier to confirm tumor location and extension, plan myelotomy, and estimate the extent of the lesion (**Figure 9**).

Epilepsy Neurosurgery

One of the most common causes of drug intractable epilepsy is focal cortical dysplasia (FCD). In epilepsy surgery, considering that normal and dysplastic brain tissues are often indistinguishable, we have utilized iUS to localize epileptogenic lesions and, thereby, improve surgical outcomes. Cortical characteristics demonstrated perfect concordance between iUS (thickness and hyper-echoic of cortex, subcortical white matter) and MRI T2-weighted/FLAIR images (hyperintense cortical and

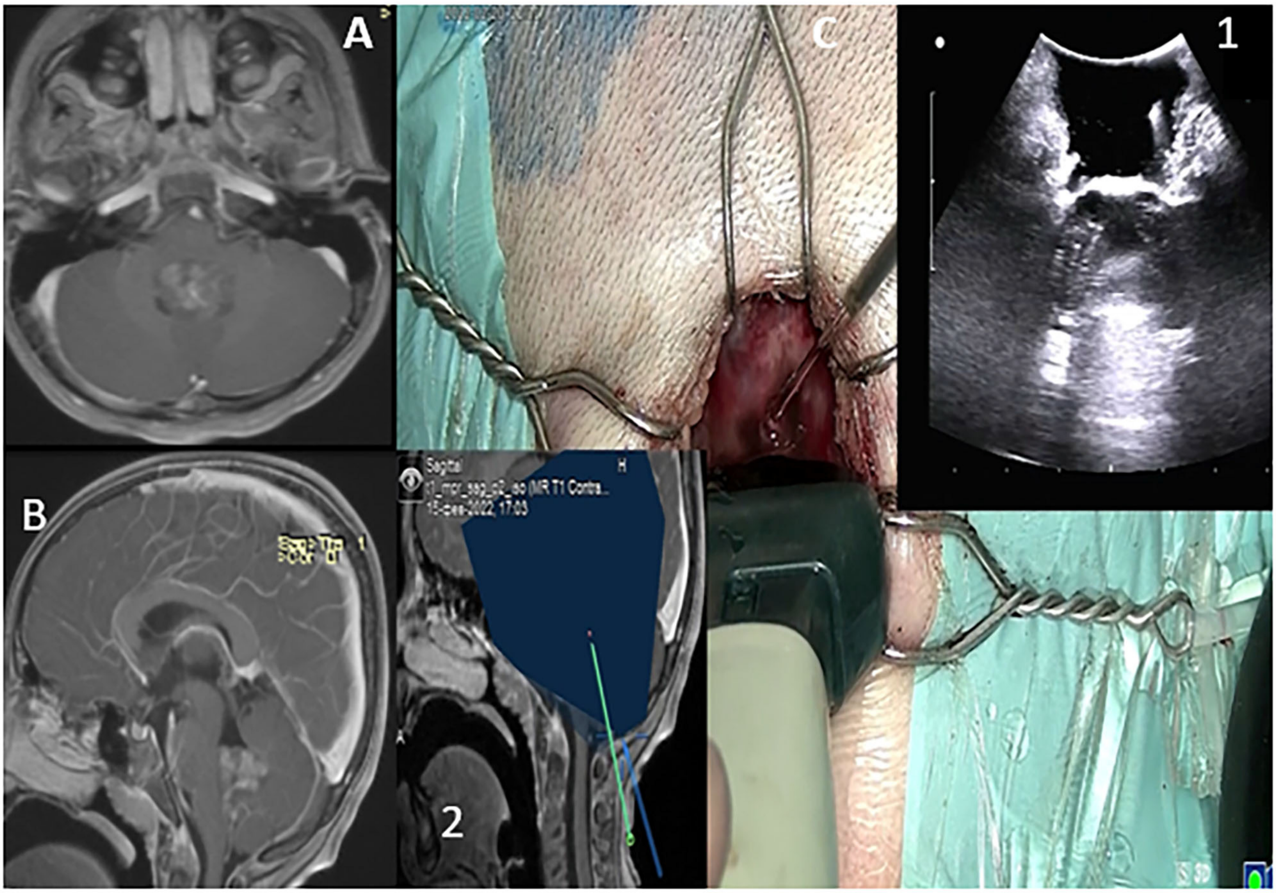

FIGURE 6 | T1WI in sagittal and axial sections depicting 4th ventricular lesion **(A,B)**. Probe is placed over the dura to acquire standard B-mode imaging scans *via* a sub occipital approach. The lesion is depicted as hyperechoic incaved between cerebellar tonsils **(C,1)**. The trajectory to the lesion is also depicted **(C,2)**.

subcortical changes), especially in Focal cortical type II. The lesion margins on IUS pictures are even clearer than on MRI images. As a result, we believe that iUS is a valuable tool for epilepsy surgery (**Figure 10**).

DISCUSSION

As a neuro-navigation modality, iUS navigation in neurosurgery requires a review in terms of utility and user-friendliness, assisting resection extent, and financial burden in terms of purchasing it in neurosurgical centers. The survey conducted suggested there appears to be widespread global availability and familiarity with iUS. Additionally, the general opinion appears to be that the application of iUS during neurosurgery provides relatively quick and accurate information on lesion location and boundaries without negatively affecting intraoperative workflow. The investigators have observed that the introduction of high-resolution iUS during neurosurgery at the study site has provided a relatively convenient and user-friendly modality for intraoperative identification, localization, and characterization of neurosurgical lesions.

Relative to other modes of intraoperative neuronavigation such as MRI and CT-scan, some of the key features and potential advantages of iUS that the investigators have noted include:

- Provision of real-time information on lesion location and extent even in the face of "brain shift"; This maximizes lesion resection while minimizing the negative effects on surrounding healthy tissue.
- Significant reduction in surgical time. A time duration evaluation use of intraoperative MRI was evaluated in a study conducted by Sacino et al. Their study observed that they had an operative time range of 1.5–3 h of additional surgery as a result of the technicalities of performing iMRI. The preparation and transportation of the patient to the MRI cabinet, conducting the MRI, and returning to the operation room were major factors that contributed to additional operative time. Additionally, when back in the

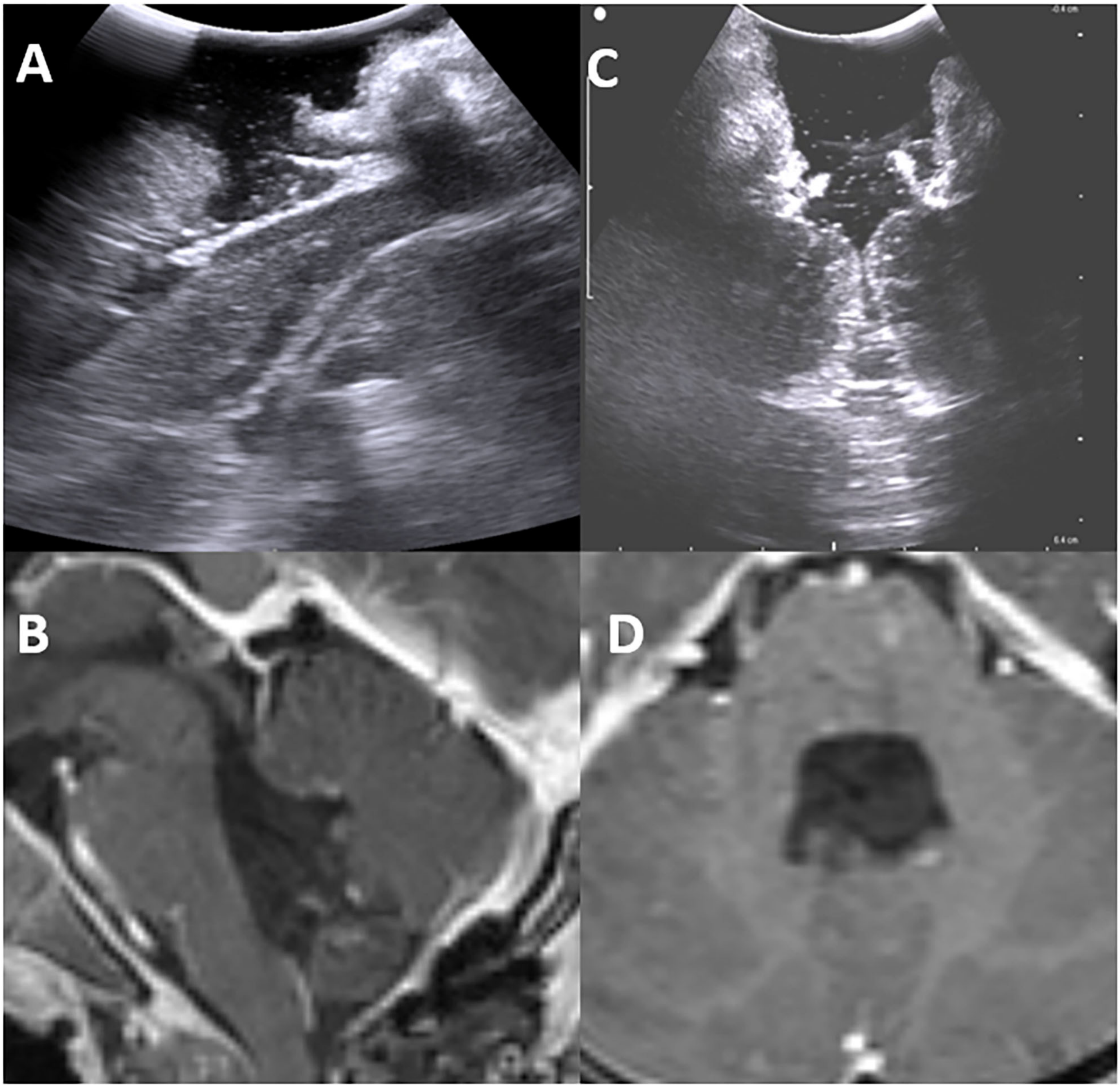

FIGURE 7 | Post-operative intraoperative ultrasound images in sagittal and axial view showing total resection of the lesion **(A,C)** in concordance with postoperative MRI -TIWI in sagittal and axial views **(B,D)**.

theater, re-sterilization, and re-gowning of the patient, nurses, and surgeon compounded into the time factor (7). This was in sharp contrast to our experience in which using iUS did not influence the operational flow. The approximate time taken for each IUS navigation screening session was as follows: (1) prior to dura opening-—1–2 min; (2) after dura opening, lesion localization and delineation are 1–2 min. Control for residual lesion post-resection is 1–2 min.

- Cost-effectiveness about acquisition, running, and maintenance of iUS apparatus – It is important to appreciate that the prohibitively high costs associated with CT- and MRI-based neuronavigation techniques limit their availability and use in LMICs (9).
- Non-invasive nature and associated safety for both patient and neurosurgeon.
- Intraoperative repeatability.

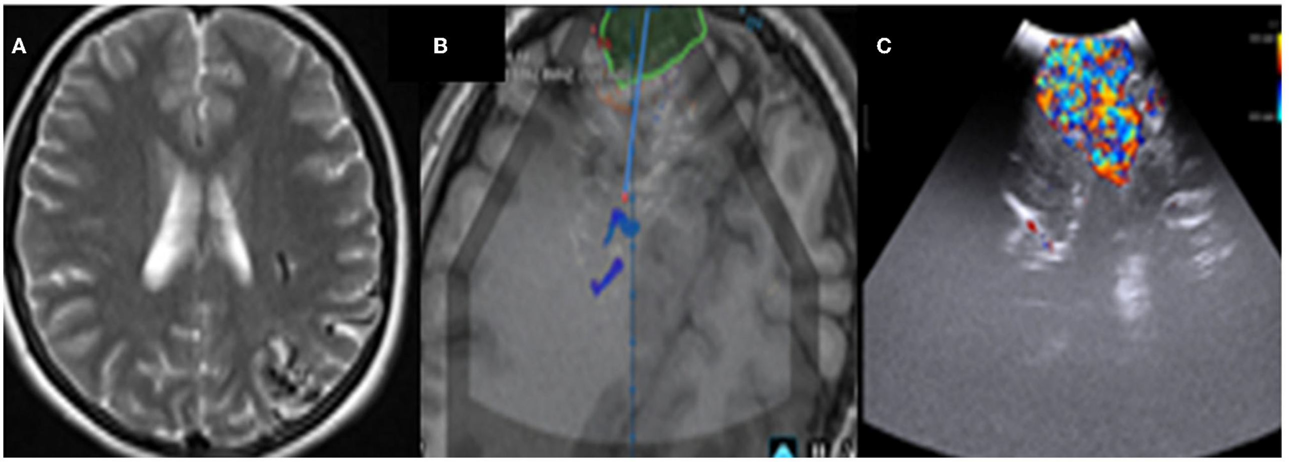

FIGURE 8 | (A) Pre-operative MRI depicting an occipital arteriovenous-malformation (AVM). **(B)** Intraoperative ultrasound integrated with brain lab system clearly identifying the AVM. **(C)** Doppler mode.

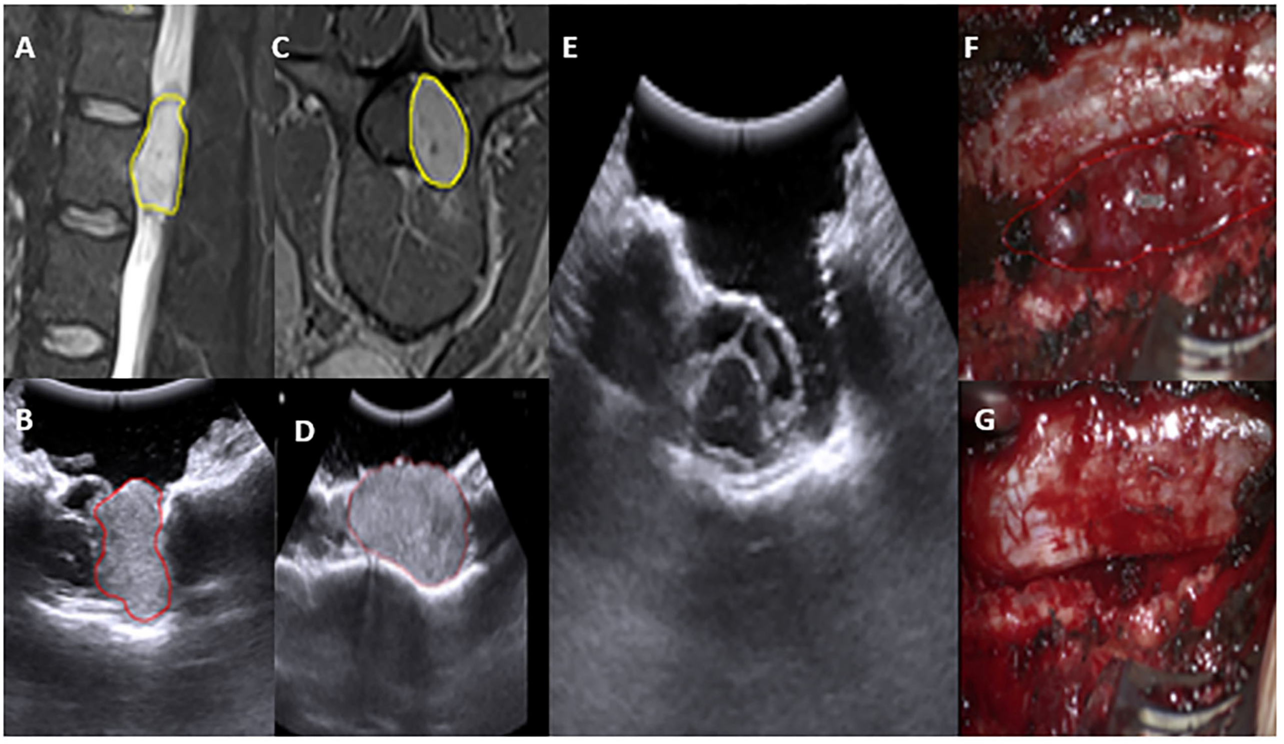

FIGURE 9 | Preoperative MRI T2WI sagittal and axial view depicting an extradural L2–3 lesion **(A,C)** yellow. In concordance, IUS depicting the lesion-location with spinal cord boundary **(B,D)**. Post-operative IUS Clearly shows total resection **(E)**. Intraoperative images, prior and post-resection **(F,G)**.

Unfortunately, as is the case with any technique applied in many fields, iUS has some disadvantages, key of which is the steep learning curve. However, the investigators are of the opinion that the rate at which different surgeons will acquire the skill to effectively employ iUS is largely a function of their years of surgical experience (2, 9).

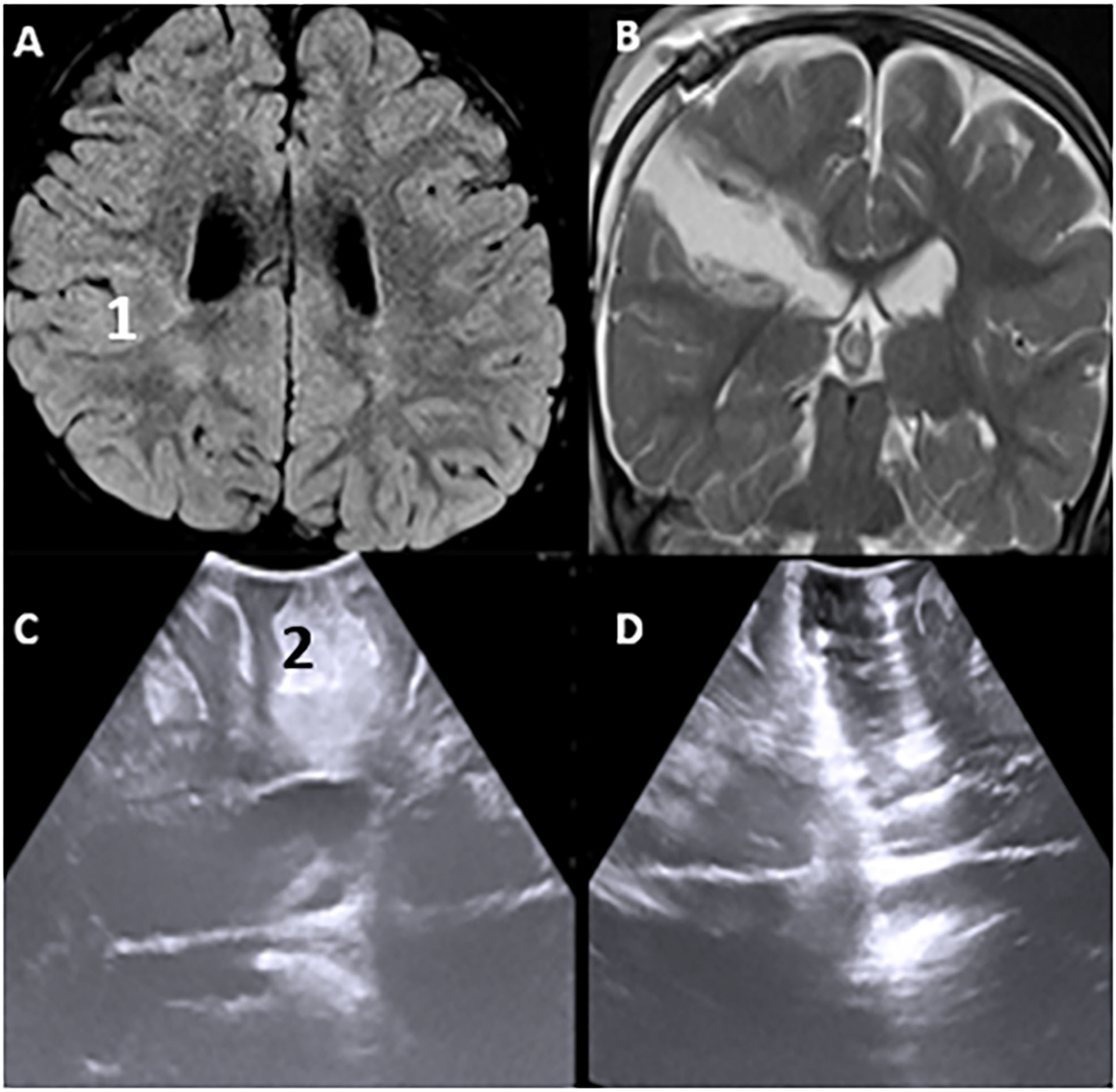

FIGURE 10 | Pre-operative Hyperintence axil MRI FLAIR rt FCD type IIb **(A,1)** in concordance with pre-resection intraoperative hyper echoic cortical and subcortical IUS features **(C,2)**. Post-operative coronal T2WI **(B)** and intraoperative post-resection IUS showing complete resection of the lesion **(D)**.

CONCLUSION

The application of iUS in neurosurgical practice will continue to evolve in the face of improvements in surgical techniques, as well as new and improved technologies.

DATA AVAILABILITY STATEMENT

The original contributions presented in the study are included in the article/supplementary material, further inquiries can be directed to the corresponding author.

ETHICS STATEMENT

Written informed consent was obtained from the individual(s) for the publication of any potentially identifiable images or data included in this article.

AUTHOR CONTRIBUTIONS

KS, RS, II, and AS: conceptualization. KS, LB, and LM: data curation. KS, AS, and RS: formal analysis. KS: investigation and project administration. RS and LB: resources. LB, RS, II, and LM:

software. LB and LM: supervision. KS, RS, and II: validation. KS and RS: roles/writing—original draft and writing—review and editing. All authors contributed to the article and approved the submitted version.

REFERENCES

1. Akeret K, Bellut D, Huppertz HJ, Ramantani G, König K, Serra C, et al. Ultrasonographic features of focal cortical dysplasia and their relevance for epilepsy surgery. *Neurosurg Focus.* (2018) 45:E5. doi: 10.3171/2018.6.FOCUS18221
2. Sastry R, Bi WL, Pieper S, Frisken S, Kapur T, Wells W 3rd, et al. Applications of ultrasound in the resection of brain tumors. *J Neuroimaging.* (2017) 27:5–15. doi: 10.1111/jon.12382
3. Prada F, Gennari AG, Quaia E, D'Incerti L, de Curtis M, DiMeco F, et al. Advanced intraoperative ultrasound (ioUS) techniques in focal cortical dysplasia (FCD) surgery: a preliminary experience on a case series. *Clin Neurol Neurosurg.* (2020) 198:106188. doi: 10.1016/j.clineuro.2020.106188
4. Tringali G, Bono B, Dones I, Cordella R, Didato G, Villani F, et al. Multimodal approach for radical excision of focal cortical dysplasia by combining advanced magnetic resonance imaging data to intraoperative ultrasound, electrocorticography, and cortical stimulation: a preliminary experience. *World Neurosurg.* (2018) 113:e738–46. doi: 10.1016/j.wneu.2018.02.141
5. Goren O, Monteith SJ, Hadani M, Bakon M, Harnof S. Modern intraoperative imaging modalities for the vascular neurosurgeon treating intracerebral hemorrhage. *Neurosurg Focus.* (2013) 34:E2. doi: 10.3171/2013.2.FOCUS1324
6. Ghinda D, Zhang N, Lu J, Yao CJ, Yuan S, Wu JS. Contribution of combined intraoperative electrophysiological investigation with 3-T intraoperative MRI for awake cerebral glioma surgery: comprehensive review of the clinical implications and radiological outcomes. *Neurosurg Focus.* (2016) 40:E14. doi: 10.3171/2015.12.FOCUS15572
7. Sacino MF, Ho CY, Murnick J, Tsuchida T, Magge SN, Keating RF, et al. Intraoperative MRI-guided resection of focal cortical dysplasia in pediatric patients: technique and outcomes. *J Neurosurg Pediatr.* (2016) 17:672–8. doi: 10.3171/2015.10.PEDS15512
8. Bø HK, Solheim O, Kvistad KA, Berntsen EM, Torp SH, Skjulsvik AJ, et al. Intraoperative 3D ultrasound-guided resection of diffuse low-grade gliomas: radiological and clinical results. *J Neurosurg.* (2019) 132:518–29. doi: 10.3171/2018.10.JNS181290
9. Kaale AJ, Rutabasibwa N, McHome LL, Lillehei KO, Honce JM, Kahamba J, et al. The use of intraoperative neurosurgical ultrasound for surgical navigation in low- and middle-income countries: the initial experience in Tanzania. *J Neurosurg.* (2020) 134:1–8. doi: 10.3171/2019.12.JNS192851

Conflict of Interest: The authors declare that the research was conducted in the absence of any commercial or financial relationships that could be construed as a potential conflict of interest.

Publisher's Note: All claims expressed in this article are solely those of the authors and do not necessarily represent those of their affiliated organizations, or those of the publisher, the editors and the reviewers. Any product that may be evaluated in this article, or claim that may be made by its manufacturer, is not guaranteed or endorsed by the publisher.

frontiers | Frontiers in Surgery

REVIEW
published: 16 May 2022
doi: 10.3389/fsurg.2022.903578

Endoscopic Transnasal Approaches to Petrous Apex

*Alexander Kovalev[1], Rinat Sufianov[2], Daniel Prevedello[3], Luís Borba[2,4], Luciano Mastronardi[2,5], Tatiana Ilyasova[6], Roy Thomas Daniel[7], Mahmoud Messerer[7], Marcio Rassi[2,8] and Guang Zhang[9]**

[1]Department of neurooncology, Federal Center of Neurosurgery, Tyumen, Russia, [2]Department of Neurosurgery, Sechenov First Moscow State Medical University (Sechenov University), Moscow, Russia, [3]Department of Neurological Surgery, The Ohio State University, Columbus, OH, United States, [4]Department of Neurosurgery, Federal University of Paraná, Curitiba, Brazil, [5]Division of Neurosurgery, San Filippo Neri Hospital, Roma, Italy, [6]Department of Internal Diseases, Bashkir State Medical University, Ufa, Republic of Bashkortostan, Russia, [7]Department of Neurosurgery, University Hospital of Lausanne, Lausanne, Switzerland, [8]Department of Neurosurgery, A.C. Camargo Cancer Center, São Paulo, SP, Brazil, [9]Department of Neurosurgery, The First Affiliated Hospital of Harbin Medical University, Harbin, China

OPEN ACCESS

Edited by:
*Daming Zhang,
First Affiliated Hospital of Harbin Medical University, China*

Reviewed by:
*Galina Dorovskikh,
The Omsk State Medical University, Russia
Aferin Beilerli,
Harbin Medical University, China*

***Correspondence:**
*Guang Zhang
zhangguang@hrbmu.edu.cn*

Specialty section:
This article was submitted to Neurosurgery, a section of the journal Frontiers in Surgery

Received: 24 March 2022
Accepted: 21 April 2022
Published: 16 May 2022

Citation:
Kovalev A, Sufianov R, Prevedello D, Borba L, Mastronardi L, Ilyasova T, Daniel RT, Messerer M, Rassi M and Zhang G (2022) Endoscopic Transnasal Approaches to Petrous Apex. Front. Surg. 9:903578. doi: 10.3389/fsurg.2022.903578

Endoscopic extended transnasal approaches to the apex of the temporal bone pyramid are rapidly developing and are widely used in our time around the world. Despite this, the problem of choosing an approach remains relevant and open not only between the "open" and "endoscopic transnasal" access groups but also within the latter. In the article, we systematized all endoscopic approaches to the pyramid of the temporal bone and divided them into three large groups: medial, inferior, and superior—in accordance with the anatomical relationship with the internal carotid artery—and also presented their various, modern (later described), modifications that allow you to work more targeted, depending on the nature of the neoplasm and the goals of surgical intervention, which in turn allows you to complete the operation with minimal losses, and improve the quality of life of the patient in the early and late postoperative period. We described the indications and limitations for these accesses and the problems that arise in the way of their implementation, which in turn can theoretically allow us to obtain an algorithm for choosing access, as well as identify growth points.

Keywords: petrous apex, approach, transnasal, endoscope, temporal bone

INTRODUCTION

Pathology, localized in the area of the apex of the pyramid, traditionally remains "difficult to achieve" due to the neurovascular structures located around it. To date, the problem of choosing an approach for pathology localized in this area remains open due to the fact that none of them can be called "perfect." A number of pathologies localized in the area of the apex of the pyramid require radical (or close to it) removal with a minimal risk of complications, which is very difficult to perform with a transcranial or transfacial approach. Often, when performing these operations, the traumatism of the approach exceeds the traumatization during the main stage; accordingly, tumors of the skull base of the median localization can be defined as "extremely complex" and often inoperable (or difficult to operate) from standard transcranial approaches. In recent decades, endoscopic transnasal approaches have become increasingly common in daily practice, having a number of undeniable advantages. Still, to date, indications, contraindications, and limitations for endoscopic transnasal approaches have not yet been clearly defined. The aim of the current study was to analyze the current literature on this issue and systematize the data.

ENDOSCOPIC TRANSNASAL APPROACHES TO THE APEX OF THE PYRAMID

The choice of surgical approach is often determined by the surgical task: drainage, partial removal (or biopsy), and total removal. The relationship between the tumor and the ICA is critical, and it is around this that the classification of transnasal approaches is based (1). We divided the approaches into three groups, according to the course of the ICA: medial, inferior, and superior (**Table 1**). The latter is an approach directly to the Meckel cavity, which is anatomically closely related to the upper part of the pyramid apex and can be considered as separate access because in some cases work in this area is required.

The most common types of extra- and intracranial pathology in the area of the pyramid apex include cholesterol granuloma, chondrosarcoma, apicitis, chordoma, meningioma, epidermoid cyst, and schwannoma. From the above list, we can conclude that these pathologies require the setting of completely different surgical tasks.

Medial Approach Group

Medial Approach

Initially, an extended sphenoidotomy with posterior septectomy is performed. Anatomical landmarks within the sphenoid sinus are determined: platform, sella turcica, clivus, optic nerve canal, medial and lateral optocarotid recess, canal of the internal carotid artery, and lingual process of the sphenoid bone. Depending on the degree of sinus pneumatization, navigation equipment may be required (1, 2).

Then, work is carried out directly in the sinus itself, medial to the internal carotid artery. Most often, we are talking about the drainage of a cholesterol granuloma; thus, it is possible to create a wide window for long-term drainage of the granuloma cavity.

Medial Approach with Transposition of ICA

It is used in the case when the expansion of the tumor is minimal in the medial direction, and it is advisable to lateralize the internal carotid artery by a few millimeters. Extended sphenoidotomy and posterior septectomy are routinely performed. In addition, a transpterygoid approach is performed to identify the Vidian nerve, which is a key anatomical landmark to the anterior genu of the ICA; then, by drilling the nerve canal at the medial and lower edge, we approach the second genu of the internal carotid artery (3). Another important anatomical landmark for determining the position of the ICA can be the pterygoclival ligament (4). A vertical (paraclival) segment of the internal carotid artery is drilled from the bone canal, which allows the artery to be lateralized by a few millimeters and to obtain a wider exposure to the top of the pyramid (1).

Contralateral Transmaxillary Corridor

It is a modernized medial approach (or addition to the approach) to the apex of the pyramid using a more parallel angle to the course of the internal carotid artery due to the approach through the anterior wall of the contralateral maxillary sinus, which in turn leads to minimization of manipulations with the internal carotid artery and, accordingly, a lower risk of damage (5). An extended sphenoidotomy and a posterior septectomy are performed. Then, maxillotomy is performed along Caldwell-Luc on the

TABLE 1 | Endoscopic transnasal approaches to petrous apex.

Transnasal approach		Short description	References
Medial approaches group	Medial	It is used when the tumor expands medially to the ICA	(1)
	Medial with ICA transposition	Minimal medial tumor expansion or more posterolateral locationDecompression of the internal carotid artery provides lateral displacement of the artery and creates a larger, several millimeters, medial window	(1)
	Contralateral transaxillary corridor	Providing greater access to the apex of the pyramid with less need for manipulation of the ICA	(5)
Infrapetrosal approaches group	Infrapetrosal	The performance of the surgical task is not available through the sphenoid sinus, it is used with a more lateral and lower location of the tumor. Requires dissection of the auditory tube and foramen lacerum	(1)
	Translacerum	Indicated alone for pathology limited to the lower part of the pyramidal apex, especially in the area of the laceration, and in combination with other approaches for more extensive lesions, the auditory tube is preserved	(7)
	Inferomedial approach	This is a combination of two approaches (medial and inferior petrosal), which allows you to mobilize the ICA for work in the dorsolateral direction and work intracranially	(2)
Suprapetrosal access to the Meckel cavity (can be used as an addition to the above) approaches	A quadrangular space is created for access, bounded by the horizontal petrosal part of the ICA below, the ascending vertical cavernous/paraclival ICA medially, the CN VI above (in the cavernous sinus), and the maxillary trigeminal nerve (V2) laterally		(8)

contralateral side (5). Maxillotomy expands to the maximum to the zygomatic prominence and the wall of the maxillary sinus laterally, to the exit point of the infraorbital nerve from above, while maintaining the nasomaxillary protrusion medially and without damaging the roots of the teeth from below. Then, medial maxillectomy was performed, which gave a more parallel course of the instruments relative to the petrosal part of the internal carotid artery.

Inferior Approaches Group

Transpterygoid Infrapetrosal

It is used when the surgical task cannot be performed only through the sphenoid sinus and the pathological formation is located below and lateral to the anterior knee of the internal carotid artery. In addition to extended sphenoidotomy, this requires a transpterygoid approach, as well as dissection of the Eustachian tube and lacerum foramen. Approach to the pterygopalatine fossa is performed, the tissues of the pterygopalatine fossa are displaced laterally to the rotundum foramen—the exit points of the second branch of the trigeminal nerve, the nerve, and artery of the pterygoid canal are crossed, and then by drilling along the medial and lower edge of the Vidian canal, they exit to the second knee of the internal carotid artery (3, 6). The base of the pterygoid processes and the upper part of the medial and lateral pterygoid plates are removed. The cartilaginous segment of the Eustachian tube is resected. Dissection along the posterior edge of the lateral pterygoid plate allows identification of the third branch of the trigeminal nerve. The inferior surface of the petrous apex is achieved by drilling the bone between the horizontal segment of the internal carotid artery and the Eustachian tube, medial to the third branch of the trigeminal nerve (1).

Translacerum

The lacerum foramen is formed by the incomplete fusion of the three main bone structures that make up the central base of the skull: the sphenoid bone, the petrous apex of the temporal bone, and the clival part of the occipital bone (2). An extended sphenoidotomy and a transpterygoid approach are performed from the side of interest to us; the bone tissue around the Vidian nerve is removed to the foramen lacerum. The medial half of the base of the pterygoid process is further removed to expose the upper part of the cartilaginous segment of the auditory tube. The fibrous cartilage overlying the foramen lacerum is cut (starting at the medial-inferior edge) toward the top of the auditory tube, and the cartilage and fibrous ligament inside the foramen lacerum are removed to expose the anterior genu and the horizontal segment of the petrous internal carotid artery (in live surgery for this Doppler must be used). A triangular space is created between the lower part of the petrous carotid artery and the Eustachian tube, through which the lower part of the apex of the pyramid could be approached. The subsequent removal in the region of the apex of the pyramid is performed through the space thus created between the lower edge of the horizontal segment of the petrous part of the internal carotid artery and the upper edge of the auditory tube (7).

Inferomedial Approach

It is a combination of inferior and medial access and suitable for resection of large tumors that grow into several anatomical regions.

Suprapetrosal Approach (to the Meckel Cavity)

The most common pathologies in this location are invasive adenoid cystic carcinomas, meningiomas, schwannomas, and invasive pituitary adenomas. An extended sphenoidotomy and a transpterygoid approach are performed to expose the structures of the cavernous sinus. The bone structures covering the cavernous sinus are removed. It is possible to enter Meckel's cavity through a quadrangular space bounded by the horizontal petrous part of the ICA from below, the ascending vertical cavernous/paraclival ICA medially, CN VI from above (in the cavernous sinus), and the maxillary trigeminal nerve (V2) from the side (**Figures 1** and **2**) (8). Opening of the DM is performed in the medial-lateral direction—from the second knee to V2. It is critical to remain below the level of the sixth nerve through the Dorello canal just behind and above the apex of the pyramid and the ICA, which cannot be damaged (9).

LIMITATIONS AND FUTURE PERSPECTIVES

The variability in the spread of tumors to neighboring areas of the skull base and their relationship with neighboring neurovascular structures do not allow us to determine whether one particular surgical approach is the best or the only option. Here, it is critical to take into account the preoperative histology and clearly understand the goals of the surgery in order to achieve the best possible outcome (10). Endoscopic transnasal approaches are more acceptable than open surgery in some patients and have a number of clear advantages (11).

In relation to the foramen lacerum, surgically, the apex of the pyramid of the temporal bone can be divided into two parts: the medial apex of the pyramid (above) and the lower apex of the pyramid (lower and lateral) (2). The medial approach is ideal for long-term drainage of the granuloma, especially when the granuloma grows medially with a well-pneumatized sinus (1). Its advantages are relatively little traumatization of the structures of the nasal cavity, the absence of the need to compromise the integrity of the Vidian nerve and the absence of the likelihood of palatal numbness after transection of the descending palatine artery (12). In addition, if we are talking about surgery for a cholesterol granuloma, draining it through the nasal cavity and especially directly into the sphenoid sinus is the most physiological. The abducens nerve, which is the upper limit of the approach, is a limitation of its implementation (2). For a greater work maneuver, a medial approach with transposition of the ICA is used due to the displacement of the artery laterally, which is advisable when the tumor expansion is somewhat less in the medial direction.

Freeman et al. in their experimental work carried out lateralization of the ICA using a self-retaining vascular retractor and showed that the artery could potentially be

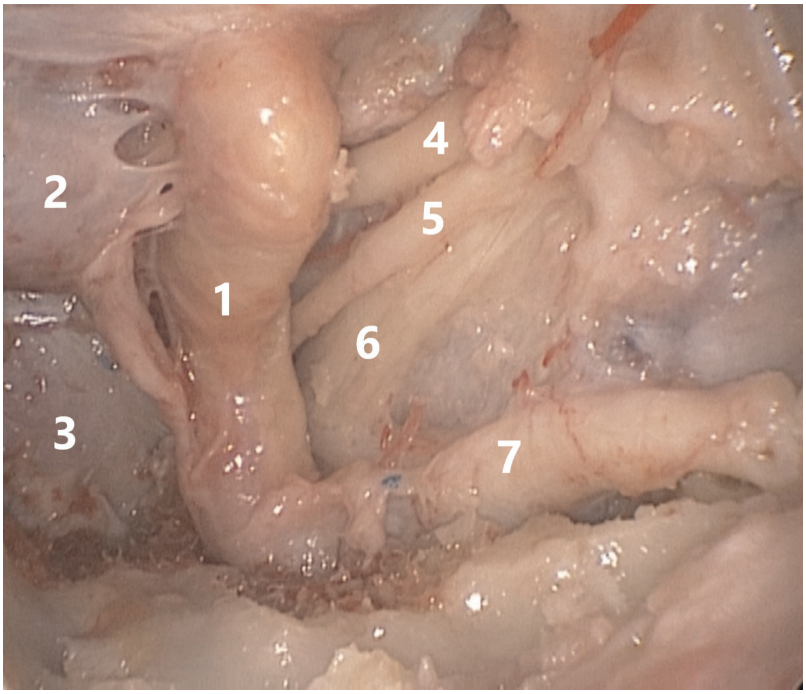

FIGURE 1 | 1—internal carotid artery, 2—hypophysis, 3—clivus, 4—oculomotor nerve, 5—abducens nerve, 6—ophthalmic nerve, 7—maxillary nerve.

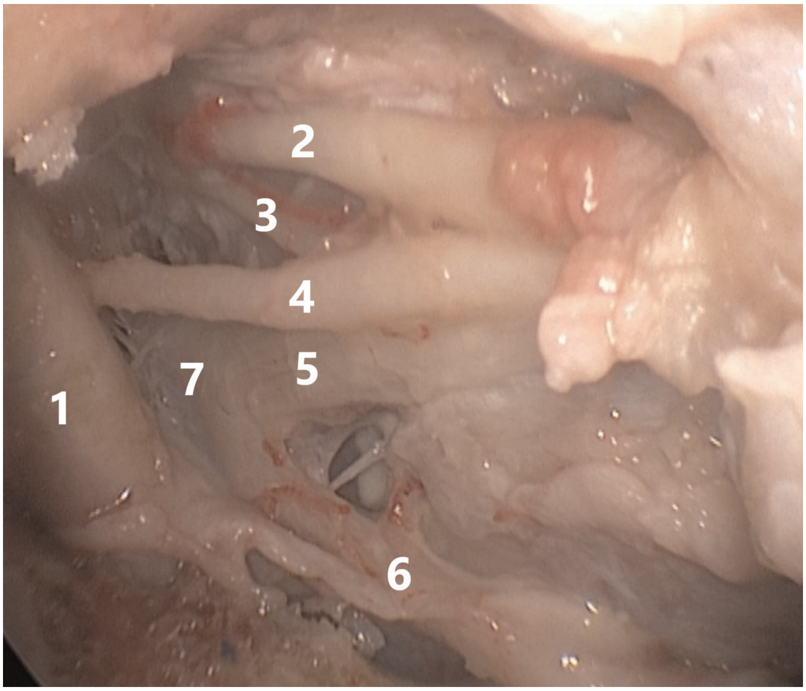

FIGURE 2 | Relationship between the structures of the cavernous sinus and the Gasser node: 1—internal carotid artery, 2—oculomotor nerve, 3—trochlear nerve, 4—abducens nerve, 5—ophthalmic nerve, 6—maxillary nerve, 7—Gasser node.

displaced 4.75 mm laterally (the work was carried out only on cadaveric material), which could potentially turn out to be sufficient to complete the task; however, this manipulation is associated with certain risks, both from the sinonasal part and catastrophic bleeding from the ICA (13). It is necessary to be very careful in choosing this approach since this approach as a "monomethod" is not suitable for a strongly lateral or low location of the tumor. One of the main limiting factors is the pear-shaped aperture. As an alternative, and sometimes addition to the above approaches, you can specify the contralateral transmaxillary access. It is logical to assume that the wider the window between the ICA and the meninges of the posterior cranial fossa, the farther in the lateral direction it is possible to work. The potential advantages of this approach are the ability to preserve the Vidian nerve and the auditory tube, take the nasoseptal flap from the ipsilateral side, and avoid unnecessary manipulation of the ICA in four out of five patients and, as a result reduce the risk of damage to it (5). If necessary, it can be additionally used, and the transposition of the ICA to increase approach. Also, it can be used instead of bottom access. Potential complications of this approach are known to all—oroantral fistula, damage to the branches of the infraorbital nerve, hyperostosis, cheek abscess, dental complications, and facial asymmetry. In some cases, especially in very inferior and lateral lesions, a transpterygoid infrapetral or an open lateral approach may be preferred (5).

Van Gompel et al. in their anatomical study showed that in corpses without anatomical changes, the open approach to the top of the pyramid achieved almost 50% more volumetric resection than the endoscopic approach (14). In addition, while the open approach completely affects the upper part of the apex of the pyramid, the endoscopic approach occupies a niche in the approach to lesions of the lower part of the apex of the pyramid. The authors proposed to refer to the endoscopic approach as "inferior anterior petrosectomy," which more clearly defines the role of each approach to the entire apex of the pyramid of the temporal bone along the lower surface of the entire petrous part of the ICA. Comparing it with the medial approach, it can be accurately noted that the restriction of work in the lateral direction is removed here, namely, the limiting maneuver laterally, the paraclival segment of the ICA. The approach is excellent for surgical treatment of solid masses. For the treatment of cystic diseases requiring long-term drainage of the cavity, the outflow tract may be somewhat more difficult due to the increased risks of scarring; the use of wide lumen stents can help solve this problem (1). Potential disadvantages also include damage to the Vidian nerve, relatively large traumatization of the sinonasal region, and damage to the auditory tube—which inevitably leads to a decrease in the patient's quality of life. In the future, works describing approaches with preservation of the integrity of the auditory tube with various options for its transposition are important; one of these approaches is translacerum, which can be performed both independently and as part of another lower approach. To date, there are many problems in removing the tumor around the anterior knee of the ICA, which is one of the most difficult anatomical areas. In clinical use, the translacerum approach was proved to be effective and provided sufficient space for work in the area of the pyramid apex; complete and partial removal was achieved in three and one cases, respectively (15). Its indisputable advantage is the ability to preserve the Vidian nerve and the auditory tube; there are no risks of developing otitis media and conductive hearing loss. In our opinion, the approach looks very promising, as it allows one to choose the most direct and minimally invasive path to the area of interest but at the same time requires the most accurate planning before the operation, as well as a team with good experience. If the most extensive and aggressive resection is required, as well as when dealing with intradural formations, the inferomedial approach is worth choosing, which is a combination of two approaches that allow achieving the widest possible resection. It may be suitable for dorsolateral surgery and is promising for the treatment of petroclival meningiomas and, if possible, the total removal of chordomas, which require maximum bone resection.

In a study by Funaki et al. (16), the abducens dural foramen was located 4.9 mm (range 4–6 mm) above the posterior end of the pterygoid canal. The lateral clival artery can be used as a guide to locate the abducens nerve, as it usually runs just medial to the intradural segment of the abducens nerve (2). On the other hand, the approach allows you to work in the area below the CN VI and above the midline. Typically, the tumor displaces the abducens nerve laterally or posteriorly and creates a corridor through which surgeons can maneuver instruments (17). On the plus side, this approach offers an efficient approach to vascular supply to meningiomas in this area, especially to the dorsal meningeal artery and its branches, and improves visualization of the occult inferior petroclival region (17, 18). Another advantage of this approach is direct access to the tumor without any manipulation of the cranial nerves, thus allowing one of the main principles of skull base surgery—do not cross the nerve—to be followed. However, this approach carries several risks, including ICA injury, nerve damage, and nasal liquorrhea. They should be carefully examined before the operation. If the formation is located above the laceration and grows into the Meckel cavity or is located only in this area, it makes sense to consider the upper approach to the Meckel cavity; it is not a direct approach to the top of the pyramid but is sometimes included as an area into which the formations grow or can be used as a site for taking a biopsy. None of the open approaches can reach the entire Meckel cavity (anterolateral, lateral, and posterolateral) due to difficulty in exposing the anteroinferior medial part of the cavity (19). The endoscopic approach is a relatively safe and direct approach to the Meckel cavity and can be used to treat a tumor in the Meckel cavity (20). It requires precise planning, including a clear understanding of the objectives of the surgery, careful preparation of the team, and a well-equipped operating room, as there is a risk of damage to the ICA and nerves. It is equally important to note that the surgical multidisciplinary team should master all approaches (open and endoscopic) and not be a team of "one approach" because approaches to the paramedian skull base are the most difficult of all endoscopic endonasal methods. Because of their technical complexity, surgeons are advised to master

FIGURE 3 | Area highlighted in green is the group of medial approaches, that in red is the area of the lacerated foramen, that in yellow is the access to the Meckel cavity, and that in blue is the group of infrapetrosal approaches; 1—internal carotid artery, 2—Vidian nerve, 3—pharyngeal mouth of the auditory tube, 4—posterior sections of the vomer, 5—base of the pterygoid process.

endoscopic endonasal anatomical approaches targeting the midline structures (sagittal plane) before proceeding with paramedial (coronal plane) pathologies (21). One of the main disadvantages of transnasal surgery is the difficult control of hemostasis, the presence of complications on the sinonasal side, and the risks of postoperative liquorrhea.

CONCLUSIONS

Endoscopic transnasal approaches provide a direct path to the top of the pyramid and have shown their effectiveness, including below the level of the foramen lacerum, which is a potential advantage over open approaches (**Figure 3**). Additional advantages include minimal brain traction, absence of cosmetic changes, and other specific complications associated with open approaches. The implementation of this group of approaches requires an experienced team and an equipped operating room. Specific problem areas are the difficulty of controlling hemostasis from the main arteries, nasal liquorrhea, and complications from the nasal cavity. The development and use of approaches that minimally reduce the quality of life are promising while preserving the Vidian nerve (prevention of dry eye syndrome) and the auditory tube (the resulting conductive hearing loss requires tympanostomy), but these solutions should not jeopardize the implementation of the main stage, do not forget about the principle of "as much as you need, but as little as possible." In achieving these goals, it is equally important to develop special power curved tools that allow you to work in deep space, safely and "around the corner."

AUTHOR CONTRIBUTIONS

Conceptualization: AK, RS, DP, AS, RTD, MM, MR, and GZ. Data curation: AK, LB, and LM. Formal analysis: AK, AS, and RS. Investigation: AK. Project administration: GZ, AS, LB, and DP. Resources: RS and LB. Software: LB, RS, TI, RTD, MM, MR, and LM. Supervision: GZ, AS, DP, LB, RTD, MM, and MR. Validation: AK, RS, and TI. Roles/writing—original draft: AK, RS, and LM. Writing—review and editing: AK, AS, and RS.

REFERENCES

1. Zanation AM, Snyderman CH, Carrau RL, Gardner PA, Prevedello DM, Kassam AB. Endoscopic endonasal surgery for petrous apex lesions. *Laryngoscope*. (2009) 119(1):19–25. doi: 10.1002/lary.20027. PMID: 19117306
2. Borghei-Razavi H, Truong HQ, Fernandes Cabral DT, Sun X, Celtikci E, Wang E, et al. Endoscopic endonasal petrosectomy: natomical investigation, limitations, and surgical relevance. *Oper Neurosurg (Hagerstown)*. (2019) 16(5):557–70. doi: 10.1093/ons/opy195
3. Kassam AB, Vescan AD, Carrau RL, Prevedello DM, Gardner P, Mintz AH, et al. Expanded endonasal approach: vidian canal as a landmark to the petrous internal carotid artery. *J Neurosurg*. (2008) 108(1):177–83. doi: 10.3171/JNS/2008/108/01/0177
4. Tayebi Meybodi A, Little AS, Vigo V, Benet A, Kakaizada S, Lawton MT. The pterygoclival ligament: a novel landmark for localization of the internal carotid artery during the endoscopic endonasal approach. *J Neurosurg*. (2018) 18:1–11. doi: 10.3171/2017.12.JNS172435
5. Patel CR, Wang EW, Fernandez-Miranda JC, Gardner PA, Snyderman CH. Contralateral transmaxillary corridor: an augmented endoscopic approach to the petrous apex. *J Neurosurg*. (2018) 129(1):211–9. doi: 10.3171/2017.4.JNS162483
6. Bootz F, Keiner S, Schulz T, Scheffler B, Seifert V. Magnetic resonance imaging–guided biopsies of the petrous apex and petroclival region. *Otol Neurotol*. (2001) 22(3):383–8. doi: 10.1097/00129492-200105000-00019
7. Taniguchi M, Akutsu N, Mizukawa K, Kohta M, Kimura H, Kohmura E. Endoscopic endonasal translacerum approach to the inferior petrous apex. *J Neurosurg*. (2016) 124(4):1032–8. doi: 10.3171/2015.1.JNS142526
8. Kassam AB, Gardner P, Snyderman C, Mintz A, Carrau R. Expanded endonasal approach: fully endoscopic, completely transnasal approach to the middle third of the clivus, petrous bone, middle cranial fossa, and infratemporal fossa. *Neurosurg Focus*. (2005) 19(1):E6. PMID: 16078820
9. Iaconetta G, Fusco M, Cavallo LM, Cappabianca P, Samii M, Tschabitscher M. The abducens nerve: microanatomic and endoscopic study. *Neurosurgery*. (2007) 61(3 Suppl):7–14; discussion 14. doi: 10.1227/01.neu.0000289706.42061.19
10. Wachter D, Behm T, Gilsbach JM, Rohde V. Neurosurgical strategies and operative results in the treatment of tumors of or extending to the petrous apex. *Minim Invasive Neurosurg*. (2011) 54(2):55–60. doi: 10.1055/s-0031-1275290

11. Saraceno G, Agosti E, Qiu J, Buffoli B, Ferrari M, Raffetti E, et al. Quantitative anatomical comparison of anterior, anterolateral and lateral, microsurgical and endoscopic approaches to the middle cranial fossa. *World Neurosurg*. (2020) 134:e682–e730. doi: 10.1016/j.wneu.2019.10.178
12. Raza SM, Gidley PW, Kupferman ME, Hanna EY, Su SY, DeMonte F. Site-specific considerations in the surgical management of skull base chondrosarcomas. *Oper Neurosurg (Hagerstown)*. (2018) 14(6):611–9. doi: 10.1093/ons/opx171
13. Freeman JL, Sampath R, Casey MA, Quattlebaum SC, Ramakrishnan VR, Youssef AS. Transposition of the paraclival carotid artery: a novel concept of self-retaining vascular retraction during endoscopic endonasal skull base surgery technical report. *Acta Neurochir (Wien)*. (2016) 158(8):1625–9. doi: 10.1007/s00701-016-2873-6
14. Van Gompel JJ, Alikhani P, Tabor MH, van Loveren HR, Agazzi S, Froelich S, et al. Anterior inferior petrosectomy: defining the role of endonasal endoscopic techniques for petrous apex approaches. *J Neurosurg*. (2014) 120(6):1321–5. doi: 10.3171/2014.2.JNS131773
15. Muto J, Prevedello DM, Ditzel Filho LF, Tang IP, Oyama K, Kerr EE, et al. Comparative analysis of the anterior transpetrosal approach with the endoscopic endonasal approach to the petroclival region. *J Neurosurg*. (2016) 125(5):1171–86. doi: 10.3171/2015.8.JNS15302
16. Funaki T, Matsushima T, Peris-Celda M, Valentine RJ, Joo W, Rhoton Jr AL. Focal transnasal approach to the upper, middle, and lower clivus. *Neurosurgery*. (2013) 73(2 Suppl Operative):ons155–90; discussion ons190-1. doi: 10.1227/01.neu.0000431469.82215.93
17. Jacquesson T, Simon E, Berhouma M, Jouanneau E. Anatomic comparison of anterior petrosectomy versus the expanded endoscopic endonasal approach: interest in petroclival tumors surgery. *Surg Radiol Anat*. (2015) 37(10): 1199–207. doi: 10.1007/s00276-015-1497-5
18. Fernandez-Miranda JC, Gardner PA, Snyderman CH, Devaney KO, Mendenhall WM, Suárez C, et al. Clival chordomas: a pathological, surgical, and radiotherapeutic review. *Head Neck*. (2014) 36(6):892–906. doi: 10.1002/hed.23415
19. Kassam AB, Prevedello DM, Carrau RL, Snyderman CH, Gardner P, Osawa S, et al. The front door to meckel's cave: an anteromedial corridor via expanded endoscopic endonasal approach- technical considerations and clinical series. *Neurosurgery*. (2009) 64(3 Suppl):ons71–82; discussion ons82-3. doi: 10.1227/01.NEU.0000335162.36862.54
20. Bai ZQ, Cai EY, Wang SQ, Li ZJ, Wang SB. Nasal cavity-maxillary sinus-pterygopalatine fossa-Meckel's cave: a preliminary anatomic study of an endoscopy-based operative approach. *Neurosci Bull*. (2009) 25(6):376–82. doi: 10.1007/s12264-009-0605-0
21. de Lara D, Ditzel Filho LF, Prevedello DM, Carrau RL, Kasemsiri P, Otto BA, et al. Endonasal endoscopic approaches to the paramedian skull base. *World Neurosurg*. (2014) 82(6 Suppl):S121–9. doi: 10.1016/j.wneu.2014.07.036

Conflict of Interest: The authors declare that the research was conducted in the absence of any commercial or financial relationships that could be construed as a potential conflict of interest.

frontiers | Frontiers in Surgery

PERSPECTIVE
published: 16 May 2022
doi: 10.3389/fsurg.2022.901759

Diagnostic Investigations as a Basis for Optimising Surgical Management of Vertebrobasilar Insufficiency Syndrome

Gennady Chmutin[1], *Gennady Antonov*[2], *Egor Chmutin*[1], *Aleksei Fedyanin*[1], *Matvey Livshitz*[1,3], *Boris Oleynikov*[1,3]*, *Zokirzhon Zokhidov*[1] and *Alina Shumadalova*[4]

[1]Department of Nervous Diseases and Neurosurgery, Peoples' Friendship University of Russia (RUDN University), Moscow, Russia, [2]Department of Neurosurgery, 3rd Central Military Clinical Hospital named after A.A. Vishnevsky under the Ministry of Defense of the Russian Federation, Krasnogorsk, Russia, [3]Department of Neurosurgery, Federal State Budgetary Institution of Medical Department of Moscow Morozov Children's City Clinical Hospital of Medical Department of Moscow, Moscow, Russia, [4]Department of General Chemistry, Bashkir State Medical University, Ufa, Russian Federation

OPEN ACCESS

Edited by:
Ozal Beylerli,
Federal Center of Neurosurgery, Russia

Reviewed by:
Annanepesov Sakhid,
Turkmen State Medical University, Turkmenistan
Boxian Zhao,
Harbin Medical University, China

***Correspondence:**
Boris Oleynikov
4ar5@mail.ru

Specialty section:
This article was submitted to Neurosurgery, a section of the journal Frontiers in Surgery

Received: 22 March 2022
Accepted: 13 April 2022
Published: 16 May 2022

Citation:
Chmutin G, Antonov G, Chmutin E, Fedyanin A, Livshitz M, Oleynikov B, Zokhidov Z and Shumadalova A (2022) Diagnostic Investigations as a Basis for Optimising Surgical Management of Vertebrobasilar Insufficiency Syndrome. Front. Surg. 9:901759. doi: 10.3389/fsurg.2022.901759

Vertebrobasilar insufficiency (VBI) is one of the most common forms of cerebrovascular pathology. The progression of the VBI, especially in the context of inadequate therapy, often leads to the formation of a persistent neurological deficits within the framework of dyscirculatory encephalopathy and the consequences of a stroke in the vertebrobasilar system. This study demonstrate the importance of objective methods of patient investigation to optimize the choice of the most effective methods of surgical treatment for VBI in cases of ineffective medical treatment. We have shown that the optimization of the diagnostic algorithm contributes to the correct individualized determination of types of surgical treatment for patients with VBI. It was found that, in addition to traditional diagnostic methods, the use of radiographic methods (ultrasound Doppler, multispiral computed tomography with contrast enhancement) is invaluable for choosing the tactics of surgical treatment. We propose a significant outcome indicator like the blood flow reactivity index to determine the postoperative improvement of blood flow in the vertebral arteries. In addition, the need to perform cerebral angiography and consultations with related specialists to exclude pathologies with a similar clinical picture is emphasized.

Keywords: diagnosis of vertebrobasilar insufficiency syndrome vertebrobasilar insufficiency, diagnosis, methods, therapy, anastomosis, stroke

INTRODUCTION

Ischemic disorders in the vertebrobasilar system occur in 30% of all cerebrovascular diseases and 70% of cases presenting with clinical features of transient ischemic attacks. Mortality from ischemic strokes in the vertebrobasilar system is twice as high as the death rate from strokes in the carotid system (1–6). Therefore, objective screening methods should help to optimize the choice of the most effective surgical treatments for vertebrobasilar insufficiency (VBI) in cases of ineffective medical treatment.

In modern studies, several prevailing factors causing narrowing of the segments of the vertebral artery (VA) and its stenosis are established, associated with age-related changes and stenosis of other major blood vessels**.** These factors make it much more difficult to identify clinical and neurological signs of vascular pathology and predetermine the use of topical diagnostics to guide treatment (7, 8). However, unified methods of localizing causes and clinical signs to determine the type of surgical treatment of VBI have not been developed. The system of diagnosing various manifestations of VA pathologies taking into account extramural compression and deformation leading to brain vascular insufficiency is not sufficiently researched (3, 5, 6, 9). We review the use of instrumental diagnostic methods for vertebrobasilar insufficiency and create an algorithm to optimize the choice of the surgical technique based on various patient characteristics.

MATERIALS AND METHODS

The Study design is a single-center retrospective-prospective cohort-controlled clinical trial involving 100 patients who were treated at the 3rd Central Military Clinical Hospital named after A.A Vishnevsky (Krasnogorsk, Russia) from 2009 to 2019. In all 100 VBI patients were confirmed and various significant stenotic-occlusive lesions of the V1 segment of the VAs were identified. The presence of pathological tortuosity of the VAs was also recorded. This study was approved by the 3rd Central Military Clinical Hospital named after A.A Vishnevskyand implemented in accordance with the principles of the Helsinki Declaration (Adopted by the 18th General Assembly of the WMA). Written informed consent was obtained from all subjects. The general patient distribution by clinical diagnosis was analyzed as indicated in **Figure 1**.

As shown in **Figure 1** above, it indicates the reliability of the clinical diagnosis based on the associated clinical picture. Since the data are obtained in percentage form, it is important to note that the clinical signs of one patient could have several of these characteristics. Thus, the chances of making an error in the clinical diagnosis were eliminated. In addition, the sex-age factor was excluded, since the distribution of 100 patients by sex and age formed a comprehensive picture of the examination and the reliability of the results obtained based on the data of the sample characteristics. The average age of the patients was 72.2 years and the risk of the disease was highest between the ages of 45 and 89. In this study, 58% were men, and 42%, were women. In 50% of patients, diffuse encephalopathy syndrome (DES) was present in the vertebrobasilar system (VBS) (stage 1 DES - 1 case; stage 2 DES - 42 cases; and stage 3 DES - 7 cases), 7% had a history of transient ischemic attack (TIA) in VBS, and 4% had a history of VBI in VBS. Comorbidities were present in 98% of patients. These are presented in **Table 1**.

Depending on the leading lesion of any arterial segment involved in the blood supply to VBS in the presence of stenotic-occlusive lesions of the V1 segment of the VA, all 100 patients were divided into 2 groups: the surgical treatment group ($n = 50$) and sonservative treatment group ($n = 50$).

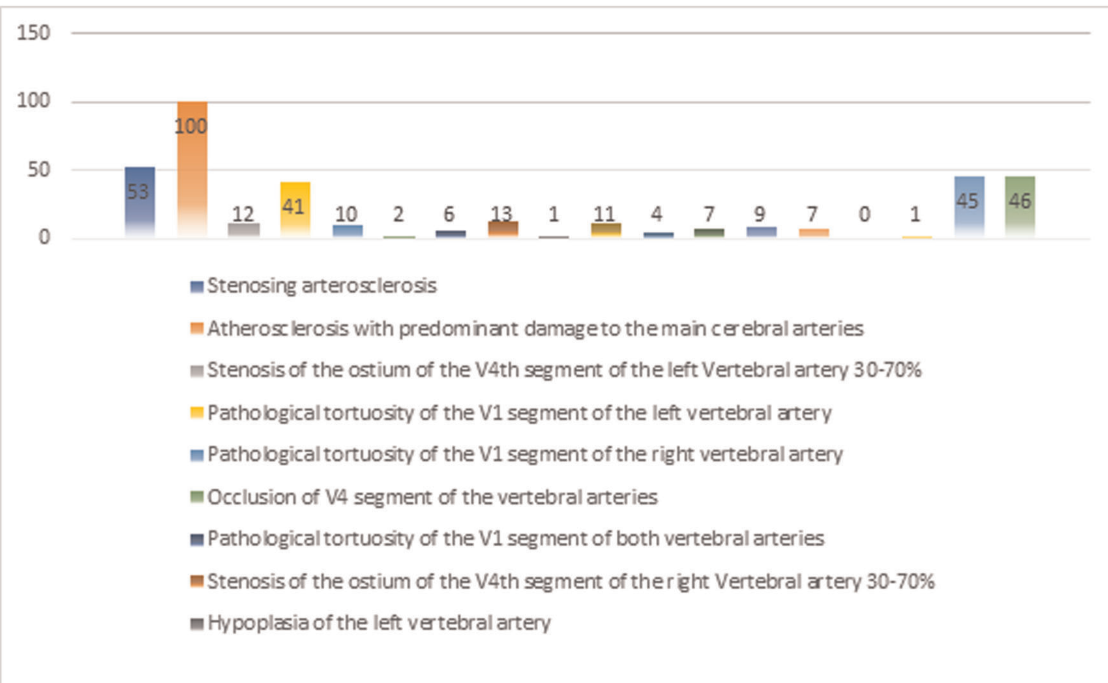

FIGURE 1 | Clinical diagnosis (in % of the total).

TABLE 1 | Comorbidities identified in the study patients.

Concomitant diseases	Number of cases
Hypertension grade 1	1
Hypertensive pain grade 2	34
Hypertension grade 3	10
Diffuse encephalopathy grade 2	42
Diffuse encephalopathy grade 3	7
Diffuse encephalopathy grade 1	1
Osteochondrosis of the spine	32
Otosclerosis, mixed form	0
Parkinson syndrome	2
Ischemic heart disease, angina pectoris I	1
Ischemic heart disease, angina pectoris II	26
Ischemic heart disease, angina pectoris III	3

Choosing the type of surgical treatment for patients with VBI is an unresolved medical problem. The key difficulty in the diagnostic process lies in the multiple possible etiologies of this pathology. The process of determining the differential diagnosis is quite time-consuming and, in our opinion, this is one of the reasons for the small number of operations for patients with VBI syndrome. The problem with choosing diagnostic methods to establish the need for surgical intervention among patients with VBI is discussed by many surgeons. This is important to determine the identifying signs of this pathology, differentiating it from other conditions with a similar clinical picture (10), namely: demyelinating processes in the central nervous system, diseases of the inner and middle ear, tumors of central vestibular structures (stem, cerebellum or cortex), carotid sinus syndrome, anemia, thyroid diseases, etc. In addition, the neurosurgeon or vascular surgeon does not conduct diagnostic measures to diagnose the VBI alone, each patient requires consultation and examination by a neurologist, ophthalmologist, ENT (ear, nose, and throat) specialist, functional and radiology diagnostics specialist to exclude all "non-vascular" diseases that may mimic VBI.

The primary technique of VA assessment is the study of blood flow volume to exclude VA hypoplasia. After using this algorithm **Figure 2**, we will analyze the procedure of patient examination by a neurosurgeon to establish the diagnosis of VBI:

Stage 1: General and clinical neurological examination of the patient (including the provocative test).

A. General clinical examination:
   - Assessment of radial artery pulses or the establishment of the presence of auscultative VA murmur in the neck or supraclavicular region;
   - Presence of blood pressure asymmetry on the hands of more than 20 mmHg.

B. Clinico-neurological examination (by a competent neurosurgeon):
   - Compression diagnostics tests (Ethan's test, VA compression test, dizziness test, etc.).

Stage 2: identifying the level of obstruction in the suspected vessels.

- doppler u/s of the brachiocephalic artery: analysis of the diameter of arteries, velocity and volume analysis of the blood flow;
- loading tests to determine perfusion reserve (turning and tilting of the head);
- Analysis and calculation of the reactivity index of VA;
- calculation of the total blood volume;
- Transcranial doppler.

Stage 3: use of radiologic diagnostic methods:

- Brain computerized tomography (CT)/magnetic resonance imaging (MRI): morphology of subtentorial and supratentorial structures of the brain;
- CT or MRI-angiography: main arteries of the brain, anatomy of the posterior cerebral artery (PCA), excluding trifurcation of carotid arteries);
- cerebral angiography of each segment of the VA, patency, morphological and functional status of the posterior circulation including compression tests.

RESULTS AND DISCUSSION

As a result of the analysis of neurological disorders, statistical indicators were determined for surgical treatment in the presence of the entire clinical complex of discoordination, vestibular-ataxia syndrome, auditory and visual disorders. Based on the proposed diagnostic algorithm, it is possible to predict the type of surgical treatment using the above indicators.

Group 1: Anastomosis ($n = 6$)

The inclusion criteria for the anastomosis included:

1. Predominant clinical features of VBI,
2. No significant defects of the VA and subclavian artery,
3. Carotid stenosis more than 70%,
4. Lack of decompensation in the vertebrobasilar system.

The data for the clinical features of the patients in 1st group was as tabulated below (**Supplementary Figure 3A**).

Of the 6 patients, vertebral circulation was closed (group 1.A) in 4 (66.7%) and open in 2 (33.3%) (group 1.B). Preoperative clinical manifestations of VBI in group 1 patients ($n = 6$): Dyscirculatory encephalopathy in VBI ($n = 2$, 33.3%), TIA in VBI ($n = 1$, 16.7%) and acute cerebrovascular accident in VBI ($n = 2$, 50.0%).

After full investigations, all patients underwent anastomosis surgery. **Supplementary Figure 4** indicates the cumulative survival of the patients.

Group 2: Resection of the Tortuous Segment ($n = 35$)

Features of diffuse encephalopathy in the VB system were seen in 15 (42.9%) patients, TIA in 7 (20%) patients, 13 (37.15%) presented with acute vascular compromise in the VBS. Abnormalities of coordination, auditory and visual systems were the most common preoperatively. However, postoperatively, auditory symptoms persisted in most patients (**Supplementary Figure 3B**).

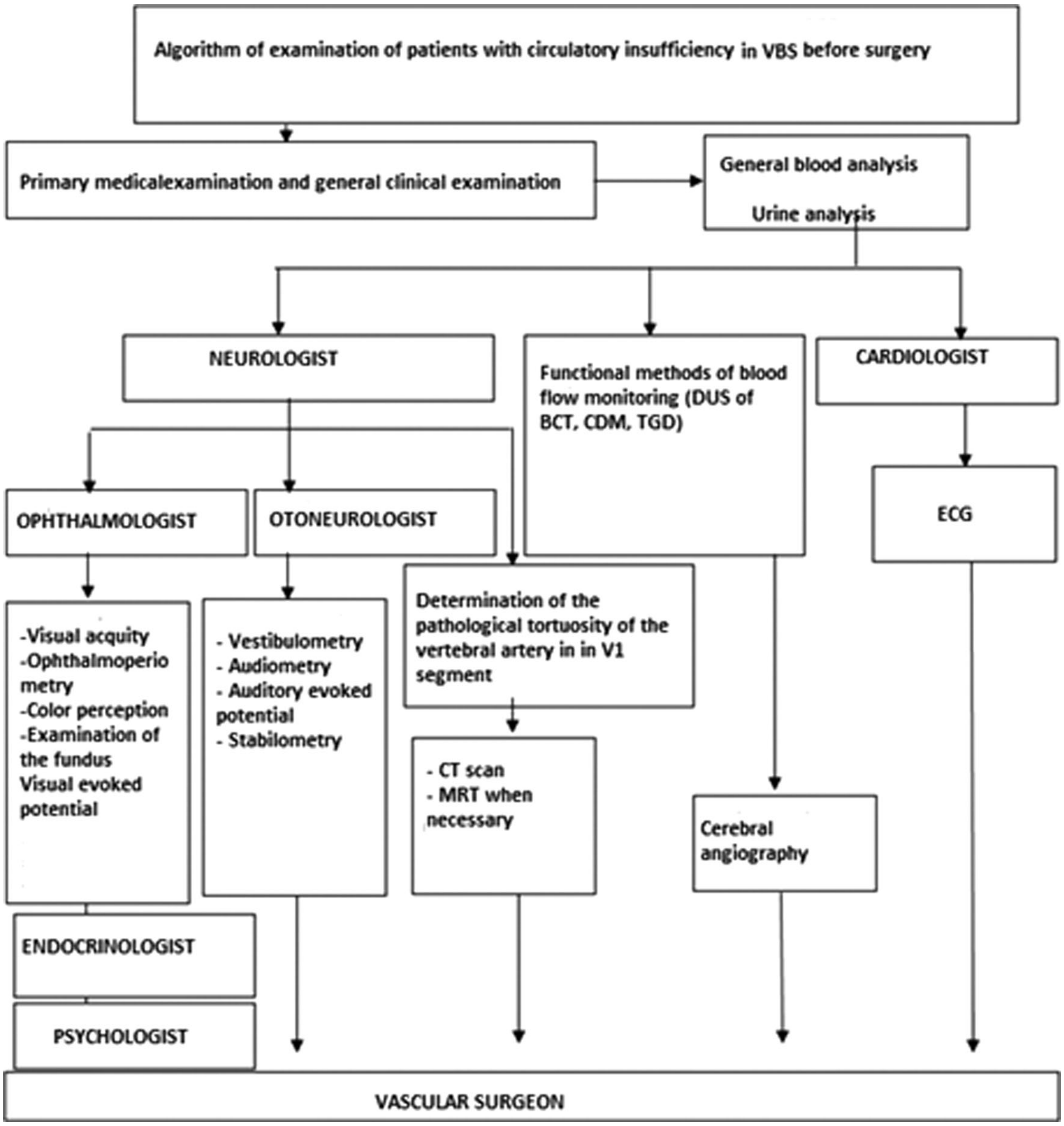

FIGURE 2 | Algorithm for examination of patients with vertebrobasilar insufficiency (VBI). Note: DUS, Doppler ultrasound; BCT, Brachiocephalic trunk; VBI, Vertebrobasilar insufficiency; ECG, Electrocardiogram; CT, Computed tomography; MRT, Magnetic resonance tomography.

The inclusion criteria for this group included:

1. Severe atherosclerotic lesions of the V1 segment of the VA,
2. Vertebral-subclavian steal phenomenon syndrome.

Based on the characteristics of the lesion on the V1 segment of the VA, the group was further divided into two types:

- IIA - 30 (85.7%) patients with occlusion of the V1 segment of VA,
- IIB - 15 (24.3%) patients with local, limited subtotal stenosis of the V1 segment of the VA (greater than 70%).

Both groups had reconstruction of the V1 segment of the VA. The division of patients by type of performed operations is presented in **Supplementary Figure 5**. The patients were followed up for a maximum of 3 years. The patients showed minimal improvement in the first year. However, by year 3, almost 75% of these patients had shown improvement (**Supplementary Figure 6**).

Group 3: Reconstructive Surgery ($n = 5$)

These patients underwent Arteriolysis, X-ray endovascular stenting, and Arterioplasty.

The inclusion criteria in this group included:

1. chronic ischemia in the distribution of the VB system;
2. VA atherosclerosis in the V1 segment of the VA;

TABLE 2 | Characteristics of blood flow in the V1 vertebral artery (VA) segment depending on the type of vertebrobasilar insufficiency (VBI).

Parameters	Dyscirculatory encephalopathy	TIA in VBS	Stroke in VBS	Control group (conservative treatment)
Age at the moment of surgery	59.06 ± 8.28	69.12 ± 7.70	70.27 ± 7.60	76.12 ± 7.70
Time from the onset of the disease to surgery	4.61 ± 2.97	4.80 ± 2.84	3.97 ± 2.27	–
Blood flow to the VA, mL/min	62.13 ± 20.60	67.70 ± 22.18	63.13 ± 17.48	62.98 ± 29.11
Blood flow after the VA, mL/min	117.79 ± 23.99	116.57 ± 17.54	115. 92 ± 17.48	120.88 ± 23.54
Increase in blood flow in VA, mL/min	54.56 ± 22.33	55.96 ± 19.73	52.80 ± 17.73	55.96 ± 19.73
Total blood flow in both VAs before surgery/ treatment, mL/min	207.81 ± 36.29	210.16 ± 23.37	216.16 ± 23.37	220.11 ± 28.82
Total blood flow in both VAs after surgery/ treatment, mL/min	262.76 ± 36.29	264.08 ± 42.62	271.36 ± 23.99	234.18 ± 14.32
Increase in total blood flow in both Vas, mL/ min	54.96 ± 30.80	53.92 ± 36.21	55.20 ± 24.96	14.07 ± 28.87
Increase in total blood flow in both VAs, mL/ min	59.79 ± 23.41	61.13 ± 25.75	56.19 ± 23.09	53.65 ± 25.65
Reactivity index before surgery/treatment	0.181 ± 0.043	0.171 ± 0.070	0.197 ± 0.038	0.198 ± 0.020
Reactivity index before surgery/treatment	0.298 ± 0.068	0.296 ± 0.080	0.314 ± 0.026	0.215 ± 0.082
Increase in reactivity index	0.117 ± 0.051	0.125 ± 0.076	0.116 ± 0.042	0.017 ± 0.072

TIA, Transient ischemic attack; VBS, Vertebrobasilar system; –, Not determined.

TABLE 3 | Characteristics of blood flow in the V1 segment of vertebral artery (VA). depending on the type of surgery performed.

Parameter	Transition of the VA to CCA (*n* = 67) M ± SD	Anastomosis M ± SD	Resection of tortuosity M ± SD	Reconstructive surgery M ± SD
Age at the moment of surgery	60.45 ± 8.66	69.97 ± 7.33	76.46 ± 8.05	70.09 ± 6.94
Time from the onset of the disease to surgery	4.73 ± 3.28	4. 53 ± 2.73	4.50 ± 1.80	3.69 ± 1.99
Blood flow to the VA, mL/min	65.08 ± 18.34	58.12 ± 19.10	75.11 ± 21.52	57.48 ± 15.83
Blood flow after the VA, mL/min	120.83 ± 20.60	111.52 ± 18.38	118.71 ± 24.63	113.95 ± 17.21
Increase in blood flow in VA, mL/min	55.18 ± 23.42	52.14 ± 16.38	46.29 ± 18.19	56.48 ± 17.30
Total blood flow in both VAs before surgery/ treatment, mL/ min	214.27 ± 22.59	209.35 ± 25.63	212.96 ± 26.24	211.49 ± 24.24
Total blood flow in both VAs after surgery/treatment, mL/min	271.33 ± 26.23	252. 74 ± 252.74	271.14 ± 30.37	268.91 ± 20.25
Increase in total blood flow in both Vas, mLl/min	59.26 ± 23.20	57. 00 ± 21.46	58.18 ± 27.29	57.42 ± 23.43

CCA, Common carotid artery; M, Mean; SD, Standard deviation.

3. Bony compression of VA in 2 segments was excluded;
4. Transient ischemic attacks;
5. Stroke in the VB system.

The preoperative and postoperative clinical features in these patients are tabulated in **Supplementary Figure 3C**.

One of the main factors for the neurosurgeon to consider when choosing the operative technique is the analysis of the V1 segment variability (11, 12), which was an exclusion factor for group 3 and an inclusion factor in group 4.

Group 4: Resection of the tortuous segment (*n* = 4)

The inclusion criteria included:

1. See criteria for group 3;
2. coiled V1 segment of the VA;
3. High mortality risk.

Assessment of clinical features of patients in group 4 is shown in **Supplementary Figure 3D**.

In this group, surgery on the V1 segment of the VA was performed as follows: 2 parients underwent angioplasty, stenting of the right vertebral artery (RVA), 1 patient underwent left scalenotomy, and 1 patient underwent eversion carotid endarterectomy on the left with resection of the pathological loop and redressing of the left vertebral artery (LVA).

In practice, we propose using the presented diagnostic algorithm, with the mandatory inclusion of the following elements: (1) to emphasize the need to exclude diseases with a similar clinical picture; (2) CT-angiography of the 4 segments of the VA and the basilar artery (BA); (3) analysis of the curvature of the vertebral circulation; (4) establishing the type of collateral compensation; (5) and the use of a significant outcome indicator like the blood flow reactivity index (**Supplementary Figure 7**).

The conservative treatment group which was receiving medical treatment ($n = 50$) was included to function as controls for comparison with the surgical treatment group (**Table 2**). Following the use of the above algorithm, the selected types of operations produced improvement in blood flow through the VAs in equal measure (**Table 3**).

When analyzing the volumetric blood flow rates, it was noted that among the operated patients, a decrease in the clinical features of VBI was observed in patients with an increase in the total volumetric velocity of blood flow in the VA of more than 250 mL/min ($p < 0.05$). An increase in the total volumetric blood flow of more than 250 mL/min was observed in most patients after various types of operations on the 1st segment of the VA.

Favorable outcomes including a decrease or disappearance of the clinical features of VBI were observed in most patients with an increase in total volumetric blood flow through the VA to 250 mL/min or more, and unfavorable outcomes i.e. deterioration or return of the clinical features of VBI was seen in patients with post-surgical total volume blood flow in the VA of less than 250 mL/min and all patients of the control group.

CONCLUSION

The use of the diagnostic algorithm contributes to the accurate prediction of the type of surgical intervention for various patients with vertebrobasilar insufficiency. In addition to traditional diagnostic methods, the gold standard investigations to guide the surgical intervention are radiological investigations including ultrasonic Doppler, contrast-enhanced multispiral CT, and CT-angiography. The need to perform cerebral angiography and multidisciplinary specialist consultations to exclude pathologies with a similar clinical picture cannot be overemphasized.

DATA AVAILABILITY STATEMENT

The original contributions presented in the study are included in the article/**Supplementary Material**, further inquiries can be directed to the corresponding author/s.

ETHICS STATEMENT

The studies involving human participants were reviewed and approved by The studies involving human participants were reviewed and approved by the Ethics Committee of by the 3rd Central Military Clinical Hospital named after A.A Vishnevsky, Krasnogorsk, Russia. Written informed consent to participate in this study was provided by the participants' legal guardian/next of kin.

AUTHOR CONTRIBUTIONS

Conceptualization, Writing - original draft and Project administration: GC, GA and EC; Writing - review and editing, Investigation and Resources: AF and ML; Formal analysis and Methodology: O; Data curation, Validation and Visualization: ZZ and AS; Funding acquisition: Gennady Chmutin; Supervision: GC. All authors contributed to the article and approved the submitted version.

SUPPLEMENTARY MATERIAL

The Supplementary Material for this article can be found online at: https://journal.frontiersin.org/article/10.3389/fsurg.2022.901759/full#supplementary-material.

REFERENCES

1. Jithoo R, Nadvi S, Robbs J. Vertebral artery embolism post subclavian artery injury with occipital lobe infarction. *Eur J Vasc Endovasc Surg*. (2000) 19(1): 85–6. doi: 10.1053/ejvs.1999.0905
2. Khalil A, Nashef SA. An alternative surgical approach to subclavian and innominate stenosis: a case series. *J Cardiothorac Surg*. (2010) 5(1):1–4. doi: 10.1186/1749-8090-5-73
3. Kim KD, Hoffman GA, Bae HW, Redmond A, Nunley PD, Tahernia AD, et al. 119. Ten-year outcomes of one-and two-level cervical disc arthroplasty: results from a US multicenter study. *Spine J*. (2019) 19(9):S57. doi: 10.1016/j.spinee.2019.05.132
4. Wang K-F, Duan S, Zhu Z-Q, Liu H-Y, Liu C-J, Xu S. Clinical and radiologic features of 3 reconstructive procedures for the surgical management of patients with bilevel cervical degenerative disc disease at a minimum follow-up period of 5 years: a comparative study. *World Neurosurg*. (2018) 113:e70–e6. doi: 10.1016/j.wneu.2018.01.157
5. Wu T-k, Wang B-y, Cheng D, Rong X, Lou J-g, Hong Y, et al. Clinical and radiographic features of hybrid surgery for the treatment of skip-level cervical degenerative disc disease: a minimum 24-month follow-up. *J Clin Neurosci*. (2017) 40:102–8. doi: 10.1016/j.jocn.2017.02.030
6. Yang L, Chen J, Yang C, Pang X, Li D, Wu B, et al. Cervical intervertebral disc degeneration contributes to dizziness: a clinical and immunohistochemical study. *World Neurosurg*. (2018) 119:e686–e93. doi: 10.1016/j.wneu.2018.07.243
7. Xu G, Fan X, Ma M, Liu X. Reconfiguration of the carotid artery after angioplasty and stenting: a case report and review of the literature. *Interv Neurol*. (2015) 4(1-2):38–42. doi: 10.1159/000438777
8. Novikov JVSIN, Grachev SA, Shepin MA, Volkov EA. Experience of surgical prevention of ischemic stroke in the vertebrobasilar system. *Angiol Vasc Surg*. (2016) 22(2):263–5.
9. Arnold M, Bousser MG, Fahrni G, Fischer U, Georgiadis D, Gandjour J, et al. Vertebral artery dissection. *Stroke*. (2006) 37(10):2499–503. doi: 10.1161/01.STR.0000240493.88473.39
10. Karasev MD SM, Shugushev Z. Secondary prevention of cerebrovascular accidents in patients with asymptomatic stenosis of the vertebral arteries. *Circ Pathol Card Surg*. (2021) 25(1):20–31. doi: 10.21688/1681-3472-2021-1-20-31
11. Debette S, Grond-Ginsbach C, Bodenant M, Kloss M, Engelter S, Metso T, et al. Differential features of carotid and vertebral artery dissections: the CADISP study. *Neurology*. (2011) 77(12):1174–81. doi: 10.1212/WNL.0b013e31822f03fc
12. Schievink WI. Spontaneous dissection of the carotid and vertebral arteries. *N Engl J Med*. (2001) 344(12):898–906. doi: 10.1056/NEJM200103223441206

Conflict of Interest: The authors declare that the research was conducted in the absence of any commercial or financial relationships that could be construed as a potential conflict of interest.

ORIGINAL RESEARCH
published: 19 May 2022
doi: 10.3389/fsurg.2022.895444

Significance of Pseudomeningocele After Decompressive Surgery for Chiari I Malformation

Artur Balasa[1], *Przemysław Kunert*[1]*, *Mateusz Bielecki*[1], *Sławomir Kujawski*[2] *and Andrzej Marchel*[1]

[1]*Department of Neurosurgery, Medical University of Warsaw, Warsaw, Poland,* [2]*Department of Exercise Physiology and Functional Anatomy, Ludwik Rydygier Collegium Medicum in Bydgoszcz Nicolaus Copernicus University in Toruń, Bydgoszcz, Poland*

OPEN ACCESS

Edited by:
Albert Sufianov,
Federal Center of Neurosurgery, Russia

Reviewed by:
Hidehito Kimura,
Graduate School of Medicine, Kobe University, Kobe, Japan
Rinat Sufianov,
I.M. Sechenov First Moscow State Medical University, Russia

***Correspondence:**
Przemysław Kunert
przemyslaw.kunert@wum.edu.pl

Specialty section:
This article was submitted to Neurosurgery, a section of the journal Frontiers in Surgery

Received: 13 March 2022
Accepted: 12 April 2022
Published: 19 May 2022

Citation:
Balasa A, Kunert P, Bielecki M, Kujawski S and Marchel A (2022) Significance of Pseudomeningocele After Decompressive Surgery for Chiari I Malformation. Front. Surg. 9:895444. doi: 10.3389/fsurg.2022.895444

Background: Pseudomeningoceles (PMCs) as abnormal collections of cerebrospinal fluid are quite common findings on follow-up MRI after Chiari decompression surgery (CDS). However, the importance of their identification has not been truly determined, especially when PMCs are described occasionally in the process of radiological follow-up. We retrospectively analyzed surgical outcomes and imaging findings after CDS depending upon the occurrence and thickness of PMCs.

Methods: A total of 76 adult patients who underwent CDS were analyzed. The clinical and radiological outcomes of patients with a pseudomeningocele (wPMC) were evaluated and compared to those of patients without a pseudomeningocele (w/oPMC). Radiological morphometric measurements were performed and compared between groups. Comparisons of the maximal PMC thickness were made within the wPMC group.

Results: PMCs were recognized in 27 (35.5%) patients, of whom 3 (11.1%) required reoperation. Differences in satisfactory result rates regarding gestalt assessment and Chicago Chiari Outcome Scale were statistically insignificant between the w/oPMC and wPMC groups ($p = 1$ and $p = 0.56$, respectively). The postoperative syringomyelia decrease and cerebellar tonsil elevation were similar between the groups ($p = 1$ and $p = 0.74$, respectively) in the long-term follow-up. Additionally, the clinical or radiological outcomes with radiological details were not related to PMC thickness in the long-term follow-up. However, radiological details showed the cooccurrence of PMCs with a postsurgical of cerebello-tentorial distance increase ($p < 0.05$), basion-pontomedullary sulcus distance decrease ($p < 0.05$) and tonsillo-graft distance decrease ($p < 0.05$).

Conclusions: We found no significant relationships between PMC presence or thickness and clinical or radiological outcomes. However, postoperative changes within the posterior fossa associated with PMCs resemble brain sagging, which occurs in intracranial hypotension. Therefore, extradural cerebrospinal fluid escape may also be responsible for symptoms in some patients with PMCs after CDS.

Keywords: Chiari I malformation, pseudomeningocele, surgical and radiological outcomes, decompressive surgery, complications

INTRODUCTION

The Chiari malformations originally described by Hans Chiari in 1891 (1) relate to a rare group of hindbrain abnormalities concerning both pediatric and adult patients. The most common, Chiari I malformation (CMI), consists of caudal herniation of elongated cerebellar tonsils through the foramen magnum, causing symptoms secondary to compression of the brain stem, dysfunction of the cerebellum and distortion of cerebrospinal fluid (CSF) flow (2). Disturbances of CSF flow are responsible for syringomyelia, which has been reported in 69% of adult patients (3), but the exact pathophysiology remains unclear (4, 5). For symptomatic cases, the treatment of choice is suboccipital decompression with duraplasty (6). However, duraplasty is related to a larger number of complications with a lower recurrence rate of symptoms than osseous decompression alone (7–9). Average complication rates have been estimated at 4.5%, and among the most common causes of CSF leaks, aseptic meningitis and pseudomeningocele have been reported (3). Pseudomeningoceles (PMCs) are defined as abnormal CSF collections visible on MRI due to leakage into the extradural space (10) and directly over the dural graft. Pseudomeningocele can reduce the volume of reconstituted cisterna magna because of compression on duraplasty. Eventually, they can become symptomatic due to compression of neural structures or the impeding of CSF flow through the foramen magnum. Nevertheless, pseudomeningocele is not a rare finding on follow-up MRI, but it is not considered a complication until it leads to recurrent symptoms or CSF fistula or causes unacceptable cosmetic effects (11).

The aim of this study was to determine the roles of co-occurring pseudomeningoceles and their sizes on long-term outcomes after decompressive surgery with duraplasty in patients with CMI.

MATERIALS AND METHODS

A total of 96 adult patients who underwent posterior fossa decompression (PFD) with duraplasty for symptomatic CMI from January 2003 to December 2019 at our institution were screened. Twenty of them were excluded because their preoperative radiographic studies were not accessible. The mean Chicago Chiari Outcome Scale (CCOS) of the excluded and included patients did not significantly differ (12.85 vs. 12.4; $p = 0.45$). Of 76 included patients, 60 were women, and 16 were men, with an average age of 41.8 years old (range from 18 to 66 years old). The medical data were obtained from telephone questionnaires and hospital and ambulatory charts. For analysis of the long-term clinical course, gestalt assessment (improvement, unchanged or deterioration) and Chicago Chiari Outcome Scale (CCOS) were used (12–14). The mean clinical follow-up was 58 months.

All methods were carried out in accordance with relevant guidelines and regulations.

All protocols were approved by Bioethics Committee of Medical University of Warsaw (AKBE/231/2021). Informed consent was obtained from all subjects.

IMAGING

Preoperative and follow-up MRI was performed in every case. Follow-up MRI was scheduled 6 months after surgery, and additional studies were performed earlier or later, depending on the clinical indications. Numerous patients underwent many control MRI studies, especially those with long-term follow-up. In these cases, the last study was considered. The mean neuroimaging follow-up was 39.9 months.

The presence of pseudomeningocele on follow-up MRI was defined as hyperintense fluid collection above a hypointense linear dural graft on sagittal T2-weighted MRI imaging.

Because of the variable shape, precise measurement of PMC total volume is very difficult or impossible. Therefore, size was determined by the maximal thickness of the pseudomeningocele as the perpendicular distance to the graft with the best correlation clinically with complications (15) (**Figure 1**).

Maximal tonsillo-graft distance was also measured. Additional radiological details, such as pre- and postprocedural differences in maximal cerebello-tentorial distance and basion-pontomedullary sulcus distance, were noted. The levels of pre- and postoperative tonsillar descent were also measured and compared. For a postoperative tonsil position assessment, the level of the foramen magnum was determined by restoration of the angle between the line tangent to the clivus surface and the basion-opisthion line established on preoperative images (Boogaard's angle; **Figure 1**) (16). In cases of syringomyelia in the preoperative study, their size was determined to be decreased, stable or increased. The cooccurrence of pseudomeningocele and its maximal thickness and clinical and radiological outcomes were analyzed in detail, including the poor preoperative status of 3 reoperated patients for symptomatic PMCs. Evaluation of the relationship of PMC thickness with tonsillo-graft distance and pre- and postprocedural differences in maximal cerebello-tentorial distance, basion-pontomedullary sulcus distance and tonsillar herniation was performed. In cases of pre- and postoperative distance comparisons, we received positive or negative values depending on whether a particular distance decreased or increased on follow-up MRI, respectively (**Figure 1**).

SURGICAL TECHNIQUE

Suboccipital craniectomy with C1 posterior arch removal and sometimes with partial (No. 24) or whole (No. 6) C2 laminectomy was performed with Y-shaped dural incision and with subsequent duraplasty in all cases. Depending on surgeon preference, two types of graft material were used for dural closure: nonautologous grafts or autologous grafts. The former, represented by synthetic collagen matrices, was used in 48 (63.2%) cases. Autologous grafts in this series, including previously harvested pericranium or fascia lata, were used in 28 (36.8%) cases. The arachnoid layer, 4^{th} ventricle and tonsils were left intact, and no local or lumbar drains after surgery were used (17, 18).

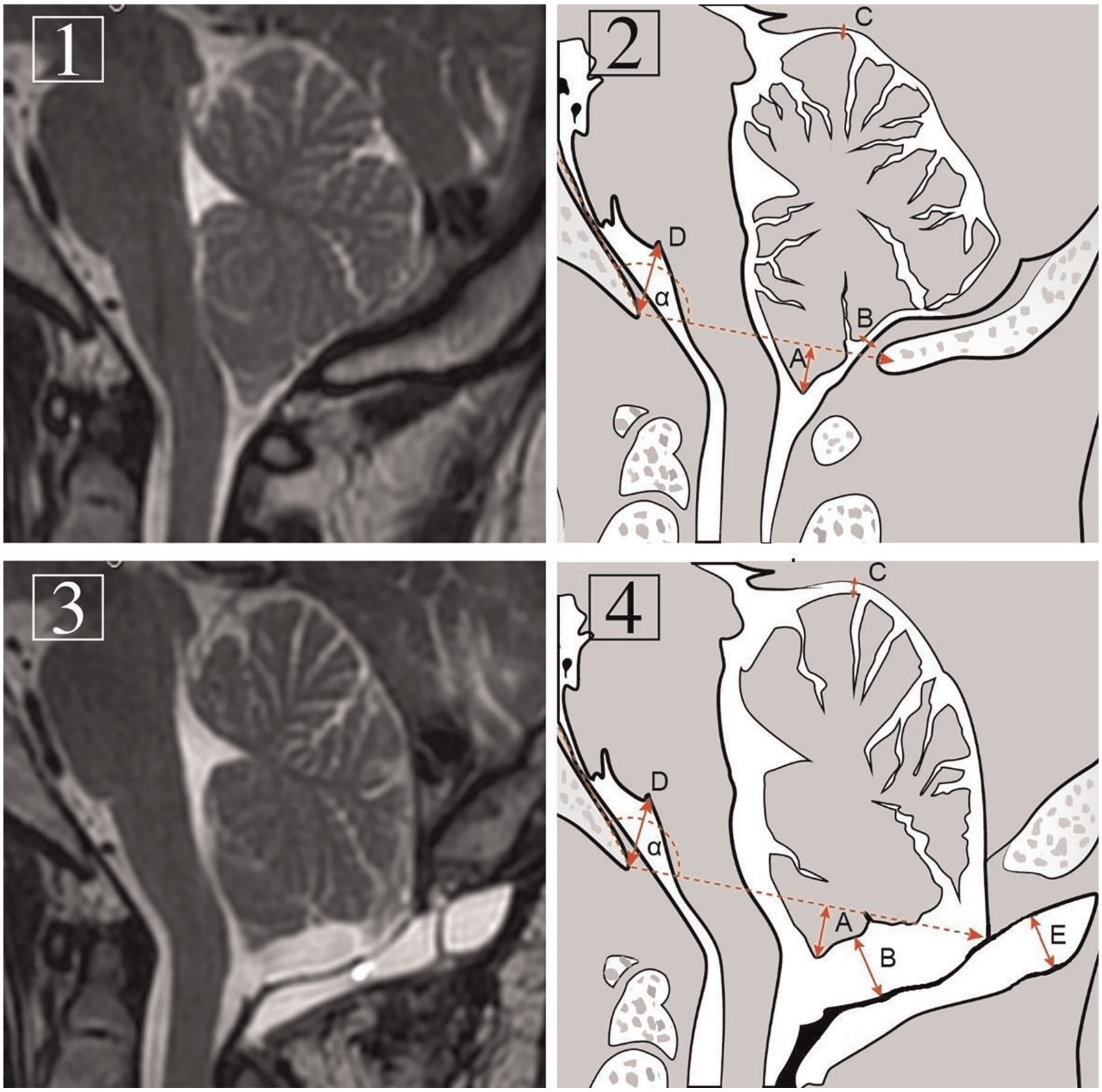

FIGURE 1 | Preoperative (**1** and **2**) and follow-up (**3** and **4**) T1-weighted MRI images of the craniocervical junction region and diagrams presenting measurements in the same midsagittal plane. Measurements included: α: Boogaard's angle. A: max. tonsillar herniation. B: max. tonsillo-graft distance. C: max. cerebello-tentorial distance. D: max. basion-pontomedullary sulcus distance. E: pseudomeningocele thickness.

STATISTICAL ANALYSIS

The Shapiro-Wilk test was used to test the assumption of normality, and Levene's test was used to examine the assumption of homogeneity. Mean values and standard deviations (SDs) are reported. Fisher's exact test was used to examine the relationship between PMC presence and changes in symptom severity expressed in a binary manner, while the chi-square test was used in the case of symptom severity changes in three categories (improvement vs. unchanged vs. deterioration). The Mann-Whitney U test was used to compare values of continuous and ordinal variables between independent groups. The significance level was set at alpha = 0.05.

RESULTS

Twenty-seven (35.5%) patients demonstrated PMC on posttreatment MRI. Only 3 (11.1%) of 27 patients required revision surgery, representing 3.9% of the overall study cohort. Satisfactory clinical results according to gestalt assessment and CCOS were obtained in 75.5% and 81.6% of patients without pseudomeningocele (w/oPMC) and 66.7% and 70.4% of patients with pseudomeningocele (wPMC), respectively ($p =$ 0.43, $p = 0.27$). For this outcome analysis, the prereoperative clinical condition of 3 reoperated patients was considered to capture the worst condition potentially related to PMC. Long-term follow-up showed even more comparable satisfactory

TABLE 1 | Comparison of clinical and radiological outcomes between patients without pseudomeningocele (w/oPMC) and with pseudomeningocele (wPMC) after decompression surgery in patients with Chiari I malformation, including preoperative status of 3 patients reoperated due to PMC and over long-term follow-up.

Comparison clinical and radiological outcomes, including preoperative status of 3 patients reoperated due to PMC				
Surgical outcomes		**Patients w/oPMC 49 pts. number of pts. (%)**	**Patients wPMC 27 pts. number of pts. (%)**	***p*-value**
Gestalt	Improvement or unchanged	37 (75.5%)	18 (66.7%)	0.43
	Deterioration	12 (24.5%)	9 (33.3%)	
CCOS[a]	≥12 (satisfactory)	40 (81.6%)	19 (70.4%)	0.27
	<12 (unsatisfactory)	9 (18.4%)	8 (29.6%)	
Syringomyelia on follow-up MRI (56 pts.)		**Patients w/oPMC with syringomyelia 36 pts. number of pts. (%)**	**Patients wPMC and syringomyelia 20 pts. number of pts. (%)**	***p*-value**
Improvement		33 (91.7%)	15 (75.0%)	0.12
Stable or deterioration		3 (8.3%)	5 (25.0%)	
Comparison of long- term clinical and radiological outcomes				
Long-term surgical outcomes		**Patients w/oPMC 49 pts. number of pts. (%)**	**Patients wPMC 25 pts. number of pts. (%)**	***p*-value**
Gestalt	Improvement or unchanged	37 (75.5%)	19 (77.7%)	1
	Deterioration	12 (24.5%)	6 (22.3%)	
CCOS[a]	≥12 (satisfactory)	40 (81.6%)	19 (77.7%)	0.56
	<12 (unsatisfactory)	9 (18.4%)	6 (22.3%)	
Syringomyelia on follow-up MRI (56 pts.)		**Patients w/oPMC with syringomyelia 37 pts. number of pts. (%)**	**Patients wPMC and syringomyelia 19 pts. number of pts. (%)**	***p*-value**
Improvement		33 (89.2%)	17 (89.5%)	1
Stable or deterioration		4 (10.8%)	2 (10.5%)	

[a]*Chicago Chiari Outcome Scale.*

results: 75.5% vs. 77.7% ($p = 1$) in gestalt and 81.6% vs. 77.7% ($p = 0.56$) in CCOS score for w/oPMC and wPMC patients, respectively (**Table 1**). Analysis of individual signs and symptoms showed no significant correlations between the wPMC and w/oPMC groups postoperatively (**Supplementary Table S1**).

Syringomyelia was present in 73.7% of patients preoperatively. A reduction in syringomyelia size was obtained in 91.7% of cases in the w/oPMC group and 75.0% of cases in the wPMC groups ($p = 0.12$). Two patients who underwent reoperation due to PMC had syringomyelia that remained unchanged after the first operation. In the long-term follow-up, including the results of 3 revision surgeries, the decrease in syrinx was similar: 89.2% vs. 89.5% for the w/oPMC and wPMC groups, respectively ($p = 1$; **Table 2**).

Pseudomeningocele was associated with a reduction in the average maximal tonsillo-graft distance on follow-up MRI (4.4 mm vs. 7.1 mm; $p < 0.05$). The cerebello-tentorial distance increased postsurgically in the wPMC group by an average of 1.2 mm, in contrast to the patients with w/oPMC, in whom it slightly decreased by an average of 0.3 mm ($p < 0.05$). Additionally, the existence of PMC was associated with a decrease in basion-pontomedullary sulcus distance by an average of 0.6 mm compared to the w/oPMC group, in which it was increased by an average of 0.6 mm ($p < 0.05$). However, we did not observe a substantial difference in tonsil elevation after surgery between the w/oPMC and wPMC groups on follow-up MRI (4.1 mm vs. 3.7 mm; $p = 0.74$; **Table 3**).

The average thickness of PMC was 8.7 mm ± 4.5 (SD) (range 2.0–21.0 mm). Relationships of PMC thickness with CCOS, individual signs and symptoms were not statistically significant (**Supplementary Table S1**). Additionally, we did not find an association between PMC thickness and changes in syrinx size on follow-up ($p = 0.59$) or other radiological details (**Table 3**).

A distinct group consisted of 3 reoperated patients due to symptomatic PMCs. Significant cerebellar subsidence coexisted in 2 patients. The average time between the operation and the onset of new symptoms was 7.7 days (range: 3–13). The predominant symptoms were severe headache, nausea, and vomiting with depressed levels of consciousness. Reduraplasty

TABLE 2 | Comparison of long-term radiological details on follow-up MRI between patients without pseudomeningocele (w/oPMC) and with pseudomeningocele (wPMC) after decompression surgery in patients with Chiari I malformation.

Radiological details on follow-up MRI	Patients w/oPMC 49 pts. mean [mm] ± SD	Patients wPMC[a] 27 pts. mean [mm] ± SD	*p*-value
Tonsillo-graft distance	7.1 ± 5.4	4.4 ± 3.3	<0.05
Pre- and postoperative difference of cerebello-tentorial distance	0.3 ± 1.0	−1.2 ± 1.4	<0.05
Pre- and postoperative difference of basion-pontomedullary sulcus distance	−0.6 ± 1.6	0.6 ± 1.5	<0.05
Pre- and postoperative difference of tonsillar herniation	4.1 ± 3.9	3.7 ± 3.1	0.74

[a]*Including the patient's clinical status before reoperation due to PMC.*

TABLE 3 | Correlation between pseudomeningocele thickness on follow-up MRI related and clinical outcome in CCOS (Chicago Chiari Outcome Scale) and radiological details.

PMC[b] thickness	2–7 mm	≥8 mm	*p*-value
No. of patients	13	14	
Mean CCOS[a] ±SD	11.4 ± 3.5	12.6 ± 2.7	0.39
Pre- and postoperative difference of tonsillo-graft distance [mm] ± SD	5.1 ± 3.8	3.8 ± 2.7	0.31
Pre- and postoperative difference of cerebello-tentorial distance [mm] ± SD	−1.5 ± 1.5	−0.9 ± 1.5	0.18
Pre- and postoperative difference of basion-pontomedullary sulcus distance [mm] ± SD	0.4 ± 1.9	0.8 ± 1.4	0.52
Pre- and postoperative difference of tonsillar herniation [mm] ± SD	3.9 ± 2.8	3.5 ± 3.5	0.75
Syringomyelia on follow-up MRI (20 pt.)	**PMC[b] thickness**		
	Patients with syringomyelia [9 pts.] No. of pts. (%)	**Patients with syringomyelia [11 pts.] No. of pts. (%)**	
Improvement	8 (88.9%)	8 (72.7%)	0.59
Stable or deterioration	1 (11.1%)	3 (27.3%)	

[a]*Including the patient's clinical status before reoperation due to PMC.*
[b]*Pseudomeningocele.*

TABLE 4 | Comparison of clinical outcomes and radiological details on follow-up MRI between reoperated and nonreoperated patients for pseudomeningocele (wPMC) after decompression surgery in patients with Chiari I malformation.

	Patients with PMC[b]		*p*-value
	Reoperated due to PMC (No. 3)	Nonreoperated (No. 24)	
Mean CCOS[a] [mm] ± SD	7.3 ± 1.2	12.3 ± 2.8	<0.05
PMC[b] thickness [mm] ± SD	11.3 ± 5.9	8.3 ± 4.5	0.37
Pre- and postoperative difference tonsillo-graft distance [mm] ± SD	3.3 ± 1.5	4.5 ± 3.4	0.73
Pre- and postoperative difference cerebello-tentorial distance [mm] ± SD	−3.7 ± 0.5	−0.9 ± 1.3	0.20
Pre- and postoperative difference basion-pontomedullary sulcus distance [mm] ± SD	0.2 ± 0.5	0.6 ± 1.8	0.73
Pre- and postoperative difference tonsillar herniation [mm] ± SD	1.2 ± 3.3	4.0 ± 3.0	0.27

[a]*Chicago Chiari Outcome Scale.*
[b]*Pseudomeningocele.*

was performed in all cases, with optimization of craniectomy size in 2. The clinical condition assessed with the CCOS in these cases before reoperation was significantly worse than that of the rest of the wPMC group (7.3 vs. 12.3; $p = 0.02$; **Table 4**). The mean CCOS of the reoperated patients improved in the long-term follow-up to 13.7 (range: 12–15), although persistent PMC was noted in 1 case on follow-up MRI. Comparison of radiological details of the reoperated PMCs to the remaining PMCs in the PMC group showed an insignificantly larger mean PMC thickness ($p = 0.37$) and a smaller reduction in tonsillo-graft distance ($p = 0.73$) in the reoperated patients. Prepostoperative differences in tonsillar herniation ($p = 0.27$), cerebello-tentorial distance ($p = 0.20$), and basion-pontomedullary sulcus distance ($p = 0.73$) were insignificantly less favorable in the reoperated patients than in nonreoperated patients with PMC (**Table 4**). We have not observed external CSF leaks in our series.

DISCUSSION

Surgical treatment for CMI has a particular predisposition to the development of CSF-related complications, including PMCs. Among predisposing factors worth mentioning are duraplasty, craniectomy, midline approach, and surgery concerning the posterior fossa (10, 15, 19). Thus, PMCs are among the most common complications after Chiari decompression surgery (20). Smith et al. noted that CM was the second most common cause of PMC after surgery for posterior fossa extraaxial tumors (10). PMC rates reported in the literature range from 2.5 to 24% (15, 21, 22). We observed PMCs in 35.5% of cases. However, we assessed even barely visible PMCs on follow-up MRI to define their exact significance. This wide disparity presumably resulted from some authors having considered PMCs recognized only on imaging studies as asymptomatic or incidental findings and not, therefore, reporting them as complications (10, 21).

According to the current state of knowledge, the appearance of PMC at the operation site might have no effect on duraplasty, or it can lead to slight reduction in recreated cisterna magna or obstruction of CSF flow, potentially leading to hydrocephalus (11). Further PMC enlargement can lead to compression of the posterior fossa neural structures. The patient either remains stable, or new symptoms can appear. PMC manifestation evolves from local pain in distended tissue or simple headache to posterior fossa syndrome or even impaired consciousness. Moreover, PMC can lead to CSF fistula and meningitis in cases of skin rupture (19).

The pathophysiology of PMC formation is unclear, but it seems that PMCs are initially formed as a result of suture CSF leakage between the dura and dural grafts or a tear in one of them. Leakage can occur immediately after an operation due to poor dural closure or could be caused by a progressive increase in intracranial CSF pressure in the course of hydrocephalus (23). However, knowing the role of CSF pressure, Valsalva maneuvers (e.g., coughing, sneezing, or defecating) likely cause a sudden increase in pressure, acting as a trigger factor in leakage (20). Symptomatic PMCs are most often observed shortly after surgery, which would suggest their onset until strong scarring among the graft, dura and neck muscles is created (15, 24).

Comparison of postoperative radiographic images of patients without and with PMC showed significant differences. A tendency to decrease the brainstem with the cerebellum in the wPMC group, defined as increased cerebello-tentorial and reduced basion-pontomedullary sulcus distances, was noted. This tendency was the opposite to that observed in the w/oPMC group, in which these structures had ascended (**Table 2**).

Considering our findings, we propose that the clinical consequences of some PMCs could develop via a similar mechanism to that of spontaneous intracranial hypotension (SIH). Spontaneous CSF fistula manifests as a small CSF reservoir (meningeal diverticula), usually associated with nerve root sleeves. CSF leakage is self-limiting, or CSF constantly leaks out in intracranial hypotension, e.g., after lumbar puncture (25–27). Similarly, postoperative leakage usually does not result in a constant increase in PMC volume. Similar to brain sagging in SIH, we noted slight hindbrain subsidence in the wPMC group, expressed as a postoperative increase in the supracerebellar space and a decrease in the basion-pontomedullary sulcus distance (**Figure 1**). The cooccurrence of cerebello-tentorial distance increases and basion-pontomedullary sulcus distance decreases in patients with PMCs might derive from the pressure gradient between the posterior fossa and PMC spaces, with a subsequent downward shift of all posterior fossa neural structures. Hypotension in the posterior fossa corresponds to partial hypotension syndrome but is not as severe as SIH in causing sagging of the whole brain (25, 28). This difference might indicate that postoperative cerebellar subsidence could be related not only to oversized occipital bony decompression but also to CSF leakage.

Raising and changing the shape of primarily herniated tonsils after decompression surgery from thin and extended to rounder and shorter are well known (16). Interestingly, despite sagging of the superior surface of the cerebellum in patients wPMC, we did not observe a significant difference in postsurgical tonsil tip ascent between the two groups, suggesting that favorable and unfavorable displacements in the posterior fossa might coexist after decompression.

Although the recreated cisterna magna was significantly smaller in patients with PMC, and the worst "prerevision" condition related to PMC was used for analysis, the comparison of the w/oPMC and wPMC groups showed no significant differences in clinical outcomes. Furthermore, the long-term observation of 25 patients with persistent PMC demonstrated that they achieved very similar clinical and radiological outcomes as their counterparts without PMC. It appears that the relative reduction in the recreated intradural space was not sufficient to block CSF flow in nonreoperated patients with PMC (29).

Pare and Batzdorf reported three cases in which PMCs were a reason for persistent syringomyelia in long-term follow-up (30). In our series, in which it was never a main cause of reoperation for PMC, all 3 revisions were performed too early after the first surgery to expect a decrease in the syrinx. We did not find any impact of the presence or size of PMCs on syringomyelia evolution.

Thus far, based on our analysis, neither the presence nor any size of PMC can be identified as a risk factor for worse outcomes. All PMCs requiring revision manifested shortly after surgery, long before scheduled follow-up MRI. Therefore, early clinical postsurgical deterioration is much more suggestive of PMC importance than any long-term radiological parameter. However, the differences in hindbrain rearrangement after decompression between patients with and without PMC shed new light on the potential mechanism increasing symptoms from some PMCs.

LIMITATIONS

Our study is limited by several factors, the most significant of which is the retrospective nature and single-center design of the research. Moreover, the cohort was represented by only 76 patients, with a significant effect on the statistical analysis of certain differences between groups. Additionally, the radiological data were based on MRI studies performed at various times after surgery and sometimes with different resolution of studies, which might have had an impact on the measured details. Standard follow-up MRI was performed without contrast, which could have shown other intracranial hypotension features. However, we obtained a relatively long-term follow-up by choosing to measure the last available MRI study. Future prospective research with a larger cohort is needed, especially to confirm our observations contained in the conclusion.

CONCLUSION

We did not find any significant relationships of pseudomeningocele presence or pseudomeningocele thickness with clinico-radiological outcomes after decompressive surgery. In rare cases, PMCs might be a cause of clinical deterioration over short postoperative periods. However, the symptoms could be secondary to hindbrain lowering caused by posterior fossa hypotension, resulting from extradural CSF leakage, rather than from narrowing of the intradural space at the foramen magnum level.

DATA AVAILABILITY STATEMENT

The original contributions presented in the study are included in the article/**Supplementary Material**, further inquiries can be directed to the corresponding author/s.

ETHICS STATEMENT

The studies involving human participants were reviewed and approved by Bioethics Committee of Medical University of Warsaw (AKBE/231/2021). Written informed consent for participation was not required for this study in accordance with the national legislation and the institutional requirements.

AUTHOR CONTRIBUTIONS

Conceptualization: AB, PK. Methodology: AB, PK. Formal analysis and investigation: AB, MB. Writing–original draft preparation: AB. Writing–review and editing: PK. Mathematical analysis: SK. Supervison: AM. All authors contributed to the article and approved the submitted version.

SUPPLEMENTARY MATERIAL

The Supplementary Material for this article can be found online at: https://www.frontiersin.org/articles/10.3389/fsurg.2022.895444/full#supplementary-material.

REFERENCES

1. Chiari H. Über veränderungen des kleinhirns infolge von hydrocephalie des grosshirns. *Dtsch Med Wochenschr* (1891) 17(42):1172–75. doi: 10.1055/s-0029-1206803
2. Steinbok P. Clinical features of Chiari I malformations. *Childs Nerv Syst*. (2004) 20(5):329–331. doi: 10.1007/s00381-003-0879-x.
3. Arnautovic A, Splavski B, Boop FA, Arnautovic KI. Pediatric and adult Chiari malformation Type I surgical series 1965–2013: a review of demographics, operative treatment, and outcomes. *J Neurosurg Pediatr*. (2015) 15(2):161–77. doi: 10.3171/2014.10.PEDS14295.
4. Holly L, Batzdorf U. Chiari malformation and syringomyelia. *J Neurosurg Spine*. (2019) 31:619–28. doi: 10.3171/2019.7.SPINE181139.
5. Klekamp J. The pathophysiology of syringomyelia - historical overview and current concept. *Acta Neurochir (Wien)*. (2002) 144(7):649–64. doi: 10.1007/s00701-002-0944-3.
6. Zhao JL, Li MH, Wang CL, Meng W. A Systematic Review of Chiari I Malformation: Techniques and Outcomes. *World Neurosurg*. (2016) 88:7–14. doi: 10.1016/j.wneu.2015.11.087.
7. Hankinson T, Tubbs RS, Wellons JC. Duraplasty or not? An evidence-based review of the pediatric Chiari I malformation. *Childs Nerv Syst*. (2011) 27(1):35–40. doi: 10.1007/s00381-010-1295-7.
8. Klekamp J, Batzdorf U, Samii M, Bothe HW. The surgical treatment of Chiari I malformation. *Acta Neurochir (Wien)*. (1996) 138(7):788–801. doi: 10.1007/BF01411256.
9. Del Gaudio N, Vaz G, Duprez T, Raftopoulos C. Comparison of dural peeling versus duraplasty for surgical treatment of Chiari Type I Malformation: results and complications in a monocentric patients' cohort. *World Neurosurg*. (2018) 117:e595–e602. doi: 10.1016/j.wneu.2018.06.093.
10. Smith GA, Strohl MP, Manjila S, Miller JP. Incidence, management, and outcome of symptomatic postoperative posterior fossa pseudomeningocele: a Retrospective single-institution experience. *Oper Neurosurg (Hagerstown)*. (2016) 12(3):298–304. doi: 10.1227/NEU.0000000000001329.
11. Mazzola CA, Fried AH. Revision surgery for Chiari malformation decompression. *Neurosurg Focus*. (2003) 15(3):E3. doi: 10.3171/foc.2003.15.3.3.
12. Aliaga L, Hekman KE, Yassari R, Straus D, Luther G, Chen J, et al. A novel scoring system for assessing Chiari malformation type I treatment outcomes. *Neurosurgery*. (2012) 70(3):656–64; discussion 664–55. doi: 10.1227/NEU.0b013e31823200a6.
13. Greenberg JK, Milner E, Yarbrough CK, Lipsey K, Piccirillo JF, Smyth MD, et al. Outcome methods used in clinical studies of Chiari malformation Type I: a systematic review. *J Neurosurg*. (2015) 122(2):262–72. doi: 10.3171/2014.9.JNS14406.
14. Bidzinski J. Late results of the surgical treatment of syringomyelia. *Acta Neurochir Suppl (Wien)*. (1988) 43:29–31. doi: 10.1007/978-3-7091-8978-8_7.
15. Gnanalingham KK, Lafuente J, Thompson D, Harkness W, Hayward R. MRI study of the natural history and risk factors for pseudomeningocoele formation following postfossa surgery in children. *Br J Neurosurg*. (2003) 17(6):530–36. doi: 10.1080/02688690310001627777.
16. Heiss JD, Suffredini G, Bakhtian KD, Sarntinoranont M, Oldfield EH. Normalization of hindbrain morphology after decompression of Chiari malformation Type I. *J Neurosurg*. (2012) 117(5):942–46. doi: 10.3171/2012.8.JNS111476.
17. Sindou M, Chavez-Machuca J, Hashish H. Cranio-cervical decompression for Chiari type I-malformation, adding extreme lateral foramen magnum opening and expansile duroplasty with arachnoid preservation. Technique and long-term functional results in 44 consecutive adult cases – comparison with literature data. *Acta Neurochir (Wien)*. (2002) 144(10):1005–19. doi: 10.1007/s00701-002-1004-8.

18. Oldfield EH, Muraszko K, Shawker TH, Patronas NJ. Pathophysiology of syringomyelia associated with Chiari I malformation of the cerebellar tonsils. implications for diagnosis and treatment. *J Neurosurg*. (1994) 80(1): 3–15. doi: 10.3171/jns.1994.80.1.0003.
19. Steinbok P, Singhal A, Mills J, Cochrane DD, Price AV. Cerebrospinal fluid (CSF) leak and pseudomeningocele formation after posterior fossa tumor resection in children: a retrospective analysis. *Childs Nerv Syst*. (2007) 23(2): 171–74; discussion 175. doi: 10.1007/s00381-006-0234-0.
20. Parker SL, Godil SS, Zuckerman SL, Mendenhall SK, Tulipan NB, McGirt MJ. Effect of symptomatic pseudomeningocele on improvement in pain, disability, and quality of life following suboccipital decompression for adult Chiari malformation type I. *J Neurosurg*. (2013) 119(5):1159–65. doi: 10. 3171/2013.8.JNS122106.
21. Foreman P, Safavi-Abbasi S, Talley MC, Boeckman L, Mapstone TB. Perioperative outcomes and complications associated with allogeneic duraplasty for the management of Chiari malformations Type I in 48 pediatric patients. *J Neurosurg Pediatr*. (2012) 10(2):142–49. doi: 10.3171/ 2012.5.PEDS11406.
22. Hoffman CE, Souweidane MM. Cerebrospinal fluid-related complications with autologous duraplasty and arachnoid sparing in type I Chiari malformation. *Neurosurg*. (2008) 62(3 Suppl 1):156–60; discussion 160–151. doi: 10.1227/01.neu.0000317387.76185.ac
23. Pirouzmand F, Tator CH, Rutka J. Management of hydrocephalus associated with vestibular schwannoma and other cerebellopontine angle tumors. *Neurosurgery*. (2001) 48(6):1246–53; discussion 1253–44. doi: 10.1097/ 00006123-200106000-00010.
24. Mehendale NH, Samy RN, Roland PS. Management of pseudomeningocele following neurotologic procedures. *Otolaryngol Head Neck Surg*. (2004) 131 (3):253–62. doi: 10.1016/j.otohns.2004.01.018.
25. Ferrante E, Trimboli M, Rubino F. Spontaneous intracranial hypotension: review and expert opinion. *Acta Neurol Belg*. (2020) 120(1):9–18. doi: 10. 1007/s13760-019-01166-8.
26. Schievink WI, Maya MM, Moser FG. Digital subtraction myelography in the investigation of post-dural puncture headache in 27 patients: technical note. *J Neurosurg Spine*. (2017) 26(6):760–64. doi: 10.3171/2016.11. SPINE16968.
27. Paldino M, Mogilner AY, Tenner MS. Intracranial hypotension syndrome: a comprehensive review. *Neurosurg Focus*. (2003) 15(6):ECP2. doi: 10.3171/foc. 2003.15.6.8
28. Kranz PG, Gray L, Malinzak MD, Amrhein TJ. Spontaneous Intracranial Hypotension: Pathogenesis, Diagnosis, and Treatment. *Neuroimaging Clin N Am*. (2019) 29(4):581–94. doi: 10.1016/j.nic.2019.07.006.
29. De Tommasi C, Bond AE. Complicated Pseudomeningocele Repair After Chiari Decompression: Case Report and Review of the Literature. *World Neurosurg*. (2016) 88(688):e681–87. doi: 10.1016/j.wneu.2015.11.056.
30. Pare LS, Batzdorf U. Syringomyelia persistence after Chiari decompression as a result of pseudomeningocele formation: implications for syrinx pathogenesis: report of three cases. *Neurosurgery*. (1998) 43(4):945–48. doi: 10.1097/00006123-199810000-00125.

Conflict of Interest: The authors declare that the research was conducted in the absence of any commercial or financial relationships that could be construed as a potential conflict of interest.

frontiers | Frontiers in Surgery

ORIGINAL RESEARCH
published: 25 May 2022
doi: 10.3389/fsurg.2022.919509

Endovascular Treatment of Acute Ischemic Stroke Due to Isolated Proximal Posterior Artery Occlusion

*Guang Zhang[1†], Yujing Zhu[1†], Yeping Ling[1], Pingbo Chen[1], Jiaxing Dai[1], Chunlei Wang[1], Shancai Xu[1], Alina Shumadalova[2] and Huaizhang Shi[1]**

[1]Department of Neurosurgery, The First Affiliated Hospital of Harbin Medical University, Harbin, China, [2]Department of General Chemistry, Bashkir State Medical University, Ufa, Republic of Bashkortostan, Russia

OPEN ACCESS

Edited by:
Ilgiz Fanilevich,
Federal Center of Neurosurgery,
Russia

Reviewed by:
Qingchun Mu,
Department of Neurosurgery,
Hainan General Hospital, China
Kun Hou,
First Affiliated Hospital of Jilin
University, China

***Correspondence:**
Huaizhang Shi
shihuaizhang@hrbmu.edu.cn

†These authors have contributed equally to this work and share first authorship

Specialty section:
This article was submitted to Neurosurgery, a section of the journal Frontiers in Surgery

Received: *13 April 2022*
Accepted: *05 May 2022*
Published: *25 May 2022*

Citation:
Zhang G, Zhu Y, Ling Y, Chen P, Dai J, Wang C, Xu S, Shumadalova A and Shi H (2022) Endovascular Treatment of Acute Ischemic Stroke Due to Isolated Proximal Posterior Artery Occlusion.
Front. Surg. 9:919509.
doi: 10.3389/fsurg.2022.919509

Background: Acute ischemic stroke (AIS) due to isolated proximal posterior cerebral artery (PPCA) occlusion is rare but associated with high morbidity and mortality rates. However, the optimal treatment strategy for patients with AIS caused by PPCA remains unclear. We discuss our single-center experience with endovascular treatment (EVT) in patients with PPCA.

Methods: Data from patients with AIS due to PPCA occlusion were retrospectively analyzed. We analyzed procedural details, the degree of reperfusion, functional outcomes, and complications. Functional outcomes were determined using the modified Rankin Scale (mRS) at 90 days, and good outcome was defined as mRS 0–2 at 90 days. Successful reperfusion was defined as modified treatment in cerebral ischemia (mTICI) 2b−3 after endovascular therapy. Safety variables included symptomatic hemorrhage (defined as an increase of four or more points in the National Institute of Health Stroke Scale score), vessel perforation or dissection, and new ischemic stroke in different territories.

Results: Seven patients were included in this study. The mean age of the patients was 64 ± 12.4 years. Successful reperfusion was achieved in all seven patients (100%). Good outcomes were achieved at 90 days in 2 patients (28.6%), and favorable outcomes were observed in five patients (71.4%). One patient underwent angioplasty as rescue therapy after three attempts. One patient died because of severe gastrointestinal bleeding 24 h after EVT, which was probably a complication of intravenous alteplase. One patient had an embolism in the basilar artery and achieved complete reperfusion after rescue thrombectomy. Another patient had a complication of vessel dissection in the PPCA and underwent stent implantation as rescue therapy. We observed no recurrence of ischemic stroke or any intracranial hemorrhage on non-contrast computed tomography 24 h after the procedure.

Conclusion: EVT may represent an alternative treatment strategy for patients with acute ischemic stroke caused by PPCA.

Keywords: acute ischemic stroke, endovascular treatment, neurological deficit, posterior cerebral artery, outcome

INTRODUCTION

Endovascular treatment (EVT) is the standard of care for patients with acute ischemic stroke (AIS) caused by large vessel occlusion (LVO) in the anterior circulation (1). Previous studies have also indicated the benefits of EVT in basilar artery occlusion (2). Acute posterior cerebral artery occlusion accounts for 5%-10% of all AIS cases (3). The territory of the proximal posterior cerebral artery (PPCA) usually has poor collaterals with a number of nerve fibers. PPCA occlusion involving thalamic perforating arteries, such as the Percheron artery, with abnormal variants can lead to severe neuropsychological deficits, visual symptoms, and unconsciousness (4, 5). However, no previous trials have focused on the effect of EVT on AIS due to PPCA occlusion (6, 7).

In this retrospective study, we aimed to present data on patients with AIS due to PPCA in clinical practice, focusing on the possibility of EVT as an alternative therapy in these patients.

METHODS

This study followed the Declaration of Helsinki and was approved by the Harbin Medical University ethics committee. Epidemiological, clinical and radiographical data were collected and reviewed. All patients or their legal guardians agreed to publication of clinical details and images. The participants provided their written informed consent to participate in this study.

All patients who underwent endovascular treatment for ischemic stroke at our institution were prospectively registered in an electronic database. For this study, we extracted data from patients with AIS due to PPCA occlusion between January 2020 and October 2021. The inclusion criteria were: (1) Acute occlusion of the PPCA, defined as the first and second segments of the posterior cerebral artery (8), as assessed by computed tomography (CT) angiography, magnetic resonance angiography (MRA), or digital subtraction angiography (DSA) before intervention; (2) Initiation of EVT within 24 h of symptom onset (**Figure 1**). The exclusion criteria were: (1) Severe preexisting disability, defined as a modified Rankin scale (mRS) score >2; (2) Secondary PPCA occlusion due to distal embolism during EVT of the basilar artery or vertebral artery occlusion; (3) Simultaneous occlusion of the anterior circulation, basilar artery, or intracranial vertebral artery.

The following data were extracted and analyzed: demographic characteristics, baseline National Institutes of Health Stroke Scale (NIHSS) scores, baseline Posterior Circulation Alberta Stroke Program Early CT Scores (pc-ASPECTS), history of previous stroke, use of intravenous

FIGURE 1 | Segmentation of PCA Proximal posterior cerebral artery was defined as first and second segment of PCA. PCA, posterior cerebral artery.

thrombolysis, time from stroke onset to groin puncture, and procedure duration. We used the NIHSS score and Glasgow coma scale (GCS) to assess the severity of AIS at the time of symptom onset, and the NIHSS and GCS scores at 24 h and at 7 days post-EVT were also recorded. The baseline pc-ASPECTS score was evaluated by two experienced neurointerventionists using non-contrast CT (NCCT) or diffusion-weighted imaging (DWI) and followed by consensus adjudication. Procedural details, including the number of retriever attempts, rescue therapies, complications, such as perforation, and vessel dissection, were also collected.

Technical Procedures

The procedure was performed under conscious sedation without heparinization. Femoral access was achieved, and a 6-French guide catheter was maneuvered into the dominant vertebral artery, and a cerebral angiogram was performed to confirm the PPCA occlusion. Under roadmap guidance, the microcatheter was navigated to the distal lumen of the occlusion site. A retrieval stent (Solitaire FR, ev3/Covidien, Irvine, CA, USA) of 4 × 20 mm was used in all cases. The stent retriever was left in place for 5 min to allow better clot integration and was retrieved through the guide catheter. Angiograms were obtained after each attempt. Repeated attempts, up to a maximum of three, were made until successful recanalization was achieved.

Outcomes and Complications

The degree of reperfusion was assessed on the final DSA image using the modified treatment in cerebral ischemia (mTICI) score. Successful reperfusion was defined as an mTICI score of 2b–3 on the final angiogram. The main outcome was the mRS score at 90 days. A good outcome was defined as an mRS score of 0–2. A favorable outcome was defined as a score of 0–3. Improved neurological function was defined as a decrease in NIHSS score of ≥4. Complications included vessel perforation, arterial dissection, intracranial hemorrhage, stroke progression, and embolism in new territories. Intracranial hemorrhage was assessed using NCCT at 24 h after the procedure. Symptomatic hemorrhage was scored by the European Cooperative Acute Stroke Study TWO (ECASS II) and was defined as an increase in the NIHSS score of >3 points or a decline in the GCS score of >2.

Statistical Analysis

Data were analyzed using descriptive statistics. Continuous variables are expressed as mean ± standard deviation or as medians and quartiles. Categorical variables are expressed as absolute values (number of patients) and relative frequencies (percentages).

RESULTS

Patient Characteristics

A total of 343 patients with AIS underwent EVT between January 1, 2020, and October 31, 2021, and seven patients were diagnosed with isolated PPCA occlusion. The median patient age was 64 ± 12.4 years. All patients were male. Occlusions were located on the right side in four patients (57%). Three patients had intracranial artery atherosclerosis, one had cardio-embolism. Three patients received intravenous alteplase therapy preceded by EVT. Six patients (85.7%) were unconscious before the procedure, and the median baseline NIHSS score was 40 (range, 21–40). The median baseline GCS score was 7 (range: 7–10). The mean time from symptom onset to recanalization was 296.7 ± 160.2 min. The procedure duration ranged from 27 to 75 min. Patient characteristics are presented in **Table 1**.

Outcomes and Complications

Patient outcome and procedure comlications are presented in **Table 2**. Successful reperfusion was achieved in all seven patients (100%). Two patients (28.6%) achieved complete reperfusion (mTICI: 3). One patient underwent angioplasty as rescue therapy after three failed retrieval attempts. Good outcomes were achieved in two patients (28.6%) and favorable outcomes were observed in five patients (71.4%). The mortality rate was 14.3%. Five (71.4%) patients had improved neurological function at 24 h post-procedure. One patient died because of severe gastrointestinal bleeding 24 h after EVT, probably as a complication of intravenous alteplase. The incidence of periprocedural complications was 28.6%. One patient had an embolism in the basilar artery and achieved

TABLE 1 | Clinical characteristics.

Patients number	1	2	3	4	5	6	7
Occlusion location	Left P1	Right P1	Left P1	Right P1	Right P1	Right P1	Left P2
Age	89	60	58	56	59	51	76
Hypertension	YES	NO	NO	NO	YES	YES	YES
Hypercholesterolemia	NO	NO	NO	NO	NO	NO	NO
Diabetes mellitus	NO	NO	NO	NO	NO	NO	NO
Previous stroke	NO	NO	NO	NO	YES	NO	YES
Atrial fibrillation	NO	NO	NO	NO	NO	NO	YES
Smoking	Yes	NO	NO	NO	Yes	NO	NO
Baseline NIHSS	40	38	36	40	40	40	21
Baseline ASPECTS	10	9	7	10	9	9	8
pre mRS	0	0	0	0	0	0	0
Baseline GCS	7	7	8	7	9	7	10
Intravenous thrombolysis	YES	NO	YES	NO	NO	NO	YES
Time from onset to groin puncture (min)	285	128	149	108	540	123	390
Time from puncture to recanalization (min)	40	62	75	30	50	70	27

P1, first segment of the posterior cerebral artery; P2, second segment of the posterior cerebral artery; NIHSS, National Institutes of Health Stroke Scale; ASPECTS, Alberta Stroke Program Early CT Score; mRS, modified Rankin scale; GCS, Glasgow coma scale.

TABLE 2 | Outcomes and complications.

Patients number	1	2	3	4	5	6	7
mTICI score	2b	2b	2b	3	3	2b	2b
Infarct location on follow up images	NA	Thalamus	Midbrainand thalamus	Occipital lobe	Occipital lobe	Thalamus and occipital lobe	Thalamus
Asymptomatic hemorrhage	NA	NO	NO	NO	NO	NO	NO
NIHSS at 24 h	NA	36	25	0	8	15	10
GCS at 24 h	NA	8	9	15	15	12	13
mRS score at 90 days	6	3	3	0	1	4	3

mTICI, modified Treatment in Cerebral Ischemia; National Institutes of Health Stroke Scale; mRS, modified Rankin Scale; GCS, Glasgow coma scale.

complete reperfusion after rescue thrombectomy. Another patient had a complication of vessel dissection in the PPCA and underwent stent implantation as rescue therapy. Endovascular procedure-related complications were not observed in the remaining five patients. We observed no recurrence of ischemic stroke or any intracranial hemorrhage on follow-up NCCT 24 h after the procedure.

Case Illustration

Case 1

Patient (No. 2) was admitted to the hospital with left limbs hemiplegia and dysarthria for 4.5 h and received intravenous alteplase (0.9 mg/Kg). Twelve h after admission, his consciousness deteriorated. His NIHSS and GCS scores were 38 and 7, respectively. NCCT did not reveal any intracranial hemorrhage. The baseline pc-ASPECTS score was nine (**Figures 2A,B**). DSA demonstrated occlusion of the right PPCA (**Figure 2C**), and the pre-mTICI score was 0. Endovascular procedures were performed with a 4 × 20-mm retrieval stent (Solitaire FR, ev3/Covidien). The final mTICI score was 2b after two attempts (**Figure 2D**). The time from onset (disturbance of consciousness) to groin puncture was 128 min, while the duration of the procedure was 62 min. Tirofiban was administered for 24 h, followed by aspirin (100 mg/day) and clopidogrel (75 mg/day). Post-procedural DWI indicated infarction in the bilateral thalamus (**Figure 2E**). MRA indicated complete recanalization of the right PCA (**Figure 2F**). The mRS score on day 90 was 3.

Case 2

Patient (No. 7) was admitted to the hospital with right hemiplegia and left oculomotor paralysis for 5 h. His NIHSS and GCS scores were 21 and 8, respectively. NCCT did not reveal any intracranial hemorrhage. The baseline pc-ASPECTS score was ten (**Figure 3A**). DSA demonstrated occlusion of the left P2 segment (**Figure 3B**), and the pre-mTICI score was 0. Endovascular procedures were performed with a 4 × 20-mm retrieval stent (Solitaire FR, ev3/Covidien). The final mTICI score was 2b after one attempt (**Figure 3C**). The time from symptom onset to groin puncture was 390 min, while the duration of the procedure was 27 min. Post-procedural DWI indicated infarction in the left thalamus (**Figure 3D**). The mRS score on day 90 was 3.

DISCUSSION

Since publication of five randomized clinical trials, EVT has become the standard therapy for patients with AIS caused by large-vessel occlusion in the anterior circulation artery (9–13). In this retrospective study, we found that EVT may be a suitable alternative treatment for PPCA occlusions. The proportion of successful reperfusions in our cases was 100%, and 28.6% of the patients achieved good functional outcomes at 90 days, with a low rate of procedure-related complications.

The perforating arteries from the P1 segment and junction of the P1-P2 supply blood to the upper midbrain, thalamus, and hypothalamus. The territory of the P2 segment includes the lateral geniculate corpus and the visual radiation adjacent to the temporal lobe (4). Therefore, occlusion of the PPCA often leads to infarction of the midbrain, thalamus, temporal lobe, and occipital lobe. Patients often present with contralateral hemiplegia and visual field defects, and have a poor outcome. Therefore, it seems necessary to provide more aggressive treatments for patients with AIS due to PPCA occlusion. In this study, six of seven patients lost consciousness after symptom onset, demonstrating that PPCA occlusion could lead to severe clinical manifestations.

In line with previous studies, 28.6% and 71.4% of patients achieved good or favorable outcomes at 90 days in this study, respectively, indicating that PPCA is an alternative therapy with an acceptable outcome. Meier et al. reported nine patients with PCA occlusion who underwent intra-arterial thrombolysis, and 67% of the patients had a favorable outcome (14). Strambo et al. compared the cognitive, visual, and disability outcomes of EVT, intravenous thrombolysis, and the best medicine therapy for isolated PPCA occlusion. Their study revealed a higher ratio of recanalization and favorable outcomes in the EVT group, and EVT did not significantly increase mortality (15). Previous studies have revealed a high successful recanalization rate, between 80% and 100%, with a low procedural complication rate of approximately 4%–7%. Good outcomes were observed in 59–66% of all patients at 90 days after EVT (16–18). Memon et al. (16) and Herweh et al. (19) presented the results of studies of 15 and 23 patients with isolated PPCA occlusion, respectively, who were treated with EVT. The successful recanalization rates were 80% and 54%, respectively. The proportions of patients with good outcomes at 90 days were

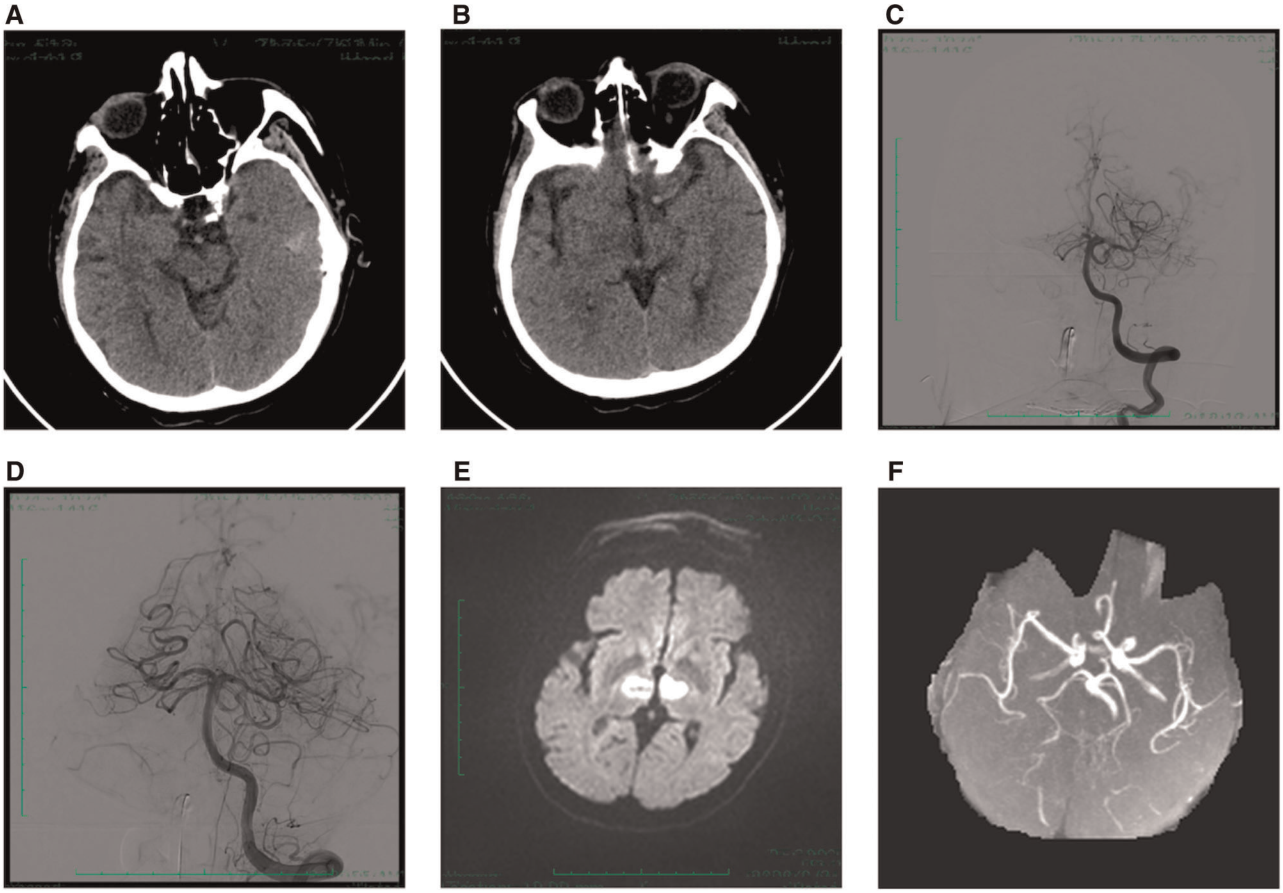

FIGURE 2 | Case 1. (**A,B**) Baseline CT indicated pc-ASPECTS score was 9. (**C**) Anterior-posterior angiogram revealed an occlusion of right PPCA. (**D**) Post-thrombectomy angiogram indicated the mTICI score was 2b. (**E**) Post-procedural DWI showed acute bilateral thalamic infarction. (**F**) MRA showed successful recanalization of right PPCA at 48 h after procedural. PPCA, proximal posterior cerebral artery; pc-ASPECTS, posterior circulation Alberta Stroke Program Early CT Score; mRS, modified Rankin Scale.

60% and 43.5%, respectively. Memon et al. reported that three patients (20%) experienced hemorrhage after the procedure, and one (6%), who had symptomatic hemorrhage, died. Herweh et al. reported a complication rate of 26% and a mortality rate of 13% within 90 days. In our study, we found one patient with asymptomatic subarachnoid hemorrhage, one patient with an embolism in a new territory, and one patient with vessel dissection, indicating the safety of EVT involving the PPCA.

In our study, we summarized the data of patients with PPCA occlusion who had undergone EVT in a single center. After evaluating the feasibility of EVT, we observed that all patients achieved successful reperfusion. Although one patient had an embolism in the basilar artery, the patient finally achieved complete reperfusion. Patient 1 received bridge therapy and died of severe upper gastrointestinal bleeding at 24 h after EVT. The patient received 0.9 mg/kg rt-PA for intravenous thrombolysis, followed by EVT. Systemic heparinization was not performed during the procedure, and as the reason for stroke was not large artery atherosclerosis, tirofiban or other antiplatelet agents were not administered during and after the procedure. Therefore, we speculated that the reasons for severe upper gastrointestinal bleeding included older age, poor general condition, and coagulopathy caused by the use of rt-PA. In the remaining six patients, no operation-related complications were observed during hospitalization or follow-up. Although our study had a high rate of successful recanalization, our good clinical outcomes were worse than those of other studies. This was because most of our patients were in coma and their baseline NIHSS scores were much higher than those of patients in the previous studies, although the neurological deficits improved in most patients after EVT.

The present study has some limitations, including its small sample size. In addition, although we extracted data from a prospective database, the case series was retrospective in nature. Third, we only analyzed patients with ischemic stroke involving PPCA occlusion who accepted EVT; i.e., those who accepted only medicine were not included in our study. Forth,

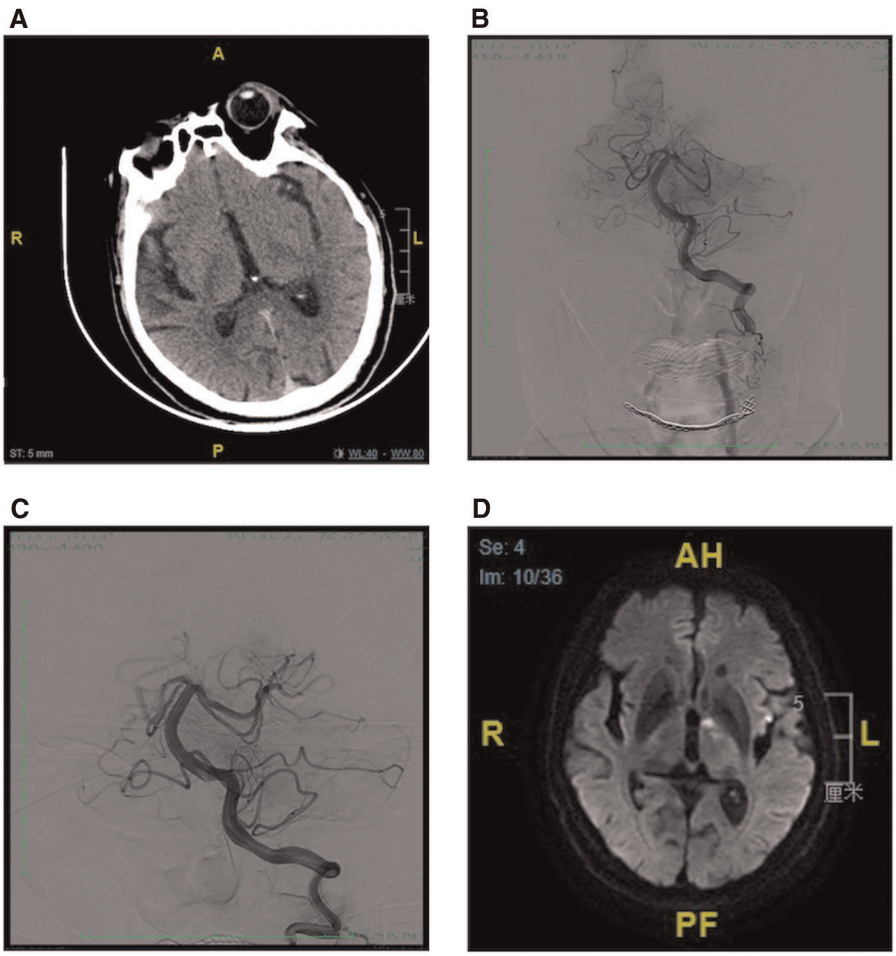

FIGURE 3 | Case 2. (**A**) Baseline CT indicated pc-ASPECTS score was 10, (**B**) Anterior-posterior angiogram revealed an occlusion of left PPCA. (**C**) Post-thrombectomy angiogram indicated the mTICI score was 2b. (**D**) Post-procedural DWI showed acute left thalamic infarction. PPCA, proximal posterior cerebral artery; pc-ASPECTS, posterior circulation Alberta Stroke Program Early CT Score; mRS, modified Rankin Scale.

patients with PPCA occlusion but who had mild symptoms might not undergo angiographic evaluation and may thus not have undergone EVT. Finally, we missed the details of these thrombus, such as thrombus length, pathologic information which potentially help to understand the etiology of PPCA occlusion.

In conclusion, our study suggests that EVT may represent an alternative treatment strategy for patients with AIS caused by PPCA occlusion. Nevertheless, further randomized studies are urgently required to verify our findings.

DATA AVAILABILITY STATEMENT

The original contributions presented in the study are included in the article/Supplementary Material, further inquiries can be directed to the corresponding author/s.

ETHICS STATEMENT

This human study was reviewed and approved by the Harbin Medical University Ethics Committee. Participants provided written informed consent to participate in this study.

AUTHOR CONTRIBUTIONS

GZ and YZ: study design, data collection, analysis, interpretation, writing of the introduction, methodology, results, discussion sections of the manuscript, and critical revision of the manuscript for important intellectual content. YL and AS: data collection, writing of the methodology and discussion sections of the manuscript and critical revision of the manuscript. PC, JD, CW, and SX: Study conception and design, writing of the results and discussion sections of the manuscript, and critical revision of the manuscript. HS: Study conception and design, study supervision, and critical revision of the manuscript for important intellectual content. All authors contributed to the article and approved the submitted version.

ACKNOWLEDGEMENTS

We would like to thank Editage (www.editage.com) for English language editing.

REFERENCES

1. Powers WJ, Rabinstein AA, Ackerson T, Adeoye OM, Bambakidis NC, Becker K, et al. Guidelines for the early management of patients with acute ischemic stroke: 2019 update to the 2018 guidelines for the early management of acute ischemic stroke: a guideline for healthcare professionals from the American Heart Association/American Stroke Association. *Stroke*. (2019) 50(12):e344–e418. doi: 10.1161/STR.0000000000000211
2. Writing Group for the BG, Zi W, Qiu Z, Wu D, Li F, Liu H, et al. Assessment of endovascular treatment for acute basilar artery occlusion via a nationwide prospective registry. *JAMA Neurol*. (2020) 77(5):561–73. doi: 10.1001/jamaneurol.2020.0156
3. Gulli G, Marquardt L, Rothwell PM, Markus HS. Stroke risk after posterior circulation stroke/transient ischemic attack and its relationship to site of vertebrobasilar stenosis: pooled data analysis from prospective studies. *Stroke*. (2013) 44(3):598–604. doi: 10.1161/STROKEAHA.112.669929
4. Maus V, Rogozinski S, Borggrefe J, Barnikol UB, Saklak M, Mpotsaris A. Clinical presentation of posterior cerebral artery occlusions - clinical rationale for a more aggressive therapeutic strategy? *eNeurologicalSci*. (2021) 25:100368. doi: 10.1016/j.ensci.2021.100368
5. Jalan P, Shrestha GS. Infarction due to occlusion of artery of percheron. *Neurol India*. (2021) 69(6):1901–2. doi: 10.4103/0028-3886.333521
6. Lindsberg PJ, Mattle HP. Therapy of basilar artery occlusion: a systematic analysis comparing intra-arterial and intravenous thrombolysis. *Stroke*. (2006) 37(3):922–8. doi: 10.1161/01.STR.0000202582.29510.6b
7. Yu W, Kostanian V, Fisher M. Endovascular recanalization of basilar artery occlusion 80 days after symptom onset. *Stroke*. (2007) 38(4):1387–9. doi: 10.1161/01.STR.0000260186.93667.a2
8. Kuybu O, Tadi P, Dossani RH. *Posterior cerebral artery stroke*. Treasure Island, FL: Statpearls (2022).
9. Berkhemer OA, Fransen PS, Beumer D, van den Berg LA, Lingsma HF, Yoo AJ, et al. A randomized trial of intraarterial treatment for acute ischemic stroke. *N Engl J Med*. (2015) 372(1):11–20. doi: 10.1056/NEJMoa1411587
10. Campbell BC, Mitchell PJ, Kleinig TJ, Dewey HM, Churilov L, Yassi N, et al. Endovascular therapy for ischemic stroke with perfusion-imaging selection. *N Engl J Med*. (2015) 372(11):1009–18. doi: 10.1056/NEJMoa1414792
11. Goyal M, Demchuk AM, Menon BK, Eesa M, Rempel JL, Thornton J, et al. Randomized assessment of rapid endovascular treatment of ischemic stroke. *N Engl J Med*. (2015) 372(11):1019–30. doi: 10.1056/NEJMoa1414905
12. Jovin TG, Chamorro A, Cobo E, de Miquel MA, Molina CA, Rovira A, et al. Thrombectomy within 8 H after symptom onset in ischemic stroke. *N Engl J Med*. (2015) 372(24):2296–306. doi: 10.1056/NEJMoa1503780
13. Saver JL, Goyal M, Bonafe A, Diener HC, Levy EI, Pereira VM, et al. Stent-retriever thrombectomy after intravenous T-Pa Vs. T-Pa alone in stroke. *N Engl J Med*. (2015) 372(24):2285–95. doi: 10.1056/NEJMoa1415061
14. Meier N, Fischer U, Schroth G, Findling O, Brekenfeld C, El-Koussy M, et al. Outcome after thrombolysis for acute isolated posterior cerebral artery occlusion. *Cerebrovasc Dis*. (2011) 32(1):79–88. doi: 10.1159/000328229
15. Strambo D, Bartolini B, Beaud V, Marto JP, Sirimarco G, Dunet V, et al. Thrombectomy and thrombolysis of isolated posterior cerebral artery occlusion: cognitive, visual, and disability outcomes. *Stroke*. (2020) 51(1):254–61. doi: 10.1161/STROKEAHA.119.026907
16. Memon MZ, Kushnirsky M, Brunet MC, Saini V, Koch S, Yavagal DR. Mechanical thrombectomy in isolated large vessel posterior cerebral artery occlusions. *Neuroradiology*. (2021) 63(1):111–6. doi: 10.1007/s00234-020-02505-w
17. Lee HN, Kim BT, Im SB, Hwang SC, Jeong JH, Chung MY, et al. Implications of mechanical endovascular thrombectomy for acute basilar and posterior cerebral artery occlusion. *J Cerebrovasc Endovasc Neurosurg*. (2018) 20(3):168–75. doi: 10.7461/jcen.2018.20.3.168
18. Clarencon F, Baronnet F, Shotar E, Degos V, Rolla-Bigliani C, Bartolini B, et al. Should posterior cerebral artery occlusions be recanalized? Insights from the trevo registry. *Eur J Neurol*. (2020) 27(5):787–92. doi: 10.1111/ene.14154
19. Herweh C, Abdalkader M, Nguyen TN, Puetz V, Schone D, Kaiser D, et al. Mechanical thrombectomy in isolated occlusion of the proximal posterior cerebral artery. *Front Neurol*. (2021) 12:697348. doi: 10.3389/fneur.2021.697348

Conflict of Interest: The authors declare that the research was conducted in the absence of any commercial or financial relationships that could be construed as a potential conflict of interest.

Publisher's Note: All claims expressed in this article are solely those of the authors and do not necessarily represent those of their affiliated organizations, or those of the publisher, the editors and the reviewers. Any product that may be evaluated in this article, or claim that may be made by its manufacturer, is not guaranteed or endorsed by the publisher.

frontiers | Frontiers in Surgery

ORIGINAL RESEARCH
published: 25 May 2022
doi: 10.3389/fsurg.2022.915310

Contralateral vs. Ipsilateral Approach to Superior Hypophyseal Artery Aneurysms: An Anatomical Study and Morphometric Analysis

Balkan Sahin[1], Serdar Onur Aydin[1], Mehmet Ozgur Yilmaz[1], Tahsin Saygi[1], Sahin Hanalioglu[2], Goktug Akyoldas[3], Oguz Baran[1,3]* and Talat Kiris[4]

[1]Microsurgical Neuroanatomy Laboratory, Koc University Hospital, Istanbul, Turkey, [2]Department of Neurosurgery, Faculty of Medicine, Hacettepe University, Ankara, Turkey, [3]Department of Neurosurgery, Koc University Hospital, Istanbul, Turkey, [4]Department of Neurosurgery, American Hospital, Istanbul, Turkey

Introduction: Surgical clipping of superior hypophyseal artery (SHA) aneurysms is a challenging task for neurosurgeons due to their close anatomical relationships. The development of endovascular techniques and the difficulty in surgery have led to a decrease in the number of surgical procedures and thus the experience of neurosurgeons in this region. In this study, we aimed to reveal the microsurgical anatomy of the ipsilateral and contralateral approaches to SHA aneurysms and define their limitations via morphometric analyses of radiological anatomy, three-dimensional (3D) modeling, and surgical illustrations.

Method: Five fixed and injected cadaver heads underwent dissections. In order to make morphometric measurements, 75 cranial MRI scans were reviewed. Cranial scans were rendered with a module and used to produce 3D models of different anatomical structures. In addition, a medical illustration was drawn that shows different sizes of aneurysms and surgical clipping approaches.

Results: For the contralateral approach, pterional craniotomy and sylvian dissection were performed. The contralateral SHA was reached from the prechiasmatic area. The dissected SHA was approached with an aneurysm clip, and maneuverability was evaluated. For the ipsilateral approach, pterional craniotomy and sylvian dissection were performed. The ipsilateral SHA was reached by mobilizing the left optic nerve with left optic nerve unroofing and left anterior clinoidectomy. MRI measurements showed that the area of the prechiasm was 90.4 ± 36.6 mm^2 (prefixed: 46.9 ± 10.4 mm^2, normofixed: 84.8 ± 15.7 mm^2, postfixed: 137.2 ± 19.5 mm^2, $p < 0.001$), the distance between the anterior aspect of the optic chiasm and the limbus sphenoidale was 10.0 ± 3.5 mm (prefixed: 5.7 ± 0.8 mm, normofixed: 9.6 ± 1.6 mm, postfixed:14.4 ± 1.6 mm, $p < 0.001$), and optic nerves' interneural angle was 65.2° ± 10.0° (prefixed: 77.1° ± 7.3, normofixed: 63.6° ± 7.7°, postfixed: 57.7° ± 5.7°, p: 0.010).

OPEN ACCESS

Edited by:
Albert Sufianov, Federal Center of Neurosurgery, Russia

Reviewed by:
Jorge Marcelo Mura, Instituto de Neurocirugía, Chile
Hidehito Kimura, Kobe University, Japan

***Correspondence:**
Oguz Baran
oguzbaran@gmail.com

Specialty section:
This article was submitted to Neurosurgery, a section of the journal Frontiers in Surgery

Received: 07 April 2022
Accepted: 03 May 2022
Published: 25 May 2022

Citation:
Sahin B, Aydin SO, Yilmaz MO, Saygi T, Hanalioglu S, Akyoldas G, Baran O and Kiris T (2022) Contralateral vs. Ipsilateral Approach to Superior Hypophyseal Artery Aneurysms: An Anatomical Study and Morphometric Analysis. Front. Surg. 9:915310. doi: 10.3389/fsurg.2022.915310

Conclusion: Anatomic dissections along with 3D virtual model simulations and illustrations demonstrated that the contralateral approach would potentially allow for proximal control and neck control/clipping in smaller SHA aneurysm with relatively minimal retraction of the contralateral optic nerve in the setting of pre- or normofixed chiasm, and ipsilateral approach requires anterior clinodectomy and optic unroofing with considerable optic nerve mobilization to control proximal ICA and clip the aneurysm neck effectively.

Keywords: superior hypophyseal artery, aneurysm, contralateral, ipsilateral, approach, microsurgical anatomy

INTRODUCTION

The superior hypophyseal artery (SHA) arises from the posteromedial surface of the internal carotid artery just distal to the distal dural ring. This terminology was first used by Day (1, 2). The SHA is responsible for the arterial supply of the pituitary stalk, optic nerves, and optic chiasm (2).

SHA aneurysms, together with carotid cave, posterior carotid wall, and carotid–ophthalmic aneurysms, are referred to as paraclinoid aneurysms (3, 4). Although SHA aneurysms are rare, they cause subarachnoid hemorrhage due to their intradural localization. Although the surgical treatment of SHA aneurysms has decreased with the development of endovascular treatment techniques, it still seems difficult to treat patients with low dome-to-neck ratios endovascularly.

First, the contralateral approach to bilateral carotid–ophtalmic aneurysms was defined by Yaşargil, and then, case series in the literature were shared by many authors (5–11). The surgical approach and clipping of SHA aneurysms are challenging for many reasons such as close proximity to important neurovascular structures, narrow surgical corridor, and difficulty in proximal control. Literature is scarce regarding the conditions and limits of the ipsilateral and contralateral approach for SHA aneurysms.

In this study, we aimed to reveal the microsurgical anatomy of the ipsilateral and contralateral approaches to SHA aneurysms and define their limitations *via* morphometric analyses of radiological anatomy, three-dimensional (3D) modeling, and surgical illustrations.

MATERIALS AND METHODS

Preparation of Specimens

In this study, five silicone-injected cadaver heads were used. Cadavers were fixed with a 10% formalin solution for at least 3 weeks. Silicone injection in all whole-head specimens was performed using the technique described by Shimizu et al. (12). Dissections were performed under ×6–40 magnification using a Zeiss Surgical Microscope (Carl Zeiss AG, Oberkochen, Germany). During the study period, all specimens were kept in a 75% alcohol solution. Three-dimensional images of each step of the dissection were obtained.

Radiological Examinations

In order to make morphometric measurements (perchiasmatic area, interneural angle, interneural length, etc.) in prefixed, normofixed, and postfixed chiasm types, we performed a thorough retrospective search on the institutional PACS for scans of patients 18–65 years who underwent any magnetic resonance imaging (MRI) of the head. We then reviewed patient charts and applied the following exclusion criteria: history of any brain or orbit tumor, enucleation of eye, optic nerve lesions, enlargement or atrophy of the optic nerve, raised intracranial pressure (treated or not), and ischemia, hemorrhage, or atrophy along the optic pathway. We included patients who had indications for MRI other than optic nerve lesions or any cranial mass effect lesions. Scans with poor visualization of the optic nerve were excluded.

A total of 75 MRIs with 18 prefixed, 36 normofixed, and 21 postfixed chiasms that met the eligibility criteria were selected. Retrospectively evaluated studies included MRI images from a 1.5 T MRI system (Magnetom Siemens Altea, Germany). Imaging parameters included FOV180, slice thickness of 0.8, TR-5.83, TE-2.53, frequency of 63.68 MHz, NEX-1, bandwidth of 399 Hz/Px, and measurements were done using a 64-bit medical image viewer for OS X. Horos DICOM viewer, an open-source software based upon OsiriX, was used to view the sectional MRI images and perform morphometric measurements.

In sagittal images evaluated for the location of the optic chiasm, the optic chiasm overlying the tuberculum sellae was termed as prefixed, the optic chiasm overlying the diaphragm sellae was termed as normal, and the optic chiasm overlying the dorsum sellae was termed as postfixed chiasm (**Figure 1A**). The angle between the medial (inner) border of the intracranial portion of bilateral optic nerves, termed the interneural angle, and between the medial aspect of the optic tracts, termed the optic tract angle, were calculated from the axial reformatted images along the intracranial optic nerves and optic tracts (**Figure 1B**). Parameters h, A, and B were defined to estimate the size of the prechiasmatic cistern. Parameter h (mm) is the distance between the anterior margin of the optic chiasm and the limbus sphenoidale, parameter A (mm) is the distance between the bilateral optic nerves at the entrance to the optic canal, and parameter B (mm) is the distance between the bilateral optic nerves forming the optic chiasm. Parameters h, A, and B were measured on an MRI slice made parallel to the long axis of the optic nerves

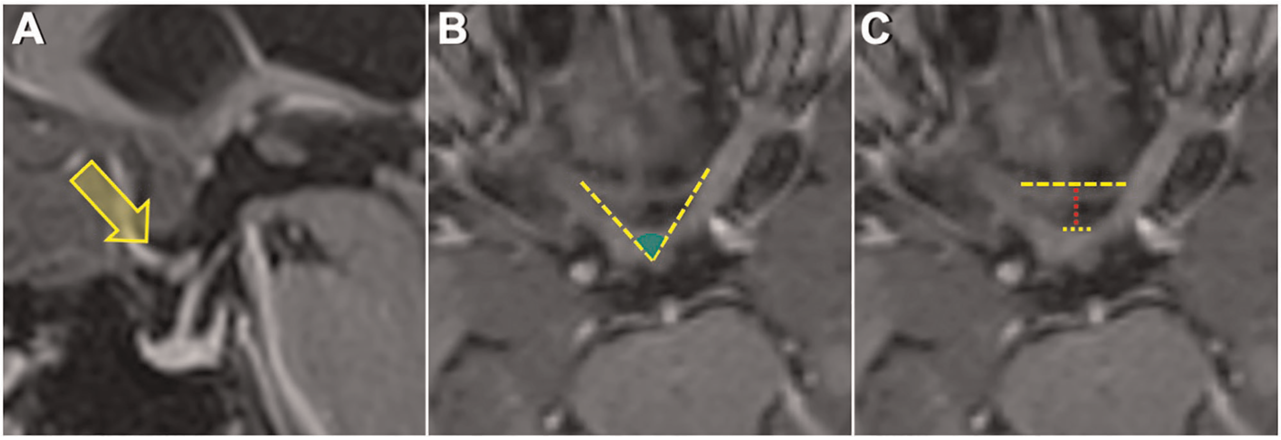

FIGURE 1 | (**A**) Sagittal MRI image showing a prefixed chiasm—overlying tuberculum sella. (**B**) Measurement of the interneural angle on axial reformatted images along the intracranial optic nerves. (**C**) Upper dashed yellow line shows the distance between the bilateral optic nerves at the entrance to the optic canal. The lower dashed yellow line shows the distance between the optic nerves just before they form the optic chiasm. The dashed red line shows the distance from the anterior aspect of the optic chiasm to the limbus sphenoidale.

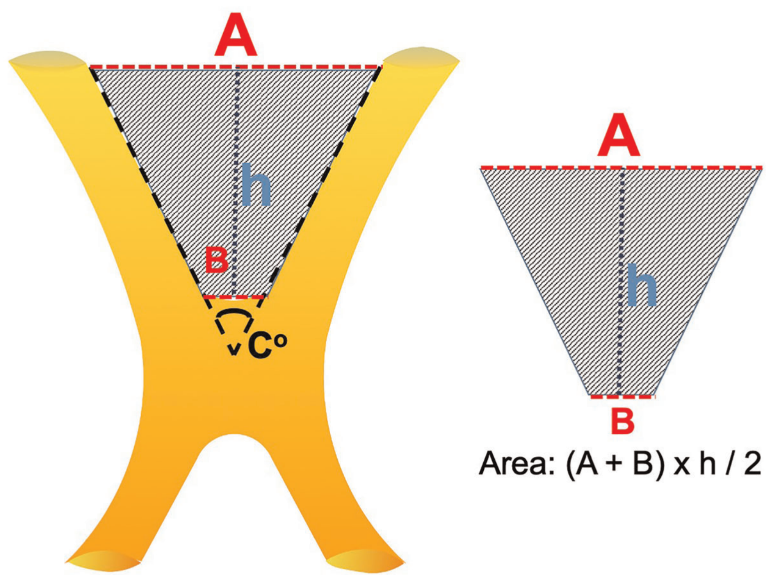

FIGURE 2 | Graphic representation of the prechiasmatic space. *h*, the distance from the anterior aspect of the optic chiasm to the limbus sphenoidale; A, the distance between the bilateral optic nerves at the entrance to the optic canal; B, the distance between the optic nerves just before they form the optic chiasm. Prechiasmatic area (scanned area) calculated by using the trapezoid area formula: $[(A + B) \times h]/2$.

(**Figure 1C**). The estimated size of the prechiasmatic area was calculated using the following formula: $(A + B) \times h/2$ (**Figure 2**).

Reconstruction of the Virtual 3D Simulation Model

All 3D planning and modeling studies were carried out with Mimics Innovation Suite 22.0 software (Materialise, Leuven, Belgium). Briefly, DICOM files of MRI or computed tomography (CT) scans were imported into Mimics. Radiological images were visualized on axial, coronal, and sagittal planes. The masking process was undertaken using hounsfield unit (HU) values on two-dimensional radiological images. Segmentation of various structures was done according to anatomical borders. Different imaging sequences were used for the segmentation of different intracranial structures: CT for bone, time of flight (TOF) MR angiography for arteries, and T2-weighted MRI for the optic nerve. All CT and MRI scans were merged and aligned with the Align Global Registration module. Surface rendering was used to produce 3D models of different anatomical structures. Then, a design module (3-matic 14.0, Materialise, Leuven, Belgium) was used for fine-tuning and detailed modeling. For this specific study, we artificially created variations to the existing anatomy (pre- and postfixed optic nerve, addition of SHA, addition of aneurysms of different sizes). This allowed us to simulate a surgical scenario by freely rotating, positioning, and trimming the model virtually. The optic nerve was made transparent to visualize the underlying SHA.

Statistical Analysis

The Statistical Package for the Social Sciences for Windows (version 15.0; IBM Corporation, Armonk, NY, USA) was used for statistical analysis. Results were expressed as mean, standard deviation, and percentage scores wherever appropriate. Measurements were compared in the prefixed, normofixed, and postfixed chiasms using a one-way ANOVA test. A p-value <0.05 was used to denote statistical significance.

RESULTS

Anatomical Aspects of the Ipsilateral and Contralateral Approach

Contralateral Approach

The right pterional approach was used in the first stage of dissection. After dural opening, proximal sylvian dissection was performed. MCA bifurcation, M1, lenticulostriate arteries, early temporal branch, ipsilateral and contralateral ICA, carotid bifurcation, A1, anterior clinoid process, ipsilateral and contralateral optic nerves, prechiasmatic area, and optic chiasma were identified (**Figures 3A,B**). The SHA originating from the medial surface of the ophthalmic segment of the ICA was identified by a slight elevation of the left optic nerve with the opening of the prechiasmatic cistern. Again, in the same exposure, the left PComA was in the field of view. It was observed that the SHA extended toward the pituitary gland, pituitary stalk, and optic nerve. Terminal branches from the artery were seen to extend from below the chiasm to the floor of the third ventricle (**Figures 3C,D**).

Ipsilateral Approach

In the left pterional approach to a different specimen, following sylvian dissection, MCA bifurcation, superior and inferior trunk, anterior clinoid process, carotid artery, and optic nerve were revealed (**Figure 4A**). When the dissection was extended, the SHA was identified in the left opticocarotid triangle. Subsequently, intradural anterior clinoidectomy was performed. The falciform ligament is defined and incised. Cutting the falciform ligament was beneficial for mobilizing the optic nerve. The optical canal is defined, and the optic roof is removed (**Figures 4B,C**). After optic unroofing, the optic nerve was mobilized. After mobilization, it was observed that the SHA originated from the medial of the ICA-ophthalmic segment, extended medially and posteriorly, and a surgical corridor was created (**Figure 4D**).

Figures 5, **6** show the 3D model and artistic depiction of the ipsilateral and contralateral approaches. Virtual 3D model simulations included bilateral SHA aneurysm scenarios and represented three different chiasm variations based on real measurements (mean values obtained in the following section were used for simulations).

Anatomic dissections along with 3D virtual model simulations and illustrations demonstrated that (i) the contralateral approach would potentially allow for proximal control and neck control/clipping in smaller SHA aneurysm with relatively minimal retraction of the contralateral optic nerve in the setting of pre- or normofixed chiasm and (ii) the ipsilateral approach requires anterior clinodectomy and optic unroofing with considerable optic nerve mobilization to effectively control proximal ICA and clip the aneurysm neck.

Morphometric Analysis

A total of 75 patients [37 males (49.3%) and 38 females (50.7%)] were included in the study. Chiasm types were 18 (24%) prefixed, 36 (48%) normofixed, and 21 (28%) postfixed. Prefixed chiasm group's age was 41.8 ± 10.6 years, normofixed chiasm group's age was 37.9 ± 13.9 years, and postfixed chiasm group's age was 38.9 ± 12 years. There was no significant difference in sex and age distribution groups.

The distance between the bilateral optic nerves at the entrance to the optic canal in all patients was 14.7 ± 1.9 mm, in the prefixed group was 12.8 ± 1.6 mm, in the normofixed group was 14.8 ± 1.5 mm, and in the postfixed group was 16 ± 1.4 mm, and there was no significant difference (**Figures 1**, **2**).

The distance between bilateral optic nerves where they form the optic chiasm in all patients was 13.1 ± 0.9 mm, in the prefixed group was 3.5 ± 0.9 mm, in the normofixed group was 2.9 ± 0.8 mm, and in the postfixed group was 3.1 ± 1.0 mm, and there was no significant difference (**Figures 1**, **2**).

The distance between the anterior aspect of the optic chiasm to the limbus sphenoidale in all patients was 10.0 ± 3.5 mm, in the prefixed group was 5.7 ± 0.8 mm, in the normofixed group was 9.6 ± 1.6 mm, and in the postfixed group was14.4 ± 1.6 mm, and there was no significant difference between distribution groups (**Figures 1**, **2**) ($p < 0.001$).

The optic nerves' interneural angle in all patients was 65.2° ± 10.0°, in the prefixed group was 77.1° ± 7.3°, in the normofixed group was 63.6 ° ± 7.7°, in the postfixed group was 57.7° ± 5.7°, and there was no significant difference between distribution groups (**Figure 7**) ($p = 0.010$).

The length of the medial side of the right optic nerve in all patients was 11.3 ± 3.0 mm, in the prefixed group was 8.0 ± 1.1 mm, in the normofixed group was 10.8 ± 1.5 mm, and in the postfixed group was 15.1 ± 1.5 mm, and there was no significant difference between distribution groups ($p < 0.001$).

The length of the medial side of the left optic nerve in all patients was 11.2 ± 2.8 mm, in the prefixed group was 7.9 ± 1.0 mm, in the normofixed group was 10.9 ± 1.6 mm, and in the postfixed group was 14.7 ± 1.2 mm, and there was no significant difference between distribution groups ($p < 0.001$).

The area of the prechiasm in all patients was 90.4 ± 36.6 mm^2, in the prefixed group was 46.9 ± 10.4 mm^2, in the

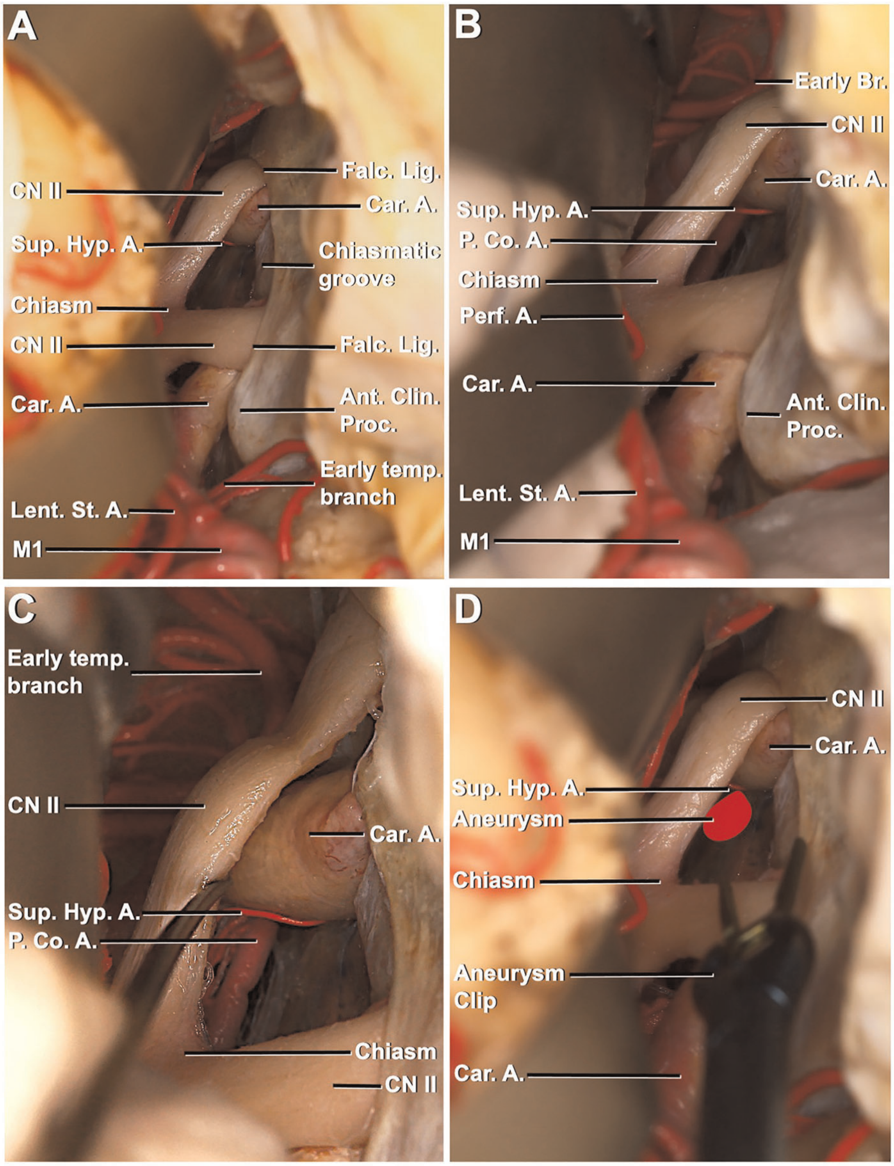

FIGURE 3 | Right pterional exposure of the preoptic chiasm and circle of Willis, contralateral approach to the left superior hypophyseal artery. (**A**) Right frontotemporal bone flap is elevated, and the dura is opened. The right frontal and temporal lobes have been retracted to expose the right carotid artery entering the dura medial to the anterior clinoid process. Right–left optic nerves, optic chiasma, prechiasmatic area, left carotid artery, and left superior hypophyseal artery are visible. (**B**) Exposure has been extended between the chiasm and frontal lobe to the left posterior communicating artery (PCoA) left superior hypophyseal artery arising from the ophthalmic segment. (**C**) PCoA, the course of the left superior hypophyseal artery, is exposed through left optic nerve mobilization. (**D**) Aneurysm of the left superior hypophyseal has been illustrated and approached with an aneurysm clip to mimic the contralateral surgical approach.

normofixed group was $84.8 \pm 15.7\ mm^2$, and in the postfixed group was $137.2 \pm 19.5\ mm^2$, and there was no significant difference between distribution groups (**Figure 8**) ($p < 0.001$).

DISCUSSION

This study is the first investigation to combine cadaveric dissections with morphometric radiologic analyses and 3D simulations to examine the superior hypophysial artery with a focus on its aneurysms. Here, we first described relevant anatomy using cadaveric dissections. Then, we presented morphometric measurements appropriate for ipsilateral and contralateral approaches for SHA aneurysms. Finally, we provided virtual 3D simulations of surgical scenarios using morphometric data to inform surgical decision-making.

The superior pituitary artery was first described by von Lusckha (13). Dawson (14) detailed information on the SHA

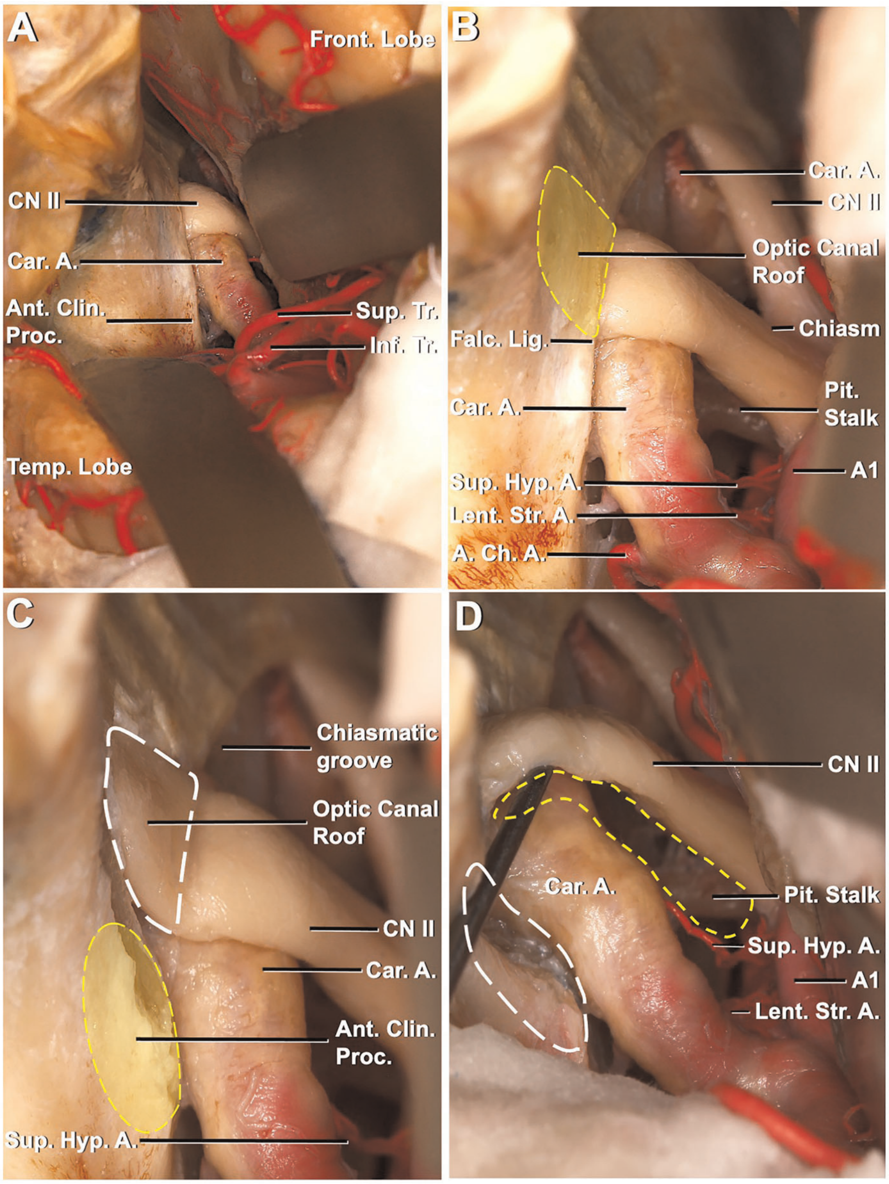

FIGURE 4 | Left pterional exposure of the preoptic chiasm and circle of Willis, the ipsilateral approach to the left superior hypophyseal artery. (**A**) Left frontotemporal bone flap is elevated, and the dura is opened. The left frontal and temporal lobes have been retracted to expose the left carotid artery entering the dura medial to the anterior clinoid process. The left optic nerve, anterior clinoid process, and prechiasmatic area are seen. (**B**) Exposure has been extended between the chiasm and the frontal lobe. Pituitary stalk and left superior hypophyseal artery are seen between the left optic nerve and left carotid artery. The optic canal roof is depicted by a dashed yellow line. (**C**) Optic canal roof, depicted by a dashed white line, is removed. The anterior clinoid process is depicted by a dashed yellow line. (**D**) Anterior clinoid process, depicted by a dashed white line, is removed and the left optic nerve is mobilized. The corridor for the ipsilateral approach to the left superior hypophyseal artery is seen (dashed yellow line) between the left optic nerve and the mobilized left carotid artery.

anatomy and reported that it originated from the ICA. Over time, information has revealed that SHA is actually a vascular complex originating from the medial aspect of the segment of the ICA between the ophthalmic artery and the posterior communicating artery (15–17). Recently, the term primary and secondary SHA was used for the first time in the study of Truong et al. (18), in which 110 SHAs originating from 60 ICAs were examined in the endoscopic study in which they examined the surgical anatomy of SHA. According to their findings, two SHAs, proximal and distal, were detected at a rate of 70%. The primary term was used for proximal SHA that feeds the optic nerve, optic chiasm, and infundibulum and travels in the preinfundibular space; the secondary term for SHA that feeds the infundibulum, tuber cinereum, optic tracts, and mammillary bodies and extends in the retroinfundibular or parainfundibular space. Moreover, they

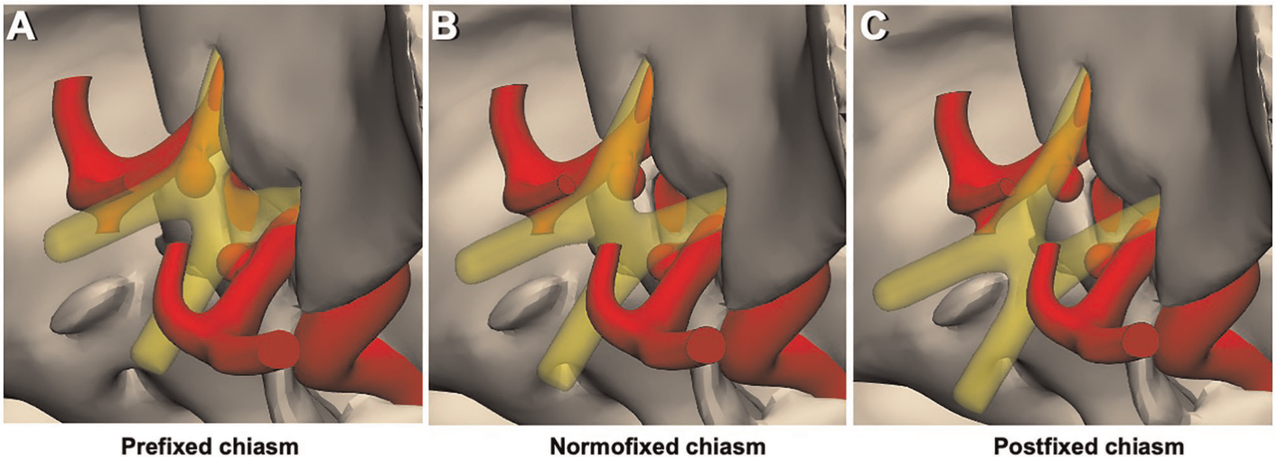

FIGURE 5 | 3D models of chiasm types and the relationship of the prechiasmatic area – aneurysms. (**A**) Prefixed chiasm type, regardless of its size and shape, the aneurysm remains below the optic chiasm. Consequently, there is not enough space for the contralateral approach. (**B**) Normofixed chiasm type provides sufficient space for the contralateral approach, depending on the shape and size of the aneurysm. (**C**) Postfixed chiasm type provides sufficient space for the contralateral approach, more than the normofixed chiasm type, depending on the shape and size of the aneurysm.

stated that there is a single SHA of 18.3% and a third SHA of 8.3%. In addition, they stated that the primary SHA originates from the ophthalmic segment of the ICA at a rate of 1/3 and the clinoidal segment of the ICA at a rate of 2/3 from the distal of the distal dural ring and from the proximal of the distal dural ring, and even half of them originate from the carotid cave. They showed that it has complicated and variational anatomy (18).

The complicated anatomy of SHA is a factor that makes surgery challenging. Complex procedures such as the complexity of the surgical anatomy of the area of SHA, the proximity of SHA to important neurovascular structures in the suprasellar area (optic nerve, chiasm, pituitary stalk, other arterial branches), the need for anterior clinoidectomy to provide proximal control of the ICA and to define the proximal aspect of the aneurysmal neck, optic nerve decompression and mobilization, and opening of the carotid collar are the factors that increase the degree of surgical difficulty in aneurysms (19). In addition, the authors mentioned the problem of accessing the infrachiasmatic space and the difficulty in dissection of SHA (14, 17). In our study, similar to the literature, it was found that it was not possible to provide proximal control in large aneurysms, especially in the contralateral approach.

One of the most important complications that develop due to these difficulties is visual deficits. In two cases presented by El Refaee et al. (20), SHA was occluded during SHA aneurysm surgery, and it was reported that superior quadranopsia developed in one of the patients. Johnson et al. (21) stated that homonymous hemianopsia developed after the operation in a patient who underwent SHA aneurysm embolization. Horiuchi et al. (22) stated that a visual deficit of 13% was observed in a series of 70 patients with SHA aneurysms, and it was commented that unilateral sacrification could not always be performed in SHA aneurysms.

Another problem in SHA aneurysms is the direction of the surgical approach. The common approach in ophthalmic segment aneurysms of the ICA is the ipsilateral pterional approach (23, 24). On the contrary, some authors suggest that surgery should be performed from the contralateral side in paraclinoid and ophthalmic ICA, especially in the ophthalmic segment and SHA aneurysms, since the aneurysm originates from the medial wall of the ICA, but they state that the problem of proximal control also poses a serious disadvantage (10, 11, 25, 26). In the presence of a bilateral aneurysm, a bilateral approach with unilateral craniotomy is recommended (11, 26–28). Finally, another type of surgical approach used in ophthalmic ICA aneurysms is the subfrontal interhemispheric approach (10).

The distance to the lesion and the prechiasmatic space are very important in the contralateral approach. We think that the type of chiasm is one of the most important points in the contralateral approach. In the study of de Oliveira et al. (25) on the contralateral approach to aneurysms, it was stated that the preference for the contralateral approach in ophthalmic ICA aneurysms depends on the size and projection of the aneurysm and its relations with the optic nerve, carotid artery, and anterior clinoid process. It has been stated that anatomical variations of the chiasm, such as the prefix chiasm, may interfere with the contralateral approach since access to the aneurysm is made between the optic nerves. Ophthalmic ICA aneurysms are divided into four types according to their projections, and the most common type is the subchiasmal type that projects medially and originates from the medial surface, but Nishio et al. (10) also drew attention to the effect of the proximity of the neck of the aneurysm to the exit point of the ophthalmic artery on surgery. They stated that the inability to see the origin of the ophthalmic artery in ipsilateral surgery complicates the ipsilateral approach. Since

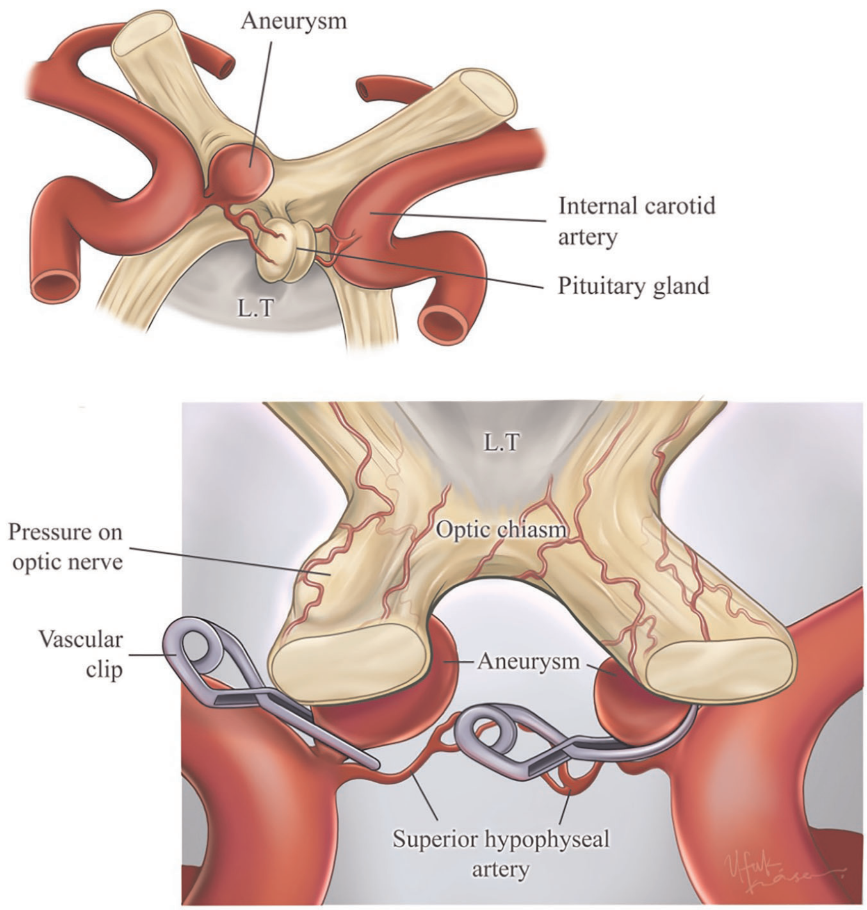

FIGURE 6 | Illustration of superior hypophyseal artery aneurysms, contralateral–ipsilateral aneurysm clipping. The right superior hypophyseal artery has aneurysms that are not suitable for the contralateral approach because of the aneurysm size and the challenge of reaching the aneurysm dome. Also, this aneurysm's pressure on the optic nerve has been illustrated. This aneurysm is suitable for the ipsilateral approach. On the other hand, the illustrated left superior hypophyseal artery aneurysm is suitable for the contralateral approach because of the aneurysm size (small). Also, this aneurysm allows reaching the aneurysm dome by the contralateral approach. Printed with permission from Ufuk Köse.

the ipsilateral optic nerve blocks the view of the origin of the ophthalmic artery and the medial aspect of the ipsilateral ICA, mobilization of the optic nerve is necessary to view these areas. For this reason, it has been reported that it is necessary to open the roof of the optic canal, remove the anterior clinoid process and tuberculum sella, and in some cases even a part of the optic nerve. Because of these maneuvers, postoperative visual impairment may be a serious problem in the ipsilateral approach (10). In the contralateral approach, the medial and inferior aspects of the ophthalmic segment of the ICA and the origin of the contralateral ophthalmic artery can be seen without the need for manipulation of the optic nerve; therefore, the aneurysm originating from the anterior, medial, and inferior of the ophthalmic ICA can be reached without causing visual impairment with a contralateral approach (10). Despite these advantages, the contralateral approach may not be suitable for large and ruptured aneurysms. Another handicap of the contralateral approach is that it can cause bilateral olfactory nerve damage and develop a permanent sense of smell (10). In the setting of large and anteromedially protruding aneurysms and prefixed chiasm, which prevents a contralateral approach, a combined contralateral pterional and interhemispheric approach has also been proposed (29). However, if the aneurysm neck is small and there is a space between the anterior wall of the aneurysm and tuberculum sellae, it might be possible to clip even giant aneurysms through a contralateral approach without optic injury (30).

Carotid cave aneurysms, one of the segments where SHA can originate, can be given as an example of a special type of intracranial aneurysm where the surgical approach is the most challenging. In the carotid cave aneurysm series of 31 cases by Sheikh et al. (28), the contralateral approach was applied to four patients, and the contralateral approach was recommended in this type of aneurysm because it does not cause optic damage and can be easily applied in multiple and bilateral aneurysms. Kakizawa et al. (7) reported the necessary parameters for the contralateral approach for ICA-ophthalmic aneurysms. They identified that the direction of the aneurysm

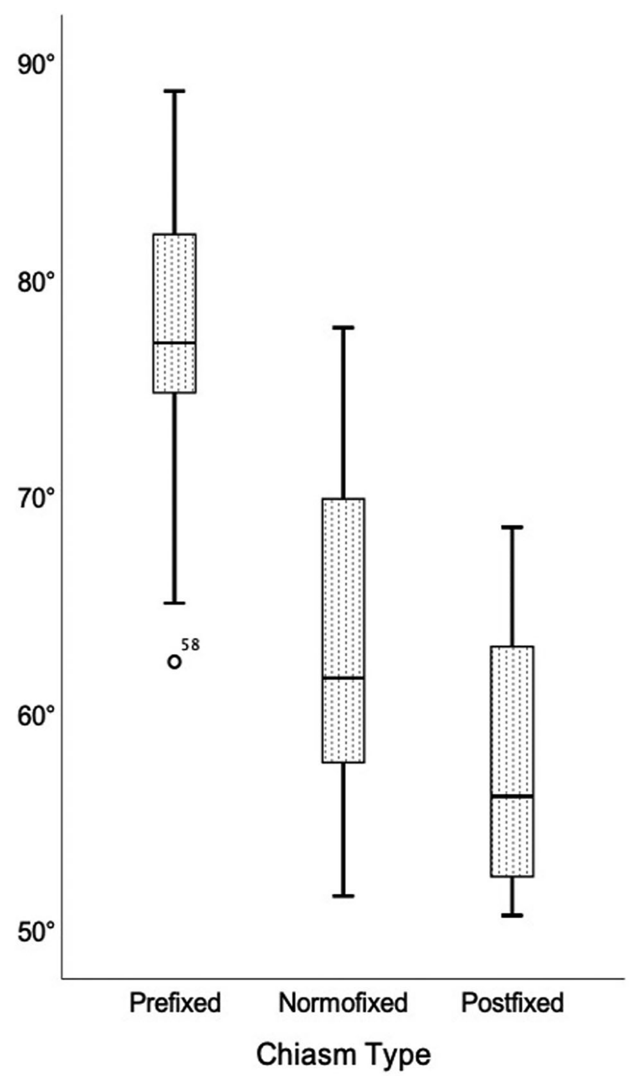

FIGURE 7 | Comparison of the interneural angle in prefixed, normofixed, and postfixed optic chiasm types.

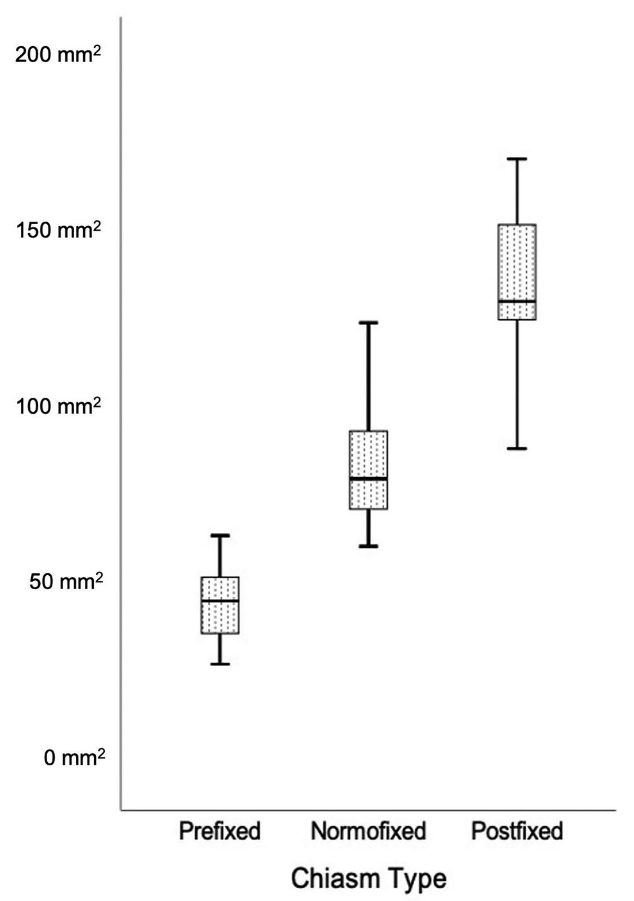

FIGURE 8 | Comparison of the prechiasmatic space in prefixed, normofixed, and postfixed optic chiasm types.

from ICA on the anteroposterior angiogram and the distance between the medial aspect of the distal dural ring and the proximal aneurysm neck on the lateral angiogram were two important factors in predicting the difficulty in the contralateral approach.

Although there are many studies on ophthalmic ICA aneurysms in the literature, there are limited studies on isolated SHA aneurysms. Although it has been stated that most paraclinoid aneurysms are associated with SHA, occlusion may not cause any deficit during the treatment of SHA aneurysm, and therefore, SHA can occasionally be sacrificed in some cases; there is no way to predict whether or not an obliteration of SHA would cause visual deficits (31). Despite the peculiarities of SHA aneurysms and their differences from other ophthalmic segment aneurysms, there is limited literature on isolated SHA aneurysms. Neurosurgeons dealing with these aneurysms need more focused guidance for these pathologies, considering the complex anatomy of SHA and the expectation of no deficits in the postoperative period in unruptured aneurysms. Most of the available studies on isolated SHA aneurysms are clinical series presentations. In the series of eight cases by Chen et al. (32), surgery was performed with the contralateral approach in nonruptured SHA aneurysms, and it was stated that no complications, including the optic deficit, developed and the contralateral approach was safe and technically possible in unruptured aneurysms. Godbole et al. (19) presented a new classification based on parameters such as aneurysm size, origin, relationship with important structures, and type (saccular, fusiform) over 14 disease series including ruptured and unruptured SHA aneurysms. They argued that detailed information about anatomical variations is necessary in order to achieve satisfactory results in their study, where they stated that, according to their results, there was no interpretation of the optic deficit in five patients, optic deficit was absent in seven patients, and optic deficit occurred in two patients (19).

In parallel to Godbole et al. (19), we identified conditions and limitations of ipsilateral and contralateral approaches to SHA aneurysms combining anatomical study with morphometric analyses and 3D simulations. The findings of the study may aid neurosurgeons in choosing the proper approach for SHA aneurysms. Hereby, we stress the utmost importance of patient-specific radiological anatomy. Indeed, even the intraoperative monitoring of visual evoked potentials might not be sufficient to prevent visual deficits in these surgeries (33–36).

Strengths and Limitations

This study combined different methodologies to study the microsurgical anatomy of SHA and its aneurysms. Robust morphometric analysis and its integration with the 3D virtual model simulation are its strengths. However, it has certain limitations, too. First, we did not study anatomic variations of SHA. Second, we did not examine angiographic variations related to SHA aneurysms. Third, although simulations can be potentially enriched by introducing endless variations, they only provide anatomic relationships but do not inform about the challenges faced in real-world settings such as adherence of aneurysm wall to adjacent structures and the extent to which optic nerves can be mobilized. Further studies with the incorporation of angiographic images into simulations can better inform decision-making processes.

CONCLUSION

This study is the first investigation to combine cadaveric dissections with morphometric radiologic analyses and 3D simulations to examine superior hypophysial artery with a focus on its aneurysms. Anatomic dissections along with 3D virtual model simulation and illustrations demonstrated that (i) the contralateral approach would potentially allow for proximal control and neck control/clipping in smaller SHA aneurysm with relatively minimal retraction of the contralateral optic nerve in the setting of pre- or normofixed chiasm and (ii) the ipsilateral approach requires anterior clinodectomy and optic unroofing with considerable optic nerve mobilization to effectively control proximal ICA and clip the aneurysm neck. Careful examination of preoperative imaging studies and patient-specific 3D modeling may further help surgeons choose the right approach to tackle SHA aneurysms.

DATA AVAILABILITY STATEMENT

The raw data supporting the conclusions of this article will be made available by the authors without undue reservation.

AUTHOR CONTRIBUTIONS

BS: conceptualization, methodology, investigation, format analysis, data curation, visualization, and writing – original draft preparation; SOA: validation, investigation, and data curation; MOY: validation and formal analysis; TS: formal analysis, resources, and visualization; SH: software, validation, and resources; GA: validation and resources; OB: conceptualization, methodology, investigation, format analysis, visualization, and writing – original draft preparation; TK: conceptualization and supervision. All authors contributed to the article and approved the submitted version.

FUNDING

This study was partly supported by the Turkish Neurosurgical Society.

ACKNOWLEDGMENTS

This study was partly supported by the Turkish Neurosurgical Society. The authors thank Osman Tunc for his assistance in 3D modeling.

REFERENCES

1. Day AL. Aneurysms of the ophthalmic segment. A clinical and anatomical analysis. *J Neurosurg*. (1990) 72:677–91. doi: 10.3171/jns.1990.72.5.0677
2. Krisht AF, Barrow DL, Barnett DW, Bonner GD, Shengalaia G. The microsurgical anatomy of the superior hypophyseal artery. *Neurosurgery*. (1994) 35:899–903; discussion 903. doi: 10.1227/00006123-199411000-00014
3. Batjer HH, Kopitnik TA, Giller CA, Samson DS. Surgery for paraclinoidal carotid artery aneurysms. *J Neurosurg*. (1994) 80:650–8. doi: 10.3171/jns.1994.80.4.0650
4. Barami K, Hernandez VS, Diaz FG, Guthikonda M. Paraclinoid carotid aneurysms: surgical management, complications, and outcome based on a new classification scheme. *Skull Base*. (2003) 13:31–41. doi: 10.1055/s-2003-820555
5. Gurian JH, Viñuela F, Guglielmi G, Gobin YP, Duckwiler GR. Endovascular embolization of superior hypophyseal artery aneurysms. *Neurosurgery*. (1996) 39:1150–4; discussion 1154–6. doi: 10.1097/00006123-199612000-00016
6. Kwon O-K, Kim SH, Oh CW, Han MH, Kang H-S, Kwon BJ, et al. Embolization of wide-necked aneurysms with using three or more microcatheters. *Acta Neurochir (Wien)*. (2006) 148:1139–45; discussion 1145. doi: 10.1007/s00701-006-0876-4
7. Kakizawa Y, Tanaka Y, Orz Y, Iwashita T, Hongo K, Kobayashi S. Parameters for contralateral approach to ophthalmic segment aneurysms of the internal carotid artery. *Neurosurgery*. (2000) 47:1130–6; discussion 1136–7. doi: 10.1097/00006123-200011000-00022
8. Sheikh B, Ohata K, El-Naggar A, Baba M, Hong B, Hakuba A. Contralateral approach to junctional C2-C3 and proximal C4 aneurysms of the internal carotid artery: microsurgical anatomic study. *Neurosurgery*. (2000) 46:1156–60; discussion 1160–1. doi: 10.1097/00006123-200005000-00027
9. Clatterbuck RE, Tamargo RJ. Contralateral approaches to multiple cerebral aneurysms. *Neurosurgery*. (2005) 57:160–3; discussion 160–3. doi: 10.1227/01.neu.0000163601.37465.6e
10. Nishio S, Matsushima T, Fukui M, Sawada K, Kitamura K. Microsurgical anatomy around the origin of the ophthalmic artery with reference to contralateral pterional surgical approach to the carotid-ophthalmic aneurysm. *Acta Neurochir (Wien)*. (1985) 76:82–9. doi: 10.1007/BF01418465
11. Fries G, Perneczky A, van Lindert E, Bahadori-Mortasawi F. Contralateral and ipsilateral microsurgical approaches to carotid-ophthalmic aneurysms.

Neurosurgery. (1997) 41:333–42; discussion 342–3. doi: 10.1097/00006123-199708000-00001
12. Shimizu S, Tanaka R, Rhoton AL, Fukushima Y, Osawa S, Kawashima M, et al. Anatomic dissection and classic three-dimensional documentation: a unit of education for neurosurgical anatomy revisited. *Neurosurgery*. (2006) 58:E1000; discussion E1000. doi: 10.1227/01.NEU.0000210247.37628.43
13. von Luschka H. *Die Hirnanhang und die Streissdruse des Menschen*. Berlin: G Reimer (1860).
14. Dawson BH. The blood vessels of the human optic chiasma and their relation to those of the hypophysis and hypothalamus. *Brain*. (1958) 81:207–17. doi: 10.1093/brain/81.2.207
15. Gibo H, Lenkey C, Rhoton AL. Microsurgical anatomy of the supraclinoid portion of the internal carotid artery. *J Neurosurg*. (1981) 55:560–74. doi: 10.3171/jns.1981.55.4.0560
16. Leclercq TA, Grisoli F. Arterial blood supply of the normal human pituitary gland. An anatomical study. *J Neurosurg*. (1983) 58:678–81. doi: 10.3171/jns.1983.58.5.0678
17. Gibo H, Kobayashi S, Kyoshima K, Hokama M. Microsurgical anatomy of the arteries of the pituitary stalk and gland as viewed from above. *Acta Neurochir (Wien)*. (1988) 90:60–6. doi: 10.1007/BF01541268
18. Truong HQ, Najera E, Zanabria-Ortiz R, Celtikci E, Sun X, Borghei-Razavi H, et al. Surgical anatomy of the superior hypophyseal artery and its relevance for endoscopic endonasal surgery. *J Neurosurg*. (2018) 131:154–62. doi: 10.3171/2018.2.JNS172959
19. Godbole C, Behari S, Bhaisora KK, Sardhara J, Srivastava A, Mehrotra A, et al. Surgery for superior hypophyseal artery aneurysms: a new classification and surgical considerations. *Neurol India*. (2017) 65:588–99. doi: 10.4103/neuroindia.NI_229_17
20. El Refaee E, Baldauf J, Balau V, Rosenstengel C, Schroeder H. Is it safe to sacrifice the superior hypophyseal artery in aneurysm clipping? A report of two cases. *J Neurol Surg A Cent Eur Neurosurg*. (2013) 74(Suppl 1): e255–60. doi: 10.1055/s-0033-1349336
21. Johnson JN, Elhammady M, Post J, Pasol J, Ebersole K, Aziz-Sultan MA. Optic pathway infarct after Onyx HD 500 aneurysm embolization: visual pathway ischemia from superior hypophyseal artery occlusion. *J Neurointerv Surg*. (2014) 6:e47. doi: 10.1136/neurintsurg-2013-010968.rep
22. Horiuchi T, Goto T, Tanaka Y, Kodama K, Tsutsumi K, Ito K, et al. Role of superior hypophyseal artery in visual function impairment after paraclinoid carotid artery aneurysm surgery. *J Neurosurg*. (2015) 123:460–6. doi: 10.3171/2014.12.JNS141218
23. Rhoton AL, Rhoton AL, Congress of Neurological Surgeons. *Rhoton cranial anatomy and surgical approaches*. Philadelphia: Lippincott Williams & Wilkins (2003).
24. Yasargil MG, Fox JL. The microsurgical approach to intracranial aneurysms. *Surg Neurol*. (1975) 3:7–14.
25. de Oliveira E, Tedeschi H, Siqueira MG, Ono M, Fretes C, Rhoton AL, et al. Anatomical and technical aspects of the contralateral approach for multiple aneurysms. *Acta Neurochir (Wien)*. (1996) 138:1–11; discussion 11. doi: 10.1007/BF01411716
26. Nakao S, Kikuchi H, Takahashi N. Successful clipping of carotid-ophthalmic aneurysms through a contralateral pterional approach. Report of two cases. *J Neurosurg*. (1981) 54:532–6. doi: 10.3171/jns.1981.54.4.0532
27. Vajda J, Juhász J, Pásztor E, Nyáry I. Contralateral approach to bilateral and ophthalmic aneurysms. *Neurosurgery*. (1988) 22:662–8. doi: 10.1227/00006123-198804000-00007
28. Sheikh B, Ohata K, El-Naggar A, Hong B, Tsuyuguchi N, Hakuba A. Contralateral approach to carotid cave aneurysms. *Acta Neurochir (Wien)*. (2000) 142:33–7. doi: 10.1007/s007010050004
29. Shiokawa Y, Aoki N, Saito I, Mizutani H. Combined contralateral pterional and interhemispheric approach to a subchiasmal carotid-ophthalmic aneurysm. *Acta Neurochir (Wien)*. (1988) 93:154–8. doi: 10.1007/BF01402900
30. Hongo K, Watanabe N, Matsushima N, Kobayashi S. Contralateral pterional approach to a giant internal carotid-ophthalmic artery aneruysm: technical case report. *Neurosurgery*. (2001) 48:955–7; discussion 957–9. doi: 10.1097/00006123-200104000-00059
31. Goto T, Tanaka Y, Kodama K, Kusano Y, Sakai K, Hongo K. Loss of visual evoked potential following temporary occlusion of the superior hypophyseal artery during aneurysm clip placement surgery. Case report. *J Neurosurg*. (2007) 107:865–7. doi: 10.3171/JNS-07/10/0865
32. Chen S, Kato Y, Kumar A, Sinha R, Oguri D, Oda J, et al. Contralateral approach to unruptured superior hypophyseal artery aneurysms. *J Neurol Surg A Cent Eur Neurosurg*. (2013) 74:18–24. doi: 10.1055/s-0032-1326944
33. Cedzich C, Schramm J. Monitoring of flash visual evoked potentials during neurosurgical operations. *Int Anesthesiol Clin*. (1990) 28:165–9. doi: 10.1097/00004311-199002830-00006
34. Harding GF, Bland JD, Smith VH. Visual evoked potential monitoring of optic nerve function during surgery. *J Neurol Neurosurg Psychiatry*. (1990) 53:890–5. doi: 10.1136/jnnp.53.10.890
35. Sasaki T, Itakura T, Suzuki K, Kasuya H, Munakata R, Muramatsu H, et al. Intraoperative monitoring of visual evoked potential: introduction of a clinically useful method. *J Neurosurg*. (2010) 112(2):273–84. doi: 10.3171/2008.9.JNS08451
36. Wiedemayer H, Fauser B, Armbruster W, Gasser T, Stolke D. Visual evoked potentials for intraoperative neurophysiologic monitoring using total intravenous anesthesia. *J Neurosurg Anesthesiol*. (2003) 15:19–24. doi: 10.1097/00008506-200301000-00004

Conflict of Interest: The authors declare that the research was conducted in the absence of any commercial or financial relationships that could be construed as a potential conflict of interest..

Publisher's Note: All claims expressed in this article are solely those of the authors and do not necessarily represent those of their affiliated organizations, or those of the publisher, the editors and the reviewers. Any product that may be evaluated in this article, or claim that may be made by its manufacturer, is not guaranteed or endorsed by the publisher.

frontiers | Frontiers in Surgery

MINI REVIEW
published: 06 June 2022
doi: 10.3389/fsurg.2022.915253

Fourth Ventricle Tumors: A Review of Series Treated With Microsurgical Technique

Rinat Sufianov[1,2], David Pitskhelauri[1] and Andrey Bykanov[1]*

[1]Department of Neurooncology, N. N. Burdenko National Medical Research Center of Neurosurgery, Ministry of Health of the Russian Federation, Moscow, Russia, [2]Department of Neurosurgery, Sechenov First Moscow State Medical University (Sechenov University), Moscow, Russia

Tumors of the IV ventricle represent 1–5% of all intracranial lesions; they are implicated in 2/3 of the tumors of the ventricular system. According to modern standards, the first treatment stage for this pathology is microsurgical removal. Currently, for the removal of neoplasms of the IV ventricle and brainstem, the median suboccipital approach is widely used, followed by one of the microapproaches. Moreover, with the development of microsurgical techniques, keyhole approaches are now beginning to be utilized. However, surgical treatment of these tumors remains a challenge for neurosurgeons due to the proximity of functionally important anatomical structures (the brainstem, the cerebellum, pathways, vessels, etc.) of the posterior cranial fossa. Therefore, surgery in this area is associated with the possible occurrence of a wide range of postoperative complications. The authors provide a review of series of fourth ventricle tumors treated with microsurgical technique.

Keywords: IV ventricle, tumors of the IV ventricle, median suboccipital approach, minimally invasive suboccipital approach, posterior fossa, keyhole approach, brainstem

OPEN ACCESS

Edited by:
Ilgiz Fanilevich Gareev
Federal Center of Neurosurgery, Russia

Reviewed by:
Liang Yanchao, Harbin Medical University, China
Qiuyi Jiang, Harbin Medical University, China

Correspondence:
Rinat Sufianov
rinat.sufianov@gmail.com

Specialty section:
This article was submitted to Neurosurgery, a section of the journal Frontiers in Surgery

Received: *07 April 2022*
Accepted: *02 May 2022*
Published: *06 June 2022*

Citation:
Sufianov R, Pitskhelauri D and Bykanov A (2022) Fourth Ventricle Tumors: A Review of Series Treated With Microsurgical Technique. Front. Surg. 9:915253. doi: 10.3389/fsurg.2022.915253

INTRODUCTION

Tumors of the IV ventricle represent 1–5% of all intracranial lesions (1–4); among tumors of the ventricular system, they are diagnosed in 2/3 of cases (3). According to the modern standards, the first stage of treatment for this pathology is microsurgical removal (5). However, surgical treatment of these tumors remains a challenge for neurosurgeons due to the proximity of functionally important anatomical structures (the brainstem, the cerebellum, pathways, vessels, etc.) of the posterior cranial fossa. Therefore, surgery in this area is associated with the possible occurrence of a wide range of postoperative complications. To date, despite the general trend toward minimally invasive surgery, the standard median suboccipital approach is commonly used for removing tumors of the IV ventricle and brainstem. According to the literature, a median suboccipital approach to the posterior cranial fossa is associated with a high risk of CSF leakage (up to 27% of cases) and pseudomeningocele (up to 23% of cases) (6). The goal of this paper is to review the different variations of the median suboccipital approaches used to surgically treat fourth ventricular pathologies. A summary of the analyzed articles can be seen in **Table 1**.

TABLE 1 | Analyzed series of the surgically treated patients with 4 ventricular and brainstem tumors.

Year Authors	1997 Kellogg (46)	1999 Ziyal (27)	2001 Matsushima (9)	2002 Gnanalingham (6) Craniectomy	2002 Gnanalingham (6) Craniotomy	2003 Jean (28)	2004 Gok (25)	2004 El-Bahy (30)	2007 Rajesh (29)	2010 Zaheer N.S. (24)	2012 Karakhan (3)	2013 Han (15)	2015 Tomasello (21)	2016 Bo Qiu (31)	2018 Ferguson (2)	2018 Kalinovsky (23)	2018 Babichev (22)	2018 Kushel (26)	2018 Pitskhelauri (47)
Average patients age	N\A	49.2 (23–63)	25.1 (1–70)	0.3–15 (5.56)	0.2–14 (5.96)	52 (26–69)	20 (1–56)	20.6 (5–45)	Under 10 y.o.	8 (1–17)	16–68	23 (6–58)	22.5 (2–66)	8.7 (2.5–14)	35.5	39.3 (19–61)	37.7 (32.8–42.4)	N\A	36 (17–66)
Patient position	Prone	Semi-prone	N\A	Sitting 98%	Lateral decubitus	Sitting	N\A	Prone, oblique	Prone	N\A	Prone	Prone	Prone	70% Lateral	Semisitting	Sitting	Sitting	Sitting 67.1%	
Osteoplastic craniotomy	N\A	N\A	N\A	0%	100%	N\A	N\A	N\A	N\A	100%	N\A	N\A	0%	5 × 4 cm	44 (80%)	100%	N\A	100%	95.7%
Craniectomy	N\A	N\A	N\A	100%	0%	N\A	N\A	N\A	100%	0%	N\A	N\A	100%	5 × 4 cm	11(20%)	0%	N\A	N\A	4.3%
Resection of C1 arch	N\A	N\A	N\A	4%	4%	100%	N\A	N\A	N\A	N\A	N\A	9 (18%)	15 (33%)	N\A	N\A	13 (39.4%)	56.10%	N\A	11 (15.7%)
Dural incision	Y-shaped	Y-shaped	N\A	N\A	N\A	Y-shaped	Y-shaped	N\A	N\A	U-shaped	N\A	Y-shaped	Y-shaped	Y-shaped	N\A	U-shaped	Y- or U-shaped	V- or Y-shaped	Y-shaped
Telovelar approach	Cerebello-medullary	Subtonsillar-transcerebellomedullary	N\A	N\A	N\A	N\A	Trans-cerebellomedullary	100%	100%	100%	92.9% (in other cases - supracerebellar)	36%	100%	19.20%	26 (48%)	100%	16 (39%)	N\A	N\A
Unilateral approach	N\A	N\A	31.60%	N\A	N\A	N\A	100%	N\A	N\A	N\A	N\A	N\A	N\A	17 (65.4%)	N\A	N\A	N\A	N\A	N\A
Bilateral approach	N\A	N\A	68.40%	N\A	N\A	N\A	N\A	N\A	N\A	N\A	N\A	N\A	100%	9 (34.6%)	N\A	N\A	N\A	N\A	N\A
Median aperture approach	N\A	N\A	N\A	N\A	N\A	N\A	N\A	N\A	N\A	N\A	N\A	64%	N\A	80.80%	N\A	0%	25 (61%)	N\A	100%
Transvermian approach	N\A	N\A	N\A	N\A	N\A	N\A	N\A	0%	N\A	0%	N\A	N\A	N\A	N\A	24 (44%)	0%	N\A	N\A	N\A
Shunting procedures preop	N\A	N\A	N\A	N\A	N\A	1 (33.3%)	N\A	N\A	N\A	6 (30%)	0	7 (14%)	N\A	3 (11.5%)	16%	N\A	12 (29.3%)	N\A	N\A
Shunting procedures intraop	N\A	N\A	N\A	N\A	N\A	N\A	N\A	N\A	N\A	N\A	N\A	N\A	N\A	9 (34.6%)	14 (25%)	N\A	N\A	154 (73%)	N\A
Shunting procedures postop abs (%)	N\A	50%	N\A	23%	15%	N\A	N\A	N\A	N\A	6 (30%)	N\A	7 (14%)	2(4.5%)	1 (3.8%)	12 (22%)	1 (3%)	N\A	2 (0.95%)	0%
Hematomas	N\A	N\A	N\A	N\A	N\A	N\A	1 (4.8%)	N\A	N\A	N\A	N\A	N\A	N\A	N\A	1 (2%)	1 (3%)	N\A	5 (2.4%)	N\A
Meningitis	N\A	N\A	N\A	20%	11%	N\A	N\A	N\A	N\A	N\A	N\A	N\A	N\A	N\A	3 (5%)	N\A	1 (2.4%)	1 (0.47%)	N\A
CSF leak abs (%)	N\A	N\A	N\A	27%	4%	N\A	N\A	N\A	N\A	2 (10%)	N\A	N\A	N\A	N\A	4 (7%)	0%	4 (9.8%)	6 (2.8%)	11.4%

Main Surgical and Anatomical Landmarks of the Suboccipital Cerebellar Surface

When removing tumors of the IV ventricle, it is essential to know the anatomical structures and landmarks of the suboccipital surface of the cerebellum, especially its fissures. The tonsillobiventral fissure is located between the upper-lateral border of the tonsil and the biventral lobule. During surgery, the dissection of this fissure is performed via the supratonsillar approach (7, 8).

The lower-medial surface of the tonsil is divided from the medulla and the uvula by the cerebellomedullar fissure, which consists of the tonsillomedullar and tonsillouvular fissures. The anterior wall of the cerebellomedular fissure is formed by the posterior surface of the medulla, the inferior medullary velum, and the tela choroidea. The posterior wall is formed by the uvula, the tonsil, and the biventral lobule laterally (9–11).

The floor of the tonsillouvular fissure is adjacent to the inferior half of the IV ventricular roof. The inferior half of the roof is formed by the inferior medullary velum, the tela choroidea, the nodule and the uvula. The inferior medullary velum is a butterfly shaped structure that blends into the ventricular surface of the nodule medially (12). It is a membranous layer and does not contain eloquent nervous tissue (13, 14). At the fastigium, it bends inferiorly from the superior medullary velum and blends with the tela choroidea at the level of the lateral recesses. The tela choroidea is a triangular fold of the pia mater (13, 15–17).

Different Approaches to Classifying Fourth Ventricular Tumors

To date, there is no commonly accepted classification system for fourth ventricular tumors. The main controversy is whether to classify tumors that spread secondary to the ventricular cavity and deform the it as tumors of the IV ventricle. In almost half of the cases, the origin site of tumor growth is the floor of the IV ventricle (3).

In the publications from the beginning of the 20th century, the prevailing opinion was that, from an anatomical point of view, IV ventricle tumors should include only those located in its cavity, i.e., growing from its floor or ependyma of the vascular plexus, according to articles of M. Yu Rappoport, I. Ya Razdolsky, Hennenberg, Cushing, O. Marburg, and Lerrebuhle (18, 19).

The majority of contemporary authors expand the concept of the term “tumor of the IV ventricle”. For instance, Yasargil in his seminal work in 1994 classified both those tumors that develop primarily in its cavity (subependymoma, ependymoma, choroidpapilloma) and those tumors that grow secondarily to its cavity (astrocytomas, medulloblastomas, etc.) as IV ventricular tumors (20). Karakhan (3) and Tomasello (21) built their classifications of IV ventricular tumors according to the same principle (intraventricular filling and subependymal protrusion).

Yasargil distinguishes tumors of the IV ventricle according to the topographic localization of the tumors, which occupy the upper-median/paramedian, lower-median/paramedian, posterior, and lateral locations (20).

In their publications, Ferguson and Babichev divided IV ventricular tumors into those with central, caudal, lateral, and oral brainstem distributions (2, 22). Karakhan divided IV ventricular neoplasms into intraventricular, with supra-, retro-, infra- and latero-compression (3) (**Table 2**).

The most common tumor types in the IV ventricle and brainstem are medulloblastomas (2, 10, 15, 21–26) (7–93.3%), metastases (2, 3, 21, 25, 27, 28) (4.8–46.4%), ependymomas (2, 3, 9, 15, 21–30) (6.7–38%), astrocytomas (grade I–IV) (2, 3, 9, 21–26, 28, 30) (7.3–33%), subependymomas (2, 22) (9–19.5%), chorioidpapillomas (2, 9, 21–23, 26, 30) (2.2–14.6%), and hemangioblastomas (2, 3, 9, 15, 21–23, 25) (4.9–14.3%).

TABLE 2 | IV ventricle tumor classifications.

Year	Author	IV ventricle tumor classification
1935	M.Y. Rappoport (18)	Lesion located in the IV ventricular cavity, growing from its floor, ependyma of the choroid plexus
1940	I.Y. Razdolsky (19)	Lesion developed from the walls of the IV ventricle (ependyma and subependymal glia), endothelium, stroma, blood vessels, choroid plexus, ventral cerebellar vermis.
1994	M.G. Yasargil (20)	I.I Lesions grow primarily within the IV ventricle II.II Lesions secondarily spread into the IV ventricular cavity Topographically: 1)Upper median and paramedian location 2)Lower median and paramedian location 3)Posterior (fastigial) location 4)Lateral location
2018	K.N.Babichev (22)	In relation to the floor of the IV ventricle: 1)Central extension 2)Caudal extension (through the median aperture) 3)Lateral extension (through the lateral aperture into the cerebellar-pontine cistern) 4)Oral-brainstem extension (infiltrating the brainstem) 5)Mixed
2015	V.B. Karakhan (3)	In relation to the IV ventricular cavity: 1)Intraventricular filling 2)Extraventricular compression (subependymal protrusion) Topographic variants: 1)Intraventricular 2)Supraventricular compression (from the superior medullary vellum) 3)Retroventricular compression (from the inferior medullary vellum) 4)Infraventricular compression (from the brainstem) 5)Lateroventricular compression (from the lateral aspects of the medulla)
2018	S.D. Ferguson (2)	1)No extension beyond the 4th ventricle 2)Caudal extension (into the foramen of Magendie) 3)Lateral extension (into the foramen of Luschka) 4)Anterior extension (invasion of the brainstem) 5)Extension in multiple directions

The Clinical Picture of Tumors of the IV Ventricle

The symptoms that occur in patients with tumors of the fourth ventricle are either a consequence of an increase in intracranial pressure due the restriction in the outflow of cerebrospinal fluid through the cavity of the 4th ventricle or the compression of the walls of the 4th ventricle by the tumor (4).

For this reason, tumors of the IV ventricle are characterized by symptoms of increased ICP (headache, nausea, vomiting); symptoms of cerebellar damage, in particular, ataxia, intentional tremor, cerebellar dysarthria; and dysfunction of the cranial nerves (from V to XII). Motor and sensory disorders are less common and occur in cases where there is significant size and spread of the tumor (19).

According to the analyzed series, the most common symptoms were headache (2, 22, 28, 30, 31) (33–100%), nausea, vomiting (2, 22, 28, 31) (38–100%), diplopia (27, 28, 31) (26.9–33.3%), gait disturbance (2, 22, 27, 28, 30) (33–100%), visual impairment (2, 22) (9.8–29%), dizziness (2, 22, 28, 31) (15.4–66.7%), bulbar syndrome (22, 27, 28, 31) (17, 1–50%), sensory and pyramidal disorders (2, 22, 23, 31) (7–69.2%) and changes in mental status (2, 22, 31) (2–17.2%).

Surgical Treatment of Tumors of the IV Ventricle

In the 1920s, the only methods of surgical intervention for tumors of the fourth ventricle were punctures of the lateral ventricles, punctures of the corpus callosum, and subtemporal decompressive trepanations. These manipulations were palliative and did not produce favorable results.

The first surgical operation for a tumor of the IV ventricle was performed by Germanides (1894), and the first successful surgical interventions were performed by Oppenheim (1912) and Krause (1913). Cushing developed a surgical technique for these pathologies, which consisted of a wide exposure of both halves of the posterior cranial fossa. Martel began to operate on such patients while they were sitting and with drainage of the surgical wound (19). However, the overall mortality in pathologies of the fourth ventricle at the beginning of the 20th century remained high. For example, in the work of Razdolsky I.Ya, the postoperative mortality was 31% (19).

To date, along with the development of microsurgical techniques, anesthesia, new methods of intraoperative neurophysiological monitoring, and a detailed study of the anatomy of the 4th ventricle, the results of surgical treatment have improved significantly, but nevertheless, treating this pathology is a difficult task for modern neurosurgeons.

Variants of the Neurosurgical Approaches to Tumors of the 4th Ventricle

Craniotomy Stage

The classic approach to tumors of the 4th ventricle is the suboccipital approach (32). After the abovementioned approach is performed, the cerebellar hemispheres, vermis and medulla are exposed. Compared to keyhole approaches, this technique has advantages and disadvantages. The advantages are that there is exposure of more anatomical structures and, thus, better orientation in the surgical wound and freedom of manipulation. However, this approach is associated with large muscle and soft tissue incisions, large exposure of the brain tissue to environmental influences (microscope light, etc.) and an increased risk of sinus damage. The authors prefer both resection (21, 29) and osteoplastic (23, 24, 26) craniotomy. Both options have advantages and disadvantages; however, according to Gnanalingham's study that compared the complications of craniotomy and craniectomy, the number of CSF leaks and pseudomeningoceles was significantly higher in the craniectomy group of patients (27 vs. 4% and 23 vs. 9%, respectively) (6).

The literature also describes a suboccipital median approach with an attached flap (33). The essence of the method lies in the fact that when performing a craniotomy, a bone flap is left on the atlantooccipital membrane. When the wound is closed, the bone is fixed into place more easily and is more stable. According to the authors, this technique reduces the risk of CSF leakage and postoperative headaches due to better preservation of the anatomy of the atlantooccipital joint and the natural soft tissue layers.

If the tumors are located below the Chamberlain line, it is possible to perform a resection of the C1 arch (13, 15, 22, 23).

When analyzing the latest published works, one can note a clear trend toward an increase in the use and indications for minimally invasive approaches (34–36).

Several clinical cases of median keyhole approaches to the IV ventricle have been described. Among them, depending on the "entrance gate" to the IV ventricle, two types of surgeries are distinguishable: a) the median suboccipital approach (34–37) and b) the approach through the posterior atlanto-occipital membrane without bone resection (38).

Some authors believe that in the absence of tumor spread to the cranial parts of the IV ventricle at the micro stage, it is possible to apply an approach through the median aperture by cutting the tela choroidea from the foramen of Magendie laterally without cutting the inferior medullary velum upward.

Bo Qiu's article described the removal of the ependymomas of the IV ventricle in several cases, and in 80.8% of the cases, it was enough to cut the tela choroidea for adequate removal of the tumors. He also believes that with an approach through the median aperture, with proper retraction of the tonsils and uvula, one can clearly visualize the lateral recess and the lower ¾ of the cavity of the IV ventricle (31). Due to the uselessness of performing an upward incision of the inferior medullary velum and the choice of the optimal trajectory, the size of the craniotomy can be significantly minimized.

Suboccipital keyhole approaches allow the exposure of the tonsils, vermis and medulla. They provide a smaller soft tissue incision, less risk of traction of the cerebellum and other anatomical structures, less environmental impact (microscope light) and less risk of sinus damage. At the same time, when performing a keyhole approach, the surgeon is limited in manipulations and is required to have high qualification and experience.

In his monograph "Keyhole approaches in neurosurgery" in 2008 (34), Perneczky described a midline suboccipital keyhole technique with a working corridor diameter of 3 cm, including the space above the posterior atlantooccipital membrane. Perneczky also proposed variations of the suboccipital approach depending on the localization of the tumor in the cavity of the IV ventricle (34).

Charlie Teo described a keyhole approach to the IV ventricle using a mini-telovelar approach, suggesting that the cerebellar hemispheres do not always need to be fully exposed and that reducing the size of the craniotomy reduces the amount of laterally dissected muscles. In his opinion, the bone should only be resected until the border of trepanation is level with the upper pole of the tumor of the IV ventricle (35).

In 2019, David Pitskhelauri published a series of 200 patients who had surgery using the burr-hole technique, and a minimally invasive suboccipital approach was used in 17 patients. The size of the craniotomy was 14 mm, and the length of the incision was 3–4 cm (36).

In 2020, Corniola described a clinical case of microsurgical removal of a small subependioma of the caudal parts of the IV ventricle using a 1 cm resection of the occipital bone (37).

The median minimally invasive suboccipital approach, in addition to being used for the removal of tumors of the posterior cranial fossa with a median localization, is also used for the treatment of other pathologies of the central nervous system.

Hamada (39) used a small craniotomy, and Rauf (40) performed an endoscopic aqueductoplasty in an isolated IV ventricle through a suboccipital burr hole, 2–3 cm below the superior nuchal line. Toyota (41), with a small craniotomy, and Gallo, using a 4 cm incision and minimal resection of the occipital bone (42), used an endoscopic approach into the isolated IV ventricle to perform aqueductoplasty.

It is worth noting the work of Bergsneider (38), which described an endoscopic approach to the IV ventricle through the foramen magnum without bone resection. The author successfully used a flexible endoscope to remove cysticercus cysts in the IV ventricles of 5 patients.

Micro Stage

The first approach to the IV ventricle is considered to be the transvermian approach, which was described by Walter Dandy. It consisted of dissection of the cerebellar vermis (43). However, its application is currently limited due to the significant neurological deficits that are caused by this approach (44).

Currently, different variations of the approach to tumors of the IV ventricle through the cerebellar-medullar fissure, as described by Matsushima et al., have been generally accepted (16). In terms of surgical significance, he compared the cerebellomedullar fissure in the subtentorial space with the Sylvian fissure in the supratentorial space. Depending on the location of the tumor in the IV ventricle, Matsushima et al. subdivided the approach through the cerebellomedullary fissure into several methods. The "extensive opening method" is used when tumors are localized deep in the cavity of the IV ventricle or are paramedian near the cerebral aqueduct. In this case, both the uvulotonsillar and medullotonsillar spaces are dissected bilaterally. The "lateral wall opening method" involves a unilateral dissection of the cerebellomedullar fissure to access the central areas of the IV ventricle. In the case of lateralization of a mass lesion, the authors recommended dissecting the contralateral fissure. With the "lateral recess opening method", in cases where the tumor is located in the most distal parts of the lateral recess, a unilateral dissection of the tonsillomedullar fissure is used (9).

Additionally, one of the approaches to the IV ventricle is through the foramen of Magendie, which is often enlarged by the tumor, and with situational dissection of the tela choroidea (22).

There is also a transcortical approach to the IV ventricle through the cerebellar hemisphere using a tubular retractor, which was described by Jamshidi et al. in a series of 3 patients. Taking into account the data of the navigation system, the surgical corridor is built in such a way as not to damage the deep nuclei of the cerebellum (45).

Most authors currently use variations of the cerebellomedullar fissure approach (3, 9, 21, 23, 24, 27, 29, 30, 46). In some series, the authors have used both of the approaches through the cerebellomedullar fissure and through the foramen of Magendie with dissection of the choroid plexus (15, 22, 31). Ferguson et al. published a series of patients who had surgery that utilized the telovelar and transvermian approaches (2). It can be noted that there is a growing trend toward the use of approaches through the cerebellomedullar fissure and a departure from the transvermian approach, which is used situationally for tumors originating from the cerebellar vermis.

Complications of Surgical Treatment

In most of the described case series, the symptoms of neurological status deterioration in the postoperative period have included the following: general worsening of neurological symptoms (2, 21–23, 29) (4.5–46.7%), cerebellar mutism (2, 15, 21, 23, 24, 29–31) (0–38%), worsening of bulbar disorders (2, 21–23, 25, 28) (2.2–38%), oculomotor disorders (21, 23, 25, 27, 29, 46) (4.5–20%), gait disturbances (2, 22, 28–30) (25–56%), and facial nerve deficits (23, 25, 27, 29, 46) (3–18.2%).

Postoperative hematomas have been described in 2–4.8% of cases (2, 23, 25, 26).

The incidence of CSF leakage in the analyzed series varied from 0 to 27% (2, 6, 22–24, 26, 47), and the incidence of postoperative meningitis was noted in 0.47% - 20% of the cases (2, 6, 22, 26).

During the perioperative period, intraoperative air embolism occurred as a complications in 9.5% of patients who had surgery while sitting in the study by Gok et al. (25). Symptomatic pneumocephalus was observed in two series of patients with an incidence of 4 and 0.95%, where the position of the patients was predominantly on their side and when sitting, respectively (2, 26).

In the analyzed series, postoperative CSF shunting operations due to unresolved occlusive hydrocephalus were needed in 0–50% of the cases (2, 6, 15, 21, 23, 24, 26, 27, 31, 47).

CONCLUSION

Despite the complexity of the anatomy of the fourth ventricle of the brain, recent studies have shown that microsurgical removal of tumors of this localization is feasible with an acceptable incidence of postoperative neurological deficits and surgical complications.

AUTHOR CONTRIBUTIONS

Conceptualization: [DP, RS]; Methodology: [DP, RS, AB]; Formal analysis and investigation: [RS, AB]; Writing- original draft preparation: [RS, AB]; Writing- review and editing: [RS, AB, DP]; Supervison: [DP]. All authors contributed to the article and approved the submitted version.

REFERENCES

1. Ostrom QT, Cioffi G, Waite K, Kruchko C, Barnholtz-Sloan JS. CBTRUS statistical report: primary brain and other central nervous system tumors diagnosed in the United States in 2014–2018. *Neuro Oncol*. (2021) 23: iii1–105. doi: 10.1093/neuonc/noab200
2. Ferguson SD, Levine NB, Suki D, Tsung AJ, Lang FF, Sawaya R, et al. The surgical treatment of tumors of the fourth ventricle: a single-institution experience. *J Neurosurg*. (2018) 128:339–51. doi: 10.3171/2016.11.JNS161167
3. Karakhan VB. Surgery for tumors of the fourth ventricle: the characteristics of accesses and the role of endoscopic techniques. *Head Neck Tumors*. (2015). doi: 10.17650/2222-1468-2012-0-4-10-18
4. Cohen AR. *Surgical disorders of the fourth ventricle*. Cambridge, MA: Blackwell Science (1996). p. 94–143.
5. Helmut Bertalanffy OB, Niklaus Krayenbuhl CW. Ventricular tumors. In: Winn HR, editor. *Youmans neurological surgery*. 6th ed. New York: Elsevier (2011). 1537 p.
6. Gnanalingham KK, Lafuente J, Thompson D, Harkness W, Hayward R. Surgical procedures for posterior fossa tumors in children: does craniotomy lead to fewer complications than craniectomy? *J Neurosurg*. (2002) 97:821–6. doi: 10.3171/jns.2002.97.4.0821
7. Lawton MT, Quiñones-Hinojosa A, Jun P. The supratonsillar approach to the inferior cerebellar peduncle: anatomy, surgical technique, and clinical application to cavernous malformations. *Oper Neurosurg*. (2006) 59:ONS-244-ONS-252. doi: 10.1227/01.NEU.0000232767.16809.68
8. Tayebi Meybodi A, Lawton MT, Tabani H, Benet A. Tonsillobiventral fissure approach to the lateral recess of the fourth ventricle. *J Neurosurg*. (2017) 127:768–74. doi: 10.3171/2016.8.JNS16855
9. Matsushima T, Inoue T, Inamura T, Natori Y, Ikezaki K, Fukui M. Transcerebellomedullary fissure approach with special reference to the methods of dissecting the fissure. *J Neurosurg*. (2001) 94:257–64. doi: 10.3171/jns.2001.94.2.0257
10. Matsushima T, Kawashima M, Inoue K, Matsushima K, Miki K. Exposure of wide cerebellomedullary cisterns for vascular lesion surgeries in cerebellomedullary cisterns: opening of unilateral cerebellomedullary fissures combined with lateral foramen magnum approach. *World Neurosurg*. (2014) 82:e615–21. doi: 10.1016/j.wneu.2014.04.064
11. Aydin I, Hanalioglu S, Peker HO, Turan Y, Kina H, Cikla U, et al. The tonsillouvular fissure approach: access to dorsal and lateral aspects of the fourth ventricle. *World Neurosurg*. (2018) 114:e1107–19. doi: 10.1016/j.wneu.2018.03.157
12. Mussi ACM, Rhoton AL. Telovelar approach to the fourth ventricle: microsurgical anatomy. *J Neurosurg*. (2000) 92:812–23. doi: 10.3171/jns.2000.92.5.0812
13. Tanriover N, Ulm AJ, Rhoton AL, Yasuda A. Comparison of the transvermian and telovelar approaches to the fourth ventricle. *J Neurosurg*. (2004) 101:484–98. doi: 10.3171/jns.2004.101.3.0484
14. Tubbs RS, Bosmia AN, Loukas M, Hattab EM, Cohen-Gadol AA. The inferior medullary velum: anatomical study and neurosurgical relevance. *J Neurosurg*. (2013) 118:315–8. doi: 10.3171/2012.10.JNS12794
15. Han S, Wang Z, Wang Y, Wu A. Transcerebellomedullary fissure approach to lesions of the fourth ventricle: less is more? *Acta Neurochir (Wien)*. (2013) 155:1011–6. doi: 10.1007/s00701-013-1689-x
16. Matsushima T, Fukui M, Inoue T, Natori Y, Baba T, Fujii K. Microsurgical and magnetic resonance imaging anatomy of the cerebellomedullary fissure and its application during fourth ventricle surgery. *Neurosurgery*. (1992) 30:325–30. doi: 10.1227/00006123-199203000-00003
17. Rhoton AL. Cerebellum and fourth ventricle. *Neurosurgery*. (2000) 47: S7–S27. doi: 10.1097/00006123-200009001-00007
18. Rappoport MY, Klossovskiy BN. *Klinika, kliniko-anatomicheskiye paralleli i operativnyye pokazaniya pri opukholyakh IV zheludochka*. Moskva-Leningrad: Gosudarstvennoye Izdatel'stvo Biologicheskoy i Meditsinskoy Literatury (1935). p. 232–340.
19. Razdolsky IY. *Opukholi IV zheludochka golovnogo mozga*. Leningrad: Izdaniye Vtorogo Leningradskogo Meditsinskogo Instituta (1940). p. 5.
20. Yaşargil MG. *Microneurosurgery in 4 volumes IVA*. Stuttgart, New York: Thieme (1994). p. 142–144.
21. Tomasello F, Conti A, Cardali S, La Torre D, Angileri FF. Telovelar approach to fourth ventricle tumors: highlights and limitations. *World Neurosurg*. (2015) 83:1141–7. doi: 10.1016/j.wneu.2015.01.039
22. Babichev KN, Stanishevskiy AV, Svistov DV, Averyanov DA, Lakotko RS. Surgical resection of fourth ventricular tumors. Comparison of the efficiency and safety of telovelar and median aperture approaches to the fourth ventricle. *Russ J Neurosurg*. (2019) 20:10–9. doi: 10.17650/1683-3295-2018-20-4-10-19
23. Kalinovskiy AV, Chernov SV, Zotov AV, Kasymov AR, Gormolysova EV, Uzhakova EK. Surgical treatment of the tumors of the fourth ventricle through telovelar approach. *Russ J Neurosurg*. (2018) 20:8–16. doi: 10.17650/1683-3295-2018-20-2-8-16
24. Zaheer SN, Wood M. Experiences with the telovelar approach to fourth ventricular tumors in children. *Pediatr Neurosurg*. (2010) 46:340–3. doi: 10.1159/000321539
25. Gok A, Alptekin M, Erkutlu I. Surgical approach to the fourth ventricle cavity through the cerebellomedullary fissure. *Neurosurg Rev*. (2004) 27:50–4. doi: 10.1007/s10143-003-0286-5
26. Kushel Y, Danilov G, Tekoev A, Cheldiev B, Strunina Y. A single-center retrospective descriptive cohort study of 211 pediatric patients: cerebrospinal fluid leakage after fourth ventricle tumor resection. *World Neurosurg*. (2019) 129:e171–6. doi: 10.1016/j.wneu.2019.05.091
27. Ziyal IM, Sekhar LN, Salas E. Subtonsillar-transcerebellomedullary approach to lesions involving the fourth ventricle, the cerebellomedullary fissure and the lateral brainstem. *Br J Neurosurg*. (1999) 13:276–84. doi: 10.1080/02688699943682
28. Jean WC, Abdel Aziz KM, Keller JT, van Loveren HR. Subtonsillar approach to the foramen of luschka: an anatomic and clinical study. *Neurosurgery*. (2003) 52:860–6. doi: 10.1227/01.NEU.0000053146.83780.74
29. Rajesh BJ, Rao BRM, Menon G, Abraham M, Easwer HV, Nair S. Telovelar approach: technical issues for large fourth ventricle tumors. *Child's Nerv Syst*. (2007) 23:555–8. doi: 10.1007/s00381-006-0295-0
30. El-Bahy K. Telovelar approach to the fourth ventricle: operative findings and results in 16 cases. *Acta Neurochir (Wien)*. (2005) 147:137–42. doi: 10.1007/s00701-004-0407-0

31. Qiu B, Wang Y, Wang W, Wang C, Wu P, Bao Y, et al. Microsurgical management of pediatric ependymomas of the fourth ventricle via the trans-cerebellomedullary fissure approach: a review of 26 cases. *Oncol Lett*. (2016) 11:4099–106. doi: 10.3892/ol.2016.4507
32. Yaşargil MG. *Microneurosurgery in 4 volumes IVB*. Stuttgart, New York: Thieme (1996). p. 63–64.
33. Prell J, Scheller C, Alfieri A, Rampp S, Rachinger J. Midline-craniotomy of the posterior fossa with attached bone flap: experiences in paediatric and adult patients. *Acta Neurochir (Wien)*. (2011) 153:541–5. doi: 10.1007/s00701-010-0924-y
34. Perneczky A, Reisch R. Suboccipital approach. In: Tschabitscher M, editor. *Keyhole approaches in neurosurgery volume 1: Concept and surgical technique*. Wien, New York: Springer (2008). 184 p.
35. Teo C, Sughrue ME. *Principles and practice of keyhole brain surgery*. Stuttgart: Thieme (2015).
36. Pitskhelauri D, Konovalov A, Kudieva E, Bykanov A, Pronin I, Eliseeva N, et al. Burr hole microsurgery for intracranial tumors and mesial temporal lobe epilepsy: results of 200 consecutive operations. *World Neurosurg*. (2019) 126:e1257–67. doi: 10.1016/j.wneu.2019.02.239
37. Corniola MV, Meling TR. How I do it: minimally invasive resection of a subependymoma of the fourth ventricle. *Acta Neurochir (Wien)*. (2022) 164:767–70. doi: 10.1007/s00701-020-04601-5
38. Bergsneider M. Endoscopic removal of cysticercal cysts within the fourth ventricle. *J Neurosurg*. (1999) 91:340–5. doi: 10.3171/jns.1999.91.2.0340
39. Hamada H, Hayashi N, Endo S, Kurimoto M, Hirashima Y, Takaku A. Endoscopic aqueductal plasty via the fourth ventricle through the cerebellar hemisphere under navigating system guidance. Technical Note. *Neurol Med Chir (Tokyo)*. (1999) 39:950–4. doi: 10.2176/nmc.39.950
40. Raouf A, Zidan I. Suboccipital endoscopic management of the entrapped fourth ventricle: technical note. *Acta Neurochir (Wien)*. (2013) 155:1957–63. doi: 10.1007/s00701-013-1843-5
41. Toyota S, Taki T, Oshino S, Hashiba T, Oku Y, Hayakawa T, et al. A neuroendoscopic approach to the aqueduct via the fourth ventricle combined with suboccipital craniectomy. *Minim Invasive Neurosurg*. (2004) 47:312–5. doi: 10.1055/s-2004-830070
42. Gallo P, Hermier M, Mottolese C, Ricci-Franchi A-C, Rousselle C, Simon E, et al. The endoscopic trans-fourth ventricle aqueductoplasty and stent placement for the treatment of trapped fourth ventricle: long-term results in a series of 18 consecutive patients. *Neurol India*. (2012) 60:271. doi: 10.4103/0028-3886.98507
43. Dandy WE. *Brain tumors: general diagnosis and treatment*. Surgery of the Brain. (1945).
44. Rekate HL, Grubb RL, Sram DM, Hahn JF, Ratcheson RA. Muteness of cerebellar origin. *Arch Neurol*. (1985) 42:697–8. doi: 10.1001/archneur.1985.04060070091023
45. Jamshidi AO, Priddy B, Beer-Furlan A, Prevedello DM. Infradentate approach to the fourth ventricle. *Oper Neurosurg*. (2019) 16:167–78. doi: 10.1093/ons/opy175
46. Kellogg JX, Piatt Jr JH. Resection of fourth ventricle tumors without splitting the vermis: the cerebellomedullary fissure approach. *Pediatr Neurosurg*. (1997) 27:28–33. doi: 10.1159/000121221
47. Pitskhelauri D, Kudieva E, Moshchev D, Ananev E, Shifrin M, Danilov G, et al. Cisterna magna arachnoid membrane suturing decreases incidence of pseudomeningocele formation and incisional CSF leakage. *Acta Neurochir (Wien)*. (2018) 160:1079–87. doi: 10.1007/s00701-018-3507-y

Conflict of Interest: The authors declare that the research was conducted in the absence of any commercial or financial relationships that could be construed as a potential conflict of interest.

Publisher's Note: All claims expressed in this article are solely those of the authors and do not necessarily represent those of their affiliated organizations, or those of the publisher, the editors and the reviewers. Any product that may be evaluated in this article, or claim that may be made by its manufacturer, is not guaranteed or endorsed by the publisher.

frontiers | Frontiers in Surgery

REVIEW
published: 16 June 2022
doi: 10.3389/fsurg.2022.889906

Beyond Placement of Pedicle Screws - New Applications for Robotics in Spine Surgery: A Multi-Surgeon, Single-Institution Experience

*Troy Q. Tabarestani[1], David Sykes[1], Kelly R. Murphy[2], Timothy Y. Wang[2], Christopher I. Shaffrey[2], C. Rory Goodwin[2], Phillip Horne[3], Khoi D. Than[2] and Muhammad M. Abd-El-Barr[2]**

[1]Duke University School of Medicine, Duke University Hospital, Durham, Durham, NC, [2]Department of Neurosurgery, Duke University Hospital, Durham, Durham, NC, [3]Department of Orthopedic Surgery, Duke University Hospital, Durham, Durham, NC

OPEN ACCESS

Edited by:
Philipp Taussky,
The University of Utah, United States

Reviewed by:
Sujay Kumar Dheerendra,
Robert Jones and Agnes Hunt Orthopaedic Hospital, United Kingdom
Davide Croci,
University of South Florida, United States

***Correspondence:**
Muhammad M. Abd-El-Barr
muhammad.abd.el.barr@duke.edu

Specialty section:
This article was submitted to Neurosurgery, a section of the journal Frontiers in Surgery

Received: *04 March 2022*
Accepted: *01 June 2022*
Published: *16 June 2022*

Citation:
Tabarestani TQ, Sykes D, Murphy KR, Wang TY, Shaffrey Christopher I., Goodwin C.R, Horne P, Than KD and Abd-El-Barr Muhammad M. (2022) Beyond Placement of Pedicle Screws - New Applications for Robotics in Spine Surgery: A Multi-Surgeon, Single-Institution Experience. Front. Surg. 9:889906. doi: 10.3389/fsurg.2022.889906

Interest in robotic-assisted spine surgery has grown as surgeon comfort and technology has evolved to maximize benefits of time saving and precision. However, the Food and Drug Administration (FDA) has currently only approved robotics to assist in determining the ideal trajectory for pedicle screw placement after extensive research supporting its efficacy and efficiency. To be considered a durable and effective option, robotics need to expand beyond the indication of just placing pedicle screws. This article aims to illustrate a multi-surgeon, single-institution experience with unique applications of robotic technologies in spine surgery. We will explore accessing Kambin's Triangle in percutaneous transforaminal interbody fusion (percLIF), iliac fixation in metastatic cancer, and sacroiliac (SI) fusions. Each of these topics will be covered in depth with associated background information and subsequent discussion. We show that with proper understanding of its limitations, robots can help surgeons perform difficult surgeries in a safe manner.

Keywords: robotic-assisted, spine surgery, neurosurgery, kambin's triangle, pedicle screw, percLIF, iliac screw, sacroiliac joint fusion

INTRODUCTION

From 2012 to 2018, the use of robotic-assisted (RA) surgeries has increased in incidence from 1.8% to almost 15% for all general surgeries (1). Specifically in the realm of spine surgery, RA procedures have been examined extensively for use in pedicle screw placement during minimally-invasive spine surgery (2, 3). With decreased muscle retraction and dissection, RA screw placement has not only improved post-operative outcomes for patients but has also assisted with the safety and accuracy of pedicle screw placement (4–6). With the combination of 3-dimensional (3D) imaging techniques, higher resolution MRIs, and more advanced robotic function, RA surgeries are primed for a rapid expansion throughout the field.

One of the main advantages of RA surgeries is the ability of the robotic arm to guide the surgeon to a predefined location in 3D space and allow for specific trajectories. The application of this ability to place pedicle screws under image navigation is well-studied in the current literature (7). However, as surgeons have become more comfortable with robotic assisted surgery, they have begun using the robot for other 'off-label' applications such as planning and executing osteotomies, decompressions, and interbody fusions (8–10).

In this paper, we review a multi-surgeon, single-institution experience of unique applications of robotics as it pertains to spine surgery. We aim to exemplify three types of procedures to illustrate the expanded applications of RA surgeries: (1) accessing Kambin's Triangle in percutaneous lumbar interbody fusion (percLIF), (2) percutaneous iliac screw fixation, and (3) sacroiliac (SI) joint fusions. We highlight the advantages and disadvantages of robotic assistance in these cases, discuss their prevalence in the literature, and speak on the future directions for RA surgeries.

Application 1: Robotic-Assisted Access into Kambin's Triangle During percLIF

A procedure that has gained popularity in the care of patients with degenerative spondylolisthesis or disc disease is percLIF through Kambin's triangle (11, 12). Kambin's triangle is defined as the exiting nerve root, superior endplate of the caudal vertebral body, and superior articulating process (SAP) (13). The triangle allows surgeons to avoid a facetectomy when attempting to access the disc space, however, the space has wide variety depending on the level, ranging from 60 mm^2 at levels L1-L2 to 108 mm^2 at levels L4-L5 (13–15). Traditionally, biplanar fluoroscopy is used for localization in spine surgery, but its application might be limited in smaller areas such as Kambin's triangle. We have recently shown that robotic entrance into the disc space and interbody placement is a feasible alternative as demonstrated in a single-center, retrospective review of ten patients with spondylolisthesis who underwent RA percLIF using robot-guided trajectory to access Kambin's triangle for cage placement (16).

In these cases, the robot utilized CT anatomy to plan a trajectory into the intervertebral space through Kambin's triangle (**Figure 1**). As this trajectory enters the disc space from the inferior-most corridor through Kambin's triangle, traversing neural anatomy is safely avoided. The trajectory is then backpropagated to the skin to ensure no structures would impede entrance into the disc space. Using the robotic arm as a guide, a stab incision is made in the skin and dilators were used to widen the fascia and subcutaneous tissue until right before entering Kambin's triangle. Then, a k-wire is passed through the end effector of the robot and entered the disc space through Kambin's triangle. The k-wire is maintained, and the robot is moved out of the way. Further dilation is done until an 8 mm portal is placed, followed by adequate discectomy. Adequate discectomy was confirmed by inserting a balloon into the disc space and filling it with contrast agent which could subsequently be visualized to confirm contact with the inferior endplate of the superior vertebral body and the superior endplate of the inferior vertebral body. A k-wire was again placed through Kambin's triangle which was used to guide an obturator into the disc space. Bone morphogenetic protein (BMP) was placed in the anterior disc space, followed by implantation of the ELITE (Spineology, Minneapolis, MN) expandable interbody fusion device.

This study showed an average estimated blood loss with 68 mL compared to average ranges of 360–7,000 mL for instrumented fusions (17). For the post-operative results, no patients were lost to follow-up, no patients were readmitted, and disc heights for all the patients showed statistically significant increases with the expandable cage. More importantly, no patients experienced post-operative motor or sensory deficits. To add to the impressive precision of this RA technique, each of the patients had a smaller Kambin's triangle than the average typically reported size. Patients who underwent RA percLIF were discharged on average after 1.8 days, which compares favorably to an average LOS of 3.6 days for elective spine fusion (18). The LOS of 1.8 days remained lower in comparison to other minimally-invasive spine surgery LOS averages (19). Without the need for laminectomies or facetectomies, minimal tissue disruption was attained by using RA instrumentation finely tuned to each patient's unique spinal landscape.

Application 2: Robotic-Assisted Percutaneous Iliac Screw Fixation

Robotic assistance can also be useful for iliac screw fixation in the presence of destructive lesions of the pelvis and sacrum.

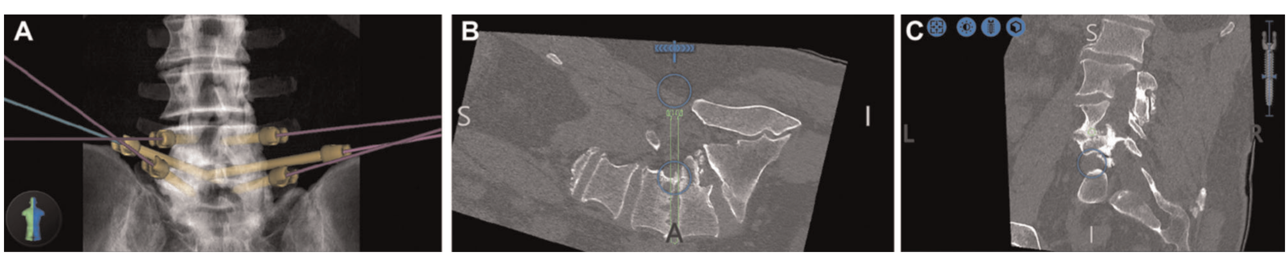

FIGURE 1 | Preoperative plan (**A**) Pedicle screws and bilateral projections into Kambin's triangle were planned. (**B**) The right projection is highlighted in green. (**C**) Coronal plan shows entrance into disc at the mid-pedicle point, which is the largest area of the safe zone within Kambin's triangle (from (16), used with permission).

Over the past years, there has been a general trend away from the Galveston rod technique/iliac screws and towards the S2-alar-iliac screw (S2AI) (20). The S2AI screw provides similar stability for the patient without the need for side connectors. However, in the presence of a more destructive and expansive sacral lesion, S2-AI screws may not be optimal (21). We have recently published our early experience of RA iliac fixation for patients with destructive sacral lesions (22). For the two cases presented here, both patients underwent percutaneous iliac screw fixation without the need for side connectors. RA navigation allowed the surgeon to plan a modified screw trajectory and entry site in line with the lumbar pedicle screws under the skin, eliminating the need for 3-D rod contouring or connectors (**Figures 2**, **3**).

The operative plan was very similar in both cases: intraoperative anterior–posterior and lateral fluoroscopic images of L4-S2 were merged with preoperative CT, Globus ExcelsiusGPS® was positioned correctly, and the screws were placed. Bilateral fluoroscopic "teardrop/outlet-oblique" views and an intraoperative CT confirmed proper alignment and placement of all screws (**Figure 4**); however, the screw positions were not assessed using any form of grading system. Neither patient had post-operative complications or instrumentation failure at their respective follow-ups.

In both cases presented, the use of S2AI screws was precluded by the extensive damage to the sacrum. Therefore, a modified iliac screw entry point was utilized with entry point slightly more medial than the traditional method, with a pre-planned trajectory of the screws using robot assistance (23, 24).

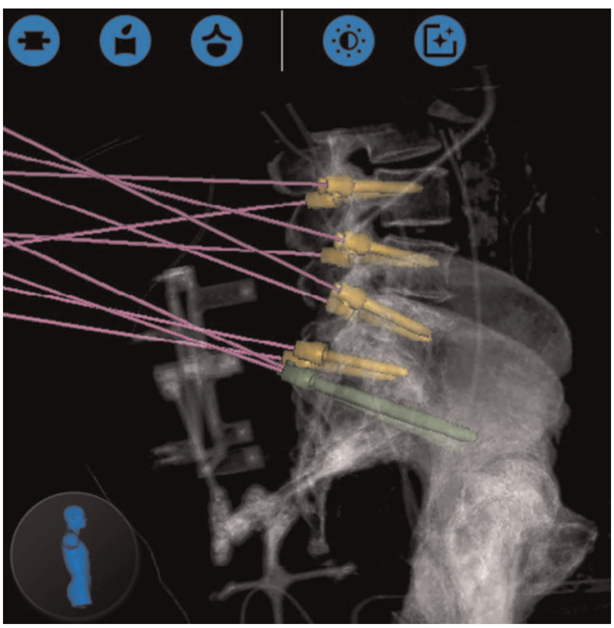

FIGURE 2 | Globus ExcelsiusGPS® preoperative planning phase showing the placement of the iliac screws prior to their insertion (from (22), used with permission).

Application 3: Robotic-Assisted SI Joint Fusion

Open SI joint fusions began in the 1920s, progressed with sacroiliac screw fixations in the 1980s, and eventually joined the minimally invasive field in 2004 (25–28). Prior to this hallmark, there were not many reports of standalone SI joint fusions, but rather mentions of them in larger instrumented spine procedures. While there was still doubt regarding the long-term efficacy, randomized clinical trials and patient follow-up studies began revealing that minimally invasive SI fusion surgery was safer and more efficacious than the usual conservative management (29, 30). As with the other minimally invasive surgeries, the fusions showed promise by reducing operative time, blood loss, and LOS (31). Even though short-term fusion rates were low, long-term radiographic analysis revealed high rate of successful bone apposition to implants (32).

The current literature supports two main approaches for SI joint fusion: dorsal or lateral transarticular, with the latter being more commonly used. In the lateral technique, screws are packed with graft materials to promote bony growth across the joint. In the dorsal approach, the implant is placed obliquely through the SI joint space (33). Both techniques have shown to be equally beneficial for post-operative fusion rates and range of motion (34). However, just as with the other techniques described, robotic assistance for SI joint fusion has yet to be fully documented in the literature. In 2021, Piche et al. provided the first known technical guide with specific case reports to describe their methodology (35). In 2022, our group at Duke University published a case series displaying this "off-label" use of the robot implementing a similar surgical technique (36).

Across all 9 patients in the cohort, three implants were planned with trajectories designed to traverse the SI joint (**Figure 5**). After general anesthesia was obtained, dynamic reference bases were placed in the contralateral posterior superior iliac crest. Anterior-posterior and lateral x-rays were then taken of the L5 vertebral body and sacrum, which were merged with a preoperative CT scan containing the pre-planned trajectories. Once the surgeon confirmed the image fusion accuracy, the robot was wheeled into the operative field until the end-effector could reach the entire work zone. The end effector was placed in the starting location and, using the robot as a guide, a high-speed drill burred a pathway for the SI screws following each respective trajectory. Intraoperatively, three screws (one above, the second short, and the third below the S1 foramen) were placed under the navigational guidance of the Globus robot. No EMG monitoring leads were placed during the procedure, but confirmatory X-rays were taken to ensure the screws remained lateral to the sacral foramina and superior to the acetabulum (**Figure 6**). Post-operatively, the patients were immediately allowed to weight-bear as-tolerated. The average operative time was 55 min, which decreased over the course of this case series. The average intraoperative radiation exposure was 13.2 mGy, average length of stay was 0.4 days, and there were no intraoperative complications or conversions.

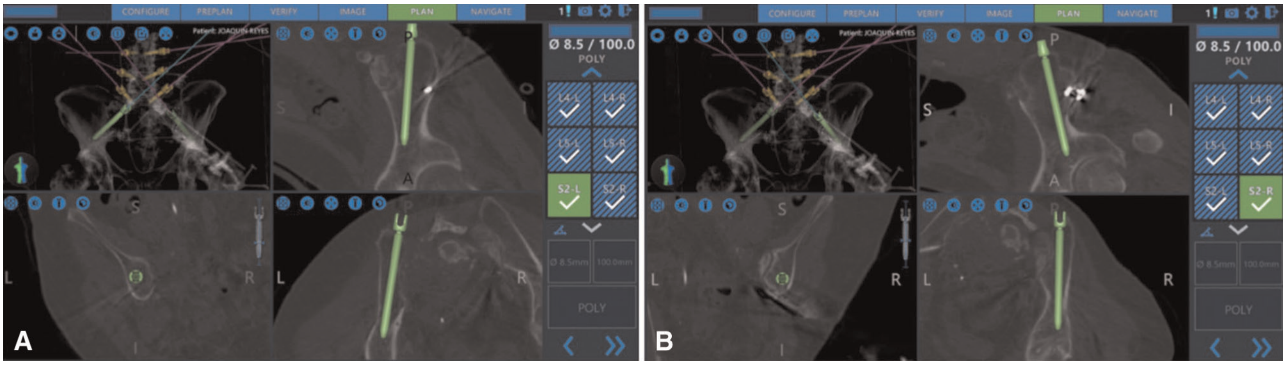

FIGURE 3 | Navigated placements of the right (**A**) and left (**B**) iliac bolts (8.5 × 100 mm) (from (22), used with permission).

FIGURE 4 | Postoperative upright x-rays for Cases 1 ((**A**) AP; (**B**) lateral) and 2 ((**C**) AP; (**D**) lateral) of the fixation construct demonstrating good screw placement (from (22), used with permission).

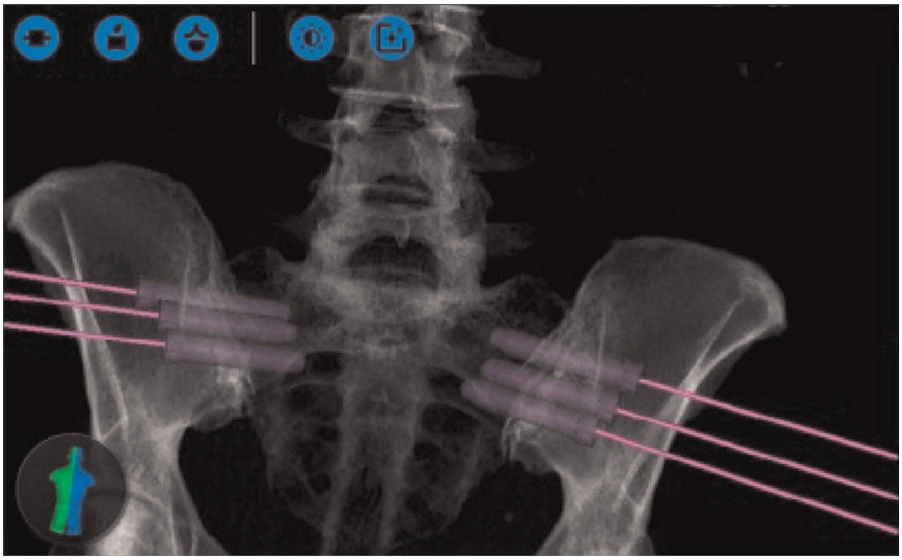

FIGURE 5 | Screw entrance plans designed on the ExcelsiusGPS interface, which requires bilateral trajectories to be mapped (from (36), used with permission).

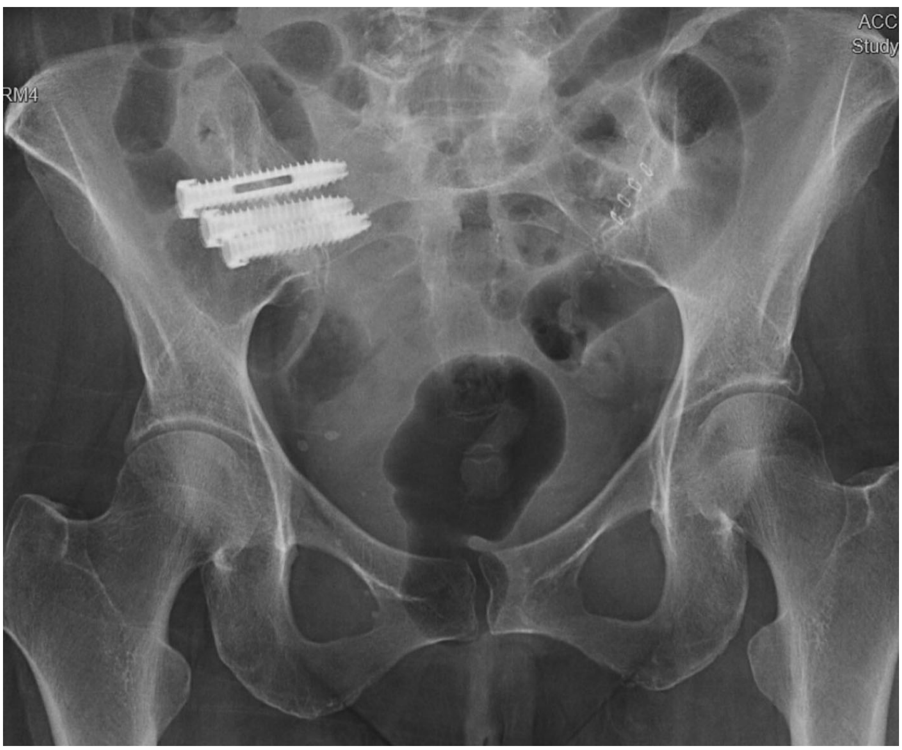

FIGURE 6 | Post-implantation X-rays demonstrating appropriate placement of the hydroxyapatite-coated titanium implants through the right SI joint (from (36), used with permission).

DISCUSSION

The history of robotics, as it relates to spine surgery, extends back almost 30 years. Since then, the dual excitement for both minimally invasive surgeries (MIS) and robotics has grown exponentially together for a multitude of reasons. As demonstrated through the applications reviewed in this article, the combination of MIS and robotic assistance into one procedure can improve various outcomes for the patient and surgeon alike. With its ability to precisely guide the surgeon to a predefined location in 3D space and allow for specific trajectories, the applications of RA spine surgery will extend beyond the placement of pedicle screws in the near future. Use of the RA method has allowed for iliac fixation in destructive sacral lesions, sacroiliac fusions, and percLIF through Kambin's Triangle. In addition to improving safety and accuracy, RA technology has allowed for faster recovery, same day discharges, minimal blood loss obviating transfusions, decreased radiation exposure, and shorter lengths of stay (16, 37).

A similar history can be traced back to the introduction of the da Vinci robot® (Intuitive Surgical; Sunnyvale, California). The first ever use of the robot was in 1997 where it assisted during a cholecystectomy. However, the skepticism of the da Vinci robot was prominent at the start of its widespread usage. Doctors complained of learning a brand-new propriety software, patients filed lawsuits for medical damages that occurred during surgeries, and hospitals were averse to the extremely high equipment prices. Slowly, as companies improved both the user interface and hardware of each product, there was increased acceptance of this technology. In 2000, the FDA approved the usage of the da Vinci robot for general laparoscopic surgeries (38). These procedures led to less blood loss, less need for blood transfusion, lower mean pain score, and shorter LOS when compared to patients undergoing the comparable open procedure (39). Just like with the da Vinci robot, the new RA techniques in spine surgery are following a similar path in their technological life cycle.

In the percLIF application, for example, we acknowledge that the technique itself is only semi-autonomous, which further indicates that the future applications for RA spine surgery should revolve around the autonomous performance of surgical actions rather than robotic localization. This will depend on research that provides haptic feedback, feedback loops, and greater robotic arm precision to perform the operator actions that spine surgery requires. This also introduces the potential for the robot to have an MIS retractor tube to dock through the system itself to provide robotic assistance in resection capabilities beyond simple localization. Recently, researchers have examined robotic lumbar facet decortication. Utilizing a preoperative plan similar to that used in percLIF, the robotic arm swings into position. Rather than placing a pedicle screw or tap, a large burr is inserted through the guide to facilitate facet decortication (40, 41). Yet another advancement was shown in the cases of iliac fixation, where we were able to successfully perform iliolumbar fixation percutaneously without the need for a side connector, which is a potential place of weakness and failure (42). Of note, this technique has been implemented by various other groups in the literature and is currently expanding its usage (43–45). Likewise, in the case of sacroiliac fusion, the robot's ability to accurately place instrumentation without soft tissue destruction is an advantage compared to traditional methods.

As discussed throughout this paper, there are a multitude of advantages to using RA technology in the realm of spine surgery. However, it remains important to also discuss the potential disadvantages as we use the robot for increased indications. The most common of these being the increased cost and subsequent decreased accessibility. These technologies are undoubtedly more expensive than the prior standard navigation platforms, but over the past few years, mass production has cut costs nearly in half as seen with the recently launched third generation Mazor X™ system (46). In terms of cost-effectiveness, there continues to be a lack of broad studies on this topic. Having said that, researchers have started comparing RA to standard technology in key variables that make up the cost-effective category including fluoroscopy time, revision rate, operative room time, and LOS. Fiani et al. reported in their systematic review paper that RA technology improved cost-effectiveness in all of these key subcomponents (46).

Further evaluating the safety, efficiency, cost, and learning curve timeline are all crucial for understanding the true benefits of RA technology versus standard navigation tools. Some of the challenges to proving these benefits include the small sample sizes of previous works thereby making randomized control studies difficult to create (47). Additionally, it is also important to look at the horizon of RA technology - augmented reality (AR). Only a few studies have examined its use in a patient model due to its higher costs and steep learning curve (48, 49). On the other hand, AR has the potential to solve a variety of the current limitations with both RA and traditional navigation technologies including line-of-sight errors, an external camera system, and surgeon attention shift (48, 50, 51). These future innovations will most likely follow the same path RA has: inception, growth, hesitance, and incremental improvement towards large-scale implementation.

CONCLUSIONS

With constant advancements in imaging, navigation, and robotics, surgeons now have even more access to tools that can improve preoperative planning, intraoperative visualization, and postoperative outcomes. Early work in spine surgeries has shown the possible applications of RA procedures beyond pedicle screw placement, but as noted in each application, further studies are needed to demonstrate the long-term clinical benefit for widespread adoption. There are numerous obstacles with integrating new technologies in the operating room including cost, learning curves, and general hesitance towards new methodologies. To begin chipping away at this tentative opinion regarding robotics, more work will need to be done on larger patient populations to continue optimizing the safety and accuracy of robotic-assisted spine surgery.

AUTHOR CONTRIBUTIONS

All authors contributed to the article conception and design. Data/literature collection and analysis were performed by TQT, DS, KM, TW and MA-E-B. The first draft of the manuscript was written by TQT and all authors critically revised previous versions of the manuscript. All authors contributed to the article and approved the submitted version.

REFERENCES

1. Sheetz KH, Claflin J, Dimick JB. Trends in the adoption of robotic surgery for common surgical procedures. *JAMA Netw Open*. (2020) 3(1):e1918911. doi: 10.1001/jamanetworkopen.2019.18911
2. Verma R, Krishan S, Haendlmayer K, Mohsen A. Functional outcome of computer-assisted spinal pedicle screw placement: a systematic review and meta-analysis of 23 studies including 5,992 pedicle screws. *Eur Spine J*. (2010) 19(3):370–5. doi: 10.1007/s00586-009-1258-4
3. Bai JY, Zhang W, An JL, Sun YP, Ding WY, Shen Y. True anteroposterior view pedicle screw insertion technique. *Ther Clin Risk Manag*. (2016) 12:1039–47. doi: 10.2147/TCRM.S99362
4. Perdomo-Pantoja A, Ishida W, Zygourakis C, Holmes C, Iyer RR, Cottrill E, et al. Accuracy of current techniques for placement of pedicle screws in the Spine: a comprehensive systematic review and meta-analysis of 51,161 screws. *World Neurosurg*. (2019) 126:664–78.e3. doi: 10.1016/j.wneu.2019.02.217
5. Zhang Q, Xu YF, Tian W, Le XF, Liu B, Liu YJ, et al. Comparison of superior-level facet joint violations between robot-assisted percutaneous pedicle screw placement and conventional open fluoroscopic-guided pedicle screw placement. *Orthop Surg*. (2019) 11(5):850–6. doi: 10.1111/os.12534
6. Fan Y, Du JP, Liu JJ, Zhang JN, Qiao HH, Liu SC, et al. Accuracy of pedicle screw placement comparing robot-assisted technology and the free-hand with fluoroscopy-guided method in spine surgery: an updated meta-analysis. *Medicine (Baltimore)*. (2018) 97(22):e10970. doi: 10.1097/MD.0000000000010970
7. Venier A, Croci D, Robert T, Distefano D, Presilla S, Scarone P. Use of intraoperative computed tomography improves outcome of minimally invasive transforaminal lumbar interbody fusion: a single-center retrospective cohort study. *World Neurosurg*. (2021) 148:e572–80. doi: 10.1016/j.wneu.2021.01.041
8. Bederman SS, Lopez G, Ji T, Hoang BH. Robotic guidance for en bloc sacrectomy: a case report. *Spine (Phila Pa 1976)*. (2014) 39(23):E1398–401. doi: 10.1097/BRS.0000000000000575
9. Li Y, Wang MY. Robotic-assisted endoscopic laminotomy: 2-dimensional operative video. *Oper Neurosurg (Hagerstown)*. (2021) 20(5):E361. doi: 10.1093/ons/opaa441
10. Liounakos JI, Wang MY. Lumbar 3-lumbar 5 robotic-assisted endoscopic transforaminal lumbar interbody fusion: 2-dimensional operative video. *Oper Neurosurg (Hagerstown)*. (2020) 19(1):E73–4. doi: 10.1093/ons/opz385
11. Wang TY, Mehta VA, Gabr M, Sankey EW, Bwensa A, Rory Goodwin C, et al. Percutaneous lumbar interbody fusion with an expandable titanium cage through Kambin's triangle: a case series with initial clinical and radiographic results. *Int J Spine Surg*. (2021) 15(6):1121–9. doi: 10.14444/8144
12. Wang MY, Grossman J. Endoscopic minimally invasive transforaminal interbody fusion without general anesthesia: initial clinical experience with 1-year follow-up. *Neurosurg Focus*. (2016) 40(2):E13. doi: 10.3171/2015.11.FOCUS15435
13. Fanous AA, Tumialán LM, Wang MY. Kambin's triangle: definition and new classification schema. *J Neurosurg Spine*. (2019) 32(3):1–9. doi: 10.3171/2019.8.SPINE181475
14. Hoshide R, Feldman E, Taylor W. Cadaveric analysis of the Kambin's triangle. *Cureus*. (2016) 8(2):e475. doi: 10.7759/cureus.475
15. Hardenbrook M, Lombardo S, Wilson MC, Telfeian AE. The anatomic rationale for transforaminal endoscopic interbody fusion: a cadaveric analysis. *Neurosurg Focus*. (2016) 40(2):E12. doi: 10.3171/2015.10.FOCUS15389
16. Dalton T, Sykes D, Wang TY, Donnelly D, Than KD, Karikari IO, et al. Robotic-assisted trajectory into Kambin's triangle during percutaneous transforaminal lumbar interbody fusion-initial case series investigating safety and efficacy. *Oper Neurosurg (Hagerstown)*. (2021) 21(6):400–8. doi: 10.1093/ons/opab325
17. Möller H, Hedlund R. Instrumented and noninstrumented posterolateral fusion in adult spondylolisthesis–a prospective randomized study: part 2. *Spine (Phila Pa 1976)*. (2000) 25(13):1716–21. doi: 10.1097/00007632-200007010-00017
18. Gruskay JA, Fu M, Bohl DD, Webb ML, Grauer JN. Factors affecting length of stay after elective posterior lumbar spine surgery: a multivariate analysis. *Spine J*. (2015) 15(6):1188–95. doi: 10.1016/j.spinee.2013.10.022
19. Skovrlj B, Belton P, Zarzour H, Qureshi SA. Perioperative outcomes in minimally invasive lumbar spine surgery: a systematic review. *World J Orthop*. (2015) 6(11):996–1005. doi: 10.5312/wjo.v6.i11.996
20. Feiz-Erfan I, Fox BD, Nader R, Suki D, Chakrabarti I, Mendel E, et al. Surgical treatment of sacral metastases: indications and results. *J Neurosurg Spine*. (2012) 17(4):285–91. doi: 10.3171/2012.7.SPINE09351
21. Sutterlin 3rd CE, Field A, Ferrara LA, Freeman AL, Phan K. Range of motion, sacral screw and rod strain in long posterior spinal constructs: a biomechanical comparison between S2 alar iliac screws with traditional fixation strategies. *J Spine Surg*. (2016) 2(4):266–76. doi: 10.21037/jss.2016.11.01
22. Park C, Crutcher C, Mehta VA, Wang TY, Than KD, Karikari IO, et al. Robotic-assisted percutaneous iliac screw fixation for destructive lumbosacral metastatic lesions: an early single-institution experience. *Acta Neurochir (Wien)*. (2021) 163(11):2983–90. doi: 10.1007/s00701-021-04894-0
23. von Glinski A, Yilmaz E, Ishak B, Hayman E, Ramey W, Jack A, et al. The modified iliac screw: an anatomic comparison and technical guide. *World Neurosurg*. (2020) 136:e608–e13. doi: 10.1016/j.wneu.2020.01.091
24. Quraishi NA, Giannoulis KE, Edwards KL, Boszczyk BM. Management of metastatic sacral tumours. *Eur Spine J*. (2012) 21(10):1984–93. doi: 10.1007/s00586-012-2394-9
25. Stark JGF, Abner; Fuentes J, Tania I, Idemmili C. The history of sacroiliac joint arthrodesis: a critical review and introduction of a new technique. *Current Orthopaedic Practice*. (2011) 22(6):545–57. doi: 10.1097/BCO.0b013e31823563d3
26. Waisbrod H, Krainick JU, Gerbershagen HU. Sacroiliac joint arthrodesis for chronic lower back pain. *Arch Orthop Trauma Surg*. (1987) 106(4):238–40. doi: 10.1007/BF00450461
27. Lippitt A. Recurrent subluxation of the sacroiliac joint: diagnosis and treatment. *Bull Hosp Jt Dis*. (1995) 54(2):94–102. PMID: 8770450
28. Giannikas KA, Khan AM, Karski MT, Maxwell HA. Sacroiliac joint fusion for chronic pain: a simple technique avoiding the use of metalwork. *Eur Spine J*. (2004) 13(3):253–6. doi: 10.1007/s00586-003-0620-1
29. Dengler JD, Kools D, Pflugmacher R, Gasbarrini A, Prestamburgo D, Gaetani P, et al. 1-year results of a randomized controlled trial of conservative management vs. minimally invasive surgical treatment for sacroiliac joint pain. *Pain Physician*. (2017) 20(6):537–50. doi: 10.36076/ppj.20.5.537
30. Polly DW, Swofford J, Whang PG, Frank CJ, Glaser JA, Limoni RP, et al. Two-year outcomes from a randomized controlled trial of minimally invasive sacroiliac joint fusion vs. non-surgical management for sacroiliac joint dysfunction. *Int J Spine Surg*. (2016) 10:28. doi: 10.14444/3028
31. Smith AG, Capobianco R, Cher D, Rudolf L, Sachs D, Gundanna M, et al. Open versus minimally invasive sacroiliac joint fusion: a multi-center comparison of perioperative measures and clinical outcomes. *Ann Surg Innov Res*. (2013) 7(1):14. doi: 10.1186/1750-1164-7-14
32. Whang PG, Darr E, Meyer SC, Kovalsky D, Frank C, Lockstadt H, et al. Long-term prospective clinical and radiographic outcomes after minimally invasive lateral transiliac sacroiliac joint fusion using triangular titanium implants. *Med Devices (Auckl)*. (2019) 12:411–22. doi: 10.2147/MDER.S219862
33. Rashbaum RF, Ohnmeiss DD, Lindley EM, Kitchel SH, Patel VV. Sacroiliac joint pain and its treatment. *Clin Spine Surg*. (2016) 29(2):42–8. doi: 10.1097/BSD.0000000000000359
34. Soriano-Baron HE. Sacro-Iliac Joint Fusion with Two Different Minimally Invasive Techniques: Posterior vs. Trans-Articular, Biomechanical Analysis. 31st Annual Meeting of the Section on Disorders of the Spine and Peripheral Nerves—Spine Summit. 2015.
35. Piche JD, Muscatelli SR, Waheed MA, Patel RD, Aleem IS. Robotic navigation system utilization for percutaneous sacroiliac screw placement: surgical setup and technique. *J Spine Surg*. (2021) 7(2):197–203. doi: 10.21037/jss-20-681
36. Wang TY, Bergin SM, Murphy KR, Mehta V, Sankey EW, Abd-El-Barr MM, et al. 313 sacroiliac joint fusion using robotic navigation: technical note and case series. *Neurosurgery*. (2022) 68(Supplement_1):69–70. doi: 10.1227/NEU.0000000000001880_313
37. Wang TY, Mehta VA, Sankey EW, Than KD, Goodwin CR, Karikari IO, et al. Awake percutaneous transforaminal lumbar interbody fusion with expandable cage and robotic-assisted navigation and instrumentation: case

report and review of literature. *Interdisciplinary Neurosurgery*. (2020) 20:100685. doi: 10.1016/j.inat.2020.100685
38. George EI, Brand TC, LaPorta A, Marescaux J, Satava RM. Origins of robotic surgery: from skepticism to standard of care. *Jsls*. (2018) 22(4). doi: 10.4293/JSLS.2018.00039
39. Tewari A, Srivasatava A, Menon M. A prospective comparison of radical retropubic and robot-assisted prostatectomy: experience in one institution. *BJU Int*. (2003) 92(3):205–10. doi: 10.1046/j.1464-410X.2003.04311.x
40. Satin AM, Albano J, Kisinde S, Lieberman IH. Minimally invasive robotic lumbar facet decortication. *Clin Spine Surg*. (2021). doi: 10.1097/BSD.0000000000001248
41. Staub BN, Sadrameli SS. The use of robotics in minimally invasive spine surgery. *J Spine Surg*. (2019) 5(Suppl 1):S31–S40. doi: 10.21037/jss.2019.04.16
42. Nanda A, Manghwani J, Kluger PJ. Sacropelvic fixation techniques - Current update. *J Clin Orthop Trauma*. (2020) 11(5):853–62. doi: 10.1016/j.jcot.2020.07.022
43. Bederman SS, Hahn P, Colin V, Kiester PD, Bhatia NN. Robotic guidance for S2-alar-iliac screws in spinal deformity correction. *Clin Spine Surg*. (2017) 30(1):E49–E53. doi: 10.1097/BSD.0b013e3182a3572b
44. Hu X, Lieberman I. Robotic-guided sacro-pelvic fixation using S2 alar-iliac screws: feasibility and accuracy. *European Spine Journal*. (2016) 26(3):720–5. doi: 10.1007/s00586-016-4639-5
45. Lee NJ, Khan A, Lombardi JM, Boddapati V, Park PJ, Mathew J, et al. The accuracy of robot-assisted S2 alar-iliac screw placement at two different healthcare centers. *J Spine Surg*. (2021) 7(3):326–34. doi: 10.21037/jss-21-14
46. Fiani B, Quadri SA, Farooqui M, Cathel A, Berman B, Noel J, et al. Impact of robot-assisted spine surgery on health care quality and neurosurgical economics: a systemic review. *Neurosurg Rev*. (2020) 43(1):17–25. doi: 10.1007/s10143-018-0971-z
47. Sørlie A, Gulati S, Giannadakis C, Carlsen SM, Salvesen Ø, Nygaard ØP, et al. Open discectomy vs microdiscectomy for lumbar disc herniation - a protocol for a pragmatic comparative effectiveness study. *F1000Res*. (2016) 5:2170.doi: 10.12688/f1000research.9015.1
48. Farshad M, Fürnstahl P, Spirig JM. First in man in-situ augmented reality pedicle screw navigation. *N Am Spine Soc J*. (2021) 6:100065. doi: 10.1016/j.xnsj.2021.100065
49. Elmi-Terander A, Burström G, Nachabe R, Skulason H, Pedersen K, Fagerlund M, et al. Pedicle screw placement using augmented reality surgical navigation with intraoperative 3D imaging: a first in-human prospective cohort study. *Spine (Phila Pa 1976)*. (2019) 44(7):517–25. doi: 10.1097/BRS.0000000000002876
50. Mehbodniya AH, Moghavvemi M, Narayanan V, Waran V. Frequency and causes of line of sight issues during neurosurgical procedures using optical image-guided systems. *World Neurosurg*. (2019) 122:e449–54. doi: 10.1016/j.wneu.2018.10.069
51. Rahmathulla G, Nottmeier EW, Pirris SM, Deen HG, Pichelmann MA. Intraoperative image-guided spinal navigation: technical pitfalls and their avoidance. *Neurosurg Focus*. (2014) 36(3):E3. doi: 10.3171/2014.1.FOCUS13516

Conflict of Interest: Khoi Than is a consultant for Bioventus, DePuy Synthes, and Integrity Implants. Than is also an honoraria of Globus and LifeNet Health. Timothy Wang has received grant funding from AlphaTec. Rory Goodwin has received grants from the Robert Wood Johnson Harold Amos Medical Faculty Development Program, the Federal Food and Drug Administration, and the NIH/NINDS K12 NRCDP Physician Scientist Award. Goodwin is also a consultant for Johnson & Johnson and Medtronic. Phillip Horne has consultancy with Globus for navigation applications.

frontiers | Frontiers in Surgery

ORIGINAL RESEARCH
published: 28 June 2022
doi: 10.3389/fsurg.2022.889402

Check for updates

How to Precisely Open the Internal Auditory Canal for Resection of Vestibular Schwannoma *via* the Retrosigmoid Approach

*Chenguang Jia[1,2†], Chengshi Xu[1,2†], Mengyang Wang[1,2†] and Jincao Chen[1,2]**

[1]Department of neurosurgery, Zhongnan Hospital, Wuhan University, Wuhan, China, [2]Brain Research Center, Zhongnan Hospital, Wuhan University, Wuhan, China

Objective: The aim of this study was to investigate how to precisely expose the intrameatal portion of vestibular schwannomas (VSs) without damaging the labyrinth.

Methods: This was a retrospective study of patients who had undergone retrosigmoid resection of a VS in our institution from April 2018 to December 2021. The patients were divided into microsurgery (MS) and navigation endoscopic-assisted (combined surgery, CS) groups and the effects of image guidance and endoscopy evaluated. The tumors in the CS group were then divided into medial and lateral types by fusion imaging and the differences between the two types analyzed.

Results: Data of 84 patients were analyzed. Residual tumor was detected by postoperative MRI at the fundus of the internal auditory canal in 5 of the 31 patients in the MS group and 1 of the 53 in the CS group. The labyrinth was damaged in four patients in the MS group but was not damaged in any of the CS group patients. The CS group included 29 lateral type and 24 medial type schwannomas. Endoscopic-assisted resection of residual tumor in the IAC was performed significantly more often on medial than on lateral tumors.

Conclusion: Navigation and endoscopy are useful in assisting the exposure of the intrameatal portion of VSs. Preoperative MRI/CT fusion imaging is helpful in preoperative evaluation and surgical planning in patients undergoing VS surgery. Tumors of the medial type require endoscopic assistance for resection.

Keywords: fusion image, endoscope, vestibular schwannoma, retrosigmoid approach, navigation

OPEN ACCESS

Edited by:
Philipp Taussky,
The University of Utah, United States

Reviewed by:
Davide Croci,
University of South Florida, United States
Brandon Sherrod,
The University of Utah, United States

***Correspondence:**
Jincao Chen
chenjincao2012@163.com

†The authors have contributed equally to this work

Specialty section:
This article was submitted to Neurosurgery, a section of the journal Frontiers in Surgery

Received: *04 March 2022*
Accepted: *09 June 2022*
Published: *28 June 2022*

Citation:
Jia C, Xu C, Wang M and Chen J (2022) How to Precisely Open the Internal Auditory Canal for Resection of Vestibular Schwannoma via *the Retrosigmoid Approach. Front. Surg. 9:889402. doi: 10.3389/fsurg.2022.889402*

INTRODUCTION

Vestibular schwannoma (VS) resection *via* the retrosigmoid approach (RS) remains challenging. Although this approach provides excellent visualization, access to the fundus of the internal auditory canal (IAC) is limited (1–5). Removal of the posterior canal wall is essential to expose the portion of the tumor residing in the IAC (2, 3, 6–11). In some cases, microscopic exposure of the tumor is incomplete, even with excessive traction of the cerebellum or extensive drilling of the posterior wall of IAC (12). Use of an endoscope may solve this problem (13–16). However, endoscopic tumor resection is a skill set that is not necessarily learned quickly, nor are microscopic skills easily transferable to the technique (17). Furthermore, numerous reports have indicated that few tumors have a remnant at the fundus of the IAC that cannot be seen with the operative microscope (15, 18–22). In the past few years, we have performed image-guided microsurgery with endoscopic assistance for patients with vestibular schwannoma. Magnetic resonance imaging (MRI) and computed tomography (CT) fusion images are used for intraoperative navigation, as either modality alone provides inadequate clinical information. Together, they are complementary, and their data can be easily and accurately integrated with the navigation system software (23, 24). The aim of this study was to investigate how to precisely expose the intrameatal portion of VSs without damaging the labyrinth.

METHODS

Patient Cohort

The cohort of this retrospective study comprised consecutive patients who had undergone RS resection of VS in our institution from April 2018 to December 2021. Patients with recurrent tumors, a history of radiation therapy, high jugular bulbar, and neurofibromatosis type 2 were excluded. Patients whose surgery was performed with the assistance of a microscope only were defined as the microsurgical group (MS group), whereas those whose surgeries were assisted by navigation and endoscopy were defined as the combined surgical group (CS group). Clinical data regarding patient age, sex, clinical presentation, neurological examination, neuroimaging, surgical findings, tumor size, and treatment outcomes were recorded and analyzed. The study was approved by the Medical Ethics Committee of Zhongnan Hospital of Wuhan University (2021037 K). Patients underwent routine follow-up every 3 months for 1 year and then yearly thereafter.

Case Classification

Schwannomas in the CS group were further classified into medial and lateral types as follows: Digital imaging and communications in medicine (DICOM) MRI and CT files were imported into the navigation system station (Medtronic Planning Station S7, Louisville, KY, USA). StealthMerge® system software (Medtronic, Dublin, Ireland) was used to automatically fuse the images. After adjustment, the outline of the tumor and posterior wall of the IAC could be clearly displayed. The line between the outermost edge of the tumor and the medial side of the sigmoid sinus was defined as the lateral safe line (LSL). Cases were classified as medial or lateral according to the relationship between the LSL and the labyrinth. Those in which the labyrinth was located lateral to the LSL were classified as lateral. Cases in which the LSL crossed the semicircular canal or crus commune were classified as medial (**Figure 1**).

Surgical Procedure

Patients underwent CT using a mobile scanner (NL3000 CereTom®; Neurologica, Danvers, MA, USA) in the operating room with 8 to 10 markers affixed to the head. DICOM files were imported into the navigation system station. After automatic fusion of the CT and MRI sequences and their verification, the images were used for intraoperative navigation. All patients were placed in a semi-seated position for surgery. After the sigmoid and transverse sinuses were localized using the navigation system, a skin incision was designed. A 4 cm craniotomy was performed posterior to the sigmoid sinus and inferior to the transverse sinus. The dura was incised and the cerebellum retracted. After partial tumor debulking, the internal acoustic pore was exposed and the dura over the posterior lip of the IAC was removed. The extent of IAC removal was determined using intraoperative image guidance. The navigation optical pointer was used for positioning, and a projection of 5–10 mm was preset to represent the predicted resection line. The lead surgeon focused on the operation under a microscope, while another neurosurgeon acted as an assistant and made judgments based on the navigation and live video monitors. The upper, lower, and outer boundaries of drilling were identified. The outermost border of the tumor and the locations of the labyrinth and petrous cells were also considered. Image guidance was used repeatedly during drilling.

The posterior IAC wall was opened using a high-speed diamond drill under continuous saline irrigation. Drilling was considered adequate if the outermost tumor margin could be exposed by gently pulling the tumor. Regardless, drilling of the posterior wall of the IAC ceased when intraoperative image guidance indicated that only 2–3 mm of bone remained over the labyrinthine structures. Tumor dissection was performed along the plane between the tumor and capsule; the capsule close to the nerves was retained. After microsurgical tumor removal was accomplished, a 0-degree/30-degree endoscope was fixed with a mechanical arm and introduced into the surgical field to visualize areas of the surgical site that the microscope could not. If endoscopic examination revealed any remaining tumor, it was carefully dissected and removed. After complete resection was confirmed and hemostasis achieved, the IAC was packed with pieces of fat under endoscopic visualization. Patients were transferred to the neurological intensive care unit after surgery was completed.

Definitions and Outcomes

The length of the IAC was measured on preoperative CT images and postoperative labyrinth integrity assessed by CT. The presence of residual tumor within the IAC was determined by endoscopic examination during surgery and MRI immediately after surgery. Additionally, postoperative facial nerve function was classified according to House–Brackmann (HB) grade, HB grades 1 or 2 being considered good whereas HB grade 3 and above were considered to denote facial nerve dysfunction. Hearing function was considered useful in patients with pure

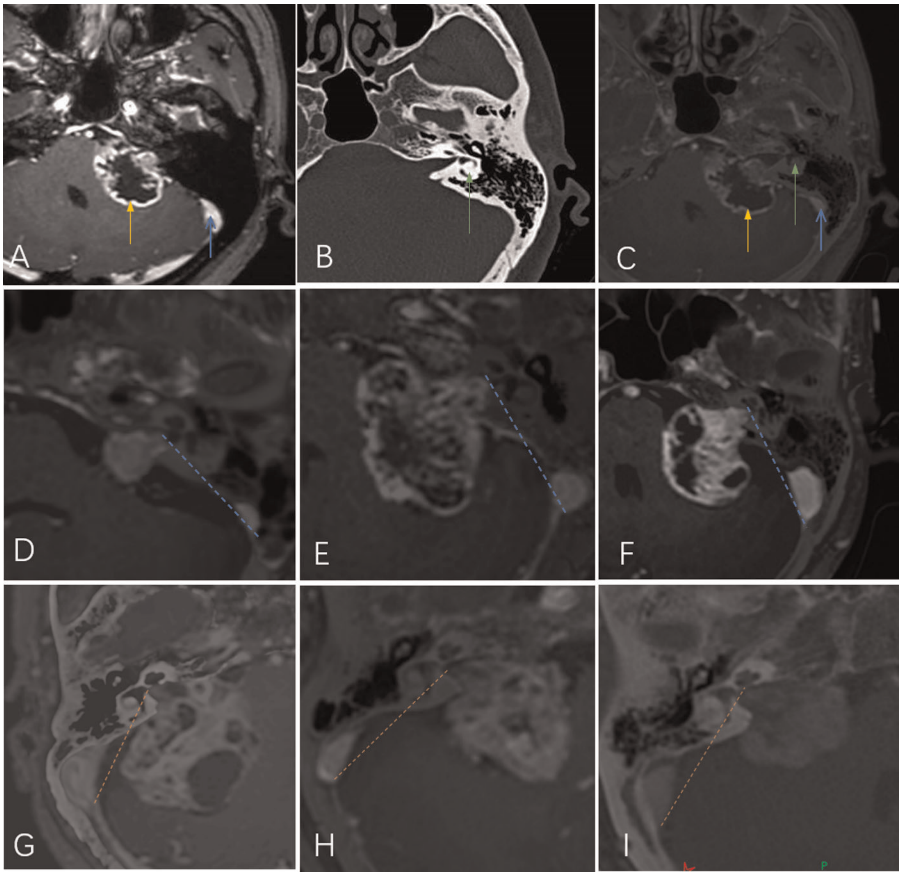

FIGURE 1 | (**A**) Magnetic resonance imaging shows the tumor (yellow arrow) and sigmoid sinus (blue arrow). (**B**) Computed tomography shows the labyrinth (green arrow). (**C**) The fused image shows the positions of all three simultaneously. The line between the outermost edge of the tumor and the medial side of the sigmoid sinus was defined as the lateral safe line (LSL; yellow- or blue-dotted line). Tumors were classified according to the relationship between the LSL and the labyrinth: lateral type (**D,E,F**) and medial type (**G,H,I**).

tone average better than 50 dB and speech discrimination score better than 50% according to Gardner-Robertson grading system. Postoperative CSF leakage, delayed hemorrhage and other complications were recorded.

Statistical Analysis

Continuous variables are presented as means with standard deviation. Categorical variables are presented as frequencies with percentage. Comparisons were performed using the chi-square test, Fisher's exact test, or Student's t-test as appropriate. Statistical analyses were performed using SPSS software version 23.0 (IBM Corp., Armonk, NY, USA). $P <$ 0.05 was considered significant.

RESULTS

Patient and vs Characteristics

Data of 84 patients were analyzed. Microsurgical removal with navigation and endoscopic assistance was achieved in 53 patients (CS group), and microsurgical removal without such assistance in 31 (MS group). Patient characteristics according to group are shown in **Table 1**. There were 29 lateral tumors and 24 medial ones in the CS group. Patient characteristics according to type are shown in **Table 2**.

Surgical Results

In the CS group, the fundus of the IAC was examined endoscopically after microsurgery, revealing and enabling removal of residual tumor tissue in five patients. Residual tumor was detected by postoperative MRI in one patient. In the MS group, postoperative MRI showed residual tumor at the fundus of the IAC in five patients. The rate of residual tumor at the fundus of the IAC was lower in the CS than in the MS group ($P = 0.02$). Postoperative facial nerve status and preservation of useful hearing are shown in **Table 1**; the differences between the two groups are not statistically significant. In the CS group, the incidence of endoscopic-assisted resection of residual tumor at the IAC was significantly higher for medial than for lateral tumors (20.8% vs. 0%, $P = 0.02$) (**Table 2**).

TABLE 1 | Patient characteristics of two groups.

	MS group	CS group	*P*-value
No.	31	53	
Age (years)	51.7 ± 11.5	53.1 ± 10.5	0.58
Sex, M:F	11:20	20:33	>0.99
Side, R:L	11:20	32:21	0.04
Tumor size (mm)	32.6 ± 9.1	28.9 ± 8.6	0.07
Length of IAC (mm)	9.0 ± 1.5	9.3 ± 1.6	0.42
Tumor residue (postoperative MR)	5	1	0.02
Normal rate of FN	64.5%	81.1%	0.12
Normal rate of FN	80.6%	90.6%	0.31
Useful hearing (post-/pre-operative)	5/12	8/16	>0.99
Labyrinth injury	4	0	0.02
Opened the air cells	3	7	0.74
CSF leak	3	2	0.35
ICH	2	1	0.55

M, male; F, female; R, right; L, left; IAC, internal auditory canal; CSF, cerebrospinal fluid. ICH, intracranial hemorrhage; FN, facial nerve.

TABLE 2 | Patient characteristics between the two types.

	Medial type	Lateral type	*P*-value
No.	24	29	
Age(years)	53.3 ± 10.3	52.9 ± 10.9	0.89
Sex, M:F	12:12	8:21	0.15
Side, R:L	17:7	15:14	0.17
Tumor size(mm)	31.5 ± 9.0	27.0 ± 7.9	0.06
Length of IAC (mm)	8.9 ± 1.6	9.6 ± 1.6	0.10
Tumor residue (endoscope)	5	0	0.02
Tumor residue (postoperative MR)	1	0	0.45

M, male; F, female; R, right; L, left; IAC, internal auditory canal.

Complications

The labyrinth was not damaged in any patient in the CS group, whereas labyrinthine injury occurred in four patients in the MS group, three of whom had no useful hearing preoperatively. Other complications are shown in **Table 1**.

Representative Case

A 56-year-old man with hearing loss and tinnitus was found to have a tumor in the right cerebellopontine angle by MRI. The tumor was classified as of medial type and excised with navigation and endoscopic assistance. Postoperative MR images showed that the tumor within the IAC had been totally resected. Postoperative CT showed that the posterior wall of IAC had been maximally drilled and the labyrinth remained intact (**Figure 2**).

DISCUSSION

The goal of VS surgery is complete resection while preserving neurological function, which is challenging (1, 4, 5, 25, 26). For large VSs, the RS approach is preferred when hearing preservation is required. Complete resection when performing the RS approach requires opening the IAC. It is essential to maintain the integrity of the labyrinth while drilling the posterior wall of the canal during this opening if hearing is to be preserved. However, because the local anatomy of the labyrinth, IAC, and tumor can vary widely, a gold standard for the angle or extent of drilling that will preserve hearing has not been established (3, 6, 10, 27–29). Therefore, it is necessary to determine the local anatomy before surgery.

Ciric et al. recommend removing no more than 8 to 9 mm of the posterior canal wall unless the posterior semicircular canal and/or endolymphatic duct are opened (30). Yokoyama et al.

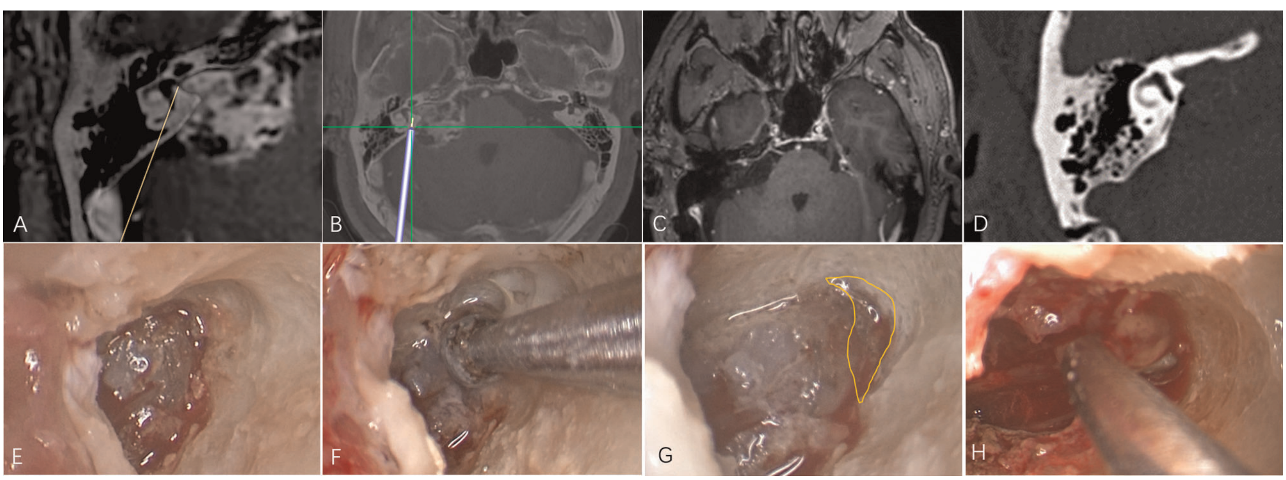

FIGURE 2 | An illustrative case. (**A**) The tumor was classified as of medial type on the basis of fusion images. (**B**) Intraoperative navigation. (**C**) Postoperative MR showing that the tumor within the IAC has been completely resected. (**D**) Postoperative CT showing maximal removal of the posterior wall of the canal. (**E**) Endoscopic image after drilling under microscope guidance. (**F**) Endoscopic drilling of the deep bone; (**G**) The area within the yellow line shows the extent of endoscopic drilling. (**H**) Endoscopic resection of residual tumor at the fundus of the IAC.

proposed the concept of the sigmoid–fundus line, an imaginary line extending from the medial side of the sigmoid sinus to the fundus of the IAC on CT (8). Samii et al. and Gharabaghi et al. concluded that if the posterior semicircular canal and crus commune are located lateral to this line, there is no risk of intraoperative injury to these structures; however, if they are located medial to the line, they are at risk (3, 9). CT does not provide a clear outline of the tumor. The purpose of posterior IAC wall drilling is to expose the lateral edge of the tumor, not the fundus of the IAC. Mohr et al. reported that approximately 60% of VSs do not completely fill the IAC (31). MRI can be used to determine the extent of tumor in the IAC, which seems to guide IAC drilling. However, MRI does not show the position of the semicircular canals because this imaging modality does not demonstrate bony structures very well. We discovered this with our use of CT/MRI fusion images for surgical navigation, which showed tumor, sigmoid sinus, posterior IAC wall, and internal IAC structures simultaneously. We were able to improve upon the sigmoid–fundus line using the fused images to define an imaginary line between the outermost edge of the tumor and the medial side of the sigmoid sinus as the LSL. The risk of Labyrinth injury can be assessed according to the relationship between the LSL and the posterior semicircular canal and crus commune before drilling.

It should be noted that the LSL is neither a surgical line of sight nor an IAC resection line. By retracting the cerebellum, the IAC can be drilled at a more medial angle than the LSL (8). However, it is not practical to precisely simulate the line of sight, because the amount of space gained by cerebellar retraction cannot be accurately assessed before surgery. In addition, the degree of traction required varies according to the patient and surgeons differ in their comfort level with applying traction. **Figure 3** shows illustrative preoperative navigation imaging, intraoperative photography, and postoperative imaging in a patient with a VS classified as lateral. As shown in panel C, the blue line represents the LSL and the blue area indicates the maximum area estimated to be removed before surgery. In general, IAC drilling starts at the posterior edge of

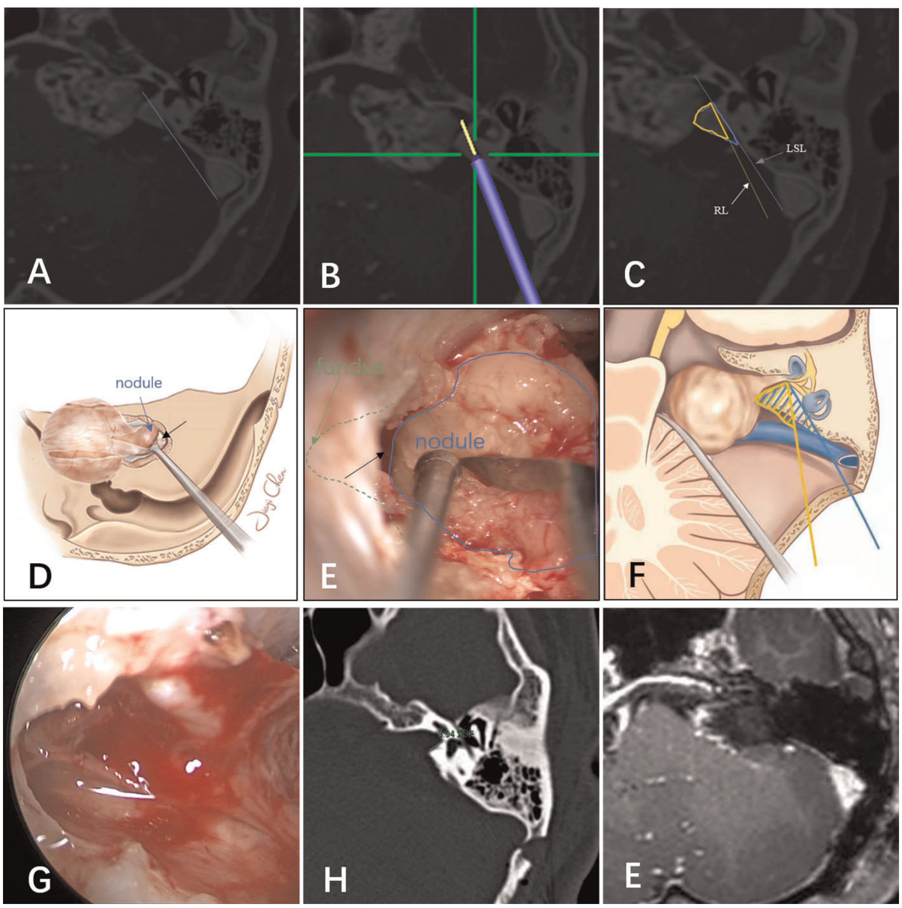

FIGURE 3 | (**A**) The tumor was classified as lateral based on magnetic resonance imaging and computed tomography fusion images. (**B**) Navigation predicted the resection line. The yellow line extending from the tip of the navigation pointer is the predicted resection line. (**C**,**F**) Illustration of the lateral safe line (blue line) and resection line (yellow line). Illustrative drawing (**D**) and microscopic view (**E**): the intrameatal portion of the tumor is displayed as a nodule (blue). The interface (black arrow) between the tumor (blue) and fundus (green) was visible by gently pulling the tumor medially. This means that the opening of the IAC was adequate. (**G**) Endoscopic examination showed no residual tumor, and the capsule near the nerves was retained. Postoperative CT(**H**) and MR(**I**) showed no tumor residue and the labyrinth was intact.

the internal acoustic pore and proceeds laterally until the outermost part of the tumor is exposed. Owing to cerebellar retraction, the actual range of drilling during surgery is less than the blue area and comprises the area in the yellow triangle. Provided that the labyrinth is not within this triangle, it should not be damaged. Therefore, in this and other tumors classified as lateral, the tumor within the IAC can be exposed safely. Illustrative drawing (**Figure 3D**) and microscopic view (**Figure 3E**) showed that the intrameatal portion of the tumor is displayed as a nodule (blue). The interface (black arrow) between the tumor (blue) and fundus (green) was visible by gently pulling the tumor medially. This means that the opening of the IAC was adequate. In these cases, no residual tumor was found during intraoperative endoscopic examination.

In medial cases, tumor exposure is likely inadequate because drilling must be stopped near the labyrinth. Marchioni et al. argue that exposure of the IAC fundus is incomplete when only the microscope is used during the RS approach and therefore a tumor located in the fundus requires blind dissection (15). Endoscopy is useful in the RS approach as an adjunct to microscopic resection and can even be implemented alone in fully endoscopic procedures (16). Shahinian et al. reported full endoscopic resection in a series of 527 patients with unilateral VS (13). You et al. recommended the use of endoscopic-assisted microsurgery (14). According to previous studies, the incidence of residual tumor detected by endoscopic examination after microscopic resection ranges between 6.5% and 48.1% (**Table 3**). In our study, the overall incidence of residual tumor in the blind corner was 9.4% and all instances were in cases classified as medial. No lateral cases had residual tumor detected in the endoscopic examination (20.8% vs. 0%; $P = 0.015$). This means that the intrameatal portion of VSs cannot be completely exposed and resected without damaging the labyrinth in one-fifth of medial cases. Therefore, we suggest that endoscopic-assisted resection should be performed for cases that are classified as medial on preoperative imaging (those in which the LSL crosses the semicircular canal or crus commune). CT/MRI fusion images assess not only the degree of tumor within the IAC, but also the position of the labyrinth relative to the tumor, which provides a more comprehensive and accurate assessment than either modality alone.

Pillai et al. concluded that approximately 70% to 80% of the posterior wall of the IAC can be drilled away without injuring the labyrinth and that such drilling can be maximized safely using image-guided surgical navigation (10). In the middle fossa approach to VSs, Miller et al. found surgical navigation to be reliable in identifying the midpoint of the IAC within 2.4 mm of accuracy (1). Furthermore, Li et al. reported localization of the facial nerve for surgical purposes using tractography and navigation (25). However, Samii et al. concluded in a preliminary clinical study that the value of navigation-assisted IAC opening is promising but limited at the present time (3, 9). Although surgical navigation has gained wide acceptance for many intracranial procedures, it is rarely used for localization of the IAC during VS surgery. There are three possible explanations. First, surgeons may have concern about navigation system accuracy. However, with the use of invasive localization markers and point-merge registration techniques, navigation can achieve sub-millimeter mean registration error (10, 32). In an accuracy study of surgical navigation in the spine, Devito et al. found that 98.3% of pedicle screws inserted using robotic guidance were either completely within the pedicle or breached it by 2 mm or less (33). Second, many experienced surgeons may believe that navigation offers limited benefits. Computer-aided navigational tools are no substitute for a thorough knowledge of temporal bone anatomy (1, 9). In our experience, VS surgery requires considerable experience to perform well. Navigation may be an imperfect but trustworthy partner in the learning process (**Figure 4**). When using it, a "safety zone" of approximately 2 mm should be set. Third, use of navigation can interrupt the operation (9). All types of surgical navigation require linking a virtual picture with the surgical field of view. Although current virtual reality technology is advancing, it is currently insufficient (34). Our solution is to perform the procedure using two surgeons, one focusing on the surgical field of vision and the navigation pointer, and the other focusing on the navigation display and the real-time picture of the operation. In addition, the cerebellum has been retracted when the navigation pointer was located in the posterior wall of the IAC, and the resection line (RL, the lateral edge of the IAC resection area, yellow line in **Figures 3B,C**) could be predicted by the navigation system. According to the RL line, the risk of labyrinth during drilling could be assessed again. If labyrinth structures were located 2 mm lateral of the RL line, repeated image guidance was not required during drilling the IAC.

CSF leakage is a common complication of VS surgery (35). Although the incidence is low, it often requires operative treatment if CSF leakage persists. Yamakami et al. state that packing of the opened IAC with pieces of fat and muscle is mandatory to prevent CSF rhinorrhea in patients with air cells near the canal (36). In addition, Tamura et al. and Corrivetti et al. argue that use of an endoscope can assist visualization and covering of opened petrosal air cells (16, 37). Endoscopic evaluation of the petrous bone may reduce the incidence of CSF leakage (17). In our study, the incidence of postoperative CSF leakage was 3.7% (2/53) in the CS group compared with 9.7% (3/31) in the MS group. This difference was not statistically significant; however, the use of navigation and endoscopic assistance in opening the IAC may nevertheless help to minimize CSF leakage. The hearing preservation is an

TABLE 3 | Endoscope check the residual tumor.

Authors & Year	Approach	Endoscope (tip angle)	Cases	Endoscope Check Residual Tumor (%)
Wackym, 1999	RS	30°	68	11 (16.2%)
Göksu, 1999	RS-RL	0°,30°,70°	32	8 (25.0%)
Kumon, 2011	RS	30°,70°	27	13 (48.1%)
Chovanec, 2012	RS	0°,30°,70°	39	4 (10.2%)
Marchioni, 2019	RS	0°,45°,70°	18	4 (22.2%)
Bi, 2022	RS	0°,30°	61	4 (6.5%)

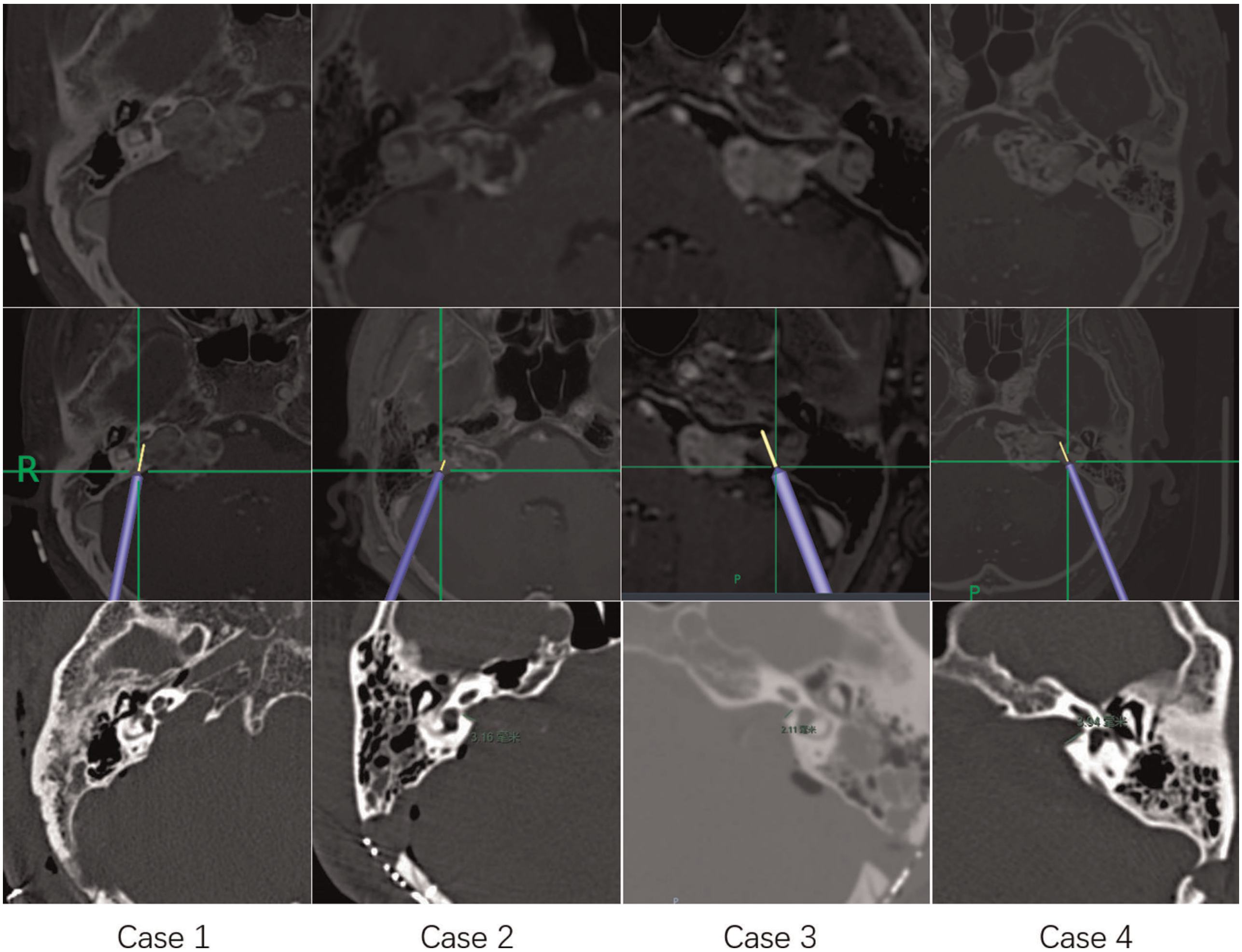

FIGURE 4 | Four illustrative cases of using navigation to locate the boundaries of drilling of the internal auditory canal.

important objective for the protection of labyrinth during surgery. However, the average diameter of the tumors in this study was close to 3 cm and most of them were Grade 3 or 4 according to the Koos classification. Only a few patients had useful hearing preoperatively, which greatly limited our analysis of hearing preservation.

CONCLUSION

Navigation and endoscopy are useful in assisting the exposure of the intrameatal portion of VSs. Preoperative MRI/CT fusion imaging is helpful in preoperative evaluation and surgical planning in patients undergoing VS surgery. Tumors of the medial type require endoscopic assistance for resection.

DATA AVAILABILITY STATEMENT

The raw data supporting the conclusions of this article will be made available by the authors, without undue reservation.

ETHICS STATEMENT

The study was approved by the Medical Ethics Committee of Zhongnan Hospital of Wuhan University (2021037K). Written informed consent for participation was not required for this study in accordance with the national legislation and the institutional requirements.

AUTHOR CONTRIBUTIONS

Conception and design: JC, CJ; Analysis and interpretation of data: CJ, MW; Technical/material support: JC, CX; Drafting the article. All authors contributed to the article and approved the submitted version.

ACKNOWLEDGMENTS

We thank Liwen Bianji (Edanz) (https://www.liwenbianji.cn) for editing the language of a draft of this manuscript.

REFERENCES

1. Miller RS, Hashisaki GT, Kesser BW. Image-guided localization of the internal auditory canal via the middle cranial fossa approach. *Otolaryngol Head Neck Surg*. (2006) 134(5):778–82. doi: 10.1016/j.otohns.2005.12.015
2. Samii M, Gerganov V, Samii A. Improved preservation of hearing and facial nerve function in vestibular schwannoma surgery via the retrosigmoid approach in a series of 200 patients. *J Neurosurg*. (2006) 105(4):527–35. doi: 10.3171/jns.2006.105.4.527
3. Gharabaghi A, Samii A, Koerbel A, Rosahl SK, Tatagiba M, Samii M. Preservation of function in vestibular schwannoma surgery. *Neurosurgery*. (2007) 60(2 Suppl 1):ONS124-7; discussion ONS7–8. doi: 10.1227/01.NEU.0000249245.10182.0D
4. Babu R, Sharma R, Bagley JH, Hatef J, Friedman AH, Adamson C. Vestibular schwannomas in the modern era: epidemiology, treatment trends, and disparities in management. *J Neurosurg*. (2013) 119(1):121–30. doi: 10.3171/2013.1.Jns121370
5. Goldbrunner R, Weller M, Regis J, Lund-Johansen M, Stavrinou P, Reuss D, et al. EANO Guideline on the diagnosis and treatment of vestibular schwannoma. *Neuro Oncol*. (2020) 22(1):31–45. doi: 10.1093/neuonc/noz153
6. Day JD, Kellogg JX, Fukushima T, Giannotta SL. Microsurgical anatomy of the inner surface of the petrous bone: neuroradiological and morphometric analysis as an adjunct to the retrosigmoid transmeatal approach. *Neurosurgery*. (1994) 34(6):1003–8. doi: 10.1227/00006123-199406000-00008
7. Cueva RA, Chole RA. Maximizing exposure of the internal auditory canal via the retrosigmoid approach: an anatomical, radiological, and surgical study. *Otol Neurotol*. (2018) 39(7):916–21. doi: 10.1097/mao.0000000000001866
8. Yokoyama T, Uemura K, Ryu H, Hinokuma K, Nishizawa S, Yamamoto S, et al. Surgical approach to the internal auditory meatus in acoustic neuroma surgery: significance of preoperative high-resolution computed tomography. *Neurosurgery*. (1996) 39(5):965–9; discussion 9–70. doi: 10.1097/00006123-199611000-00017
9. Samii A, Brinker T, Kaminsky J, Lanksch WR, Samii M. Navigation-guided opening of the internal auditory canal via the retrosigmoid route for acoustic neuroma surgery: cadaveric, radiological, and preliminary clinical study. *Neurosurgery*. (2000) 47(2):382–7; discussion 8. doi: 10.1097/00006123-200008000-00021
10. Pillai P, Sammet S, Ammirati M. Image-guided, endoscopic-assisted drilling and exposure of the whole length of the internal auditory canal and its fundus with preservation of the integrity of the labyrinth using a retrosigmoid approach: a laboratory investigation. *Neurosurgery*. (2009) 65(6 Suppl):53–9; discussion 9. doi: 10.1227/01.NEU.0000343521.88537.16
11. Wanibuchi M, Fukushima T, Friedman AH, Watanabe K, Akiyama Y, Mikami T, et al. Hearing preservation surgery for vestibular schwannomas via the retrosigmoid transmeatal approach: surgical tips. *Neurosurg Rev*. (2014) 37(3):431–44; discussion 44. doi: 10.1007/s10143-014-0543-9
12. Tatagiba M, Samii M, Matthies C, el Azm M, Schönmayr R. The significance for postoperative hearing of preserving the labyrinth in acoustic neurinoma surgery. *J Neurosurg*. (1992) 77(5):677–84. doi: 10.3171/jns.1992.77.5.0677
13. Shahinian HK, Ra Y. 527 Fully endoscopic resections of vestibular schwannomas. *Minim Invasive Neurosurg*. (2011) 54(2):61–7. doi: 10.1055/s-0031-1275335
14. You YP, Zhang JX, Lu AL, Liu N. Vestibular schwannoma surgical treatment. *CNS Neurosci Ther*. (2013) 19(5):289–93. doi: 10.1111/cns.12080
15. Marchioni D, Gazzini L, Boaria F, Pinna G, Masotto B, Rubini A. Is endoscopic inspection necessary to detect residual disease in acoustic neuroma surgery? *Eur Arch Otorhinolaryngol*. (2019) 276(8):2155–63. doi: 10.1007/s00405-019-05442-4
16. Corrivetti F, Cacciotti G, Scavo CG, Roperto R, Stati G, Sufianov A, et al. Flexible endoscopic assistance in the surgical management of vestibular schwannomas. *Neurosurg Rev*. (2021) 44(1):363–71. doi: 10.1007/s10143-019-01195-0
17. Van Gompel JJ, Agazzi S, Carlson ML, Adewumi DA, Hadjipanayis CG, Uhm JH, et al. Congress of neurological surgeons systematic review and evidence-based guidelines on emerging therapies for the treatment of patients with vestibular schwannomas. *Neurosurgery*. (2018) 82(2):E52–e4. doi: 10.1093/neuros/nyx516
18. Göksu N, Bayazit Y, Kemaloğlu Y. Endoscopy of the posterior fossa and dissection of acoustic neuroma. *J Neurosurg*. (1999) 91(5):776–80. doi: 10.3171/jns.1999.91.5.0776
19. Wackym PA, King WA, Poe DS, Meyer GA, Ojemann RG, Barker FG, et al. Adjunctive use of endoscopy during acoustic neuroma surgery. *Laryngoscope*. (1999) 109(8):1193–201. doi: 10.1097/00005537-199908000-00003
20. Kumon Y, Kohno S, Ohue S, Watanabe H, Inoue A, Iwata S, et al. Usefulness of endoscope-assisted microsurgery for removal of vestibular schwannomas. *J Neurol Surg B Skull Base*. (2012) 73(1):42–7. doi: 10.1055/s-0032-1304555
21. Chovanec M, Zvěřina E, Profant O, Skřivan J, Cakrt O, Lisý J, et al. Impact of video-endoscopy on the results of retrosigmoid-transmeatal microsurgery of vestibular schwannoma: prospective study. *Eur Arch Otorhinolaryngol*. (2013) 270(4):1277–84. doi: 10.1007/s00405-012-2112-6
22. Bi Y, Ni Y, Gao D, Zhu Q, Zhou Q, Tang J, et al. Endoscope-Assisted retrosigmoid approach for vestibular schwannomas with intracanalicular extensions: facial nerve outcomes. *Front Oncol*. (2021) 11:774462. doi: 10.3389/fonc.2021.774462
23. Nandish S, Prabhu G, Rajagopal KV. Multiresolution image registration for multimodal brain images and fusion for better neurosurgical planning. *Biomed J*. (2017) 40(6):329–38. doi: 10.1016/j.bj.2017.09.002
24. Kohyama S, Nishiura Y, Hara Y, Ogawa T, Ikumi A, Okano E, et al. A novel three-dimensional MRI-CT image fusion technique for precise preoperative evaluation and treatment of capitellar osteochondritis dissecans. *Eur Radiol*. (2021) 31(8):5721–33. doi: 10.1007/s00330-020-07680-1
25. Li H, Wang L, Hao S, Li D, Wu Z, Zhang L, et al. Identification of the facial nerve in relation to vestibular schwannoma using preoperative diffusion tensor tractography and intraoperative tractography-integrated neuronavigation system. *World Neurosurg*. (2017) 107:669–77. doi: 10.1016/j.wneu.2017.08.048
26. Killeen DE, Barnett SL, Mickey BE, Hunter JB, Isaacson B, Kutz Jr JW. The association of vestibular schwannoma volume with facial nerve outcomes after surgical resection. *Laryngoscope*. (2021) 131(4):E1328–34. doi: 10.1002/lary.29141
27. Thedinger BS, Whittaker CK, Luetje CM. Recurrent acoustic tumor after a suboccipital removal. *Neurosurgery*. (1991) 29(5):681–7. doi: 10.1097/00006123-199111000-00007
28. Blevins NH, Jackler RK. Exposure of the lateral extremity of the internal auditory canal through the retrosigmoid approach: a radioanatomic study. *Otolaryngol Head Neck Surg*. (1994) 111(1):81–90. doi: 10.1177/019459989411100116
29. Scerrati A, Lee JS, Zhang J, Ammirati M. Microsurgical anatomy of the internal acoustic meatus as seen using the retrosigmoid approach. *Otol Neurotol*. (2016) 37(5):568–73. doi: 10.1097/mao.0000000000001013
30. Ciric I, Zhao JC, Rosenblatt S, Wiet R, O'Shaughnessy B. Suboccipital retrosigmoid approach for removal of vestibular schwannomas: facial nerve function and hearing preservation. *Neurosurgery*. (2005) 56(3):560–70; discussion -70. doi: 10.1227/01.neu.0000154059.34990.b8
31. Mohr G, Sade B, Dufour JJ, Rappaport JM. Preservation of hearing in patients undergoing microsurgery for vestibular schwannoma: degree of meatal filling. *J Neurosurg*. (2005) 102(1):1–5. doi: 10.3171/jns.2005.102.1.0001
32. Pillai P, Sammet S, Ammirati M. Application accuracy of computed tomography-based, image-guided navigation of temporal bone. *Neurosurgery*. (2008) 63(4 Suppl 2):326–32; discussion 32–3. doi: 10.1227/01.NEU.0000316429.19314.67
33. Devito DP, Kaplan L, Dietl R, Pfeiffer M, Horne D, Silberstein B, et al. Clinical acceptance and accuracy assessment of spinal implants guided with SpineAssist surgical robot: retrospective study. *Spine (Phila Pa 1976)*. (2010) 35(24):2109–15. doi: 10.1097/BRS.0b013e3181d323ab
34. Barber SR, Jain S, Son YJ, Almefty K, Lawton MT, Stevens SM. Integrating stereoscopic video with modular 3D anatomic models for lateral skull base training. *J Neurol Surg B Skull Base*. (2021) 82(Suppl 3):e268–e70. doi: 10.1055/s-0040-1701675
35. Fishman AJ, Marrinan MS, Golfinos JG, Cohen NL, Roland Jr JT. Prevention and management of cerebrospinal fluid leak following vestibular schwannoma surgery. *Laryngoscope*. (2004) 114(3):501–5. doi: 10.1097/00005537-200403000-00022
36. Yamakami I, Uchino Y, Kobayashi E, Yamaura A. Computed tomography evaluation of air cells in the petrous bone–relationship with postoperative cerebrospinal fluid rhinorrhea. *Neurol Med Chir (Tokyo)*. (2003) 43(7):334–8; discussion 9. doi: 10.2176/nmc.43.334

37. Tamura R, Tomio R, Mohammad F, Toda M, Yoshida K. Analysis of various tracts of mastoid air cells related to CSF leak after the anterior transpetrosal approach. *J Neurosurg*. (2018) 130(2):360–7. doi: 10.3171/2017.9.Jns171622

Conflict of Interest: The authors declare that the research was conducted in the absence of any commercial or financial relationships that could be construed as a potential conflict of interest.

Publisher's Note: All claims expressed in this article are solely those of the authors and do not necessarily represent those of their affiliated organizations, or those of the publisher, the editors and the reviewers. Any product that may be evaluated in this article, or claim that may be made by its manufacturer, is not guaranteed or endorsed by the publisher.

frontiers | Frontiers in Surgery

TYPE Original Research
PUBLISHED 28 July 2022
DOI 10.3389/fsurg.2022.930261

Check for updates

OPEN ACCESS

EDITED BY
Philipp Taussky,
Harvard Medical School, United States

REVIEWED BY
Basil Erwin Grüter,
Aarau Cantonal Hospital, Switzerland
Brandon Sherrod,
The University of Utah, United States

*CORRESPONDENCE
Jia Yin
jianyiyin@hotmail.com

†These authors have contributed equally to this work.

‡This author share first authorship.

SPECIALITY SECTION
This article was submitted to Neurosurgery, a section of the journal Frontiers in Surgery

RECEIVED 12 May 2022
ACCEPTED 14 July 2022
PUBLISHED 28 July 2022

CITATION
Zhang Z, Wang W, Yu F, Kwok Sze Chai, Wang Y and Yin J (2022) Strategies for intraoperative management of the trigeminal nerve and long-term follow-up outcomes in patients with trigeminal neuralgia secondary to an intracranial epidermoid cyst.
Front. Surg. 9:930261.
doi: 10.3389/fsurg.2022.930261

Strategies for intraoperative management of the trigeminal nerve and long-term follow-up outcomes in patients with trigeminal neuralgia secondary to an intracranial epidermoid cyst

Zhenyu Zhang[1†], Wenhua Wang[1†‡], Feng Yu[2], Sze Chai Kwok[3,4,5], Yuhai Wang[6] and Jia Yin[1*]

[1]Department of Neurosurgery, Shanghai Tenth People's Hospital, Tongji University School of Medicine, Shanghai China, [2]Department of Neurosurgery, 960 Hospital of The People's Liberation Army of China, Jinan, China, [3]Shanghai Key Laboratory of Brain Functional Genomics, Key Laboratory of Brain Functional Genomics Ministry of Education, Shanghai Key Laboratory of Magnetic Resonance, Affiliated Mental Health Center (ECNU), School of Psychology and Cognitive Science, East China Normal University, Shanghai, China, [4]Division of Natural and Applied Sciences, Duke Kunshan University, Kunshan, China, [5]Shanghai Changning Mental Health Center, Shanghai, China, [6]Department of Neurosurgery, 904 Hospital of The People's Liberation Army of China, Wuxi, China

Background: Epidermoid cysts (ECs) are one of the most common causes of secondary trigeminal neuralgia (TGN). However, most previous studies have primarily focused on whether complete tumor resection was achieved, and few studies have discussed the primary goal of pain relief.
Objective: The present study provides intraoperative strategies for trigeminal nerve (TN) management in patients with TGN secondary to an EC and observed long-term follow-up outcomes.
Methods: A total of 69 patients with TGN secondary to an EC at our hospitals were included (January 2011–June 2021). The same surgical team performed all surgeries using a retrosigmoid approach. After EC removal, different methods for TN management were used, including microvascular decompression (MVD), sharp capsulectomy, nerve combing and embedded cholesterol crystal excision. The epidemiological, clinical, and surgical data were extracted.
Results: The total EC removal rate was 92.8% (64/69). All patients achieved initial pain relief postoperatively, and 12 patients (17.4%) experienced varying degrees of hemifacial hypesthesia, which was relieved within 3–6 months. Three patients (4.3%) reported partial pain recurrence within a median follow-up period of 5.5 (0.5–10.5) years, which was relieved completely after low-dose carbamazepine administration.
Conclusion: The primary goal of surgical tumor removal for patients with TGN secondary to an EC is relief of the main symptom of tormenting pain. The selection of an appropriate strategy for TN, including MVD, sharp capsulectomy, nerve combing or embedded cholesterol crystal excision, should depend on the patient's situation.

KEYWORDS

Cerebellopontine angle, epidermoid cyst, trigeminal neuralgia, management strategy, trigeminal nerve

Introduction

The incidence of intracranial epidermal cysts (ECs), also named intracranial cholesteatomas, accounts for approximately 1% of all intracranial tumors (1–3), and these tumors primarily occur in the cerebellopontine angle (CPA) (4, 5). EC is one of the main causes of secondary trigeminal neuralgia (TGN) (6, 7). The curative goal of patients with TGN secondary to an EC is tumor removal with recurrence prevention and avoidance of complications (8–10). However, the primary goal of treatment in patients with TGN as the first or main symptom is relief of the tormenting pain (11, 12). When pain is not relieved, even complete resection of the tumor should be considered a treatment failure, at least from the patient's perspective. Therefore, the relief of pain, reduction of facial numbness and other symptoms of cranial nerve (CN) injury, and prevention of TGN recurrence using appropriate approaches for trigeminal nerve (TN) management during the process of tumor resection are more important than tumor resection. Few studies have summarized and discussed experience and practice in this respect. This article summarizes our 10-year experience and practice in the treatment of 69 patients with TGN secondary to an EC and discusses the preferred management strategies.

Methods

Patient characteristics

All patients who underwent surgery for TGN at our hospitals from January 1, 2011, to June 30, 2021, were reviewed retrospectively. The diagnosis of TGN was made in 2,048 cases according to the criteria for classic TGN (13.1.1) of the International Classification of Headache Disorders 3 (ICHD-3). As part of the routine clinical management of TGN, all patients underwent a preoperative three-dimensional time-of-flight (3D-TOF) magnetic resonance imaging (MRI) examination. In cases of prepontine cistern enlargement or abnormal signals, contrast enhancement or 3D fast imaging using steady-state acquisition (3D-FIESTA) was applied (**Figure 1**) (13). Of the 2,048 consecutive TGN cases, the EC was diagnosed secondary to TGN in 76 cases preoperatively, surgically and pathologically. By the end of June 2021, seven patients were lost to follow-up, and 69 were ultimately included in this study for analysis. Seventeen of the 69 patients had undergone other surgical treatments (percutaneous radiofrequency thermocoagulation, percutaneous ball compression or γ-knife surgery) before admission to our hospitals, and nine of these patients had obvious postblock hypesthesia. The ethics committee of the two hospitals involved approved this study. The patient data were anonymous, and informed consent was not necessary.

Anatomical observations and surgical procedures

All patients underwent treatment with a standard suboccipital retrosigmoid approach. After the release of cerebrospinal fluid (CSF) under a microscope and retraction of the cerebellar hemisphere, a pearl-like space-occupying lesion with an intact capsule was observed at the CPA. The TN, facial-acoustic nerve, and lower CNs were compressed and encapsulated. After opening the arachnoid membrane, intracapsular resection was performed as the primary procedure, including clearing of the cholesteatomatous tumor tissue in all corners using an aspirator and dissector and the tumor tissue on the tentorium cerebellum and in the contralateral prepontine cistern by adjusting the angle of the microscope. For tumor capsules attached to the brain stem, compulsory resection was not performed to avoid damaging the penetrating vessel, which results in severe consequences. In cases where the tumor wrapped the facial-acoustic, abduction and trochlear nerves, a small aspirator tube with a well-controlled suction force was used because these nerves are thin and delicate, and excessive suction could cause direct damage. The adhered tumor capsule was cut and removed *via* sharp dissection. After clear and complete tumor removal, primary attention was focused on the management of the TN root. Different surgical procedures for TN management were performed according to the type classification, as discussed below.

Type I

There were 49 cases of this type, consisting of only an EC without vascular involvement of the TN. Eighteen cases were type Ia, in which the main portion of the tumor was located in the prepontine cistern, and the TN was pushed from the inside to the outside and became distorted but was not completely encapsuled by the tumor. When the arachnoid membrane was opened, the TN root was directly observed, and the running direction of the fiber was seen clearly. The first step in these cases was clearing the tumor portion in the CPA. TN management started by examining and clearing the root entrance/exit zone and the portion entering the Meckel cave, especially the ventral side of the nerve, to avoid missing the tumor outside of the direct surgical microscopic field. The tumor capsule attached to the TN was removed *via* sharp dissection using microscopic scissors (**Figure 2**, **Supplementary Video S1**).

Twenty-four cases were type Ib, in which the tumor tissue completely encapsulated the nerve. After retraction of the cerebellum, only the tumor was visualized directly in most cases, but the facial-acoustic nerve was seen in some cases. After partial clearing of the tumor, the normally flat TN

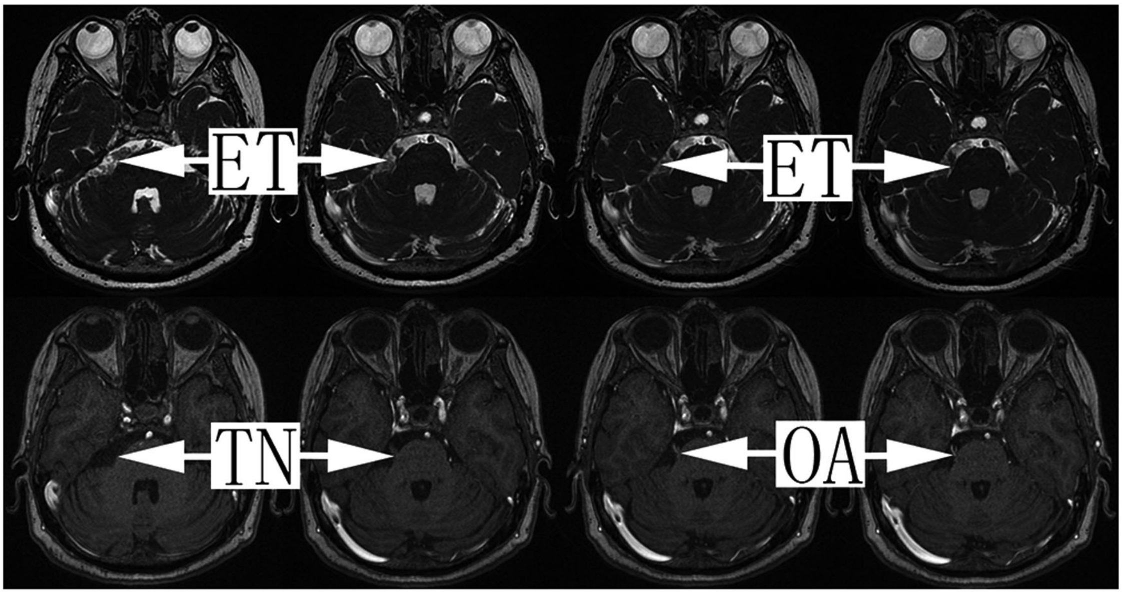

FIGURE 1
The 3D-FIESTA and 3D-TOF magnetic resonance sequence of TGN secondary to EC patients with offending arteries. Tumors of the epidermoid cyst, trigeminal nerve and offending artery are indicated by the arrows. ET, epidermoid tumor; TN, trigeminal nerve; OA, offending artery.

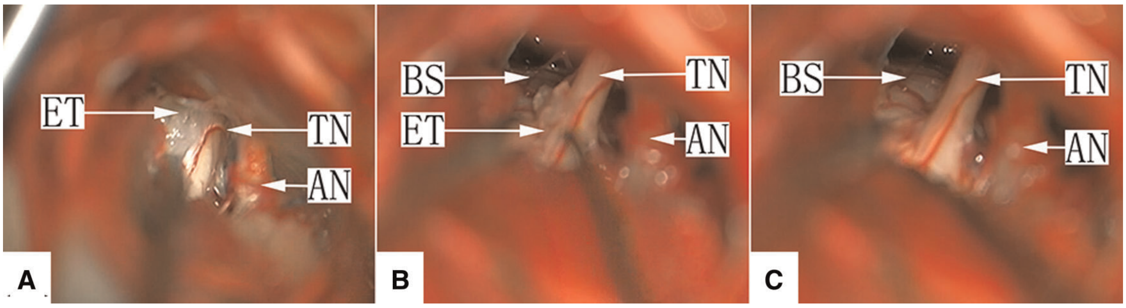

FIGURE 2
(A) Type Ia: After craniotomy and retraction of the cerebellar hemisphere under a surgical microscope, the facial-acoustic nerve, trigeminal nerve and epidermoid cyst in the lateral aspect of the prepontine cistern are seen. The tumor tissue appears white with a pearl-like luster. TN, trigeminal nerve; ET, epidermoid tumor; AN, acoustic nerve. (B): Type Ia: Most cholesteatoid tumor tissue in the prepontine cistern has been removed, with a small amount of tumor residue on the dorsal aspect of the TN root entry zone. TN, trigeminal nerve; ET, epidermoid tumor; AN, acoustic nerve; BS, brain stem. (C): Type Ia: The tumor tissue was removed completely, and the TN surface is smooth. TN, trigeminal nerve; AN, acoustic nerve; BS, brain stem.

cisternal segment had become cylindrically round like an electrical pole, with a layer of capsule-like tissue on the surface. The longitudinal nerve fibers could not be clearly identified. Simple tumor resection in cases of severe TN root invasion by the tumor may not relieve pain completely. The nerve combing procedure was applied to release the TN cisternal segment in 11 patients by making 4–8 incisions along the longitudinal axis using a homemade combing knife (**Figure 3**, **Supplementary Video S2**).

Seven cases were type Ic. Because there may be cholesterol crystals in this type of EC tumor, these stone-like hard substances may be embedded in the TN root, and sharp dissection with microscopic scissors is required to achieve sufficient decompression (**Figure 4**, **Supplementary Video S3**).

Type II

There were 20 cases of this type, in which the TN root contacted the blood vessel during EC excision. Thirteen of these cases were type IIa, in which an offending artery (OA) was found, and microvascular decompression (MVD) was

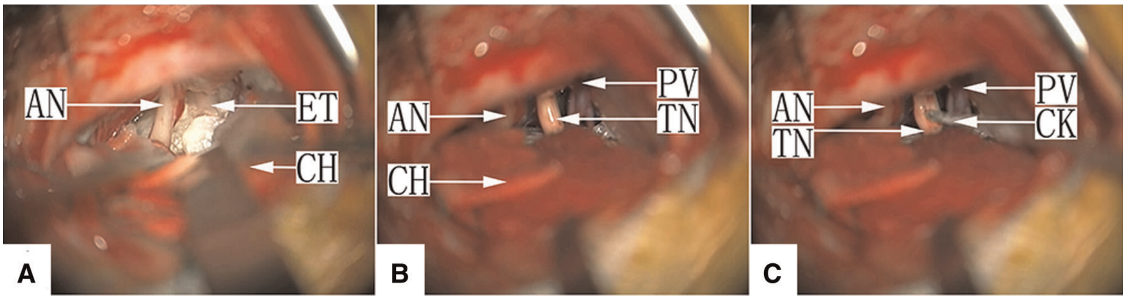

FIGURE 3
(A) Type Ib: After craniotomy and retraction of the cerebellar hemisphere under a surgical microscope, the facial-acoustic nerve is seen, the depth of which is filled with pearl-like tumor tissue, with the petrosal vein and TN buried inside. ET, epidermoid tumor; AN, acoustic nerve; CH, cerebellar hemisphere. (B) Type Ib: The tumor in the cerebellopontine angle (CPA) was removed completely. The TN in the cistern segment is cylindrically round, and its surface is covered with a pseudo-membrane. The longitudinal nerve fibers are not visible. TN, trigeminal nerve; PV, petrosal vein; AN, acoustic nerve; CH, cerebellar hemisphere. (C) Type Ib: Nerve combing of the TN. The cistern segment is performed by inserting the combing knife into the nerve and moving it longitudinally. TN, trigeminal nerve; AN, acoustic nerve; CH, cerebellar hemisphere; CK, combing knife.

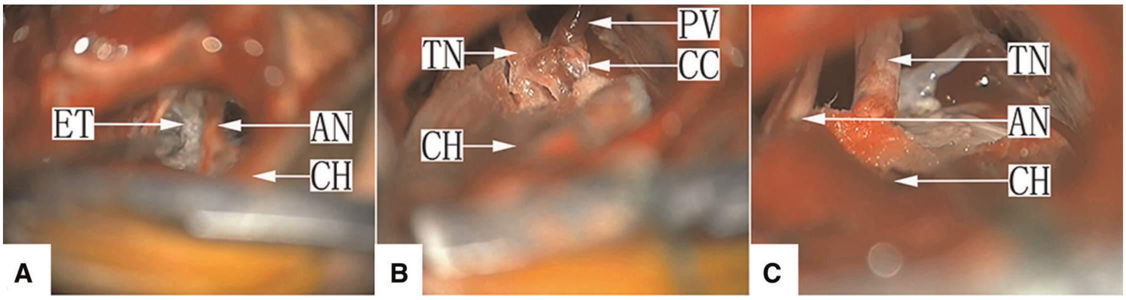

FIGURE 4
(A) Type Ic: After craniotomy and retraction of the cerebellar hemisphere under a surgical microscope, the facial-acoustic nerve is seen, the depth of which is filled with the pearl-like tumor tissue, and the TN is buried inside. AN, acoustic nerve; CH, cerebellar hemisphere; ET, epidermoid tumor. (B) Type Ic: The tumor tissue in the CPA was excised, and the TN root closely adhered to a cholesteatoid crystal with a petrosal vein on the surface. CH, cerebellar hemisphere; PV, petrosal vein; TN, trigeminal nerve; CC, cholesteatoid crystal. (C) Type Ic: The trigeminal nerve was decompressed completely after removal of the cholesteatoid crystal embedded at the TN root *via* sharp dissection at the expense of the petrosal vein. CH, cerebellar hemisphere; AN, acoustic nerve; TN, trigeminal nerve.

performed (**Figure 5**, **Supplementary Video S4**). The remaining 7 cases were type IIb, in which an offending vein (OV) was found. OVs smaller than 1 mm were usually snipped after electrocoagulation, and MVD was used for relatively thick OVs (**Figure 6**, **Supplementary Video S5**).

Follow-up evaluations were performed 6 and 12 months post-operatively and then annually thereafter and included routine physical examination, MRI and facial sensory testing in most cases. Telephone interviews were performed if the patients failed to visit our clinic at the scheduled time. In addition to other CN complications, we primarily evaluated the initial pain relief, pain recurrence, and any type of sensory disturbance using the Barrow Neurological Institute (BNI) pain intensity score and the facial numbness score (14). Complete pain relief was defined as a BNI pain score of I. Partial pain relief was defined as a BNI pain score of II or III.

Results

Sixty-nine of the 2,048 cases were included in the study. The mean age of the 69 EC patients was 49.8 (17–77) years. Most patients were women (68%, 47/69). The mean disease duration was 61.5 (1–480) months, and the mean follow-up duration was 5.5 (0.5–10.5) years. The affected areas and other clinical characteristics are shown in **Table 1**.

All patients had sutures removed and were discharged 5–7 days post-operatively. Immediate and complete pain relief (BNI pain score I) was achieved in all 69 cases. Postoperative

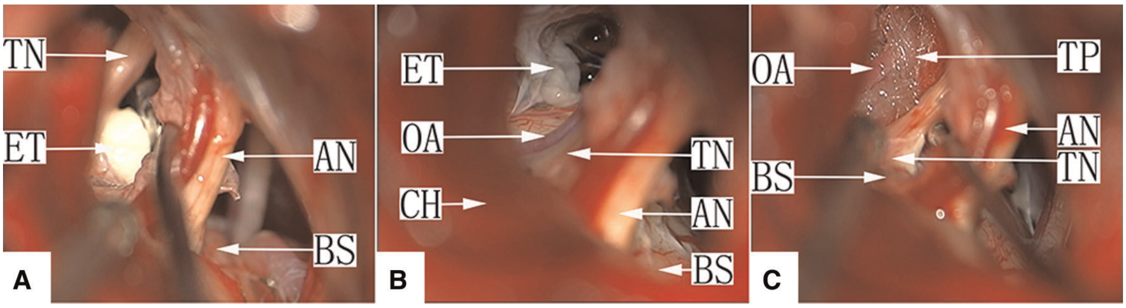

FIGURE 5
(A) Type IIa: After craniotomy and retraction of the cerebellar hemisphere under a surgical microscope, the facial-acoustic nerve and the epidermoid cyst in the prepontine cistern in the median aspect of the nerve are seen. After removal of the tumor tissue, TN was observed. AN, acoustic nerve; TN, trigeminal nerve; ET, epidermoid tumor; BS, brain stem. (B) Type IIa: After removal of most of the epidermoid cyst in the prepontine cistern, the TN root was exposed. Two arteries are seen on its ventral side, which created compression on the nerve. AN, acoustic nerve; TN, trigeminal nerve; ET, epidermoid tumor; BS, brain stem; OA, offending artery; CH, cerebellar hemisphere. (C) Type IIa: Microvascular decompression was performed by separating the offending artery (OA) at the TN root using a Teflon pad. AN: acoustic nerve; TN: trigeminal nerve; BS: brain stem; OA: offending artery; TP: Teflon pad.

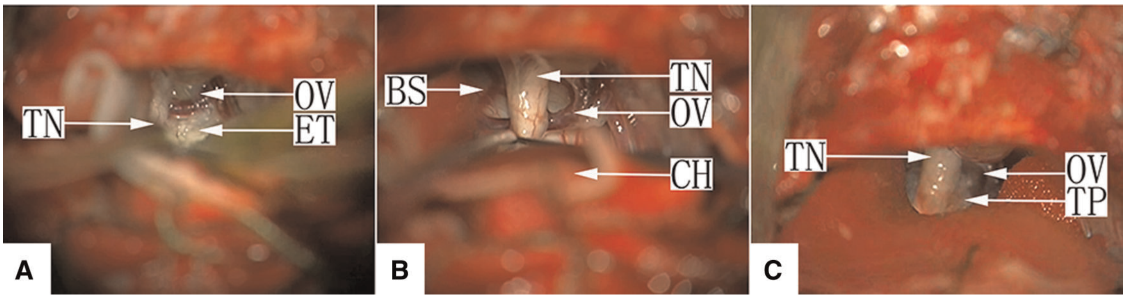

FIGURE 6
(A) Type IIb: After craniotomy and retraction of the cerebellar hemisphere under a surgical microscope, the facial-acoustic nerve, TN and the epidermoid cyst in the prepontine cistern in the median aspect of the nerve are seen. The tumor tissue appears white with a pearl-like luster, and a petrosal vein branch is seen on the surface. TN, trigeminal nerve; ET, epidermoid tumor; OV, offending vein; (B) Type IIb: The tumor tissue in the CPA was removed, and a petrosal vein branch is seen intraneurally passing through the TN root. TN, trigeminal nerve; OV, offending vein; BS, brain stem; CH, cerebellar hemisphere. (C) Type IIb: Microvascular decompression was performed by separating the petrosal vein branch intraneurally passing through the TN root using a Teflon pad on both sides. TN, trigeminal nerve; OV, offending vein; TP, Teflon pad.

MRI demonstrated total resection in 64 cases and subtotal resection in the other five cases because the tumors on the supratentorial and contralateral CPA parts were relatively large. The main complication was unilateral facial hypesthesia, which occurred as a new symptom or exacerbation of the original bradyesthesia in 12 cases, including three of the 11 type Ib EC patients who underwent combing. This bradyesthesia was relieved 3–6 months post-operatively in all patients. Other presenting complications included acute subdural hematoma in three cases (detected on routine CT checkup 24 h post-operatively), which presented as a thin-layer hematoma with no clinical symptoms and were absorbed spontaneously within one month in all cases, aseptic meningitis in eight cases, diplopia in seven cases, including trochlear nerve injury in four cases and abducens nerve injury in three cases, and hearing loss in five cases. During the follow-up period of 0.5–10.5 years, no significant enlargement of the tumor was observed in the five patients in whom subtotal resection was achieved. Three patients (4.35%) reported partial pain recurrence (BNI pain score II–III) two and three years post-operatively. Treatment for recurrence in these patients included the use of low-dose carbamazepine (<200 mg/d), which provided a satisfactory analgesic effect. Pain-free survival was defined as the time to recurrence of facial pain after surgery. Kaplan–Meier curves were constructed based on pain-free survival (**Figure 7**). The different types of TN involvement and the occurrence of related complications are shown in **Table 2**.

TABLE 1 Clinical characteristics of the patients.

	Cohort size ($n = 69$)
Affected side, No. (%)	
Right	27 (39.1%)
Left	42 (60.9%)
Symptom	
Cranial nerve V	
TGN territory involved	
V1	6
V2	9
V3	13
V1 + 2	5
V2 + 3	26
V1 + 2 + 3	10
Post-block hypesthesia	9
Cranial nerve VII	
Hemifacial spasm	3
Cranial nerve VIII	
Hearing difficulty	5
Tinnitus	3

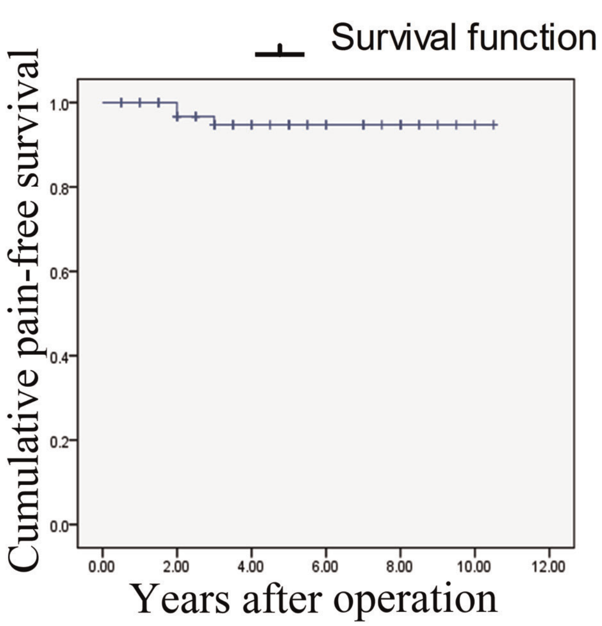

FIGURE 7
Kaplan–Meier survival pain-free analysis. Recurrence of pain occurred in three patients (at 2, 2, and 3 years post-operatively).

TABLE 2 Different types of TN involvement and the occurrence of related CN complications and surgical outcomes.

	Subtotal ($n = 5$)	CN complications ($n = 20$[a])			
		IV ($n = 4$)	V ($n = 12$)	VI ($n = 3$)	VII ($n = 5$)
Type I					
a ($n = 18$)	1	1	4	1	2
b ($n = 24$)	3	2	5		2
c ($n = 7$)			2		
Type II					
a ($n = 13$)	1	1	1	2	
b ($n = 7$)					1

[a]As some patients had injury to multiple cranial nerves after operation, the sum of the cranial nerve cases ($n = 24$) is larger than the total number of the complication cases ($n = 20$).

Discussion

The occurrence of ECs in the CPA is rare, but we have treated numerous cases at our TGN center because the most common onset symptom is TGN. The 69 patients with TGN secondary to an EC included in our series were primarily characterized by a young mean age, pain in the V2 and V3 regions, and a similar onset of symptoms and typical vascular compression presenting as simple TGN (15). The total tumor removal rate was 92.8% (64/69). The simple lateral suboccipital retrosigmoid approach may not expose the distal part of the tumor, and the combined use of the anterior transpetrosal approach or combined transpetrosal approach may be necessary (16, 17); alternatively, endoscopy may be a better means of completely removing the tumor (18, 19). However, a combined approach in this area may cause unexpectedly extensive trauma and require more surgical time. The incidences of perioperative complications, sequalae and tumor recurrence were low in our series. Other than the symptoms of TGN, the symptoms of injury to other CNs, such as diplopia, were restored within approximately six months in most cases. While restoration of hearing loss is relatively difficult, unilateral hearing loss does not have a significant impact on daily activities.

The key for the successful treatment of TGN secondary to an EC is pain relief. The immediate pain relief rate was 100% in our study, and long-term follow-up observation only revealed partial pain recurrence in three cases (4.3%). The incidence of nerve-related complications was also low. Hemifacial hypesthesia was the main symptom, but its postoperative clinical presentation was mild and caused an insignificant impact on patients' daily activities. The symptoms were relieved in 3–6 months in most patients.

A few studies have reported research on TGN secondary to an EC. Kabata (2002) analyzed 28 cases and emphasized that straightening the neuraxis by cutting and removing the adherent tumor capsule and arachnoid membrane was mandatory for the relief of pain and prevention of pain recurrence. With a mean follow-up period of 11.5 years, they detected pain recurrence symptoms in three patients (10.7%). However, their postoperative TN injury rate was as high as

64.3% (18/28). Together with other CN (III-V) injuries, the overall incidence accounted for approximately two-thirds of all patients. Therefore, an excellent outcome was achieved in only 57.1% (16/28) (20). Guo (2011) reported 48 similar cases in which TGN was not relieved after surgery in two cases (a second surgery was performed), and pain recurred in another patient. They noted that resecting the attachment of the tumor capsule to CN V was critical for relieving pain, although this method may damage the nerve (21). Other studies on ECs have only reported intracranial resection of the tumors, with few cases of TGN as the onset symptom (22, 23). These studies demonstrate that the pain relief rate in the management of TGN secondary to an EC is not sufficient, and the rate of TN injury remains high. The etiology of TGN secondary to an EC must be identified and eliminated to achieve the goal of pain relief.

The pathogenesis of TGN secondary to an EC is likely related to the following three conditions: (1) nerve compression from vascular compression; (2) direct compression of the nerve by the tumor; and (3) irritation of the chemicals within the EC or aseptic inflammation of the TN. These factors may work independently or synergistically on the TN to cause demyelination of the nerve and formation of pseudosynaptic connections, which ultimately result in abnormal TN tactile conduction (23, 24).

The principle of our surgical strategy for TN management is removal of the above factors.

1. Strategy for TGN management. Some researchers have advocated conservative management strategies for ECs involving the CN (25). We partially agree that caution should be taken in handling CNs other than the TN, such as the trochlear, abduction, facial and auditory nerves, and use of an aspirator should be avoided. However, pain relief is the primary goal, and we advocate a more positive attitude in treating the TN using a proper method. The present study primarily describes three strategies for TGN management in different situations: (1) sharp dissection of the tumor capsule adhering to the nerve; (2) excision of embedded cholesterol crystals; and (3) combing of the nerve wrapped by the pseudocapsule inside the tumor. Lagares reported that TNs within ECs may undergo pathological changes, including axonal loss and demyelination, with the presence of abundant collagen infiltrates and myelin debris. Myelin-denuded axons have been found in close apposition in some areas, allowing axon-to-axon interactions (26). These findings are consistent with those of previous studies on patients with vascular compression-related TGN. Therefore, nerve combing is generally used instead of MVD when no OV is found (27–29). We used nerve combing to destroy the pseudomembrane formed after nerve demyelination and release the pseudomembrane wrapping the nerve to ensure pain relief.
2. OVs may cause TGN in EC patients. The only controversy is that some researchers believe that the OV is the only cause (30). We found that 30% (20/69) of the cases in our series had OVs, which we carefully examined. An attentive review of the TN by 3D-TOF MRI may be helpful, especially near the TN root entry/exit zone and Meckel cave. With respect to OV management, an OV smaller than 1 mm in diameter may be sacrificed by cutting after cauterization, but removal should be avoided for relatively large OVs (>2 mm in diameter) to reduce hemorrhage and the risk of infarction, which is different from the opinion advocated in most studies that all TGN-related OVs should be sacrificed.

The present study has some limitations. First, it was only a retrospective study. Second, TN combing is an innovative method that has not been generally accepted. Therefore, more studies are required to provide verification of its efficacy and long-term outcomes.

Conclusion

The primary goal of EC removal as a treatment is relief of the tormenting pain. Caution should be taken to avoid oversight of any possible OVs for decompression. The selection of an appropriate strategy for TGN, including sharp capsulectomy, nerve combing or embedded cholesterol crystal excision, should depend on the extent of tumor invasion into the TN.

Data availability statement

The original contributions presented in the study are included in the article/**Suplementary Material**, further inquiries can be directed to the corresponding author/s.

Ethics statement

The studies involving human participants were reviewed and approved by Ethics Committee of the Shanghai Tenth People's Hospitals. Written informed consent for participation was not required for this study in accordance with the national legislation and the institutional requirements.

Author contributions

ZZ and FY performed the data analyses, wrote the manuscript. ZZ and WW revised the manuscript and contributed equally to this work. YW contributed significantly to analysis and manuscript preparation. SCK helped perform the analysis with constructive discussions. JY was the operator and contributed to the conception of the study. All authors contributed to the article and approved the submitted version.

Funding

This work was supported, in part, by the National Natural Science Foundation of China (#81,671,201 by Jia Yin and #81,871,598 by Yuhai Wang). Tenth people's hospital clinical research funding (YNCR2A002) by Jia Yin.

Conflict of interest

The authors declare that the research was conducted in the absence of any commercial or financial relationships that could be construed as a potential conflict of interest.

Publisher's note

All claims expressed in this article are solely those of the authors and do not necessarily represent those of their affiliated organizations, or those of the publisher, the editors and the reviewers. Any product that may be evaluated in this article, or claim that may be made by its manufacturer, is not guaranteed or endorsed by the publisher.

Supplementary material

The Supplementary Material for this article can be found online at: https://www.frontiersin.org/articles/10.3389/fsurg.2022.930261/full#supplementary-material.

References

1. Gonzalez AG. Differential diagnosis of tumors at the cerebellopontine recess. *Bull Johns Hopkins Hosp*. (1948) 83:187–212. PMID: 18877371

2. Hamel E, Frowein RA, Karimi-Nejad A. Intracranial intradural epidermoids and dermoids. Surgical results of 38 cases. *Neurosurg Rev*. (1980) 3:215–9. doi: 10.1007/BF01650025

3. Ulrich J. Intracranial epidermoids: a study on their distribution and spread. *J Neurosurg*. (1964) 21:1051–8. doi: 10.3171/jns.1964.21.12.1051

4. Rubin G, Scienza R, Pasqualin A, Rosta L, Da Pian R. Craniocerebral epidermoids and dermoids. A review of 44 cases. *Acta Neurochir (Wien)*. (1989) 97:1–16. doi: 10.1007/BF01577734

5. Yamakawa K, Shitara N, Genka S, Manaka S, Takakura K. Clinical course and surgical prognosis of 33 cases of intracranial epidermoid tumors. *Neurosurgery*. (1989) 24:568–73. doi: 10.1227/00006123-198904000-00013

6. Mohanty A, Venkatrama SK, Rao BR, Chandramouli BA, Jayakumar PN, Das BS. Experience with cerebellopontine angle epidermoids. *Neurosurgery*. (1997) 40:24–30. doi: 10.1097/00006123-199701000-00004

7. Schiefer TK, Link MJ. Epidermoids of the cerebellopontine angle: a 20-year experience. *Surg Neurol*. (2008) 70:584–90. doi: 10.1016/j.surneu.2007.12.021

8. Ogleznev K, Grigoryan Y, Slavin KV. Parapontine epidermoid tumours presenting as trigeminal neuralgias: anatomical findings and operative results. *Acta Neurochir (Wien)*. (1991) 110:116–9. doi: 10.1007/BF01400677

9. Talacchi A, Sala F, Alessandrini F, Turazzi S, Bricolo A. Assessment and surgical management of posterior fossa epidermoid tumors: report of 28 cases. *Neurosurgery*. (1998) 42:242–52. doi: 10.1097/00006123-199802000-00020

10. Vernon V, Naik H, Guha A. Surgical management of cerebellopontine angle epidermoid cysts: an institutional experience of 10 years. *Br J Neurosurg*. (2022) 36 (2):203–12. doi: 10.1080/02688697.2020.1867058

11. Revuelta-Gutiérrez R, Díaz-Romero Paz RF, Vales-Hidalgo LO, Hinojosa-González R, Barges-Coll J. Cerebellopontine angle epidermoid cysts. Experience of 43 cases with long-term follow-up. *Cir Cir*. (2009) 77:257–65. PMID: 19919786

12. Zhang YQ, Yu F, Zhao ZY, Men XZ, Shi W. Surgical treatment of secondary trigeminal neuralgia induced by cerebellopontine angle tumors: a single-center experience. *World Neurosurg*. (2020) 141:e508–13. doi: 10.1016/j.wneu.2020.05.226

13. Nguyen JB, Ahktar N, Delgado PN, Lowe LH. Magnetic resonance imaging and proton magnetic resonance spectroscopy of intracranial epidermoid tumors. *Crit Rev Comput Tomogr*. (2004) 45:389–427. doi: 10.3109/10408370490903543

14. Pinzi V, Marchetti M, De Martin E, Cuccarini V, Tramacere I, Ghielmetti F, et al. Multisession radiosurgery for intracranial meningioma treatment: study protocol of a single arm, monocenter, prospective trial. *Radiat Oncol*. (2020) 15:26. doi: 10.1186/s13014-020-1478-7

15. Yu F, Yin J. Young-onset trigeminal neuralgia: a clinical study and literature review. *Acta Neurochir (Wien)*. (2021) 163:1617–21. doi: 10.1007/s00701-021-04848-6

16. Darrouzet V, Franco-Vidal V, Hilton M, Nguyen DQ, Lacher-Fougere S, Guerin J, et al. Surgery of cerebellopontine angle epidermoid cysts: role of the widened retrolabyrinthine approach combined with endoscopy. *Otolaryngol Head Neck Surg*. (2004) 131:120–5. doi: 10.1016/j.otohns.2004.02.023

17. Sakamoto H, Kohno M, Matsushima K, Ichimasu N, Nakajima N, Yoshino M. Importance of appropriate surgical approach selection for radical resection of cerebellopontine angle epidermoid cysts with preservation of cranial nerve functions: our experience of 54 cases. *Acta Neurochir (Wien)*. (2021) 163:2465–74. doi: 10.1007/s00701-021-04840-0

18. Cecchini G, Sorenson TJ, Graffeo CS, Vitale G, Di Biase F. Two-operator endoscopic resection of left cerebellopontine angle epidermoid. *World Neurosurg*. (2019) 132:398. doi: 10.1016/j.wneu.2019.09.008

19. Hu Z, Guan F, Kang T, Huang H, Dai B, Zhu G, et al. Whole course neuroendoscopic resection of cerebellopontine angle epidermoid cysts. *J Neurol Surg A Cent Eur Neurosurg*. (2016) 77:381–8. doi: 10.1055/s-0035-1558818

20. Kobata H, Kondo A, Iwasaki K. Cerebellopontine angle epidermoids presenting with cranial nerve hyperactive dysfunction: pathogenesis and long-term surgical results in 30 patients. *Neurosurgery*. (2002) 50:276–86. doi: 10.1097/00006123-200202000-00008

21. Guo Z, Ouyang H, Cheng Z. Surgical treatment of parapontine epidermoid cysts presenting with trigeminal neuralgia. *J Clin Neurosci*. (2011) 18:344–6. doi: 10.1016/j.jocn.2010.07.110

22. Shen CC, Wang YC, Wei SH, Chang CS, Chan YC, Leu CH. Microsurgical management of intracranial epidermoid cysts. *Zhonghua Yi Xue Za Zhi (Taipei)*. (1998) 61:313–23. PMID: 9684507

23. Hasegawa M, Nouri M, Nagahisa S, Yoshida K, Adachi K, Inamasu J, et al. Cerebellopontine angle epidermoid cysts: clinical presentations and surgical outcome. *Neurosurg Rev*. (2016) 39:259–67. doi: 10.1007/s10143-015-0684-5

24. Howng SL, Kwan AL, Hwang SL, Chien TC. Intracranial epidermoid cysts. *Gaoxiong Yi Xue Ke Xue Za Zhi*. (1990) 6(2):81–7. PMID: 2352319

25. Farhoud A, Khedr W, Aboul-Enein H. Surgical resection of cerebellopontine epidermoid cysts: limitations and outcome. *J Neurol Surg B Skull Base*. (2018) 79:167–72. doi: 10.1055/s-0037-1606220

26. Lagares A, Rivas JJ, Jiménez L, Cicuendez M, Avendaño C. Central demyelination in the pathogenesis of trigeminal neuralgia associated with cerebellopontine angle tumors: case report with ultrastructural trigeminal root analysis. *Neurosurgery*. (2010) 66:E841–842. doi: 10.1227/01.NEU.0000367550.30165.A7

27. Jie H, Xuanchen Z, Deheng L, Kun G, Fengyang X, Xiang C, et al. The long-term outcome of nerve combing for trigeminal neuralgia. *Acta Neurochir (Wien)*. (2013) 155:1703–8. doi: 10.1007/s00701-013-1804-z

28. Ko AL, Ozpinar A, Lee A, Raslan AM, McCartney S, Burchiel KJ. Long-term efficacy and safety of internal neurolysis for trigeminal neuralgia without neurovascular compression. *J Neurosurg*. (2015) 122:1048–57. doi: 10.3171/2014.12.JNS14469

29. Urculo E, Elua A, Arrazola M, Torres P, Torres S, Undabeitia J. Trigeminal root massage in microsurgical treatment of trigeminal neuralgia patients without arterial compression: when, how and why. *Neurocirugia (Astur: Engl Ed)*. (2020) 31:53–63. doi: 10.1016/j.neucir.2019.07.003

30. Xia L, Zhong J, Zhu J, Wang YN, Dou NN, Liu MX, et al. Cholesteatoma of cerebellopontine angle presented as trigeminal neuralgia. *J Craniofac Surg*. (2014) 25:1540–2. doi: 10.1097/SCS.0000000000000778

Advantages of publishing in Frontiers

OPEN ACCESS
Articles are free to read for greatest visibility and readership

FAST PUBLICATION
Around 90 days from submission to decision

HIGH QUALITY PEER-REVIEW
Rigorous, collaborative, and constructive peer-review

TRANSPARENT PEER-REVIEW
Editors and reviewers acknowledged by name on published articles

Frontiers
Avenue du Tribunal-Fédéral 34
1005 Lausanne | Switzerland

Visit us: www.frontiersin.org
Contact us: frontiersin.org/about/contact

REPRODUCIBILITY OF RESEARCH
Support open data and methods to enhance research reproducibility

DIGITAL PUBLISHING
Articles designed for optimal readership across devices

FOLLOW US
@frontiersin

IMPACT METRICS
Advanced article metrics track visibility across digital media

EXTENSIVE PROMOTION
Marketing and promotion of impactful research

LOOP RESEARCH NETWORK
Our network increases your article's readership